Metagenomic Exploration of the Effects of Depth and Temperature on the Microbiome Structure and Function of the Gorgonian *Eunicella Singularis* and the Cold Water Scleractinia *Desmophyllum pertusum*

Exploració metagenòmica dels efectes de la profunditat i la temperatura sobre l'estructura i la funció del microbioma de la gorgònia Eunicella singularis i el corall d'aigua freda Desmophyllum pertusum

Mohammad Mutlaq S. Binsarha

Metagenomic Exploration of the Effects of Depth and Temperature on the Microbiome Structure and Function of the Gorgonian *Eunicella Singularis* and the Cold Water Scleractinia *Desmophyllum pertusum*

Exploració metagenòmica dels efectes de la profunditat i la temperatura sobre l'estructura i la funció del microbioma de la gorgònia Eunicella singularis i el corall d'aigua freda Desmophyllum pertusum

Mohammad Mutlaq S. Binsarhan

A Thesis in the Field of Marine Microbial Ecology
for the Degree of Doctorate of Marine Science

Doctoral Program: Doctorat de Ciencies de la Terra
Thesis Supervisor: **Dr. Ramiro Ernesto Logares Haurié**
Thesis Tutor: **Dr. Antonio Miguel Calafat Frau**

University of Barcelona
July 2024

UNIVERSITAT DE BARCELONA

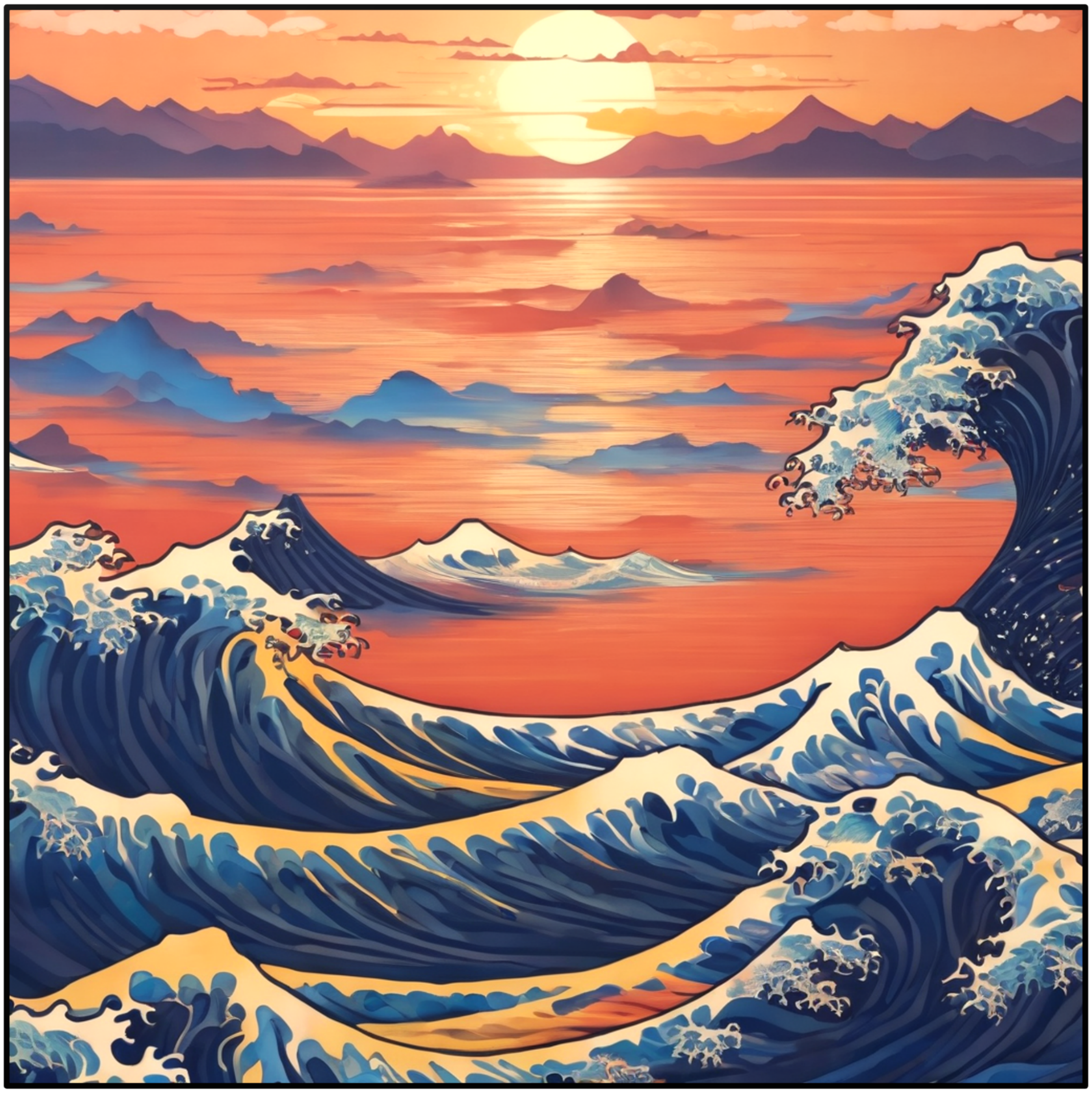

“Be like the ocean beautiful, unpredictable, and mysterious.”

Dedication

To my mother, *whose unwavering support and love have been my anchor throughout this journey.*

To my adviser, *Professor Ramiro Logares, for your guidance, patience, and invaluable insights that shaped this work.*

To my so*n,* ***Jasir,*** *who is the spark of my energy and my motivation to be a better version of myself. I hope to make you proud.*

To Hussain Alsharee*f, who stood by my side in my struggles and whose inspiration and encouragement fueled my determination to complete this thesis.*

To my friends, *who stood by me with encouragement and laughter during challenging moments.*

To all those whose names may not be mentioned but whose impact has been felt, thank you for being a part of this academic endeavor.

This work is dedicated to you.

Acknowledgments

I would like to express my deepest gratitude to the following individuals and institutions who played pivotal roles in the completion of this thesis:

My Adviser, Dr. Ramiro Logares: *Your unwavering support, expert guidance, and insightful feedback were invaluable throughout the research process. Your mentorship has not only shaped the academic content of this thesis but has also influenced my growth as a researcher.*

Research Collaborators: *I extend my appreciation to my research collaborators,* ***Dr. Pierre Galand****,* ***Dr. Javier de Campo, Dr. Rammon Massana****, for their dedication, expertise, and collaborative spirit. Our collective efforts significantly enriched the quality of this research.*

Participants in the Study: *I am grateful to the individuals who participated in the study, especially* ***Dr. Francisco Latorre****. Their willingness to share their insights and experiences contributed immensely to the depth and validity of the research findings.*

KingAbdulAziz University and the Saudi Cultural Mission in Madrid: *I acknowledge their provided financial support. This support played a crucial role in facilitating the necessary resources for data collection and analysis.*

Table of Contents

List of Figures

Summary

Corals play an essential role in marine environments and their morphological structure provides microbes with different habitat types. In turn, the microbes provide corals with important compounds that contribute to coral fitness and health. Corals have been suggested to hold distinct microbes within the anatomical layer, such as the Skeleton, Surface mucus layer (SML), Tissue, and Gastric cavity. Furthermore, many factors can influence the structure and function of the microbiome, making it more challenging to understand. Coral age, taxonomy, disease, depth zones, and many other abiotic factors could shape coral microbiomes and are responsible for their stability. Disturbances in the relationship's stability between coral hosts and their associated microbes increase the chance of coral infections and bleaching, leading to mortality. Therefore, studying the influence of each factor on the microbiome could lead to a better understanding of the nature and dynamics of this complex system. However, many questions remain regarding how microbes are acquired and function in corals. In this thesis, we explored the coral microbiome and its relationship with two abiotic variables, depth and temperature. High-throughput meta-omics approaches have been used to investigate coral microbiomes. Some limitations may hinder the full benefits of meta-omics; however, these powerful tools open doors for understanding the coral microbiome.

Our comprehensive analysis of the Mediterranean *Eunicella singularis* microbiome revealed significant differences between shallow and mesophotic colonies at both taxonomic and functional levels. While shallow water colonies prominently featured *Symbiodinium*, essential for coral energy production through photosynthesis, its absence in the mesophotic zone indicates a shift in microbial community structure. In deeper environments, the microbial community exhibited higher abundances of functional genes

related to carbohydrate, energy, amino acid, cofactor, and vitamin metabolism. This potentially allows the microbiome to utilize carbon and nitrogen from various sources, such as glutathione, steroids, fatty acids, and aromatic hydrocarbons, which might help sustain coral nutrition through enhanced nutrient availability. Additionally, Metagenome-Assembled Genomes (MAGs) analysis identified microbiome taxa, such as DT-91 (Order Pseudomonadales) and *Endozoicomonas*, involved in nutrient recycling, vitamin production, and secretion systems, highlighting their role in microbiome fitness. These findings underscore potential microbial adaptation mechanisms to environmental conditions, emphasizing their potential role in facilitating coral resilience and adaptation to different contexts. Further investigations are needed to determine whether these genes are actively expressed in the microbial community and to assess the extent of their influence on both the coral's health and its associated microbiome.

Our study of the potential influence of prolonged thermal stress on the cold-water coral *D. pertusum* revealed a significant impact on the microbiome structure at both taxonomic and functional levels. Metagenomic analyses supported previous research, showing an increase in Rhodobacterales under thermal stress conditions. Moreover, our analyses indicated an increase in the carbon metabolic genes, such as methylotrophy and glycoside hydrolase enzymes, which may destabilize the microbiome and promote the growth of opportunistic pathogenic organisms. Indeed, we found an increase in pathogenic marker genes within the *D. pertusum* microbiome as temperature increased. Interestingly, the microbial taxa associated with these markers, such as those related to type 1 and 3 secretion systems, also increased in abundance in thermally stressed microbiomes. Additionally, we observed an increase in genes associated with diazotrophic activity, including denitrification and nitrification, which could disrupt the nitrogen cycle balance between the coral and its microbiome, potentially increasing the susceptibility to diseases and mortality. Together, these findings underscore the influence of increasing temperature on the taxonomic and functional structure of the cold-water coral microbiome. However, further research is required to investigate the gene expression profiles associated with formaldehyde assimilation, denitrification, and nitrification. Examining the expression levels of these metabolic pathways would provide deeper insights into their activity and regulation, contributing to a more comprehensive understanding of their roles in the microbiome's response to environmental stressors such as temperature increase.

Resum

Els coralls juguen un paper essencial en els ambients marins i la seva estructura morfològica proporciona als microbis diferents tipus d'hàbitats. Al seu torn, els microbis proporcionen als coralls compostos importants que contribueixen al benestar i la salut dels coralls. S'ha suggerit que els coralls contenen microbis específics dins de les capes anatòmiques, com ara l'esquelet, la capa de mucositat superficial (SML), el teixit i la cavitat gàstrica. A més, molts factors poden influir en l'estructura i funció del microbioma, fent-ne més difícil la comprensió. L'edat del corall, la taxonomia, les malalties, les zones de profunditat i molts altres factors abiòtics podrien modelar els microbiomes dels coralls i són responsables de la seva estabilitat. Les pertorbacions en l'estabilitat de la relació entre els hostes del corall i els seus microbis associats augmenten la probabilitat d'infeccions i blanqueig dels coralls, conduint a la seva mortalitat. Per tant, estudiar la influència de cada factor en el microbioma podria portar a una millor comprensió de la naturalesa i la dinàmica d'aquest complex sistema. No obstant això, queden moltes preguntes sobre com s'adquireixen i funcionen els microbis en els coralls. En aquesta tesi, vam explorar el microbioma dels coralls i la seva relació amb dues variables abiòtiques, la profunditat i la temperatura. S'han utilitzat enfocaments metaòmics d'alt rendiment per investigar els microbiomes dels coralls. Algunes limitacions poden obstaculitzar els beneficis complets de les metaòmiques; tanmateix, aquestes eines poderoses obren portes per comprendre el microbioma dels coralls.

La nostra anàlisi exhaustiva del microbioma de l'Eunicella singularis mediterrània va revelar diferències significatives entre les colònies superficials i mesofòtiques tant a nivell taxonòmic com funcional. Mentre que les colònies d'aigües poc profundes presentaven de manera destacada Symbiodinium, essencial per a la producció d'energia del corall a través de la fotosíntesi, la seva absència a la zona mesofòtica indica un canvi en l'estructura de la comunitat microbiana. En ambients més profunds, la comunitat microbiana va mostrar una major abundància de gens funcionals relacionats amb el

metabolisme de carbohidrats, energia, aminoàcids, cofactors i vitamines. Això possiblement permet al microbioma utilitzar carboni i nitrogen de diverses fonts, com el glutatió, els esteroides, els àcids grassos i els hidrocarburs aromàtics, la qual cosa podria ajudar a mantenir la nutrició del corall mitjançant una major disponibilitat de nutrients. A més, l'anàlisi dels Genomes Obtinguts per Metagenòmica (MAGs) va identificar tàxons del microbioma, com DT-91 (Ordre Pseudomonadales) i Endozoicomonas, involucrats en el reciclatge de nutrients, la producció de vitamines i els sistemes de secreció, destacant el seu paper en la salut del microbioma. Aquests descobriments subratllen els mecanismes potencials d'adaptació microbiana a les condicions ambientals, ressaltant el seu paper potencial en la resiliència i l'adaptació dels coralls a diferents contextos. Són necessàries més investigacions per determinar si aquests gens s'expressen activament a la comunitat microbiana i per avaluar l'abast de la seva influència en la salut del corall i el seu microbioma associat.

El nostre estudi sobre la influència potencial de l'estrès tèrmic prolongat en el corall d'aigua freda D. pertusum va revelar un impacte significatiu en l'estructura del microbioma tant a nivell taxonòmic com funcional. Les anàlisis metagenòmiques van recolzar investigacions anteriors, mostrant un augment dels Rhodobacterales en condicions d'estrès tèrmic. A més, les nostres anàlisis van indicar un augment en els gens metabòlics del carboni, com la metilotrofia i les enzims glicòsids hidrolases, que podrien desestabilitzar el microbioma i promoure el creixement d'organismes patògens oportunistes. De fet, vam trobar un augment en els gens marcadors de patogenicitat dins del microbioma de D. pertusum a mesura que augmentava la temperatura. Curiosament, els tàxons microbians associats a aquests marcadors, com aquells relacionats amb els sistemes de secreció de tipus 1 i 3, també van augmentar en abundància en microbiomes sotmesos a estrès tèrmic. A més, vam observar un augment en els gens associats amb l'activitat diazotròfica, incloent la desnitrificació i la nitrificació, que podrien alterar l'equilibri del cicle del nitrogen entre el corall i el seu microbioma, potencialment augmentant la susceptibilitat a malalties i mortalitat. Aquests descobriments subratllen la influència de l'augment de la temperatura en l'estructura taxonòmica i funcional del microbioma del corall d'aigua freda. No obstant això, es requereixen més investigacions per explorar els perfils d'expressió genètica associats amb l'assimilació de formaldehid, la desnitrificació i la nitrificació. Examinar els nivells d'expressió d'aquestes vies metabòliques proporcionaria una comprensió més profunda de la seva activitat i regulació, contribuint a una comprensió més completa dels seus papers en la resposta del microbioma als factors d'estrès ambientals com l'augment de la temperatura.

1. INTRODUCTION

1. Introduction

1.1. The history of ocean investigations

Our oceans cover approximately two-thirds of the Earth (Yuh et al., 2011) and play a key role in the global climate (Rahmstorf, 2002). They hold millions of living organisms from all domains of life (Mariño-Tapia et al., 2014). In the early stages of ocean and coral investigation, scholars faced the challenge of overcoming entrenched beliefs in mythology, superstition, and folklore. The earliest credible account of coral can be traced back to Theophrastus (c. 372–c. 285 BC), an Aristotle's successor at the Lyceum in Athens. Theophrastus, based on specimens from the Mediterranean, initially perceived coral as a type of stone, briefly mentioning it in his work on minerals, titled "Peri lithon" (On Stones). The Latin translation, "De lapidus," preserved much of Greek learning in the subsequent Roman era. Theophrastus introduced the term "coral" as "kouralion," later translated into Latin as "curalium" and evolving into "corallo" in Italian, "corail" in French, and equivalent terms in other European languages. The surviving fragment of "Peri lithon" contains the first mention of coral's perplexing nature, describing it as similar to a stone, shaped like a root, and found in the sea.

Theophrastus faced a dilemma akin to Aristotle's (384–322 BC) classification challenges in his work "Historia animalium." Aristotle's observations noted ambiguous characteristics in marine forms, such as corals, which he deemed rocks with a plant-like appearance, leading to their later classification as "lithophytes" (stone+plant). Limited references to coral appeared in Latin literature, notably in Pliny the Elder's "Naturalis Historia" (Natural History), where he highlighted the commercial value of coral in the Mediterranean, Red Sea, and Persian Gulf. Indian incorporation into the Hellenistic Empire led to significant coral trade. Pliny humorously noted the hazards of collecting corals and pearls for wealthy women's adornment despite the dangers posed by sharks.

From ancient times to the late 16th century, corals were perceived as either mineral or plant formations, based on their physical characteristics. Red coral, particularly the flexible species "Corallium rubrum," has become a precious gem and staple in jewelry for 2000 years. Initially retrieved by swimming and diving, the practice expanded to the North African coast, as easily accessible areas along the French and Italian coasts were depleted. Red coral stems were harvested, dried, and transformed into gem-like stones for use in jewelry. These prized artifacts were widely distributed in archaeological sites across the ancient world, from Egypt and Persia to Great Britain, India, China, Japan, and various parts of Africa.

In the 18th century, ocean expeditions gained more attention due to the need to discover new commercial routes, for example, James Cook’s voyages. This British explorer, known for his voyages from 1768 to 1780, made detailed maps of the Newfoundland. He explored the ocean and achieved the initial documented European encounter with the eastern shores of Australia and the Hawaiian Islands during his three journeys to the Pacific. Additionally, he accomplished the first recorded circumnavigation of New Zealand. This was followed by Benjamin Franklin, who wrote in his letter “Sundry Maritime Observations,” the first description of the Gulf Stream, an intense, warm ocean current in the western North Atlantic Ocean. This stream moves north along the coast of Florida and then turns eastward off of North Carolina, flowing northeast across the Atlantic. Benjamin also included in his letter discussions of ship propulsion methods, hull designs, causes of disaster at sea, sea anchors, food at sea, and even the use of propellers to steer balloons. Another expedition was the one led by Alejandro Malaspina (1789-1794), which was a five-year maritime scientific exploration and fully funded by the Spanish government for scientific goals.

Then, Charles Darwin’s expedition took place in the 19th century when he sailed on HMS Beagle around the world for a five-year voyage. The primary mission of the journey, which was sponsored by the British government, was to survey the coastline and chart the harbors of South America to make better maps and protect British interests in the Americas. Darwin took the chance to explore and describe different species from 20 different stops and he successfully described more than 1500 of them. After this long, intensive trip, in 1872 the first scientific expedition took place, The Challenger expedition. During its historic voyage around the world, the expedition conducted 492 deep-sea soundings, 133 bottom dredges, 151 open water trawls, and 263 continuous water temperature observations. Approximately 4,700 previously unknown marine species have been identified to date. In the 20th century, different explorations have been made, such as the Bathyscaphe Trieste dives to the deepest point in the Mariana Trench in 1960. Also, The Ben Franklin (PX-15) drifts submerged for 30 days in the Gulf Stream in 1969.

The big jump in the science and technology fields in the 21st century, such as DNA sequencing and bioinformatics algorithms, has revolutionized the field of marine science and biology. For example, the *Sorcerer II* expeditions (2003-2010) conducted global surveys of prokaryotic metagenomes from the ocean covering 32,000 nautical miles and more than 20 different territories on four continents. In addition, the Malaspina Expedition 2010 (named after the one led by Alejandro Malaspina) was an interdisciplinary research project to assess the impact of global change on oceans and explore their biodiversity, from surface to bathypelagic waters. Also, the expedition TARA Oceans from 2009 to 2013 conducted a large environmental survey of 210 ecosystems in 20 biogeographic provinces, collecting over 35,000 samples from surface and mesopelagic waters. The amount of data generated by these expeditions is massive and enhanced our knowledge of ocean dynamics and diversity. Recently, another expedition, the TARA Pacific Expedition, focused on coral reefs across the Pacific Ocean and used a coordinated sampling effort to address questions at multiple scales using a common suite of samples. For two years (2016-2018), more than a hundred thousand kilometers, including 32 sampling sites and 3000 scuba dives collecting nearly 58,000 samples from different reefs across the Pacific, opened new doors toward understanding the coral ecosystem. This huge effort highlights the importance of coral reef ecosystems in global ocean health.

1.2. An Overview of the Coral Ecosystem

Coral zones are among the most productive and diverse marine ecosystems (Moberg & Folke, 1999; Mulhall, 2009; Y. Zhang et al., 2015). Corals are fundamental ecosystem designers that support various organisms (Bourne et al., 2016) that host thousands of species, several of which remain unknown (Hoegh-Guldberg, 1999). Estimates indicate that there are more than 60,000 animal species in coral habitats (Reaka-Kudla, 1997). This high-productivity assemblage contains an array of microorganisms, including symbionts, inhabiting coral colonies and participating in various complex interactions with the coral host (Weis et al., 2008). These interactions play a key role in the global carbon cycle (Shi et al., 2021). In addition to the crucial role of corals in preserving high biological diversity, coral reefs also play a critical role in supporting human well-being. They provide economic benefits to coastal areas through various industries, including tourism, fisheries, and pharma. These industries provide jobs and income for local communities, and coral reefs also offer coastal protection, food security, and a source of scientific discovery (Burke et al., 2011).

The phylum Cnidaria comprises approximately 10,000 species. It contains two major groups: Anthozoa and Medusozoa. Most of these are marine species, such as corals and sea anemones in the Anthozoa class, and only a few species are adapted to freshwater (Technau et al., 2015). Moreover, the Anthozoa class includes 234 species that are divided into two subclasses: Hexacorallia, which has six different orders, including anemones, scleractinians, black corals, and octocorallia, which has three distinctive orders: soft coral and sea fans, blue corals, and sea pens (McFadden et al., 2021) (Figure 1).

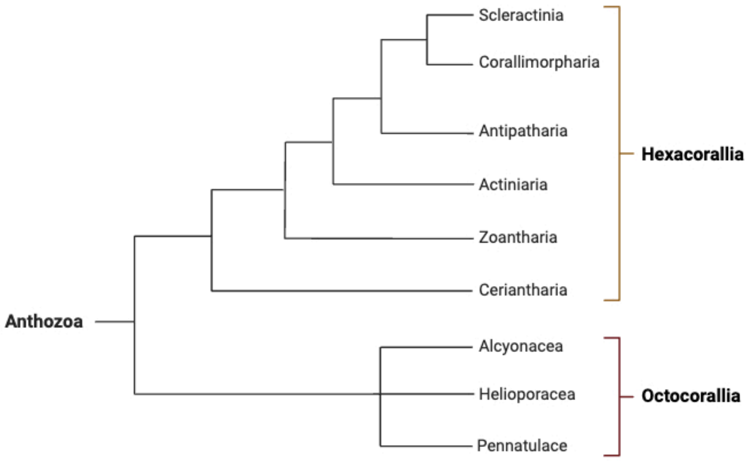

Figure 1: Phylogeny of orders in Anthozoa class, adapted from Quattrini et al. (2020) (Quattrini et al., 2020)

Corals can be polypoid and exist as colonies, clones, or solitary individuals; they may either lack a skeleton or possess a skeleton composed of minerals and/or proteins (Frias-Lopez et al., 2002). Some of them, such as scleractinian corals, secrete a crystal form of calcium carbonate, aragonite, to form their skeletons. However, some types of proteinaceous corals, such as soft and black corals, produce internal small sclerites of calcium carbonate composed of its most stable polymorph, calcite (Rahman et al., 2011), embedded in the coenenchyme (Menzel et al., 2015). Colonial coral polyps are interconnected and work together to exchange nutrients (Bonacolta et al., 2023). Their structure is comprised of two cell layers: an external ectoderm-epidermis and an internal endoderm-gastrodermis. These two layers have an acellular layer separator called the mesoglea, and each of the tissue layers contains numerous cell types, the total number and physiological functions of which are not entirely known. Furthermore, the coral polyp structure comprises a ring of tentacles surrounding the mouth, and the tubular body contains the gastrovascular cavity (Figure 2). The Endosymbiotic algae, when present, reside within gastrodermal specialized cells called 'symbiocytes' (Tresguerres et al., 2017), translocating produced organic matter to the coral host (Muscatine & Porter, 1977). Corals can reproduce sexually or asexually by producing gametes (Daly et al., 2003; Plovie, 2009). There are two modes of sexual reproduction, broadcast spawning and brooding. The broadcast spawning mode releases sperm and eggs into the surrounding water, and fertilization and embryonic development occur externally. In contrast, fertilization occurs internally in the brooding reproduction mode when the released sperm finds its way into another coral colony that holds eggs inside the polyp. Then, the larvae brood internally and mature larvae are released.

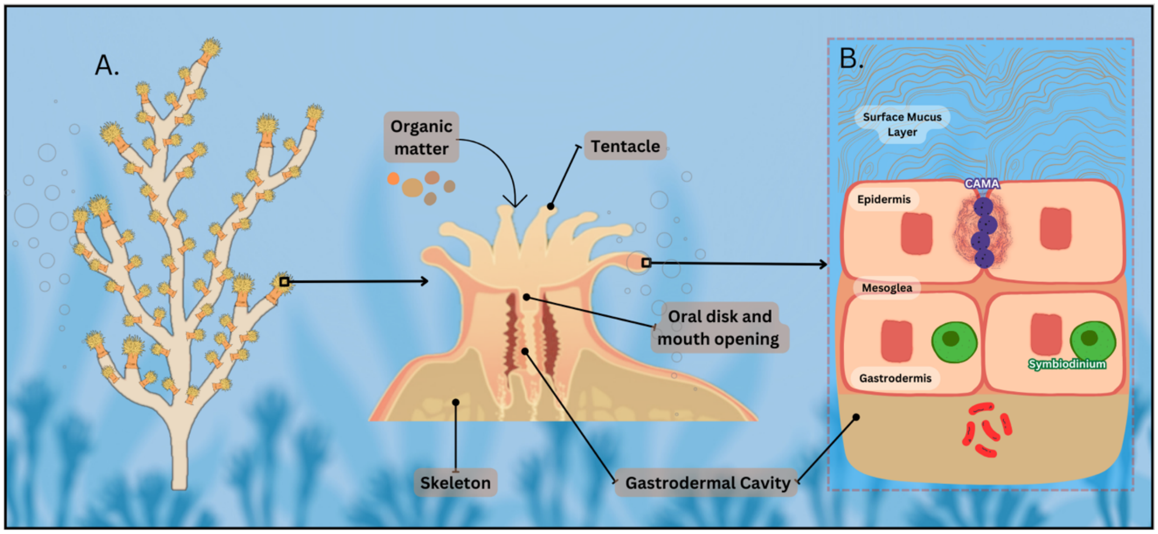

Figure 2: Illustration of the coral polyp anatomy showing **A.** the general coral polyp structure and **B.** the different cellular layers and the *Symbiodinium* residing within the gastrodermal cell symbiocytes

1.3. Coral Holobiont and Ecosphere

Coral hosts include distinct microbes in their surrounding environment (Bayer, Neave, et al., 2013; Bourne et al., 2016; van de Water et al., 2017). Many corals have a symbiotic relationship with the photosynthetic dinoflagellate *Symbiodinium* (Weis et al., 2008). They also include a large diversity of symbiotic microbes (Galand et al., 2023), including protists, fungi, archaea, bacteria, and viruses, some of which have species-specific associations (Carlos et al., 2013; Glasl et al., 2016; Hochart et al., 2023; van Oppen & Blackall, 2019). These symbionts are fundamental to almost every aspect of the coral host, including its function and health (Bordenstein & Theis, 2015). They provide many beneficial services to their hosts, such as nitrogen, carbon, and sulfur fixation, as well as antibiotics (Wegley et al., 2007). Specifically, bacteria-dinoflagellate-coral interactions provide access to nutrients and metabolic pathways to the coral host (D Ainsworth et al., 2015). Furthermore, corals provide different microbial niches, including the inner tissue layers (M. Lesser et al., 2008), surface mucus layers (Kooperman et al., 2007; Rohwer et al., 2002), gastrovascular cavities (Herndl & Velimirov, 1985), and skeleton (Shashar et al., 1997). Each coral tissue layer typically holds a distinct microbial community (Agostini et al., 2012; Apprill et al., 2016; Chiu et al., 2012; Pollock et al., 2018; Rosenberg et al., 2007; M. J. Sweet et al., 2011). In addition, most prokaryotes can be found in the mucus layer (Garren & Azam, 2010) or the skeleton (Yang et al., 2019). The variation in gene composition across the different layers suggests the functional specialization of each microbial community (Kimes et al., 2010). This assemblage of organisms that live with corals constitutes the coral holobiont (Thurber et al., 2009; Water et al., 2018). The global decrease in coral reefs has drawn attention to their microbiome and functions (Rosenberg et al., 2007), as the cnidarian-microbiota interaction is partially understood (Water et al., 2018).

One important association is the coral–microeukaryote interaction. These include ciliates, dinoflagellates, apicomplexans, and chromerids, which can establish either positive or negative interactions with corals (Janouškovec et al., 2012). Furthermore, dinoflagellate-coral interactions are vital to symbiotic corals. For instance, *Symbiodinium* provides the host coral with fixed carbon and organic matter (van Oppen & Blackall, 2019). Another example is the endolithic algae *Ostreobium* sp., which is commonly found in the vast majority of scleractinian corals (Gonzalez-Zapata et al., 2018; Odum & Odum, 1955), including Symbiodinium-less stony corals such as *Tubastrea micranthus* (Pernice et al., 2020a). They play an important role in coral hosts. They may fix carbon (Shashar et al., 1997) and exchange photosynthates such as carbohydrates and lipids with coral tissues (Gonzalez-Zapata et al., 2018; Odum & Odum, 1955; Pernice et al., 2020a). This implies that there is a well-established metabolic relationship between endolithic algae and corals; however, the molecular translocations and exchange processes between endolithic *Ostreobium* and coral tissues remain to be investigated (Ricci et al., 2019). In addition to its beneficial role in the coral nutrition cycle, the green alga *Ostreobium* is the most significant agent in the microbial carbonate removal process of coral skeletons, accounting for up to 90% (Grange et al., 2015; Tribollet, 2008). This process involves dissolving calcium carbonate ($CaCO_3$), a fundamental component of scleractinian coral skeletons, thereby rendering the coral structure fragile.

Endolithic fungi are assumed to play a role in nitrogen cycling by reducing nitrate and nitrite to ammonia and accumulating ammonia for biosynthesis (Wegley et al., 2007). Ciliates are bacterial grazers (M. Sweet & Bythell, 2012) and are commonly found as part of the coral holobiont. They may opportunistically feed on coral-associated bacteria and control their populations (Bonacolta et al., 2022). Furthermore, they might help to control the abundance of potentially harmful bacteria and other microorganisms, contributing to a healthy coral microbiota. However, ciliates are assumed to be associated with coral diseases, such as skeleton eroding band (SEB) or brown band (BrB) syndrome. In the case of SEB, the ciliate *Halofolliculina corallasia* generates a speckled black band (Page & Willis, 2008); however, in the case of BrB, *Porpostoma guamensis* contributes to visible symptoms (Lobban et al., 2011) like brown zones on the infected tissue. Recent surveys have identified abundant apicomplexan (primary parasitic protist) sequences in many healthy corals (Kwong et al., 2019), which could indicate parasitism (Bourne et al., 2016). The coral-associated alveolate *Chromera velia* shares a common ancestor with dinoflagellates and exhibits ultrastructural characteristics typical of apicomplexans (Kořený et al., 2011). It can establish endosymbiotic or parasitic associations with coral larvae (Cumbo et al., 2013). However, recent studies indicate that these relationships remain unclear (Mathur et al., 2018; Mohamed et al., 2018).

Some unicellular eukaryotic predators, such as thraustochytrids and labyrinthulids, contribute to coral holobionts by regulating the bacterial and archaeal populations. These microorganisms have been observed in the coral mucus layer (Ainsworth et al., 2017) and have been found to exhibit an ecological resemblance to aquatic fungi (Raghukumar & Ravindran, 2012). In addition, these protists may contribute polyunsaturated fatty acids to the coral (Ainsworth et al., 2017). Furthermore, the coral mucus layer inhibits different types of ciliates, such as C. *verminus* and *Holosticha* sp.; however, they become more abundant in diseased tissues. Ravindran et al. 2020 found that ciliates, when growing at high abundances in bacteria-free mucus substrate, prefer nutrients in mucus instead of bacteria. Additionally, certain ciliates, specifically *Holosticha* sp., have been observed to invade host cells and voraciously consume Symbiodiniaceae cells and tissues (Raghukumar & Ravindran, 2012). Furthermore, certain fungi can invade small-scale calcium carbonate structures and interact with *Ostreobium* cells (R. A. Littman et al., 2009). These fungi are capable of consuming endolithic algae and coral polyps (Golubic et al., 2005; Prog et al., 1995) and are known for their detrimental effects on both stony and soft corals (Alker et al., 2001; Golubic et al., 2005; Priess et al., 2000; Prog et al., 1995; Work et al., 2008). They also contribute to the bioerosion of coral skeletons (Glynn & Manzello, 2015; Tribollet & Golubic, 2011).

Another important interaction involves coral prokaryotes. Archaea typically display low abundance in the coral microbiome, yet they carry essential functions, such as nutrient recycling. The most prevalent archaeal phyla are *Thaumarchaeota*, *Euryarchaeota* (Huggett & Apprill, 2019), and *Crenarchaeota*, which contribute to nitrogen fixation by removing ammonia through nitrification, denitrification (Siboni et al., 2008), and ammonia oxidation (Siboni et al., 2008; Wegley et al., 2007). Other common archaea in the coral microbiome are anaerobic methanotrophs and anaerobic nitrate reducers (Siboni et al., 2008; Wegley et al., 2004). In contrast, bacteria are more abundant, and their symbiosis is vital for coral health and adaptation to environmental fluctuations (van de Water, Voolstra, et al., 2018). The bacterial classes Gammaproteobacteria, Alphaproteobacteria, Bacteroidetes, Cyanobacteria, Firmicutes, and Tenericutes are the dominant bacteria in corals (Huggett & Apprill, 2019).

Corals hold distinct bacterial communities (Bourne et al., 2016) with specific roles, such as nutrient fixation. For example, specific cyanobacteria can fix nitrogen in nitrogen-limited waters surrounding corals (M. Lesser et al., 2008). Despite their multiple benefits, bacteria can cause coral diseases. An example of a negative bacterial interaction is Black Band Disease. It is characterized by a thick microbial layer developed on top of coral tissue that is typically dominated by one or two types of cyanobacteria, sulfate-reducing bacteria such as *Desulfovibrio* sp., sulfur-oxidizing bacteria such as *Beggiatoa* sp. (Sharma & Ravindran, 2020; Weil et al., 2016) and members of Arcobacter (Meyer et al., 2017). However, some bacterial community members in corals can play a significant role in strengthening coral immunity and controlling pathogens (Villela, 2020) through the production of antibiotics (Bourne et al., 2009). In addition, it has recently been suggested that probiotics can help treat unhealthy corals by providing them with antimicrobial substances (Teplitski & Ritchie, 2009). For instance, *Serratia marcescens*, a pathogen associated with whitepox disease, produces Glycosidases and N-acetyl-glucosidase to utilize the coral mucus layer as a source of nutrition. As a protection mechanism, native coral microbes are believed to reduce *S. marcescens* growth and inhibit its enzymatic activity by blocking chemical signals and disrupting chemical transporters (Krediet et al., 2013). Overall, this symbiotic relationship is crucial for the stability, function, and protection of corals (Hagedorn et al., 2015).

Moreover, there is a wide variety of bacterial communities in the coral skeleton, and the skeletal environment is more diverse in prokaryotes than coral tissues or mucus (Pollock et al., 2018). The predominant bacterial classes in the skeleton are Alphaproteobacteria and Gammaproteobacteria (Marcelino & Verbruggen, 2016; Meron et al., 2012). Furthermore, filamentous marine cyanobacteria, including *Plectonema terebrans*, *Mastigocoleus testarum*, and *Halomicronema excentricum*, were among the earliest prokaryotes identified from green bands in coral skeletons (Pernice et al., 2020b). The presence of bacteriochlorophylls in the green and deeper bands of coral skeletons indicates a high abundance of cyanobacteria and anoxygenic phototrophic bacteria (Magnusson et al., 2007; Ralph et al., 2007). However, there have been limited investigations into the range of bacteria in coral endoliths, and these studies have frequently overlooked the possible variability in bacterial diversity within this compartment of corals (Pernice et al., 2020b).

1.4. What shapes the coral microbiome?

Several biotic and abiotic factors influence coral microbial communities. Among biotic factors, coral age, taxonomy, diseases, and other microbiome members play a significant role in shaping microbiome structure. The coral host itself can affect the diversity of the microbiome through mechanisms such as promoting growth by providing essential nutrients (Lima et al., 2023) or releasing antimicrobial substances that hinder bacterial growth within the mucus layer (Bakshani et al., 2018). Moreover, the involvement of other microbiome members, such as *Halobacteriovorax* spp. (Welsh et al., 2017) and viral phages may shape the bacterial community (Teplitski & Ritchie, 2009). Furthermore, the surrounding environmental conditions may also influence the microbiome structure of a wide range of coral species (Pantos et al., 2015). Conditions include factors such as water depth, geographical location, seasonal variations, chemical fluctuations in the surrounding water, disturbances in marine sediments, and temperature alterations. Furthermore, corals are subjected to some of these factors daily (Ainsworth et al., 2010), which can affect the stability of the coral microbiome (Pantos et al., 2015; Villela, 2020).

1.4.1. Coral Age

Multiple hypotheses have been proposed to understand coral microbial selection mechanisms and to determine whether this process is genetically or environmentally modulated. One hypothesis suggests that the bacterial community is vertically transmitted from parents to offspring during the brooding period before larvae are released into the water (Sharp et al., 2012), after which the coral acquires other bacterial taxa from the surrounding environment (Ricardo et al., 2016). Another hypothesis suggests that corals acquire their bacterial communities directly from the environment during broadcast spawning (Leite et al., 2017; Ricardo et al., 2016). Corals can obtain their associated bacteria by using both strategies (van Oppen & Blackall, 2019). However, coral larvae may have a higher microbial diversity (Epstein, Torda, et al., 2019; Lema et al., 2014; R. Littman et al., 2009) and be more dynamic (Damjanovic et al., 2019). In turn, the adult colony shows stability in its microbial composition compared to the juvenile stage (Hernandez-Agreda et al., 2018). The observed disparity in microbial composition between juvenile and adult coral colonies suggests that coral age can influence microbiome diversity. However, the specific role of the microbiome in juvenile coral remains unclear. Metabolomics can provide insights into the dynamic nature and functional aspects of coral microbiomes at various stages of life.

1.4.2. Taxonomy

Researchers have proposed that the two main Scleractinia coral divisions, Robusta and Complexa, have species-specific microbial communities (Chu & Vollmer, 2016; van de Water et al., 2015; Wegley et al., 2007). Previous studies have suggested that coral species may contain few species-specific core bacteria. For example, *Spirochaetales* dominate the red coral microbiome and are stable at both the spatial and temporal scales (van de Water, Allemand, et al., 2018). In contrast, *Cladocora ceaspistosa*, which is deemed the only true reef in the Mediterranean Sea, has different dominant bacteria belonging mainly to Alphaproteobacteria and Gammaproteobacteria (Rubio-Portillo et al., 2018). Gammaproteobacteria dominate the Red Sea coral, *Acropora* spp., microbiome, especially *Endozoicomonas* (Bayer, Neave, et al., 2013), which appears as ubiquitous coral symbionts (Hochart et al., 2023). Pollock et al., 2018 (Pollock et al., 2018), hypothesized that corals, throughout their evolution, have selected some microbial species as phylosymbiotic members. The term phylosymbiosis refers to the relationship between a group of phylogenetically related hosts and symbiotic organisms. Pollock et al. found that the order of scleractinian corals showed signs of microbial phylosymbiosis in tissues and skeletons but not in the mucus layer. In Octocorals, evidence of microbiome phylosymbiosis has been observed. It has been suggested that species of *Eunicella*, *Leptogorgia*, and *Paramurcia* share certain bacterial orders, such as Alteromonadales and Oceanospirillales, particularly the family *Endozoicomonadaceae* (Keller-Costa et al., 2021) However, *Eunicella* species, for example, exhibit indications of phylosymbiosis with Sphingomonadales (Keller-Costa et al., 2016) and Poribacteria (Keller-Costa et al., 2021). In contrast, *Leptogorgia* species display a phylosymbiotic relationship with

Mollicutes (Keller-Costa et al., 2021). Additionally, *Paramurcia* species demonstrate phylosymbiosis with Rhodobacterales and Flavobacteriales (Bonacolta et al., 2023).

Furthermore, a huge effort has been made over the past two years to sample from 32 different sites across the Pacific (Tara Pacific expedition) (Belser et al., 2023). They sampled two scleractinian coral species, Pocillopora meandrina (977 colonies) and Porites lobata (945 colonies), and one hydrocoral, Millepora platyphylla (619 colonies). Using these samples, Galand et al. 2023 analyzed their microbiomes and revealed a high presence of one microbial ASV belonging to Endozoicomonadaceae in most coral samples. However, some low-abundance ASVs were also observed, showing a sort of specification with coral species. For instance, Millepora was associated with Cytophagales and Kiloniellales, Porites with Vibrionales and Rhodobacterales, and Pocillopora with Cytophagales and Vibrionales, with prevalences of 90% and 87%, respectively (Galand et al., 2023). Environmental gradients in water quality, light, and temperature can influence coral microbial communities more strongly than coral taxonomy (Hernandez-Agreda et al., 2016; R. A. Littman et al., 2009). Moreover, in the early life stages of coral colonies, it has been suggested that the environment is the main factor determining the coral microbiome, not coral species (Epstein, Torda, et al., 2019; Lema et al., 2014; R. Littman et al., 2009). In conclusion, the evolutionary history of corals may have played a significant role in shaping the diversity of their microbiomes, particularly the skeletal and tissue microbiomes. Understanding the taxonomic preferences of the coral microbiome provides valuable insights into the ecological and evolutionary relationships between corals and their associated microbes.

1.4.3. Disease

The relationship between coral hosts and dinoflagellates is well known, and dysbiosis, a shift in the composition and diversity of the associated microorganisms, can cause bleaching and coral diseases. Identifying the causative agents of coral diseases can be challenging because of the complex nature of coral holobionts. Some of the diseases like Black Band Disease can infect both Hexacorallia and Octocorallia. However, many diseases were found to be species-related (Table.1). For example, Stony Coral Tissue Loss Disease (SCTLD) can infect Hexacorallia (Aeby et al., 2019). This is a serious issue for Florida and Caribbean reefs in the 21st century, with the potential to cause substantial damage to ecosystem services and affect economies. Stony Coral Tissue Loss Disease (SCTLD) results in widespread coral mortality, affects several coral species, and displays variable disease symptoms depending on the species, including differences in tissue loss rates, lesion morphology, and occurrence (Aeby et al., 2019). Although the transmission sources and causative agents of the disease are not entirely clear, it is evident that seawater is involved in the transmission (Alvarez-Filip et al., 2022). In addition, some SCTLD-associated bacterial taxa, such as Alteromonadales, Vibrionales, Peptostreptococcales–Tissierellales, and Rhodobacterales, may play a role in disease progression (Rosales et al., 2023). Microscopic analysis of SCTLD-affected coral tissues did not reveal the presence of bacteria that contributed to tissue death. Instead, the examination indicated the death of coral cells and endosymbiotic dinoflagellates, suggesting a breakdown in the symbiotic relationship between the host and endosymbionts. It remains uncertain which of the two dies first, leading to the death of the other (Work et al., 2021).

Another example of disease-specificity is Aspergillosis. It is believed to be caused primarily by Aspergillus sydowii and infects Octocorallia, especially, Sea Fan (Gorgonia spp.) (Weil et al., 2016). A molecular study comparing the genetic structure of *A. sydowii*, including isolates from diseased corals, humans, and environmental sources, found that it is a single global population with sufficient gene flow to prevent differentiation across geographic locations or sources (K. Kim & Rypien, 2015). Nevertheless, certain fungi, such as *Penicillium chrysogenum* and *P. mallochii*, have been detected in afflicted colonies and have also been discovered in unaffected gorgonian corals (X.-Y. Zhang & Qi, 2019). These findings imply that these fungi are integral constituents of thriving microbial communities. The factors that lead to aspergillosis or the development of other fungal pathogens in coral reefs are unknown (Soler-Hurtado et al., 2016).

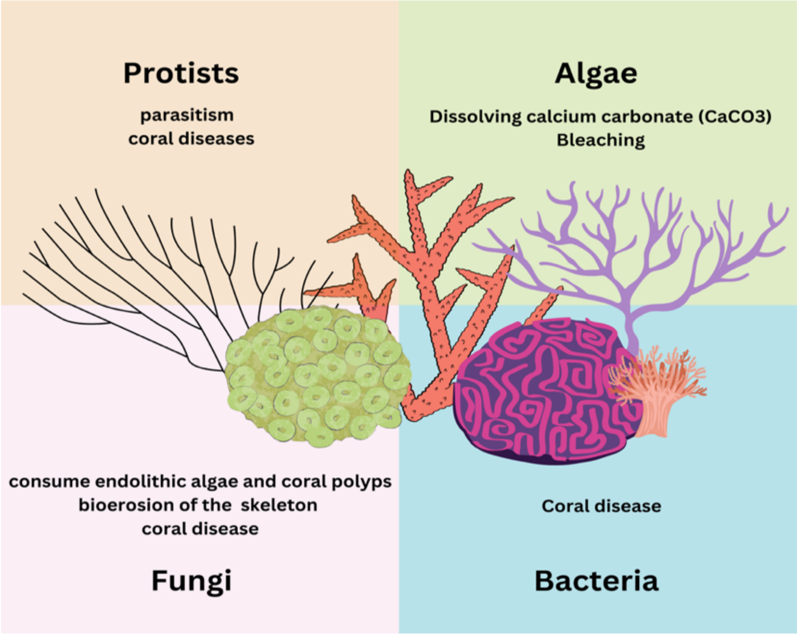

Figure 3: The negative interactions within the coral holobiont, highlighting the roles of different components. Algae could contribute to coral fragility either by dissolving the coral skeleton or loss of symbiosis; protists play a role in coral parasitism and disease; fungi are involved in coral skeleton and tissue damage; and certain bacteria are associated with various coral diseases.

Numerous studies have been conducted to determine the etiological agents of coral diseases. Nonetheless, the causative agents of several coral diseases are unknown, and they may provide insights into the microbiome structure of diseased corals, such as White Band Disease (WBD), which has been linked to potentially associated microbes, such as Vibrionales and Rickettsiales (Linares et al., 2016; C. S. Pereira et al., 2012). Black-band disease (BBD) is a polymicrobial disease consisting of diverse members of four functional groups, with no conclusive primary pathogens identified (Richardson, 2004). Trichoderma and Penicillium fungi are also thought to cause disorders such as fungal protozoan syndrome (FPS) (Cerrano et al., 2000) and Black Necrotic Syndrome (BNS) (Morrison-Gardiner, 2002). However, most of these studies have struggled to identify functional alterations in the microbiome or the processes by which pathogens infiltrate coral tissues and influence the microbiome.

Table.1: Some coral diseases are classified by specificity to Hexacorallia or Octocorallia and potential causative agents

Disease	Hexacorallia	Octocorallia	Causative Agent
White Plague (WP) I,II,III	+	-	Bacteria, Ciliates
Black Band Disease (BBD)	+	+	Bacteria
White Band Disease (WBD) I,II	+	-	Bacteria, Ciliates
Aspergillosis (ASP)	-	+	Fungi
Fungal-Protozoan Syndrome (FPS)	-	+	Fungi, Ciliates
Black Necrotic Syndrome (BNS)	-	+	Fungi
Gorgonian Labyrinthulomycosis (LAB) and Multifocal Purple Spots (MFPS)	-	+	Protozoan parasite genus *Aplanochytrium*
Stony Coral Tissue Loss Disease (SCTLD)	+	-	Bacteria

Moreover, coral health is intricately linked to its surrounding environment (Aeby et al., 2020), and any alterations can lead to dysbiosis (Maher et al., 2019), which can result in a range of ailments, such as tissue lesions, bleaching, and tissue loss (Mera & Bourne, 2018). Consequently, these disturbances have a significant impact on the microbial communities of affected species. Additionally, regular monitoring of the coral host and its response can provide valuable insights into disease processes. For example, analyzing coral samples regularly, especially, in locations that are more susceptible to anthropogenic activities, and pre-bleaching periods. However, given the complex structure of holobionts, this process is challenging. Visual symptoms are actively used for the diagnosis and identification of coral diseases. Therefore, there is an urgent need for improved approaches such as metagenomics, metatranscriptomics, and analyses to enhance our understanding of these illnesses and develop appropriate mitigation strategies.

1.4.4. Depth

Environmental variations in water quality, light, and temperature are thought to profoundly influence the microbial communities within corals (Hernandez-Agreda et al., 2016; R. A. Littman et al., 2009). In this context, depth is regarded as a multifaceted environmental factor that encompasses various gradients such as light and temperature.

The categorization of coral ecosystems based on their depth within the ocean has identified three distinct categories: shallow corals (<30m), upper mesophotic corals (30-60m), and lower mesophotic corals (>60m) (Bongaerts et al., 2010, 2015; Kahng et al., 2010) (Figure 4). Considerable work has been done on tropical water corals, including scleractinian and soft corals, compared with cold-water corals (CWC). Recently, they have attracted the interest of many coral researchers because they could potentially provide predictions about the state of corals in the face of global ocean changes, such as rising temperatures and acidification. Deep-sea corals, which are widely distributed worldwide at depths exceeding 50 m, play a crucial role as ecosystem engineers (Davies & Guinotte, 2011; Middelburg et al., 2015a; Roberts et al., 2006), and are vital contributors to biodiversity. As inhabitants of the deep ocean, they rely on the transportation of organic matter from the sunlit ocean surface (Cathalot et al., 2015; Oevelen et al., 2009).

Recent studies have suggested notable divergence in the microbial composition of corals across different water depths (van de Water, Voolstra, et al., 2018). In tropical-water corals, Prada et al. 2022 conducted a study to examine how depth variation affects the coral microbiome of two warm-water coral species, *Orbicella franksi* [7-8m] and *Orbicella annularis* [3-4m]. To investigate the impact of depth on these species microbiomes, they transplanted the O. *annularis* at ~9m and O. *franksi* at ~4m depth. They have discovered that Gammaproteobacteria, particularly the genus *Endozoicomonas*, exhibit higher levels of enrichment at shallow colonies microbiome. It has been proposed to dualistically metabolize dimethylsulfoniopropionate (DMSP) to produce both dimethylsulfide (DMS) and DMSP as carbon sources for growth and survival (Tandon et al., 2020a). Additionally, the family Alteromonadaceae and order Acidimicrobiales were also found to be more abundant in shallow regions (Prada et al., 2022). It hypothesized that Alteromonadaceae can neutralize the harmful effects of oxidative stress caused by reactive oxygen species (ROS) in corals using enzymatic antioxidants such as catalase, peroxidase, and superoxide dismutase (Dungan et al., 2021).

Additionally, a study by Glasl et al. in 2017 (Glasl et al., 2017) revealed that in *Madracis pharensis*, the prokaryotic community at 15m differs from that at 55 and 85 m in depth. They indicated that the presence of Chloroflexales bacteria was strongly linked to *M. pharensis* at a depth of 15 m, but their relative abundance sharply declined as the depth increased towards the upper mesophotic zone. However, this order is known to be a member of the anoxygenic photosynthesis family (Saghaï et al., 2020) and has mostly been linked to communities associated with hot springs (Hanada, 2014; Ward et al., 2018). Interestingly, Chloroflexales were found completely absent in the *Madracis pharensis* microbiome from the lower mesophotic zone (Glasl et al., 2017). In contrast, the Amoebophilaceae bacterial family was identified as a depth-related taxon of *Madracis pharensis* microbiome at 55 and 85 m, and its relative abundance within *M. pharensis* increased with increasing depth (Glasl et al., 2017). They also found alterations in the *Symbiodinium* community (type B7 in the shallow layers is completely replaced by type B15 in the mesophotic habitats) and prokaryotic community composition. It is worth mentioning that the deepest recorded photosynthetic corals (172 m depth) harbored Symbiodiniaceae together with a diverse community of bacteria, and endolithic algae from the genus *Ostreobium* (Rouzé et al., 2021). An additional example of shallow-water corals in warm environments is *Acropora spp*., whose microbiome is primarily constituted by *Endozoicomonas* (Bayer, Neave, et al., 2013), which is a ubiquitous coral symbiont (Hochart et al., 2023). These are examples of tropical water corals showing depth-variable differences in microbiome composition.

These variations were also detected in the temperate-water corals. For example, *Cladocora ceaspistosa*, which is deemed the only true reef in the Mediterranean Sea, has different dominant bacteria belonging to the Bacteroidetes, Alpha, and Gammaproteobacteria classes (Rubio-Portillo et al., 2018). These colonies were collected at a shallow depth of ~7m. The Rhodobacterales are the most abundant order in the Alpha- class while Flavobacteriales and Sphingobacteriales dominate Bacteroidetes. Interestingly, when the water becomes colder and deeper, the coral microbiome diverges.

Another example is the temperate *Eunicella labiata* microbiome. At depth ~15m, it shows enrichment of Oceanospirillales – mainly Endozoicomonas – followed by Rhodobacterales and Actinomarina (Keller-Costa et al., 2017, 2021). Another survey targeting the 16s rRNA of *Eunicella singularis* was conducted at a depth of approximately 35m. The findings indicated that the predominant component of the core microbiome was Endozoicomonas. Additionally, the microbiome exhibited a locally diverse bacterial population, including Burkholderiales, Mycoplasmatales, Spirochaetales, and Vibrionales (van de Water et al., 2017). Moreover, an analysis of another *Eunicella* species, E. *cavolini*, at different depths (24, 30, and 41m), revealed a consistent dominance of *Endozoicomonas* across all depths, with a few depth-correlated taxa such as Aquimarina and Myxococcales (Bayer, Arif, et al., 2013).

The cold-water coral *Primnoa pacifica* microbiome at ~16m was dominated by Rhabdochlamydiaceae (Goldsmith et al., 2018). Moreover, Spirochaetales dominated the cold-water red coral *Corallium rubrum* microbiome, which was collected from ~ 20 m (van de Water, Allemand, et al., 2018). Furthermore, coral species inhabiting mesophotic zones may possess unique microbiomes (Meyer et al., 2017). When diving deeper, the microbial community of the corals appeared to be different from that of the upper sea layers. For instance, the microbiome of the cold-water coral species *Desmophyllum pertusum*, formerly classified as *Lophelia pertusa* (Linnaeus, 1758), was dominant at ~300 m depth by the uncultured Alpha-proteobacteria of Rhizobiales (Jensen et al., 2019). In the Baltimore Canyon, *Paramuricea placomus* colonies were collected from a depth range of 379–382 m and the microbiome was examined. All examined colonies appeared to share Alpha-, Beta-, Delta-, Epsilon-, and Gammaproteobacteria (Kellogg et al., 2016). Additionally, the microbiome of the deep-sea coral *P. resedaeformis* was studied in a canyon approximately 400–550 m in depth. This investigation revealed the substantial presence of various families within the Proteobacteria phylum, notably including *Xanthomonadaceae*, *Pseudomonadaceae*, *Pseudoalteromonadaceae*, and *Moraxellaceae* (Goldsmith et al., 2018). In the abyssal coral (at depths between 3,000 and 6,000 m), Quintanilla et al. 2020 (Quintanilla et al., 2022) found that Primnoidae and

Isididae microbiomes are dominated by *Terasakiellaceae* and *Spongiibacteraceae* bacteria. Interestingly, they reported that *Terasakiellaceae* ASVs are associated with *Primnoidae* corals (Quintanilla et al., 2022).

1.4.5. Additional Abiotic stressors

Significant variations were observed in the composition of microbial communities inhabiting coral hosts, both spatially and temporally. Despite this variability, the core microbiomes of individual coral hosts exhibit distinct specificities and remarkable stability across different spatiotemporal scales. Furthermore, Dunphy et al. (2019) observed an increase in microbial community dissimilarity with the geographical location of the coral host, suggesting that regional processes, such as dispersal limitation and spatiotemporal environmental heterogeneity, may significantly influence microbial community composition. However, it has been proposed that the dissimilarity observed among geographically separated corals can be primarily attributed to variations in the phylotypes of Gammaproteobacteria (Dunphy et al., 2019). Additionally, some microbiome taxa such as Endozoicomonas and Campylobacteraceae may play a significant role in driving differences in microbiome structure across coral genera (Dunphy et al., 2019; Hochart et al., 2023).

Recently, the influence of geographical distribution on coral microbiome has been investigated across the Pacific Ocean. The coral microbiomes of *Pocillopora meandrina*, *Porites lobata*, and *Millepora platyphylla* were significantly correlated with geographical distance, indicating that local site-specific environmental conditions play a crucial role in shaping the microbiome composition of colonies (Galand et al., 2023). Furthermore, the soft coral *Scleronephthya gracillimum* showed significant diversity and variation in associated bacterial communities across different geographical locations. In *S. gracillimum* from Korea and Japan, the dominant group was Endozoicimonaceae, whereas Mycoplasma was dominant in *S. gracillimum* from Taiwan. Notably, corals from Taiwan had a lower relative abundance of Endozoicimonaceae but greater diversity (Woo et al., 2017). Nevertheless, by narrowing the focus to the core microbiome, it is possible to reduce the occurrence of false positives and negatives by disregarding the inherent variability of non-core microorganisms (Dunphy et al., 2019). Moreover, differences in the strength of host identity—defined by the uniqueness and stability of the microbial communities associated with each coral species—could be used to infer the susceptibility of each species to environmental disturbances and disease outbreaks. This provides crucial insights for conservation and management strategies.

Furthermore, some coral species show high diversity and rapid seasonal changes in their associated microbial communities (C.-P. Chen et al., 2011). A comparative study of three coral genera from reefs near Bocas del Toro, Panama, conducted by Dunphy et al. (2019), found a high abundance of Gammaproteobacteria in December, whereas in April and October, they were mostly absent. Another investigation of the *Acropora pruinosa* microbiome over different seasons by X. Yu et al. (2021) reported seasonal variations in its composition. The results demonstrated the dominance of Proteobacteria in spring, autumn, and winter, whereas Bacteroidetes was dominant in summer (X. Yu et al., 2021). Moreover, 12 OTUs were identified as part of the core microbiome. These 12 bacterial OTUs were shared among the samples across all seasons. The dominant core bacteria showed seasonal changes in their abundance. The bacterial BD1-7 clade was dominant in autumn (86%) and summer (71%), while Rhodococcus was dominant in spring (76%) and winter (36%). The seasonality of the microbiome was analyzed for the whole and core microbiomes. The highest abundance of the core microbiome was recorded in the autumn, accounting for > 81% of the total microbiome. The lowest abundance was observed in spring, with less than 5% of the total microbial community. However, it remains unclear whether the dynamics of bacterial composition affect the functionality of the microbiome. In addition, analyzing the microbiome genes diversity and expression between seasons may enhance our understanding of the microbiome.

Environmental disturbance of cnidarian-algae symbiosis can cause expulsion of endosymbiotic *Symbiodinium* from the coral host as a response to stress (Ainsworth et al., 2008; Leggat et al., 2006). Studies suggest that continuous climate change and anthropogenic pollution play a role in changing the microbial community assemblage associated with coral species (Y. Zhang et al., 2015). Therefore, future ocean conditions may accelerate reef deterioration and render corals more fragile (Reyes-Nivia et al., 2013). Corals usually sustain their nitrogen requirements through heterotrophic feeding and/or by absorbing dissolved inorganic nitrogen from surrounding water (Morrow et al., 2018). Moreover, the reduction in the post-bleaching photoinhibition process and recovery time was correlated with the increased nitrogen acquired through heterotrophy (Ferrier-Pagès et al., 2010; Grottoli et al., 2006; Hoogenboom et al., 2012). Interestingly, the increase in nitrifying bacteria (diazotrophic) during thermal stress (Cardini et al., 2016) suggests a link between bleaching and available nitrogen in the surrounding water (Pogoreutz et al., 2017; Vega Thurber et al., 2014; Wooldridge, 2013). Consequently, researchers have assumed that increased nitrogen intake for corals could accelerate coral recovery following a bleaching event (Morrow et al., 2018). Nevertheless, increases in water temperature and light exposure limit the nitrogen uptake ratio and may cause corals to increase the excretion of organic matter into the surrounding water (Böttjer et al., 2017; Godinot et al., 2011). In addition, the elevated water temperature and reduction in water pH were assumed to limit phosphate and nitrate uptake rates (Godinot et al., 2011). Consequently, the enrichment of organic matter and nitrogen in the water (M. P. Lesser, 2007) with the increase in temperature and light intake, and the mutualistic relationships between coral and the endosymbiotic algae *Symbiodinium,* lead to bleaching (Godinot et al., 2011; M. P. Lesser, 2007).

Plastics are another type of stressors. The impact of plastics and other pollutants on corals has recently gained increasing attention. According to Lamb et al. (2018), corals entangled with plastics have a 20-fold higher likelihood of exhibiting signs of disease. Plastic debris can negatively affect corals in various ways, such as depriving them of light and causing anoxia, and may provide a foothold for pathogens to invade (Lamb et al., 2018). Furthermore, toxicities such as petroleum toxicity and heavy metal exposure affect coral health and lead to coral injuries and death (Stoskopf et al., 2022). Petroleum hydrocarbon contamination causes dysbiosis and disruption of the microbial population, which can injure corals and alter the complex balance and functional diversity within coral holobionts (P. H. F. Pereira et al., 2023). Furthermore, a study by Gissi et al. (2019) indicated that the coral microbiome may undergo dysbiotic alterations due to exposure to Ni and Cu. However, there are notable deficiencies in our understanding of how the microbiome and cnidarian host react to stress, particularly in the context of metal exposure (Gissi et al., 2019).

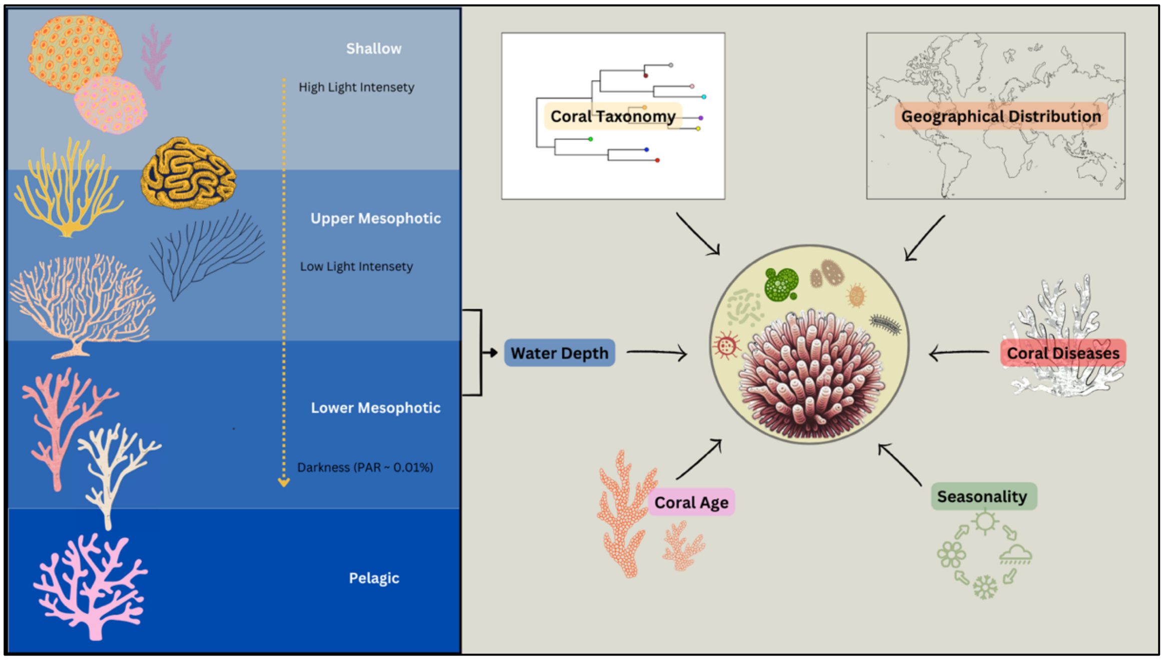

Figure 4. Schematic representation of the primary factors influencing the coral microbiome. The left panel shows the different depth zones within coral habitats.

1.5. Omics-Based Research on the Coral Microbiome

As mentioned previously, coral reefs depend on healthy coral holobionts (Bourne et al., 2016); however, the dynamics of this delicate and complex interaction between coral and the microbiome are affected by environmental disturbances (Planes et al., 2019a). This disturbance causes dysbiosis of the microbiome, which can have substantial consequences for coral and the entire reef (Belser et al., 2023). Integrating multi-omics data, such as genomics, transcriptomics, proteomics, metabolomics, epigenomics, and other omics fields, is crucial for understanding the biocomplexity of corals and their microbial symbionts (Reddy et al., 2023). This approach provides key insights into the resilience, acclimatization, and environmental adaptation of corals and coral reefs (Reddy et al., 2023), although this is more challenging for eukaryotes because of their larger genomes. In addition, eukaryotic genomes are more complex than prokaryotic genomes, with extensive non-coding regions, repetitive sequences, and introns. Additionally, sequences of bacterial origin can contaminate eukaryotic genome assemblies because environmental samples contain DNA from all domains of life. Contamination can also occur from DNA extraction kits or laboratory environments. In this section, I underscore the importance of employing omic-based approaches in coral microbiome studies and provide examples from previous research, highlighting their main findings in addition to some of the limitations and possible solutions.

Metabarcoding has opened doors for exploring microbes that cannot be cultured in the laboratory; however, it only identifies taxa. In turn, metagenomics can be used for the metabolic profiling of microbiomes. Unlike genomics, which focuses on the genetic material of a single organism, metagenomics analyzes the genetic material of entire communities in a given sample by generating large numbers of short metagenomic reads (short DNA sequences). It is useful for examining the genetic composition of microbial populations associated with coral hosts by allowing researchers to sequence and analyze the collective genomes of microorganisms. This approach helps identify the diversity and functional capabilities of the microbial communities, understand their interactions with coral hosts, and assess their roles in coral health and disease. Furthermore, constructing gene libraries for coral microbiomes will increase our knowledge of their functional diversity, providing valuable information about potential metabolic pathways and enzymes. Consequently, this allows researchers to hypothesize and investigate the complex microbial interactions within the microbiome (Planes et al., 2019b). In addition, metagenomics can also be used for taxonomic profiling of the microbiome using marker genes (such as 16S and 18S rDNA) (Salazar et al., 2021a; Vaulot et al., 2022) by mapping them to reference databases such as SILVA (Quast et al., 2012), PR2 (Guillou et al., 2012), and the Global Ocean DB (Obiol et al., 2020).

Metagenome-assembled genomes (MAGs) would help to understand the role of microbiome members. To illustrate, Robbins et al. (2019a) used MAGs to describe the potential role of the stony coral *Porites lutea*. They recovered 52 high-quality genomes of different microbiome components, including the dinoflagellate symbiont *Cladocopium* C15, Archaeal, and bacterial genomes. Based on the functional annotation of the encoded genes in the Cladocopium MAG, they obtained a view of its metabolic capacity in synthesizing some amino acids that cannot be synthesized by the coral (Shinzato et al., 2011, 2014), in addition to their role in nutrition acquisition from the surrounding water. Furthermore, they highlighted the role of archaea and bacteria in producing essential vitamins (group B) that are required for growth by both the coral host and its associated dinoflagellates. These vitamins are essential and cannot be synthesized by corals or algae (Croft et al., 2005; Salem et al., 2014). They also suggested that the prokaryotic community might be involved in carbon fixation which was previously thought that coral only acquires that from predation or their endosymbiotic *Symbiodinium*. Interestingly, they obtained information about the potential interaction between the different microbiome members, in this case, the *Cladocpium* and prokaryotes, in sulfur cycling, such as catalyzing dimethylsulfoniopropionate (DMSP) into dimethyl sulfide (DMS) (Robbins et al., 2019a; Sunda et al., 2002). Collectively, these findings indicate that metagenomics serves as a potent tool for enhancing our knowledge and understanding of intricate dynamics within the holobiont.

Furthermore, metagenome-assembled genomes (MAGs) can be used to analyze the genomic characteristics of specific taxa and compare populations of the same taxon (Hochart et al., 2023). *Endozoicomonas*, for example, is a ubiquitous bacterium associated with most coral species (Neave et al., 2016a). Neave, Michell, et al. (2017), used single cells and metagenomes from three different scleractinian corals to generate novel *Endozoicomonas* MAGs. They found that this symbiont bacterium is involved in the assimilation of ammonia through the synthesis of glutamine and glutamate. However, MAGs show different production capacities for some essential amino acids (Neave, Michell, et al., 2017; Price et al., 2014). In addition, Endozoicomonas was found to encode a phosphoenolpyruvate-dependent sugar phosphotransferase (PTS) system with specific subunits of lactose and cellobiose, suggesting a potential role in consuming degrading algal cells, particularly *Symbiodinium* algae (Neave, Michell, et al., 2017). In addition, it may play a role in communication between microbial cells through chemotaxis (Lux et al., 1995) or quorum sensing (C. S. Pereira et al., 2012).

Another application of metagenome-assembled genomes is the investigation of coral-associated microbial aggregates (CAMA). Wada et al. 2022 (Wada et al., 2022) constructed two MAGs from individual CAMAs belonging to *the genus Endozoicomonas* to study their genomic functional features. They predicted that 37 proteins in each MAG were related to single-species biofilm formation and quorum sensing. In addition, these MAGs exhibited nearly complete components of various secretory systems, including the general twin-arginine protein translocation (Tat) and types I–III and VI secretion systems (SSs). These proteins and secretion systems potentially facilitate aggregation (Cassan et al., 2021) in coral tissues, biofilm formation (Linares et al., 2016), and pathogenicity traits (Bernard et al., 2010). Additionally, MAGs were screened for eukaryotic repeat domains, identifying 26 proteins with ankyrin repeats and 13 proteins with tetratricopeptide repeats, suggesting potential roles in facilitating host-symbiont interactions. Furthermore, these *Endozoicomonas* MAGs from CAMAs were capable of sequestering and cycling phosphate between coral holobiont partners (Wada et al., 2022).

Moreover, metagenomics has been used to study coral strategies for host bacteria and the specification of host-bacterial associations. For example, it has been assumed that *Pocillopora* is associated with *Endozoicomonas* clade A (Neave, Rachmawati, et al., 2017). However, it has recently been found that in some geographical locations, *Pocillopora* is associated with different *Endozoicomonas* clades such as clades B and C (Hochart et al., 2023). In addition, Hochart et al. (2023) conducted a large-scale study across the Pacific Ocean using samples from the TARA Pacific expedition (Belser et al., 2023) on three coral genera, *Millepora*, *Pocillopora*, and *Porites,* and generated 24 *Endozoicomonadaceae* MAGs belonging to two genera: *Endozoicomonas* and *Parendozoicomonas*. They suggested that different coral genera harbor distinct Endozoicomonadaceae species. However, this distinction could be influenced by co-evolutionary history and environmental factors, leading to diverse communities through the rearrangement of prevalent *Endozoicomonas* phylotypes (Tandon, Chiou, et al., 2022a). For example, some coral species may undergo microbial shuffling to confer selective advantages, although further investigation is required (Tandon, Chiou, et al., 2022a). In addition, functional analysis of these MAGs revealed metabolic capacities such as the biosynthesis of cofactors, catabolizing dimethylsulfoniopropionate (DMSP) into dimethyl sulfide (DMS) (Tandon et al., 2020b), and chitin degradation, a widely available polysaccharide in the ocean (Keller-Costa et al., 2022). However, these metabolic pathways varied across the host lineage, associated *Endozoicomonas* clade, and available nutrition sources. These findings suggest that coral-bacterial associations appear diverse, ranging from stable co-dependent relationships established over evolutionary time to flexible opportunistic associations influenced by the environment (Hochart et al., 2023).

The popularity of metagenomic approaches in coral research has resulted in the publication of many studies that have proposed significant hypotheses regarding the roles of microorganisms in stress and bleaching, such as the hypothesis of polygenic evolution (Rose et al., 2018). However, these hypotheses are primarily based on correlational data derived from complex datasets, which makes it challenging to identify and fully understand the essential components of stress response. Additionally, generating data from various species without consistent experimental conditions makes it difficult to compare the datasets. To address this challenge, standardizing data processing and analysis across datasets could involve developing common protocols for data normalization, quality control, and statistical analysis that are applicable to different coral species and experimental conditions. The Tara Pacific expedition (Planes et al., 2019b) took the initiative, proposed a standardized protocol, and built the largest database of coral reef multi-omics data (Lombard et al., 2023). They have used a systematic sampling of two species of scleractinian corals and one hydrocoral in addition to collected water and aerosol samples, along with environmental context data sourced from taxonomic registries, gazetteers, almanacs, climatologies, operational biogeochemical models, and satellite observations (Lombard et al., 2023; Planes & Allemand, 2023). In addition, they used a specific genetic material extraction protocol for metagenomics, including an additional enzymatic step by adding lysozyme, mutanolysine, and lysostaphine and incubation for 1h at 37 °C before the Proteinase K step. This will help to achieve the best lysis of the bacterial and archaeal components of the microbiome (Belser et al., 2023).

Limited microbial DNA is another challenge when dealing with the high volume of sequences generated by the coral host. One way to address this issue is to sequence more deeply and generate more reads to obtain more biological information on coral-associated microorganisms. For instance, Tandon, Ricci, et al. (2022) applied deep sequencing to investigate two reef-building coral skeleton microbiomes, *Porites lutea* and *Isopora palifera*. They sequenced a high number ($\pm 1.3 \times 10^9$) of read pairs and constructed ~400 MAGs, including archaeal MAGs with > 90% completeness and < 10% contamination from the skeleton, some of which are unique to coral species. They found that the skeletal microbiome could use an array of eukaryotic-like proteins (ELPs), such as TPRs and ARPs, to interact with coral and associated microeukaryotes (Nguyen et al., 2014). The presence of various microbial ELPs might indicate diverse roles and different importances (Tandon, Ricci, et al., 2022). Additionally, it has been suggested that the abundance of ELPs is driven by different factors, i.e., the abundance of ARPs is more associated with bacterial lifestyles such as obligate intracellular (Jernigan & Bordenstein, 2014), whereas TPRs are linked to phylogenetic history (Jernigan & Bordenstein, 2015). In addition, their findings elucidated the presumed functional impact of the skeletal microbiome on essential metabolic processes including nitrogen fixation, dissimilatory and assimilatory nitrate, and sulfate reduction (Tandon, Ricci, et al., 2022). This comprehensive view of the functionality of the skeletal microbiome sheds light on some aspects of the complex microbiome interaction, contributing to an enriched understanding and providing new perspectives in microbiome research.

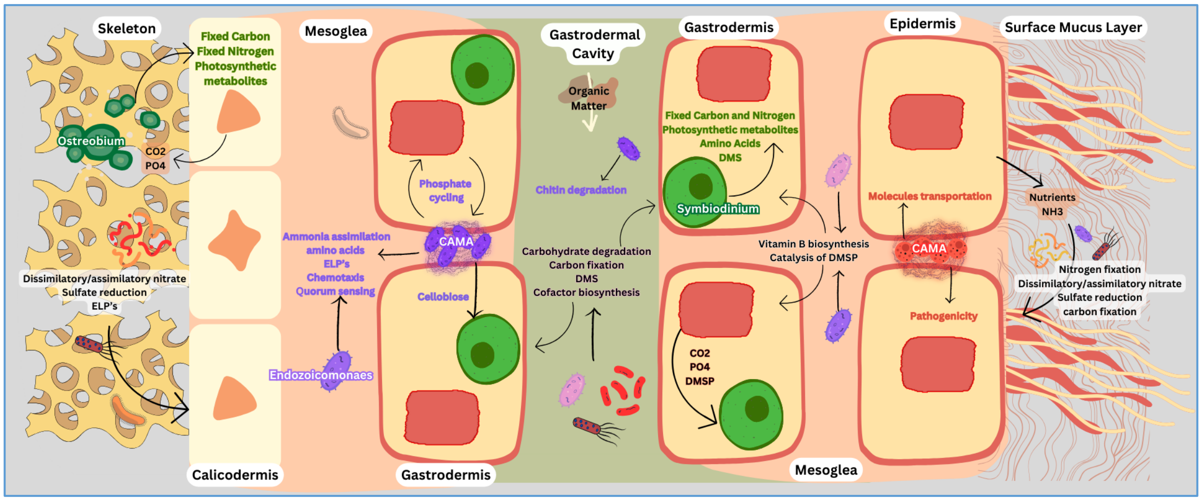

Figure 5. An illustration of coral anatomy indicates the potential roles of the microbiome within each microbial niche of the coral host, derived from metagenomic insights in coral microbiome studies.

Despite this, the popularity of meta-omic techniques in coral research has resulted in the publication of many studies that have proposed significant hypotheses regarding the roles of microorganisms in stress and bleaching, such as the hypothesis of polygenic evolution (Rose et al., 2018). Therefore, metagenomics could help coral disease research and provide valuable insights into microbiome characteristics. For example, metagenomics has been used to understand the microbial community dynamics of SCTLD. Rosales et al. (2022) compared the microbial community of healthy, diseased, and unaffected tissues from four coral species: *tephanocoenia intersepta, Diploria labyrinthiformis, Dichocoenia stokesii*, and *Meandrina meandrites*. Their results showed the presence of ciliates associated with coral diseases (Eaton et al., 2021), and genetically characterized them (Rosales et al., 2022). This provides an advantage and supports the previous histological findings of SCTLD (Landsberg et al., 2020; Meyer et al., 2019a). In addition, they retrieved 16 high-resolution MAGs that were associated with SCTLD and defined specific metabolic pathways of potential interest. In addition, MAGs were more abundant in diseased tissues, such as Campylobacterales, Rhizobiales, and Rhodobacterales. These MAGs orders have been previously reported in diseased loose tissue (Meyer et al., 2019a). Another study conducted by Cárdenas et al. 2022) investigated the prolonged exposure of the endolithic communities of two reef-building corals (*Goniastrea edwardsi* and *Porites lutea*) to thermal stress. Neither coral species showed taxonomic variation between the control and heat-treated subjects within the endolithic microbes. However, a comparison of the two endolithic microbiomes showed that *G. edwardsi* had larger functional diversity than *P. lutea*, especially in carbon fixation pathways (Cárdenas et al., 2022). Nevertheless, *P. lutea* showed higher nitrogen assimilation under stress conditions. Their results suggested that the two endolithic communities might have used different sources of carbon for energy production and metabolic functions under thermal stress (Cárdenas et al., 2022; Sangsawang et al., 2017). These studies provide an example of the application of metagenomics in coral diseases and bleaching investigations.

Meta-transcriptomics identifies the genes that are actively expressed in the microbiome. This technique has provided a significant amount of data in coral research and presents an opportunity to identify crucial pathways in the microbial community to understand their roles in coral ecosystems and their interactions with coral hosts. In coral omics, microarrays and RNA-seq have gained popularity for profiling coral transcriptomes to uncover gene expression patterns related to thermal stress (Cziesielski et al., 2019). By identifying differentially expressed genes (DEGs), researchers can investigate responses to various environmental conditions (Barshis et al., 2013; Hrdlickova et al., 2017) and help advance coral investigations (Y. Zhang et al., 2019). For example, Daniels et al 2015 (Daniels et al., 2015), have explored the stony coral *Orbicella faveolata* holobiont response to white plaque disease (WPD). The transcriptomic analysis of the microbiome indicated an increase in gene expression of heat-shock proteins and metal transporters suggesting the acquisition/transport of metals released from damaged host cells. Also, their results suggested the expression of multiple stress and virulence genes linked to *Alteromonadaceae, Rhodobacteraceae, Flavobacteriaceae, Enterobacteriaceae*, and *Vibrionaceae*, pointing toward an opportunistic nature of these bacteria (Daniels et al., 2015). Although the main causative agents of WPD are still ambiguous (Chimetto Tonon et al., 2017), understanding the functional role of the coral microbiome is crucial for understanding their interactions in the context of expressed genes.

Another study conducted by Avila-Magaña et al. (2021) used metatranscriptomic to investigate the impact of thermal stress on coral holobiont: *Pseudodiploria clivosa*, *Orbicella faveolata* and *Siderastrea radians*. Each coral species hosts a species-specific, symbiotic dinoflagellate. In addition to the differences in some key biological processes in thermally stressed corals, symbiotic algae showed different gene expression in response to thermal stress (Avila-Magaña et al., 2021). Multiple photosynthesis-related genes were differentially expressed, indicating variations in the photodamage and photoinhibition responses. The thermotolerant Breviolum B5 exhibited overexpression of *psbI* and pentatricopeptide repeat-containing protein mrl1 genes, suggesting a strategy focused on PSII core complex stabilization and RuBisCO transcript regulation to withstand higher temperatures without compromising algal photosynthetic capacity (Avila-Magaña et al., 2021; Ikeuchi et al., 1995; Johnson et al., 2010). In contrast, *Symbiodinium* A3 displayed an intermediate ability to sustain photosynthesis under heat stress, prevent chlorophyll breakdown, and maintain the PSII repair rates. This is in contrast with the more sensitive response of *B. faviinorum*. This evidence supports *Breviolum* B5 as a thermotolerant photosymbiont, *Symbiodinium* A3, which exhibits an intermediate response, whereas *B. faviinorum* is more sensitive to heat stress (Avila-Magaña et al., 2021).

Although meta-transcriptomics has only been employed in a limited number of cases, its integration with other meta-omics methodologies can validate gene expression patterns, enable the quantification of their effects, and offer insights into novel metabolic and symbiotic interactions. Mass-spectrometry-based techniques, such as proteomics and metabolomics, have led to groundbreaking discoveries in holobiont research (Mohamed et al., 2023). Metabolomics research has provided new insights into the interactions between coral holobionts (Lohr et al., 2019; Williams et al., 2021a). For instance, platelet activation factors were found to increase at coral-algal interfaces, suggesting their involvement in these interactions (Quinn et al., 2016). Certain lipid classes, such as betaine lipids and diacyl glycerides, have been linked to earlier episodes of coral bleaching and can serve as indicators of disease (Deutsch et al., 2021; Roach et al., 2020). Furthermore, dipeptides have been identified as indicators of heat stress in corals (Williams et al., 2021b). These metabolites consist of various chemical groups and can have a significant impact on the microbiome of the surface mucopolysaccharide layer (SML) (Ochsenkühn et al., 2018). One notable metabolite that has been identified is estrogen, which not only regulates stress responses, but also modifies microbiome composition (Stien et al., 2020; Vilela et al., 2021). Proteomics has been instrumental in examining how both hosts and symbionts respond to heat stress, unveiling novel thermal stress molecular biomarkers like the dipeptides lysine–glutamine and arginine–glutamine (Williams et al., 2021a). However, the absence of standardized coral metabolomics methods, limited chemical reference libraries, and a lack of knowledge of metabolite functions pose major challenges.

One of the issues is the influence of the extraction techniques on the identified compounds. While some metabolites are prone to degradation, others are not efficiently extracted (Andersson et al., 2019; Lu et al., 2020). To overcome some of these limitations, Reddy et al., 2023 enhanced the extraction method by modifying the Matyash lipid extraction method, followed by ^{1}H NMR and LC-MS analysis of the non-polar and polar metabolites (Andersson et al., 2019; Sostare et al., 2018), and the extraction yields were maximized by liquid-liquid partitioning of the freeze-dried material using a biphasic solvent mixture MTBE/MeOH/H_2O. This allows the achievement of a broad, complete metabolic overview of coral holobiont (Reddy et al., 2023). They applied this technique to natural populations of two reef-building coral genera, *Pocillopora* spp. and *Porites* spp., and one hydrocoral, *Millepora* cf. *platyphylla*, from the TARA Pacific expedition (Belser et al., 2023). They identified 24 compounds by NMR, including osmolytes, and over 200 lipids by MS analysis of corals. Although the metabolic profiles varied among coral genera, they remained consistent within the genotypes. Despite the recognized influence of endosymbiotic dinoflagellates (Symbiodiniaceae) on the metabolomic signature of coral holobionts, these dinoflagellates alone did not explain all observed differences. This indicated the collective impact of various coral holobiont members and their interactions with the environment.

1.6. ***Current Limitation of Meta-omics***

The primary objective of coral omics is to identify the fundamental genes and species involved in the response to various stressors and to elucidate the relationship between variations in this response and differences in stress resilience. The vast majority of studies have focused on tropical and subtropical stony corals; however, temperate and cold-water corals need to receive more attention in coral omics studies. Furthermore, despite the advantages of metagenomics, some limitations must be overcome, such as the presence of a significant number of genes with unknown functions, referred to as 'dark genes,' in corals and algae (Cleves, Shumaker, et al., 2020). For example, in dinoflagellates, approximately one-third of the genes are unannotated, and only a small fraction of these uncharacterized proteins have a known domain, which limits our ability to infer their functions and understand the biological processes and pathways in which they are involved (Stephens et al., 2018). Conversely, traditional molecular biology and biochemistry methods for characterizing gene or protein function are time-consuming and lack high-throughput (Mohamed et al., 2023). Utilizing gene networks has demonstrated to identify hypothetical proteins with potential significance, and could offer insights into their importance (Cleves, Tinoco, et al., 2020). In addition, the functionality of these proteins can be explored using methods such as alpha-fold (Ma et al., 2022). Therefore, building a marine gene database that includes corals is required. Recently, a global ocean gene catalog that includes more than 317 million gene groups was released. This open-source database will enhance our knowledge of the diversity and role of different microbes in different marine habitats, including coral microbiome (Laiolo et al., 2024).

Furthermore, meta-transcriptomic techniques are potentially powerful; however, several challenges hinder their widespread use. One major hurdle is the high concentration of rRNA in the collected RNA samples, leading to a significant reduction in the quantity of mRNA, which is the main focus of transcriptomic research. Efforts have been made to address this issue by removing ribosomal RNA efficiently (Peano et al., 2013). Another challenge is the instability of mRNA, which is a well-known problem that can affect sample integrity before sequencing (Aguiar-Pulido et al., 2016). Moreover, distinguishing between host and microbial RNA remains challenging, despite the availability of various enrichment kits. Computational methods can be employed if the host's reference genome is accessible, as demonstrated by Pérez-Losada et al. (Pérez-Losada et al., 2015) in their research on the human airway microbiome and host-pathogen interactions.

Finally, a limitation arises from the restricted coverage of transcriptome reference databases. Although metabolomics is a promising field with lower costs than sequencing, it has several limitations (Lu et al., 2020). This has been difficult to improve because of major hurdles in identifying metabolites with low abundance and many hidden metabolites usually found in biological processes (Vohsen et al., 2019). The complexity of chemical formulae and structures poses the biggest challenge in mass spectrometry-based metabolomics, where annotations can only be reliably confirmed with comparisons to known standards (Mohamed et al., 2023). Connecting metabolites with their corresponding generating organisms is a key challenge in studying holobionts. Although statistical correlation of metabolite and amplicon sequencing data can help with this endeavor (Jorissen et al., 2021), it is only useful for identifying distinct secondary metabolites. Another key challenge is determining whether a metabolite is produced by the host or the microbiome, making their identification and assignment to specific organisms more difficult. Metabolomic results must be combined with other omics data to determine the association between specific genes, enzymes, or pathways with a particular metabolite. Therefore, new approaches that deal with integrated omics are required to address these challenges (Aguiar-Pulido et al., 2016).

1.7. ***Thesis Objectives***

This thesis aims to enhance the current knowledge of the coral microbiome in the context of environmental change and the potential influence of these changes on the coral microbiome and, therefore, their health and resilience. To have a comprehensive view of the topic, we have reviewed coral biology, coral microbiome, and advanced technology that has improved our understanding of the coral microbiome. In addition, we reviewed the main biotic and abiotic factors that could potentially influence the stability and resilience of the corals and their microbiome. Also, we discussed the current advances in the coral microbiome studies and current limitations which give a better view of the current gaps and remaining unknown aspects.

Through reviewing the coral microbiome, we have noticed that there are limited studies that have used primerless, deep shotgun metagenome sequencing to determine the influence of environmental gradients (i.e., depth) on octocoral, specifically, gorgonian corals. Interestingly, the gorgonian coral *Eunicella Singularis* is the only symbiotic gorgonian in the Mediterranean and can live with (in shallow depths) and without (in mesophotic depths) Symbiodinium. This makes it important to understand the dynamics of microbiome functions between symbiotic and asymbiotic communities. Therefore, we investigated the effects of depth on the diversity and function of *Eunicella singularis* microbiomes to address this gap by, specifically, analyzing microbiomes from both shallow (12 m) and mesophotic (57 m) environments using deep-sequencing metagenomics. Our study sought to answer the following questions regarding the microbiome of *Eunicella singularis*:

(i) Does the composition of dominant species vary with depth?
(ii) Are there potential functional differences in the microbiomes at different depths?

(iii) What are the likely functional roles of the main members of the microbiome at various depths?

As climate change threatens ocean life, especially, corals, the study of the elevated temperature is crucial. While many investigations have focused on the tropical and subtropical corals, less attention has been given to the cold water coral species. Therefore, we will study the impact of prolonged elevated water temperature on the microbiome of the cold-water coral, the hexocorallia scleractinian *Desmophyllum Pertusum*. To accomplish this, a 60-day controlled laboratory experiment was conducted in which coral samples were exposed to three different thermal conditions: 10°C (control temperature), 13°C, and 15°C. To conduct a comprehensive metagenomic analysis of the microbiome response to temperature increases, two coral colonies were collected from each temperature treatment at the beginning (day 1) and end (day 60) of the study. Given the anticipated abundance of Rhodobacterales, our hypothesis suggests that rising temperatures will:

(i) impact the microbiome's taxonomic and functional structure
(ii) Drive bacterial assemblages towards increased prevalence of opportunistic pathogenic bacteria.
(iii) Disruptions in the microbial nitrogen cycle will lead to increased abundance and activity of denitrification genes and associated microbes.

2. MATERIALS AND METHODS

In this thesis, two separate projects were conducted to achieve the objectives of this study. The first project investigation aimed to survey whether the water depth influences the taxonomical and functional structure of the temperate water soft coral *Eunicella singularis*. The second project aimed to study the impact of thermal stress on the cold water scleractinian coral *Desmophyllum pertusum*. Each project has different sampling methods and experimental setups (Figure 6). However, both investigations shared the same bioinformatics and downstream data analysis. This section will describe first the sampling process and DNA extraction of each experiment, then, the bioinformatics analysis.

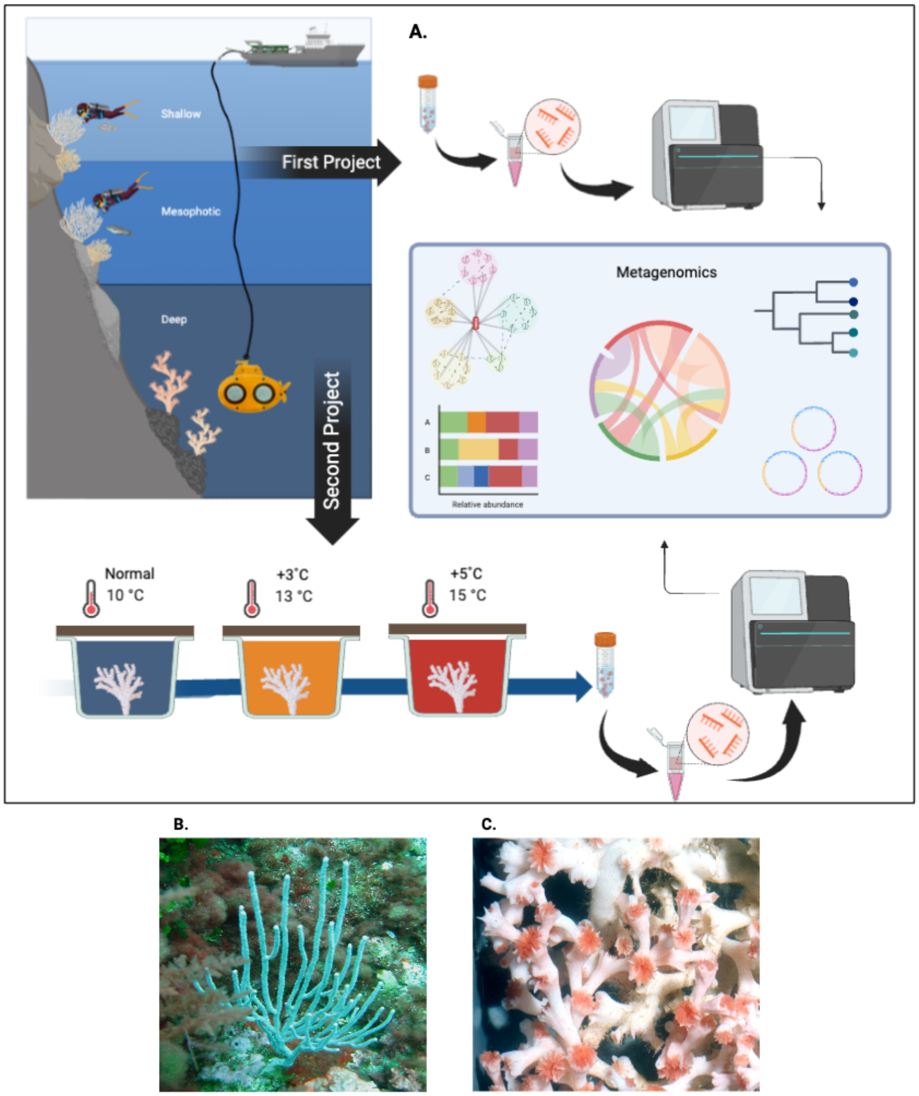

Figure 6: A. The research approach. The targeted coral species **B.** *Euncilla pingularis* (picture by: Matthieu Sontag) and **C.** *Desmophyllum Pertusum* (picture by: Alan J. Southward)

2.1. *Coral specimen collection DNA Extraction and Library Construction*

2.1.1. *Eunicella singularis*

Samples were collected from the Banyuls Sur Mer coast – South of France – by scuba diving at different depths (shallow: 12 meters, and mesophotic: 57 meters) in December 2020. Branches (10-15 cm each) of 10 Mediterranean *Eunicella singularis* colonies were sampled (5 shallow; E_12m_1 to E_12m_5, and 5 mesophotic; E_57m_1 to E_57m_5). DNA extraction was done with the Zymo DNA kit following the standard protocol. The extracted DNA was shotgun sequenced using *Illumina*, aiming for a high coverage per sample (Novaseq 2*150 bp, > 80 Gb/sample). Sequencing was done at Macrogen in Korea. The high sequencing depth aims to obtain more information about the microbiome, as we expect that most of the reads will come from the coral. Sequences have been deposited at the European Nucleotide Archive (ENA; https://www.ebi.ac.uk/ena) under the accession number PRJEB61841.

2.1.2. *Desmophyllum pertusum*

Five colonies of *Desmophyllum pertusum* were collected at a depth of 800 m in the Lampaul canyon of the Bay of Biscay, North-east Atlantic Ocean (N.47°36.703, W07°32.192) during the ChEReef research cruise in August 2021. These colonies were obtained using the remotely operated vehicle (ROV) Ariane from the R/V Thalassa and were maintained in oxygenated seawater at a temperature of 10°C using a cooling unit (ICE400, Aquavie, Connaux, France). After transportation to the laboratory (Banyuls Oceanological Observatory), the corals were acclimated to laboratory conditions for 5 months in aerated 80 L tanks, supplied with filtered (5 µm) seawater pumped from 10 m depth and fed three times a week with *Artemia salina* nauplii and marine snow plankton diet. Following this acclimatization period, the *D. pertusum* colonies were cut into nubbins containing 3-13 living polyps, glued onto PVC blocks using an aquatic epoxy resin (Hold Fast Sand, Aquarium System, Sarrebourg, France), and transferred to experimental tanks.

To examine the effects of warming on the *D. pertusum* coral holobiont, colonies were exposed to three distinct temperature conditions (10, 13, and 15°C) for 60 days. The temperature of 10°C served as the control, representing the *in situ* temperature, while 13°C (+3°C increase) represented the *in situ* temperature in the Mediterranean Sea. Furthermore, 15°C (+5°C) represented a severe warming scenario, approaching the presumed upper thermal tolerance limit for this species (Brooke et al., 2013). The experimental procedures adhered to the protocol outlined in (Chapron et al., 2021). A total of 22 to 24 nubbins were randomly allocated to each of the three 36L experimental tanks, ensuring sufficient spacing between nubbins to prevent any contact between different colonies and polyps (Orejas et al., 2019). Each experimental condition consisted of four distinct colonies. For metagenomic analysis, two nubbins were selected at each sampling time to conduct microbiome analyses.

Each experimental tank was equipped with a small water pump (NJ400, Newa Jet, Loreggia, Italy) to maintain a constant flow rate of 3 cm s−1 and facilitate water mixing. To ensure stable temperature regulation, each coral tank was placed within a larger water bath tank. Additionally, a temperature probe connected to a temperature controller (Biotherm Eco, Hobby Aquaristik, Gelsdor, Germany, precise at 0.1°C) was installed in each coral tank, along with a cooling unit (ICE400, Aquavie, Connaux, France) in the water bath. The temperature in each tank was autonomously monitored every 30 minutes using an IBUTTON probe and manually checked twice a day using a digital thermometer (Checktemp thermometer, Hanna Instrument, Woonsocket, USA). The pH, oxygen concentrations, and salinity were measured manually twice a week using probes (C3010 Multi-parameter analyzers, Consort). Before temperature changes, the nubbins were acclimated for two weeks in the experimental aquaria. Subsequently, the water temperature in the experimental tanks was gradually adjusted over 10 days until the desired temperatures were reached, following the protocol outlined by Naumann et al.

(Naumann et al., 2014). Throughout the entire experiment, the feeding routine was consistently maintained.

For the extraction of DNA, individual polyps, encompassing the skeleton, tissues, and mucus, underwent initial crushing with a sterile hammer. Subsequently, they were ground in tubes containing a garnet matrix and mechanically lysed using a FastPrep Instrument (MP, Biomedical, Illkirch-Graffenstaden, France). DNA extraction followed the manufacturer's instructions using the Maxwell Blood DNA Purification Kit LEV and the Maxwell 16 MDx Instrument (Promega, Madison, WI, United States). Next, Illumina shotgun sequencing was carried out to achieve a high coverage per sample (Novaseq 2*150 bp, > 80 Gb/sample) at Macrogen in Korea. The primary goal of this sequencing approach was to gather additional insights into the microbiome, with the anticipation that the coral would account for the majority of the reads. The sequences have been submitted to ENA and can be accessed using the accession number PRJEB68224.

2.2. ***Bioinformatic analyses***

The bioinformatics analysis is mainly composed of three main streams: Taxonomic classification, Gene-Centric, and Genome Centric (Figure 7). The taxonomic classification includes the extraction of the SSU rRNA and mapping it against reference databases. The gene-centric analysis focuses on the functional and taxonomic annotation of the genes from the community, which gives an overview of the metabolic pathways that are present in the microbiome and the taxa contributing to them. Lastly, the genome-centric analysis allows the reconstruction of genomes from metagenomic samples.

2.2.1. *Read quality check, trimming, and taxonomic profiling*

Read quality checks and adapter removal were performed using Cutadapt [v1.16] (Martin, 2011) (minimum length =75, quality cutoff = 20, nextseq-trim = 20, max-n= 0) (Martin, 2011). The taxonomic diversity in metagenomes was determined using mTAGs, a bioinformatic tool that performs taxonomic annotation of metagenomic reads that belong to the ribosomal RNA, using a 97% similarity threshold to assign reads to Operational Taxonomic Units (OTUs) (Salazar et al., 2021b). Different databases have been used to assign taxonomy, such as SILVA [SILVA-128] for prokaryotic and eukaryotic reads (Quast et al., 2012) and the PR2 (Protist Ribosomal Reference) database [4.14.0] (Guillou et al., 2012) for protist reads. For protists - to increase accuracy - the initial step involved extracting the V4 region from mTAGs and aligning the reads against a specifically curated in-house eukaryotic V4 database (Obiol, 2020). This database was implemented to enhance the precision of protistan mTAGs' classifications (Obiol et al., 2020). SeqKit [v0.16.0] was used to extract sequences, and the eukaryotic mTAGs were then aligned against the PR2 database using USEARCH [v.9.2.64] (Edgar, 2010) (id = 0.97, mincols = 105, strand = both, top_hits_only, -maxaccepts = 0, maxrejects = 0).

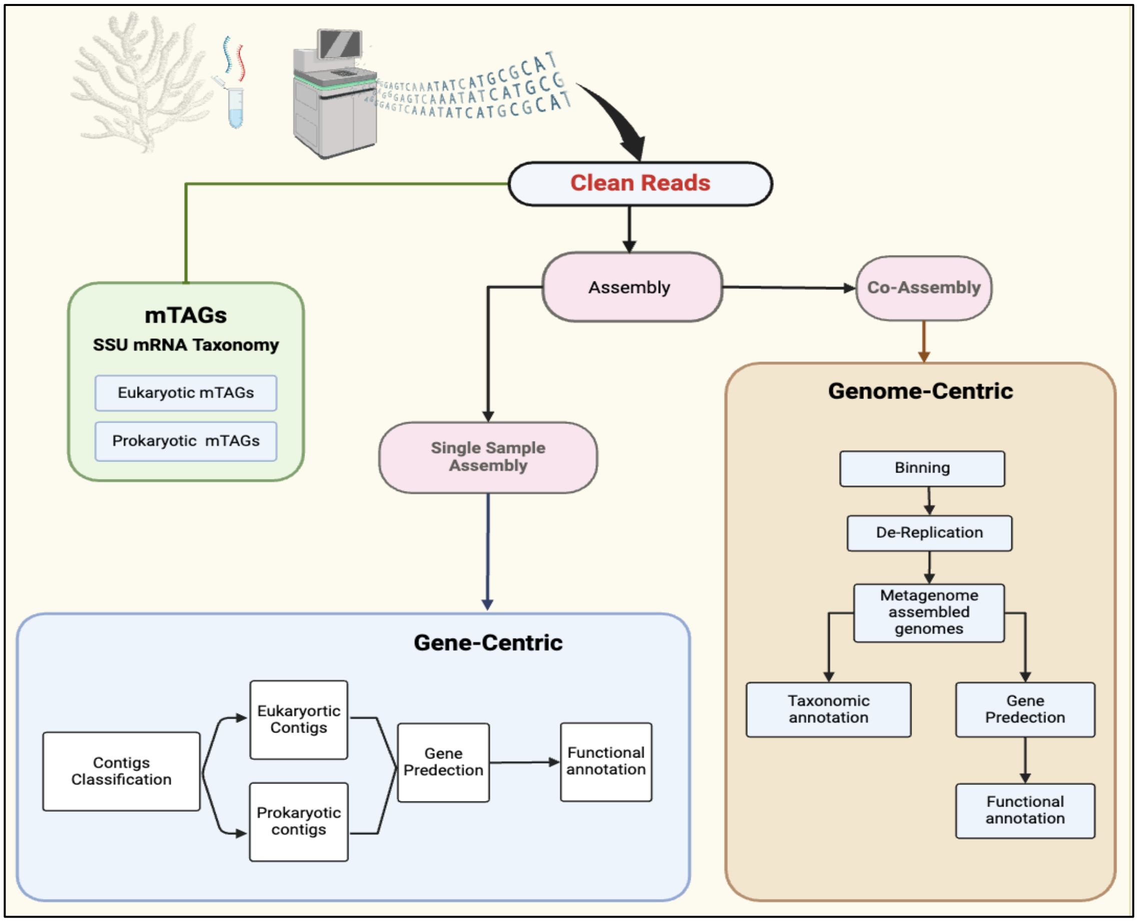

Figure 7: The main pathways of metagenomic reads processing

2.2.2. Assembly, gene catalog construction, and annotation

The single sample assemblies of the clean metagenomic reads were performed using MEGAHIT [v1.2.8], a fast de novo assembler for large and complex metagenomics data sets (D. Li et al., 2015a), using a *meta-large* preset. Prokaryotic and eukaryotic contigs were identified and separated with EukRep [v0.6.5] (West et al., 2018), using a minimum contig size of 2000 bp. Eukaryotic exons (hereafter, "genes") were predicted on eukaryotic contigs with MetaEuk [v1-ea903e5] (Levy Karin et al., 2020), using the following parameters: metaeuk-val= 0.0001, metaeuk-tcov= 0.6, maximal E-Value= 100, min-length= 40, min-exon-aa= 20. In turn, prokaryotic Open Reading Frames (ORFs; hereafter "genes") were predicted on prokaryotic contigs with MetaGeneMark [v3.38] (Zhu et al., 2010) and Prodigal [v2.6.3] (Hyatt et al., 2010). MetaGeneMark predicted both partial and complete genes, while Prodigal predicted only complete genes. Only genes ≥ 250 bp were included in the downstream analyses. Prokaryotic and eukaryotic genes from the different samples were pooled separately, and redundancy was removed by clustering them at 95% identity and 80% alignment coverage of the shorter fragment using 'linclust' (Steinegger & Söding, 2017a), from MMseqs2 [v.9-d36de] (Steinegger & Söding, 2017b).

The taxonomic annotation of prokaryotic genes was performed with the taxonomy module from MMseqs2 using the Genome Taxonomy DataBase (GTDB) [v89] (Parks et al., 2020). The eukaryotic genes were taxonomically classified with the 'taxonomy' module from MMseq2s [v11-e1a1c] using EukProt [v2], a database of genome-scale predicted proteins from various eukaryotes, including Cnidaria (Richter et al., 2022). Predicted genes were functionally annotated using Diamond [v0.9.22] (Buchfink et al., 2015), with a maximum expected value of 0.1, against the KEGG (Kyoto Encyclopedia of Genes and Genomes) database [v2019-02-11] (Kanehisa, 2019). Then, KEGG gene hits were linked to KEGG KOs with an in-house script. This linked the KEGG gene hits with their KEGG KO numbers using the file `ko_genes-sorted-by-gene.list` located in the KEGG public database path in the cluster MARBITS.

Metagenome reads were back-mapped to the catalogues using the BWA aligner [v0.7.17] (H. Li & Durbin, 2009) , unmapped reads were discarded and we considered a mapping quality threshold of 10. The number of aligned counts per gene was obtained using HTSeq [v0.13.5](Anders et al., 2015) (max-reads-in-buffer= 10^{11}, stranded = no, nonunique = all). Read counts per gene were normalized by gene length and the geometric mean abundance of 10 selected single-copy genes in each sample for prokaryotes (Salazar et al., 2019) or metagenome size in gigabases for microbial eukaryotes. Normalized gene abundance tables were generated, including the abundance of each gene in each sample. The corresponding functional abundance tables were generated by adding all normalized abundances of all genes annotated to a specific KEGG function. In addition, Diting [v0.9], (Xue et al., 2021), was used to investigate the relative abundance of metabolic and biogeochemical functional pathways in the prokaryotic community.

2.2.3. Metagenome Assembled Genomes (MAGs) construction and annotation

Metagenomes were co-assembled using MEGAHIT [v1.2.8] (D. Li et al., 2015b). Then, clean reads were mapped against the co-assembled contigs using BWA [v0.7.17] (H. Li & Durbin, 2009) to obtain contig abundance. Co-assemblies were binned using three binning programs: MetaBAT [v2.12.1] [55] (minContig = 2500), MaxBin [v2.2.5] (Y.-W. Wu et al., 2014) (min_contig_lenght = 2500, max_iteration = 50, prob_threshold = 0.9), and CONCOCT [v0.4.2] (Alneberg et al., 2013) (Length_threshold = 2500, clusters = 400) considering contigs with >2500 bp length. The three pools of bins were co-refined using Metawrap [v1.3-4bf5f8a], (Uritskiy et al., 2018), considering genome completeness of >50% and contamination of <10%. Furthermore, COMEbin [v1.0.4] (Wang et al., 2024), was used as an additional binner algorithm with the default parameters. The constructed bins were dereplicated to select the best representative genomes, hereafter MAGs, using dRep [v2.3.2] (Olm et al., 2017), with specific parameters: an Average Nucleotide Identity (ANI) threshold of 90% for the creation of primary clusters utilizing MASH and an ANI threshold of 99% for the formation of secondary clusters.

The quality of the constructed MAGs was assessed using both CheckM and CheckM2. CheckM (Parks et al., 2015) is a bioinformatics tool for assessing the quality of genomes recovered from isolates, single cells, or metagenomes. It provides robust estimates of genome completeness and contamination by using collocated sets of genes that are ubiquitous and single-copy within a phylogenetic lineage. In contrast, CheckM2 (Chklovski et al., 2024) is a bioinformatics tool that assesses bin quality using machine learning. It employs two distinct machine-learning models to predict genome completeness. The 'general' gradient boost model demonstrates a commendable ability to generalize and is specifically designed for application on organisms that are not adequately represented in GenBank or RefSeq. On the other hand, the 'specific' neural network model exhibits greater accuracy in predicting completeness for organisms that are closely related to the reference training set. CheckM2 utilizes a cosine similarity calculation to automatically determine the most suitable completeness model for each input genome. CoverM (Woodcroft et al., n.d.) was used to calculate the relative abundance of the MAGs by backmapping reads.

CompareM was used to compare the differences between genomes. The taxonomic classification of MAGs was performed using GTDB-Tk [v1.5] (Chaumeil et al., 2020). Prokka [v1.14.6] (Seemann, 2014), was used for the functional annotation of MAGs. EnrichM [v0.5.0] (Joel A Boyd, 2019) (DB = enrichm_database_v10, cutoff = 0.5), was used to identify and quantify enriched genes and pathways in metagenomic samples. Also, to investigate the KEGG functional modules' completion in MAGs. In addition, METABOLIC, a program that predicts metabolic and biogeochemical functional features from multiple genomic datasets, was used to reconstruct metabolic pathways and generate detailed diagrams of biogeochemical cycle pathways (including nitrogen, carbon, sulfur, and other elements). This allowed for a thorough analysis of the metabolic capabilities and environmental interactions of the microbial communities under study. Bioinformatics analyses were performed at the Marine Bioinformatics Service

(MARBITS; https://marbits.icm.csic.es) of the Institute of Marine Sciences (ICM-CSIC) in Barcelona.

*2.3. **Statistical analysis***

All analyses and visualizations were conducted using the statistical computing environment 'R' (4.3.1). The data and tables were processed using 'Tidyverse' (Wickham et al., 2019). We calculated the average abundance of data tables (mTAGs) to obtain a representative measure of the microbial taxa present. We applied a 0.05 percentile threshold (P5) to focus on the most significant data, filtering out the lowest 5% of values. This threshold was chosen to exclude the least abundant and potentially less relevant taxa, thereby reducing noise and improving the clarity of subsequent analyses. After filtering, the mTAGs data were normalized to standardize the dataset, ensuring that variations due to differences in sequencing depth or sample size were minimized. This normalization step helped enhance the comparability of the data, allowing us to identify and analyze the most relevant and abundant taxa more accurately. The normalization process included calculating the sum of the counts of all filtered mTAGs across the samples. Subsequently, the counts of mTAGs were divided by the corresponding sum of all counts to obtain normalized data for further analysis. Relative abundance was calculated using the function 'make_relative' from the package 'Funrar' (Grenié et al., 2017). Moreover, Niche breadth was applied to assess the microbial niche breadth using the 'MicroNiche' package (Finn et al., 2020). Niche breadth is a concept in ecology that describes the range of ecological or environmental conditions that a species can tolerate or exploit. More specifically, niche breadth refers to the range of resources that a species can use, such as food sources, habitats, or environmental conditions, and how specialized or generalized a species is in its resource use. Species with a narrow niche breadth are specialized and can only survive under specific ecological or environmental conditions, while species with a broad niche breadth are generalists and can tolerate a wider range of conditions (Finn et al., 2020).

Ecological statistical analyses were performed using the R packages ‘Vegan' (Oksanen et al., 2022), and 'Ecodist' (Goslee & Urban, 2007). The Bray-Curtis dissimilarity index was employed to quantify differences between samples based on their gene composition, mTAGs (metatranscriptomic assigned genes), and functional gene profiles. This index measures the compositional dissimilarity between samples by considering the presence and abundance of various features. Using the Bray-Curtis dissimilarity matrix, we performed principal coordinate analysis (PCoA) to visualize the relationships and differences among the samples in a reduced-dimensional space. PCoA helps identify patterns and clustering of samples based on their genetic and functional characteristics. To statistically test for significant differences in the Bray-Curtis dissimilarity matrix between sample categories (e.g., different depths or environmental conditions), we conducted permutational multivariate analyses of variance (PERMANOVAs) with 999 permutations. PERMANOVA is a robust method that assesses whether the observed dissimilarities between groups are greater than would be expected by chance, providing a p-value to indicate the significance of the differences. By using 999 permutations, we ensured a rigorous and reliable assessment of the overall differences between sample categories.

Diversity was estimated using the Shannon index, and community richness was estimated using the Chao1 index. The Shannon index considers both the number of species present and their relative abundance. The Chao1 index estimates the overall number of species found in a specific environment or community. It uses the number of singletons (species represented by a single individual or sequence) and doubletons (species represented by two individuals or sequences) observations to estimate the total number of species in a community. The Chao1 estimator assumes that rare species are more likely to be missed during sampling than abundant species and uses this information to make predictions about the number of species that are not observed. In addition, a t-test and Wilcoxon rank-sum test were used to analyze the statistical differences between the two variable points, and the Kruskal–Wallis (K–W) test was used to test possible statistical differences between the three variable points.

To further examine and visualize the abundance of MAGs, the R package 'metacoder' (Foster et al., 2017) was used to visualize, calculate, and compare differences between time point groups. The Log2 median ratio and Wilcoxon Rank-Sum test were used to assess the significance of these differences, and the Kruskal–Wallis (K–W) test was used to test possible statistical differences between the three thermal conditions. The coefficient of variation (CV), a statistical measure of the relative variability of data points in a dataset, each MAG was used to identify the most varied MAGs based on the highest corresponding CV values. It calculates the ratio of the standard deviation to the mean and allows for the comparison of variability between datasets. The low CV suggests low variability relative to the mean and the high CV suggests high variability relative to the mean

To determine the functional genes (KO's) that contributed most to the dissimilarity of the different microbiomes in both investigations, similarity percentage analysis (SIMPER) and differential abundance analysis were performed on KEGG abundances. SIMPER assesses the most differentiating KO's among groups of samples based on a ranked dissimilarity matrix, calculated, in this case, using the Bray-Curtis index. The enrichment of KEGG pathways and modules of the identified KO's based on SIMPER were analyzed using the R package 'clusterProfiler' (G. Yu et al., 2012). The differential abundance analysis for the identified KEGG genes was conducted using the 'lmFit' and 'eBayes' functions from the 'limma' package (Ritchie et al., 2015). This analysis involves comparing the abundance of features, such as genes, across different sample groups to identify significant differences. The 'lmFit' was applied to fit a linear model to the gene abundance data, incorporating potential covariates or experimental factors. Subsequently, the 'eBayes' function was utilized to compute moderated statistics, facilitating the identification of differentially abundant genes across different sample groups or conditions. Lastly, all results were visualized using 'ggplot2' (Wickham, 2016) and 'circlize' (Gu et al., 2014).

3. __RESULTS__

3.1. Gorgonian Eunicella singularis Microbiome analysis

The Gorgonian corals of the Mediterranean sublittoral ecosystems play a vital role in maintaining ecological balance, with disturbances potentially affecting the entire benthic ecosystem (Ezzat et al., 2013). Their presence facilitates numerous biochemical interactions and influences a diverse array of organisms across various water depths, ranging from continental shelves to deep-sea environments (van de Water et al., 2017). Among these corals*, Eunicella singularis,* also known as sea whip*,* is an octocoral photophilic species. It typically inhabits horizontal or sub-horizontal substrates and is found within a depth range of 10–70 m across the Western Mediterranean, Adriatic, and Aegean seas (Ghanem et al., 2018; Gori et al., 2011). Notably, *E. singularis* is unique as the sole Mediterranean gorgonian specimen known to harbor symbiotic *Symbiodinium* dinoflagellates. This symbiotic relationship supplies coral with energy through photosynthesis-driven metabolites and aids in the absorption of dissolved nutrients, enabling coral growth in shallow nutrient-poor environments (Pernice & Levy, 2014). In return, coral provides *Symbiodinium* with phosphorus, inorganic nitrogen, inorganic carbon, and habitat (Asgari, 2014).

Shallow colonies (approximately 10m in depth) of *E. singularis* can establish a symbiotic relationship with *Symbiodinium*, which contributes to the coral's energy demand (Gori, Viladrich, et al., 2012) and fulfills respiratory requirements through symbiont photosynthesis (Ezzat et al., 2013; Schubert et al., 2016). However, with increasing depth, the population density of *Symbiodinium* decreases, along with reduced chlorophyll levels (Forcioli et al., 2011), and it is completely absent in mesophotic colonies (Gori, Bramanti, et al., 2012). This disparity in *Symbiodinium* abundance highlights the importance of autotrophic processes in meeting the energy needs of shallow colonies, thereby significantly contributing to their ecological success by maximizing nutrient acquisition (Schubert et al., 2016). In contrast, in deeper areas, *E. Singularis* relies more on heterotrophy than autotrophy to meet its energy demands (Schubert et al., 2016).

While *Symbiodinium* dinoflagellates play a crucial role in coral symbiosis, other members of the microbiome, particularly coral-associated prokaryotes, also contribute significantly to coral health and fitness (Bordenstein & Theis, 2015). The coral associated bacteria are distinct from those in surrounding seawater (Bayer, Neave, et al., 2013; Bourne & Munn, 2005; van de Water, Allemand, et al., 2018). Investigations of different coral species have highlighted species-specific core bacteria (*i.e.,* bacteria that tend to be present in the microbiome of all coral colonies). Indeed, *Eunicella* spp. have shown signs of phylosymbiosis with Sphingomonadales (Keller-Costa et al., 2016) and Poribacteria (Keller-Costa et al., 2021). However, it is assumed that environmental gradients in water conditions, such as light, nutrient concentrations, and temperature, exert a notable influence on coral microbial communities (Keller-Costa et al., 2017, 2021). Numerous investigations have examined the impact of these stressors on the microbiome of *Eunicella.* For instance, a survey conducted using metabarcoding targeting the 16s rRNA gene on *Eunicella singularis* at a depth of approximately 35 m revealed that the core microbiome is primarily composed of the bacterium *Endozoicomonas*. The microbiome also contains diverse bacterial populations, including Burkholderiales, Mycoplasmatales, Spirochaetales, and Vibrionales (van de Water et al., 2017). Bayer *et al.* (Bayer, Arif, et al., 2013) delved into the microbiome of *Eunicella cavolini* at 24, 30, and 41m depth. They consistently observed the dominance of *Endozoicomonas* across all depths, accompanied by depth-correlated variations in *Aquimarina* and Myxococcales (Bayer, Arif, et al., 2013).

Another study on *Eunicella verrucosa* investigated the impact of depth within a range of 6–27 m (Ransome et al., 2014). Denaturing gradient gel electrophoresis (DGGE) and clone libraries revealed the prevalence of Gammaproteobacteria, particularly within the genus *Endozoicomonas*, across various depths. Significantly, the shallow samples (6-9 m) displayed a bacterial community that was less similar and more diverse than that of the mesophotic samples (Ransome et al., 2014). Rivière *et al.* (La Rivière et al., 2015) investigated the impact of seasonality, specifically summer and winter, on the bacterial community of *E. singularis* using terminal restriction fragment length polymorphism (T-RFLP) of the 16S rRNA gene. Despite finding no significant disparities in the bacterial community between summer and winter, the analysis of 165 clones from *E. singularis* revealed a predominance of Gamma-proteobacteria associated with the *Hahellaceae* family within the order Oceanospirillales (La Rivière et al., 2015).

Previous research has proposed that factors such as the physiology and fitness of the coral host are associated with the diversity and metabolic functions of microorganisms. Associated microbes have been proposed to provide many beneficial services to their hosts, such as nitrogen, carbon, sulfur fixation, and antibiotic production(van de Water, Allemand, et al., 2018). However, most octocoral studies have primarily focused on changes in microbiome taxonomic diversity, with limited exploration of how environmental changes affect the metabolic capacity, leaving significant gaps in our knowledge (Keller-Costa et al., 2021, 2022). Keller-Costa et al. (2021) conducted a pioneering study utilizing shotgun metagenome sequencing to explore the taxonomic, functional, and secondary metabolism characteristics of prokaryotic communities in octocorals. Their comparative analysis of healthy, necrotic octocorals, seawater, and sediment metagenomes revealed variations in the microbiome composition across different sampling groups. Specifically, they observed an increase in the abundance of *Flavobacteriaceae* and *Alphaproteobacteria* in the necrotic *E. gazella* microbiome. In turn, healthy corals exhibited a prevalence of eukaryotic-like proteins (ELPs), suggesting mechanisms for host-symbiont recognition and stable partnerships within octocorals. ELPs are believed to facilitate communication and mutualistic interactions between the coral host and its symbiotic organisms. For example, symbiotic microbes harbor ELPs to interact with the coral host and establish symbiosis without eliciting the host's immune response. By recognizing specific molecular signatures on these symbionts, ELPs enable corals to differentiate between beneficial and potentially harmful organisms (Pushpakumara et al., 2023). Conversely, the necrotic microbial community showed an increase in pathogenic features such as nitric oxide reductase and type VI secretion system genes, facilitating host invasion, virulence, and immune system attack.

3.1.1. Metagenomes and gene composition

In total, 430.6 Gb of sequencing data were obtained for the 10 *Eunicella Singularis* metagenomes (approximately 3×10^8 short reads per sample). The single-sample assemblies generated ca. 17.6×10^6 contigs for all samples. We identified 12.3×10^6 eukaryotic (70%) and 5.2×10^6 prokaryotic contigs (30%). The number of eukaryotes and prokaryotic contigs was higher in the shallow samples. However, the average eukaryotic contig size in shallow samples was larger than that in mesophotic samples. In contrast, the mesophotic samples' average prokaryotic contig size was larger than that in the shallow samples (Supplementary Figure 1; Supplementary Table 1).

After removing the predicted genes assigned to Anthozoa, the Principal Coordinates Analysis (PCoA) of the eukaryotic genes (n= 266741) indicated a significant impact of depth on gene composition (Figure 8A) (PERMANOVA, $R^2 = 0.6$, $p = 0.007$). The shallow samples had a higher mean gene diversity (Shannon index = 12.0; SD = 0.03) than the mesophotic samples (10.7; SD = 0.04) [*t*-test *p*-value = 9.66 e-11] (Figure 8B). In addition, the shallow samples showed a higher mean Chao1 richness (196679, SD = 2059) than the mesophotic samples (82850, SD = 1894) [*t*-test *p*-value = 2.81e-13] (Figure 8C). Depth also influenced the prokaryotic gene composition (PERMANOVA, $R^2 = 0.63$, $p = 0.009$) (Figure 8A). The shallow samples had a higher average prokaryotic gene diversity (Shannon index, 13.0; SD = 0.03) than the mesophotic samples (12.3; SD = 0.04) [*t*-test *p*-value = 6.29e-06] (Figure 8B). The shallow samples had a higher average Chao1 gene richness (545776.8, SD = 10554) compared to the mesophotic samples (332615.6, SD = 7042) [*t*-test *p*-value = 2.6-e9] (Figure 8C).

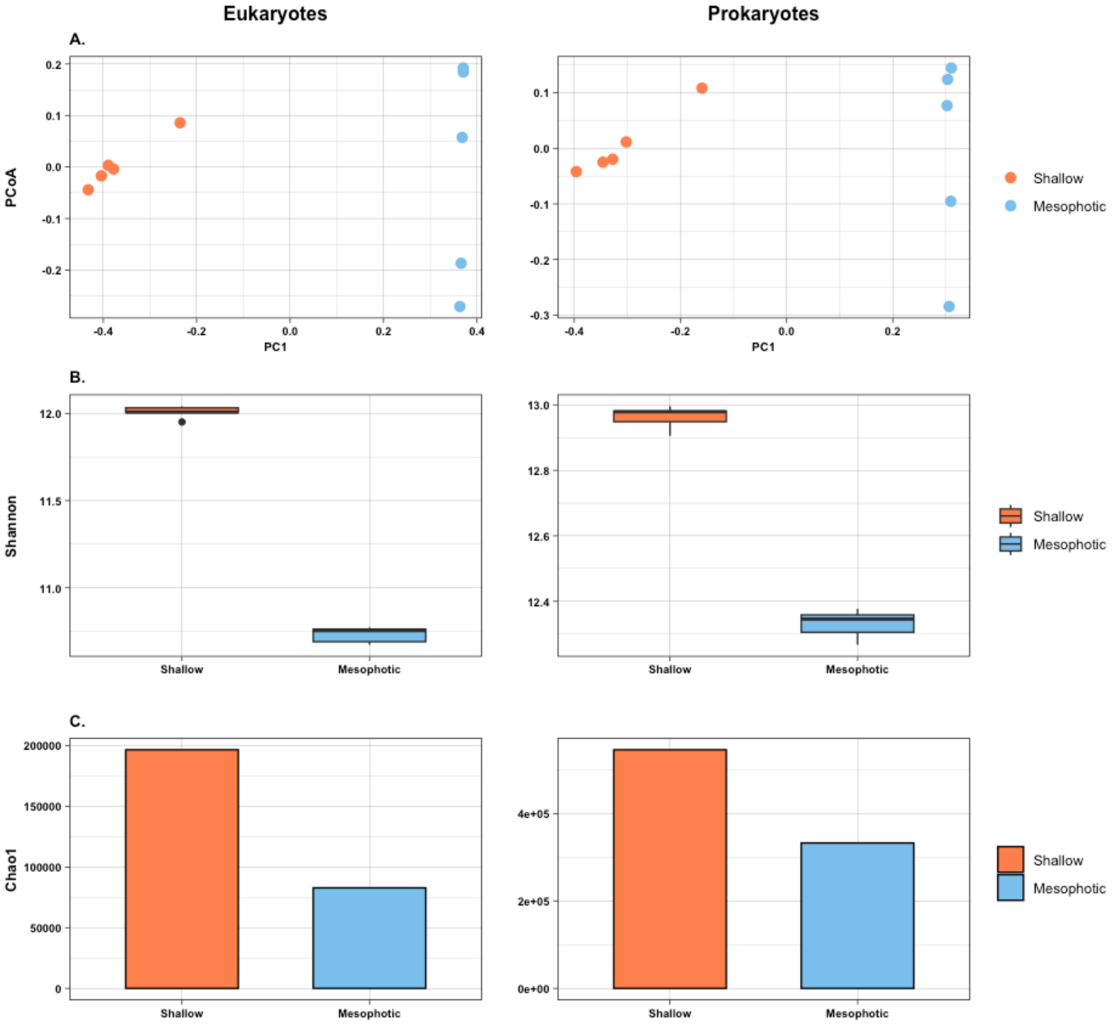

Figure 8. Effects of depth on the gene composition of *the Eunicella singularis* microbiome**. A**. PCoA ordination based on Bray-Curtis of eukaryotic and prokaryotic gene compositions. **B.** Box plot showing eukaryotic and prokaryotic gene diversity (Shannon index). **C.** Eukaryotic and prokaryotic gene richness estimates (Choa1).

3.1.2. Taxonomic composition of the coral microbiome

The mTAG analysis (rRNA SSU metagenomic fragments) yielded 1,924,784 mTAGs. These reads consisted of 27% Opisthokonta (mostly coral), 15% prokaryotes, 2% alveolates, and 1% other microeukaryotes, with the remaining 38% being unaligned or unassigned mTAGs. We excluded mTAGs identified as Cnidarian, unaligned, or unassigned from the downstream analysis. The PCoA results indicated clusters of samples corresponding to the two depths, indicating clear differences in coral microbiome composition between the shallow and mesophotic samples (PERMANOVA, $R^2 = 0.57$, $p = 0.008$) (Figure 9A). The shallow samples had higher microbial mTAGs richness and diversity (Chao1 $\mu = 162$; Shannon $\mu = 4.72$) than the mesophotic samples (Chao1 $\mu = 94$; Shannon $\mu = 4.18$) [Chao1 $p = 0.0007$; Shannon $p = 0.005$] (Figure 9B, C).

The curated taxonomic annotation revealed that the gorgonian microbiomes were composed of six main microbial phyla, including one eukaryotic (Dinoflagellata) and five prokaryotic phyla. Among the microbial eukaryotes, 33,279 mTAGs were taxonomically identified, as Dinoflagellates comprising ~ 99% of eukaryotic mTAGs. Among the dinoflagellates, the dominant genus was *Symbiodinium*. Moreover, the prokaryotic community was comprised of four bacterial classes: Alphaproteobacteria, Gammaproteobacteria, Bacilli, and Bacteroidia. Among the bacteria, the prevailing genus at both depths was *Endozoicomonas*, encompassing approximately 97% of the overall prokaryotic mTAGs, followed by the genus *Bermanella*, constituting approximately 2% of the sequences. Notably, although most prokaryotic communities were dominated by these two genera, approximately 1% of the bacterial mTAGs belonged to additional taxonomic groups. They encompassed the BD1-7 clade, *Sphingomonas*, *Mycoplasma*, *Thalassolituus*, *Halioglobus*, *Spiroplasma*, and *Aquimarina* (Figure 10A, Supplementary Table 2).

Furthermore, we analyzed the niche breadth of these microbial taxa across shallow vs. mesophotic samples using Levins' approach (Finn et al., 2020). Taxa distributed across habitats at both depths were identified as generalists (Levins. $Bn > 0.9$, p-value ≥ 0.05), whereas taxa that were not evenly distributed across depths were identified as specialists (Levins. $Bn < 0.5$, p-value < 0.05). *Symbiodinium* and *Spiroplasma* were classified as shallow-water specialists, whereas BD1-7, Thalassolituus, and Aquimarina were identified as mesophotic specialists. The genera *Endozoicomonas*, *Bermanella*, *Halioglobus*, *Mycoplasma*, and *Sphingomonas* were identified as depth generalists, indicating that they were distributed across both depths (Figure 10B; Supplementary Table 3).

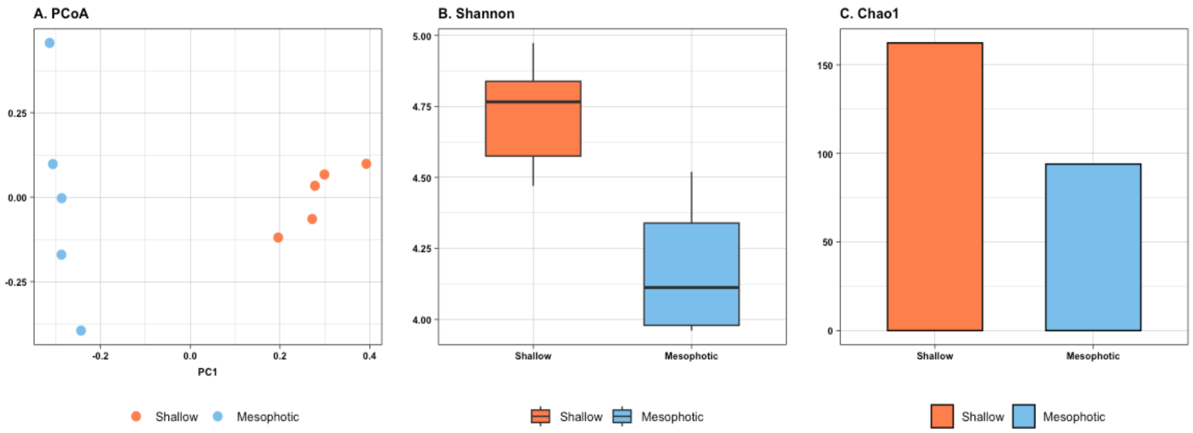

Figure 9. Microbial community composition based on mTAGs. A. PCoA ordination based on based on Bray Curtis distance. **B.** Community diversity of Shallow and Mesophotic communities **C.** Richness of Shallow and Mesophotic communities.

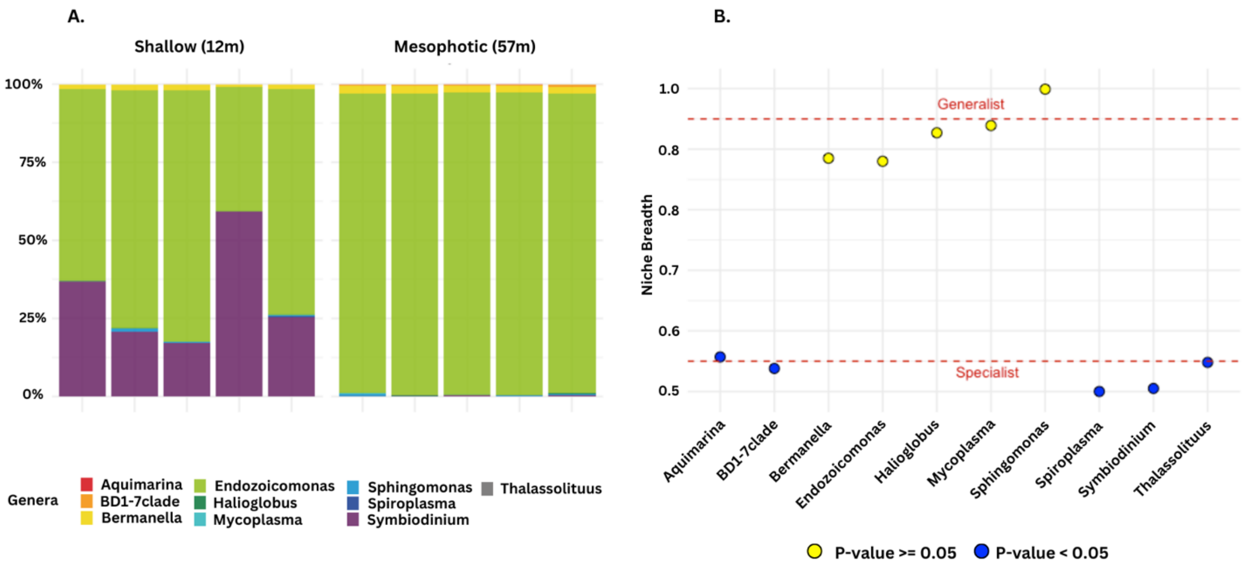

Figure 10. Taxonomic composition of E. singularis based on mTAGs. **A.** Relative abundance of the most abundant genera in shallow vs. mesophotic samples. **B.** Computed niche Breadth of the most abundant microbial genera.

3.1.3. Microbiome functional gene structure

Functional annotation of *Symbiodinium* resulted in 1,003 KEGG orthologs (KO's) (hereafter KEGG). *Symbiodinium* functional genes were absent from the mesophotic samples in accordance with the results of the taxonomic analysis. We identified 53 potential metabolic pathways, most of which were found to be shared with the prokaryotic community except for these three pathways: photosynthesis (ko00195), carbon fixation in photosynthetic organisms (ko00710), and nitrogen metabolism (ko00910) (Supplementary Table 4).

The functional annotation of prokaryotic genes against KEGG resulted in 3,129 KEGG after removing the low-abundance ones. Overall, there was no significant difference in the prokaryotic KEGG composition between depths (PERMANOVA, $p =. 0.19$; Chao1 t-test $p = 0.54$; Shannon's t-test $p = 0.07$). We further investigated the enrichment of the KEGG pathways and modules. We identified 91 metabolic pathways in the prokaryotic community, 82 of which were shared across depths. In addition, the prokaryotic community in mesophotic samples showed a higher abundance of KEGGs related mainly to KEGG pathways in four metabolic categories: carbohydrates, energy, amino acids, and cofactors and vitamin metabolism (Supplementary Figure 2). Some of the pathways that were found to have a higher abundance (p.adj < 0.05) in mesophotic samples were central metabolism (Glycolysis, Gluconeogenesis), oxidative phosphorylation (NADH-quinone oxidoreductase, cytochrome c oxidase (cbb3-type), and other prokaryotic cytochrome c oxidase), and the secretion system (Type III Secretion, Type II Secretion, Sec-SRP, and Twin arginine targeting) (Figure 11; Supplementary Table 5).

Three KEGG pathways were found only in shallow samples, including photosynthesis (ko00195, ko00196) and phosphonate and phosphinate metabolism (ko00440) (q-value < 0.05) (Supplementary Table 4). Furthermore, six pathways were limited to the mesophotic prokaryotic community: steroid degradation (ko00984), pentose and glucuronate interconversion (ko00040), methane metabolism (ko00680), pinene, camphor, and geraniol degradation (ko00907), C5-Branched dibasic acid metabolism (ko00660), and glycerophospholipid metabolism (ko00564) (q-value < 0.05) (Supplementary Table 4).

We identified 49 KEGG modules - functional units within a metabolic pathway that execute specific biological functions (Kanehisa, 2000) - in the prokaryotic community, 44 of which were shared across different depths. However, four KEGG modules were enriched in shallow samples (q-value < 0.05). These modules include phylloquinone biosynthesis (M00932), NAD(P)H: quinone oxidoreductase (M00145), glycogen degradation - glycogen to glucose-6P (M00855), and lysine degradation - L-lysine to glutarate to succinate/acetyl-CoA (M00857). In contrast, only one module showed higher enrichment in mesophotic samples: catechol meta-cleavage (M00569).

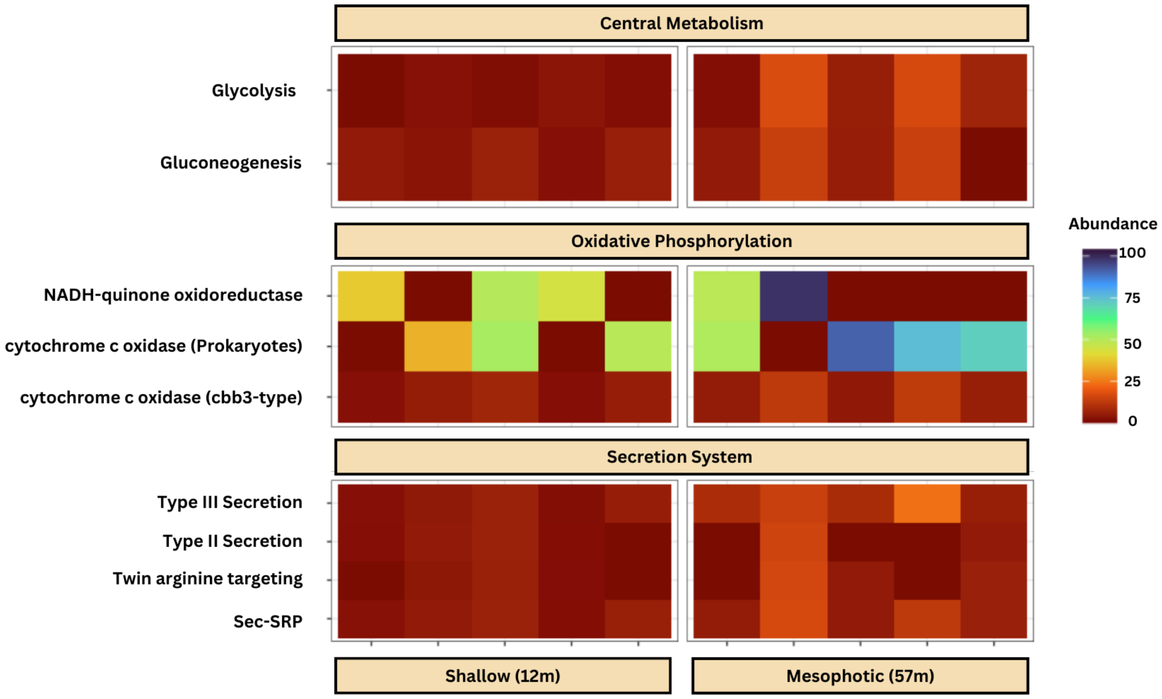

Figure 11. The relative abundances of some metabolic pathways varied with depth in the prokaryotic community.

We further aimed to identify potential metabolic pathways that were common but variable between prokaryotes and Symbiodinium. A total of 1,132 KOs were present in both Symbiodinium and prokaryotes. Among these KOs, 10 exhibited a noticeable abundance and varied significantly between the two depths (adj. P-value < 0.01). Some of these KOs were relatively more abundant in shallow samples and related to amino acid metabolism (K00558, K17398), carbohydrate and carbon metabolism (glycolysis/gluconeogenesis K01007, starch and sucrose metabolism K01179, carbon fixation K01601(*rbcL*,*ccbL*)), and photosynthesis (K02689 and K02705). Conversely, the mesophotic community showed higher relative abundances of K00232 (lipid metabolism), K00681 (amino acid metabolism), and K08678 (carbohydrate metabolism) (Figure. 12A, Supplementary Table 6).

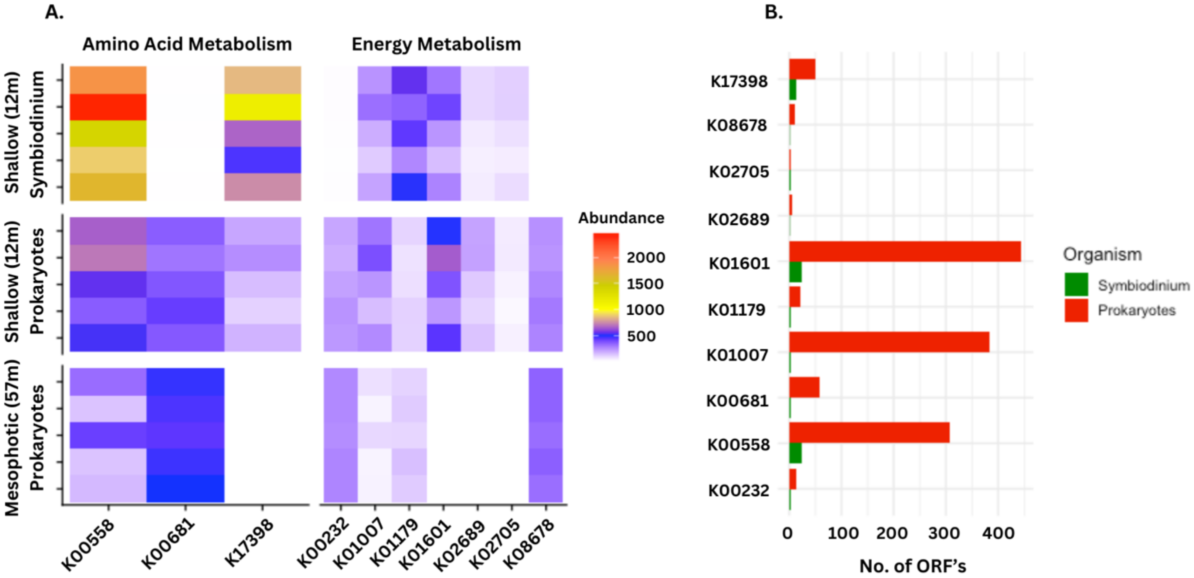

Figure 12. Relative abundance of KOs found in both ‘*Symbiodinium* and prokaryotic communities of *Eunicella Singularis* across depths (A). The number of genes (ORFs) annotated for each KO in Symbiodinium and prokaryotic communities (B).

In addition, we searched for open reading frames (ORFs) related to each of these functions. Interestingly, *Symbiodinium* showed a high number of genes annotated as DNA (cytosine-5)-methyltransferase 1 (K00558), DNA (cytosine-5)-methyltransferase 3A (K17398), and ribulose-bisphosphate carboxylase large chain (K01601) (Figure 12B). Finally, we compared the pathways shared between *Symbiodinium* and the associated prokaryotic community and found 52 shared pathways. The photosynthetic pathway (ko00195) was only found in shallow samples, indicating the absence of photosynthetic activity in the mesophotic community, as expected. In contrast, the mesophotic prokaryotic community metabolic pathways showed higher KOs diversity for the metabolism of cofactors and amino acids pathways (Supplementary Figure 3).

3.1.4. Metagenome Assembled Genomes (MAGs) analysis

We recovered 15 de-replicated prokaryotic MAGs (99% similarity) with completeness values ranging between 66.28% and 99.65% (mean ~ 83%) (Supplementary Table 7). The other 15 MAGs belonged to six bacterial classes: Cyanobacteria, GCA-001730085, Spirochaetia, Gammaproteobacteria, Alphaproteobacteria, and Bacilli. As expected, one MAG belonging to Endozoicomondaceae (MAG.25993) was dominant at all depths with more abundance in mesophotic. Interestingly, one *Endozoicomonas* MAG (MAG.17) that we retrieved had a low abundance, which did not differ between depths and thus probably did not correspond to the dominant *Endozoicomonas* identified by mTAGs. The comparison between the two MAGs, 17 and 25993, showed a significant degree of genetic similarity, with 556 orthologous genes and an orthologous fraction of 28.53%. The mean amino acid identity of 55.43 and a standard deviation of 13.35 indicate a moderate similarity between the protein-coding genes of these two genomes, albeit with some variability. This suggests that these genomes may belong to closely related taxa or have a shared evolutionary history. The other MAGs did not show statistical differences between the depths in mapped reads abundance (Reads Per Kilobase per Million mapped reads; RPKM) ($p < 0.05$), except for MAG.12, Pseudomonadales (genus DT-91), which showed higher abundance in mesophotic samples despite its low read abundance (Figure 13). Unfortunately, the 16S rRNA genes were not retrieved for most of the MAGs, hindering our ability to accurately link the most abundant MAG, identified as Endozoicomonadaceae, with the mTAGs results. This absence of 16S rRNA sequences prevented essential robust phylogenetic analysis needed to confirm the taxonomic identities and associations between MAGs and mTAGs.

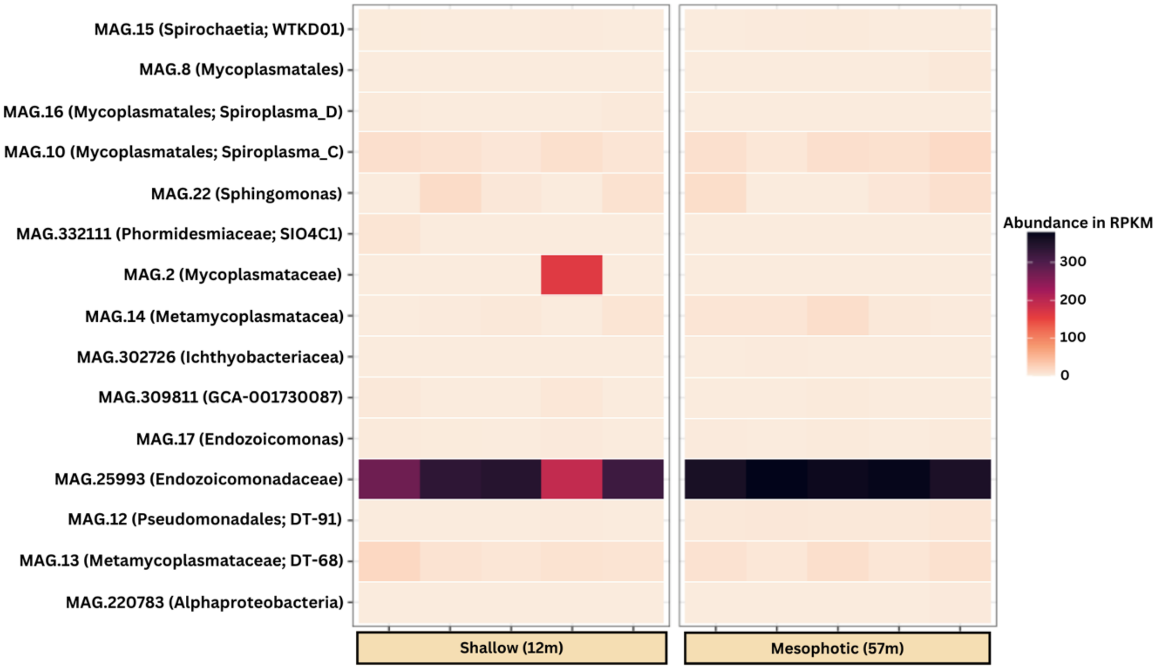

Figure 13. Abundance (in reads per kilobase per million mapped reads; RPKM) of 15 MAGs reconstructed from *E. singularis*.

We further explored the potential contribution of MAGs to previously identified metabolic functions of the microbiome. While most MAGs encoded proteins involved in central metabolism (Glycolysis, Gluconeogenesis), few MAGs encoded genes related to oxidative phosphorylation. For example, NADH-quinone oxidoreductase was found only in MAG.22 (*Sphingomonas*). In addition, the cytochrome cbb3-type was found in MAG.22 (*Sphingomonas*), MAG. 17, and 25993 (Endozoicomondaceae) only.

Cofactor and vitamin metabolism, such as menaquinone (K_2), pantothenate (B_5), pyridoxal (B_6), biotin (B_7), and cobalamin (B_{12}), were found in only six MAGs: *Phormidesmiaceae* (genus SIO4C1), Pseudomonadales (genus DT-91), Pseudomonadales (genus *Endozoicomonas*), GCA-001730085, and Sphingomonadales (genus *Sphingomonas*). The MAG of the genus DT-91 (Order Pseudomonadales) had complete modules of vitamin and cofactor metabolism, such as biosynthesis of B_5, B_6, B_7, and B_{12}. In addition, Endozoicomondaceae MAGs exhibited biosynthesis modules for several vitamins, such as B_1, B_6, B_7, and K_2. Other MAGs also showed complete modules for vitamin and cofactor metabolism, including B_7 and K_2.

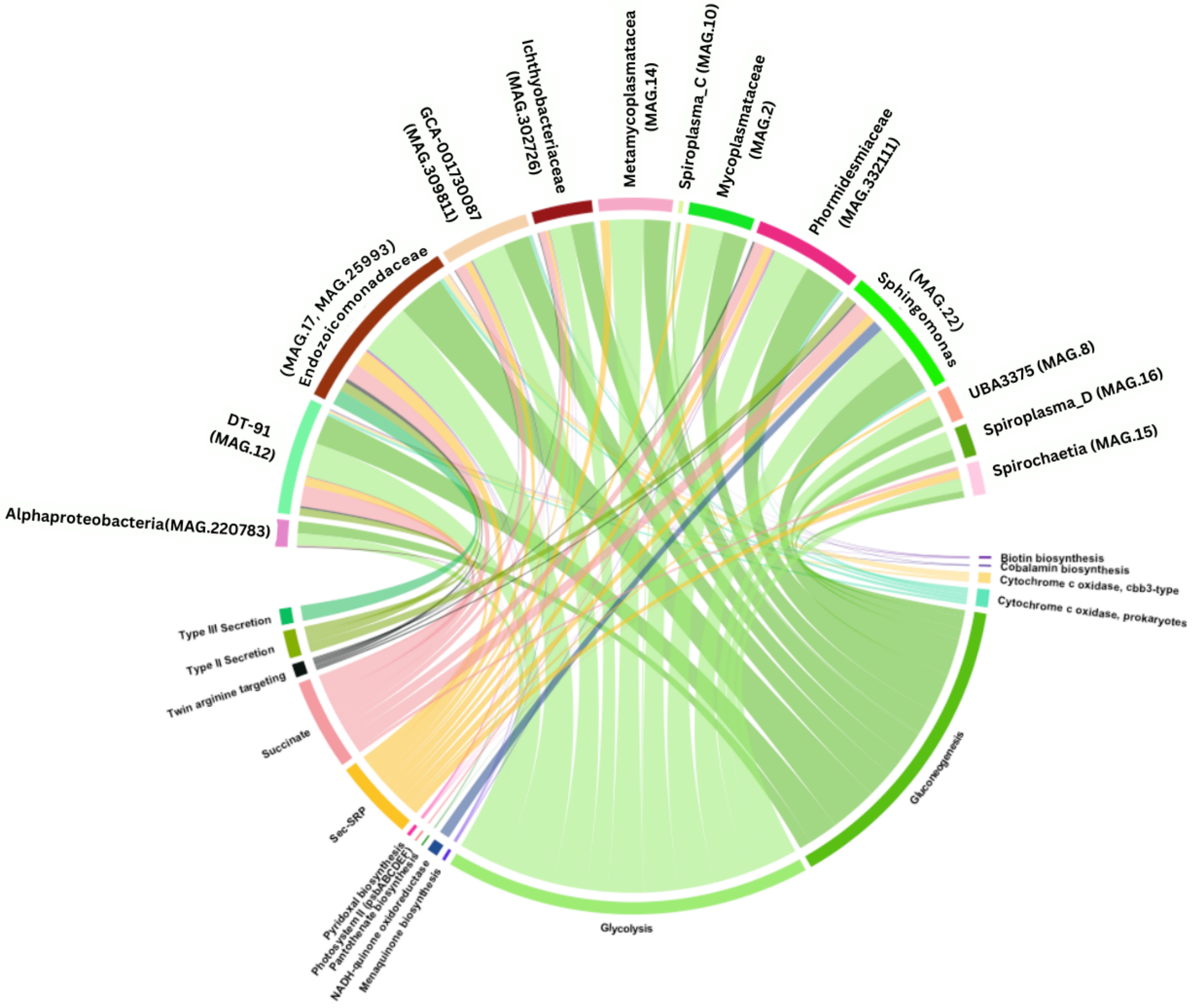

Figure 14. Chord graph for the 15 MAGs illustrating their contribution to metabolic pathways in the *E. singularis* microbiome. It connects each MAG with pathways based on the KEGG KOs encoded in their genomes.

Furthermore, eight MAGs were found to encode secretion system genes. For example, the twin-arginine translocation (Tat) system was found in eight MAGs such as MAG.12 (Pseudomonadales, genus DT-91), MAG 17 and 25993 (Endozoicomondaceae), MAG.22 (Sphingomonas), MAG.220783 (Alphaproteobacteria), MAG.302726 (Ichthyobacteriaceae), MAG.309811 (GCA-001730086), and MAG.332111

(Phormidesmiaceae). Additionally, the type II secretion system was found in the MAG.12 (Pseudomonadales, genus DT-91), MAG 17 and 25993 (Endozoicomondaceae), MAG.22 (Sphingomonas). In contrast, the Type III secretion system was only found in MAG 17 and 25993 (Endozoicomondaceae)(Figure 14; Supplementary Table 8).

3.2. Scleractinia Desmophyllum pertusum microbiome analysis

Cold water corals (CWC), also known as deep-sea corals, are frequently found in the submerged topographic structures of submarine canyons where they establish reef formations (Chapron et al., 2018). These ecosystems are vital habitats within the mesophotic zone, supporting diverse species and exhibiting greater biodiversity and biomass than the surrounding seabed (Buhl-Mortensen et al., 2016; Sundahl et al., 2020). Colonial scleractinians or stony corals can construct substantial reef structures (Roberts, 2019). Our species of interest *Desmophyllum pertusum*, an asymbiotic scleractinian coral species (Emblem et al., 2012) previously known as *Lophelia pertusa* (Linnaeus, 1758), is a CWC species that forms reefs and serves as a biodiversity hotspot in the deep ocean (Baussant et al., 2022). It is a globally distributed scleractinian coral that creates critical three-dimensional habitats in the deep ocean (Schleinkofer et al., 2019). Their main depth distribution is mainly 200-1000m (Le Goff-Vitry et al., 2004) at temperatures between 4 and 12 °C (Davies et al., 2008). However, their distribution is influenced by diverse environmental factors, such as dissolved oxygen levels and temperature (Hebbeln et al., 2020). They are typically located on continental margins and are generally present, but not limited to the Northeast Atlantic and southeastern regions of North America (Tong et al., 2022).

D. pertusum is an opportunistic feeder (Mueller et al., 2014) that prefers productive and high-current zones (Davies et al., 2008). In addition, it relies on its microbiome to cycle nutrients, degrade organic carbon, fix nitrogen (Galkiewicz et al., 2011), and reduce some end products of coral anaerobic metabolism (Neulinger et al., 2008). Molecular and culture-based methods have been used to investigate bacterial communities associated with *D. pertusum* (Kellogg et al., 2017; Meistertzheim et al., 2016; van Bleijswijk et al., 2015). For example, the involvement of the *D. pertusum* microbiome in nitrogen cycling and the transfer of fixed nitrogen and inorganic carbon into coral tissues has been demonstrated using isotope tracers (Middelburg et al., 2015b). In addition to its role in nutrition, the *D. pertusum* microbiome plays a role in enhancing the resilience of corals against pathogens through antibiotic production (Kellogg et al., 2009). Therefore, the stability of this symbiotic relationship is vital, and disturbance of the interaction between corals and their microbiome due to environmental stressors can impact coral health (Peixoto et al., 2017).

In recent years, there has been an increase in the literature on deep-sea corals (Kellogg et al., 2017). This surge in attention can be primarily attributed to growing conservation concerns, as numerous cold-water coral habitats coincide with regions where commercial fishing or oil and gas drilling activities occur (Järnegren et al., 2017). In addition, predictions of future climate scenarios suggest that deep ocean environments will experience a more rapid increase in temperature, approximately 3 °C, by the end of the century (Sweetman et al., 2017) compared to surface waters (Brito-Morales et al., 2020). Unfortunately, these organisms, including *D. pertusum,* are highly susceptible to these stressors because of their low resistance to disturbances, slow recovery rates, and poor resiliency (Matos et al., 2021). For example, ocean acidification has been proposed to increase *D. pertusum* vulnerability and reduce colony development (Vad et al., 2017). Similarly, increased ocean temperatures affect resilience to environmental conditions (Weinnig et al., 2020).

Alterations in environmental conditions, such as increased water temperature, impact the health of cold-water corals (CWC) across multiple fronts. These changes influence various aspects, including shifts in microbiome composition, alterations in organic carbon fluxes, changes in respiration rates, modifications in feeding behavior, and impacts on skeletal biomineralization, potentially rendering CWCs more vulnerable (Chapron et al., 2021; Dodds et al., 2007; Gori et al., 2014; Naumann et al., 2014). However, our understanding of the functions of CWC-associated microbiome and its potential metabolic responses to these environmental stressors remains incomplete and requires further investigation. Chapron et al. (2021) found that the microbiome of *D. pertusum* exposed to an increased water temperature (15C°) was dominated by bacteria of the *order Rhodobacterales*, which has been proposed as an indicator of thermal stress (Pootakham et al., 2019). Interestingly, some *Rhodobacterales* were able to use methanol as a carbon source through methanol assimilation (Sargeant et al., 2016), suggesting its influence on the carbon cycle.

It has been reported that the presence of chemoautotrophic and nitrogen-fixing microorganisms in the CWC microbiome maintains nitrogen balance and efficiently recycles nitrogen (Middelburg et al., 2015b). However, the specific microbes responsible for nitrogen cycling remain to be identified (Kellogg et al., 2017). This harmony between microbes and their host corals is susceptible to environmental changes. It has been proposed that increased seawater temperature leads to consistent increases in diazotroph abundance and diversity in coral reefs, potentially affecting the nitrogen cycle (Santos et al., 2014). This dysbiosis in the microbiome due to increasing water temperature may affect organic carbon fluxes and the nitrogen cycle. In addition, similar to other corals, the *D. pertusum* microbiome can contain opportunistic pathogenic components (Weinbauer et al., 2019), which have been reported in the cold-water microbiome (Penn et al., 2006). Due to thermal stress, *D. pertusum* modifies its microbiome and loses its species specificity (Thurber et al., 2009). This shift may encourage opportunistic pathogens to transition the microbiome toward the pathobiome (Ezzat et al., 2021; Thurber et al., 2009), which has been recognized to be more prevalent in cold-water corals under stress (Röthig et al., 2017), thereby leading to coral death (Chapron et al., 2021). However, further investigation is needed to fully understand the changes that occur in the microbiome.

3.2.1. Overview of metagenomic samples

The single sample assembly generated 27.88×10^6 contigs, featuring a total of 15.39×10^6 eukaryotic and 12.47×10^6 prokaryotic contigs. The total eukaryotic contig size was ~ 1.37×10^7 bp, with an N50 value of 2044 bp representing the sequence length of the shortest contig at 50% of the total assembly length. The cumulative length of prokaryotic contigs reached a substantial ~ 7.11×10^9 bp, derived from 12.47×10^6 contigs, with an N50 of 1396 bp (Supplementary Table 9).

Furthermore, we conducted a thorough analysis, focusing specifically on the prokaryotic community, using the prokaryotic gene catalog. Additionally, we analyzed prokaryotic gene composition across different environmental conditions and time points. The prokaryotic gene collection exhibited differences among the three environmental conditions (10°C, 13°C, and 15°C) at each time point (days 1 and 60). Analysis of prokaryotic gene composition revealed discernible profiles associated with each treatment. We identified a significant temporal influence on microbial community gene composition (PERMANOVA, F = 2.44, $p = 0.004$) (Supplementary Figure 4). However, the Shannon diversity and Chao1 richness were not statistically significant between the time groups (Shannon *t*-test *p*-value = 0.32, Chao1 *t*-test *p*-value = 0.28) or thermal treatments (Shannon K-W *p*-value = 0.17, Chao1 K-W *p*-value = 0.49).

3.2.2. mTAGs taxonomy and abundance

We investigated the taxonomic variation of the microbiome among time points and treatments using mTAGs. We obtained a total of 5,895,633 mTAGs; the majority were unaligned (~87%), and only ~13% had a taxonomic annotation: eukaryotic (~9.9%), and prokaryotic (~2.6%). The high percentage of unaligned sequences might be due to limitations in the method, such as insufficient mTAG generation, or the incompleteness of the reference database used for alignment. Our interest lies in the prokaryotic community; therefore, we excluded other mTAGs from the rest of the analysis. The prokaryotic mTAGs (n = 155,370) showed differences in the taxonomic composition of the microbiome between the two-time points, day 1 and day 60 (PERMANOVA, F = 4.45, $p = 0.007$) (Figure 15A). In day 1 samples, the microbiome showed similar taxonomic composition, which could be due to several factors like insufficient time for the microbiome to respond to new conditions, the initial similarity in microbial communities across samples, minimal variation introduced by the experimental conditions, natural stability of the coral microbiome, or technical and sampling variability. Interestingly, the order Vibrionales was present in all treatment samples at the two-time points; however, on day 60, it was found at a low abundance at 10 °C and increased abundance at 13 and 15 °C. In addition, the microbiomes of the samples after 60 days showed taxonomic variation between the treatments (Figure 15B). Some microbial orders were abundant in the 10 °C samples, including Alteromonadales (~27%), Cellvibrionales (~15%), and Chitinophagales (~12%). However, other microbial orders showed an increase in relative abundance with increasing temperature, especially at 15 °C, such as Rhodobacterales (~35%), Dadabacteriales (~12%), Campylobacterales (~10%), and Rhodospirillales (~8.5%) (Figure 15B; Supplementary Table 10).

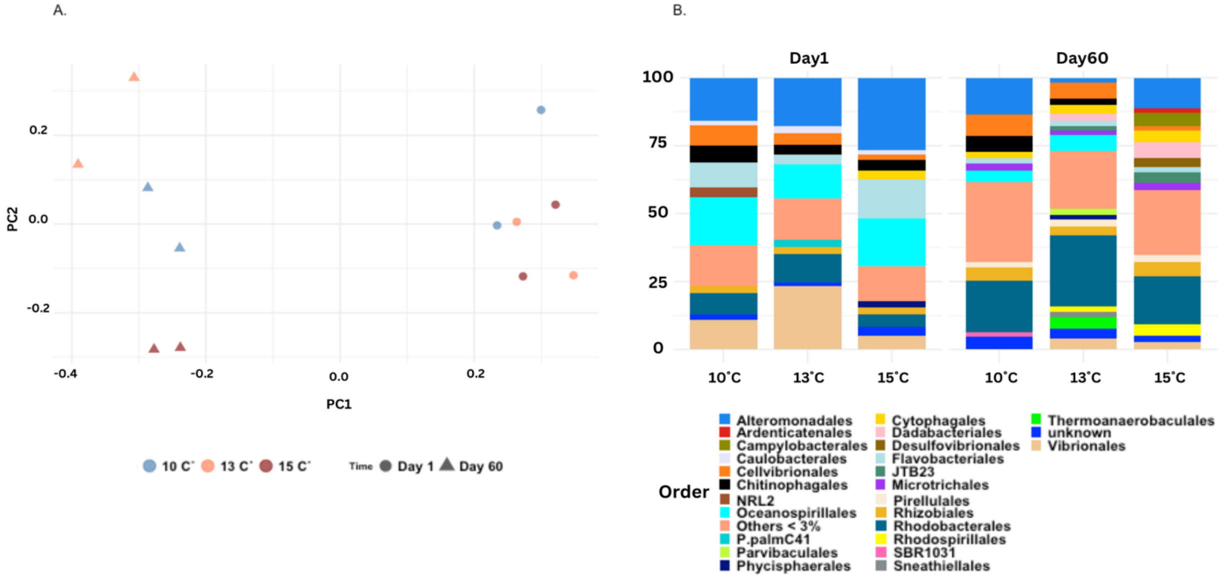

Figure 15: Prokaryotic community composition A. Non-metric multi-dimensional scaling (NMDS) based on Bray-Curtis dissimilarities among the prokaryotic mTAGs compositions of *D. pertusum* samples. Two clusters of prokaryotic SSU-rRNA genes (n= 155370) were observed at the start (day 1) and end (day 60) of the experiment at 10°C, 13°C, and 15°C. **B**. Relative abundance of the mTAGs at the order level showing the variation of the microbiome taxonomic composition between samples between day 1 and day 60 and between the thermal treatments.

3.2.3. MAG taxonomy and abundance

We recovered 281 de-replicated (99% similarity) metagenome-assembled genomes (MAGs) belonging to 20 phyla. The most abundant phyla were Proteobacteria – Alpha (~37%) and Gamma (~22%), followed by Planctomycetota (~13.5%), and Bacteroidetes (~8.5%). In addition, a few MAGs belonged to the phylum Actinobacteria (2.8%), whereas the remaining 41 MAGs included Myxococcota (~2.8%), Chloroflexota (~2.1%), Desulfobacterota (~1.8%), and other phyla. More than 42% of the MAGs had genome completeness above 90%, with the highest-quality genome belonging to the order Opitutales (completeness of 100%) (Supplementary Figure 5, Supplementary Table 11). Moreover, the MAGs' abundance (RPKM, Reads Per Kilobase per million total sequences) showed variation between the two temporal groups, revealing significant differences in the abundance distribution of MAGs between days 1 and 60 (Wilcoxon rank-sum test, $p < 0.05$) (Supplementary Figure 6, Supplementary Table 12). We identified 14 MAGs with the most abundance variation over temporal and thermal scales. Some of these MAGs showed higher abundance in day 60 samples, such as some MAGs of the orders Rhodobacteraceae – genus Mangrovicoccus (MAG.31), UBA4486 (MAG.45), Cytophagales (MAG.174,137), Pseudomonadales–genus Porticoccus (MAG.18,193), and Alteromonadaceae – genus Glaciecola (MAG. 256). This variation between the two temporal groups, especially between the control temperature (10C°) on day 1 and the experimental group on day 60, could be related to the acclimation to experimental conditions. Surprisingly, one colony showed an increase of one MAG abundance within its microbiome (MAG.245) belonging to Mycoplasmatales in both temporal groups at 10C° that was not detected in the other colonies (Supplementary Figure 7).

Since we were interested in the impact of prolonged thermal stress on the microbiome, we focused hereafter on the changes in the microbial community on day 60 across the different thermal treatments (10C°,13C°, 15C°). The MAGs RPKM abundance showed a significant variation between the three thermal conditions (K-W *p*-value < 2.2e-16) (Figure 16A). Six MAGs showed an increased abundance with thermal stress: Rhodobacteraceae – genus Sedimuntalea (MAG.184) and genus Mangrovicoccus (MAG.31,41,73), UBA4486 (MAG.45), and Desulfobacterota_D (MAG.259). In turn, a few MAGs showed decreasing abundance with increasing temperature, such as Pseudomonadales, genus Porticoccus (MAG.18,193), Mycoplasmataceae (MAG.245), Alteromonadaceae, genus Glaciecola (MAG. 256), Cytophagales (MAG.137,174), Alphaproteobacteria, and (MAG.146) (K-W p-value = 7.03e-11) (Figure 16B).

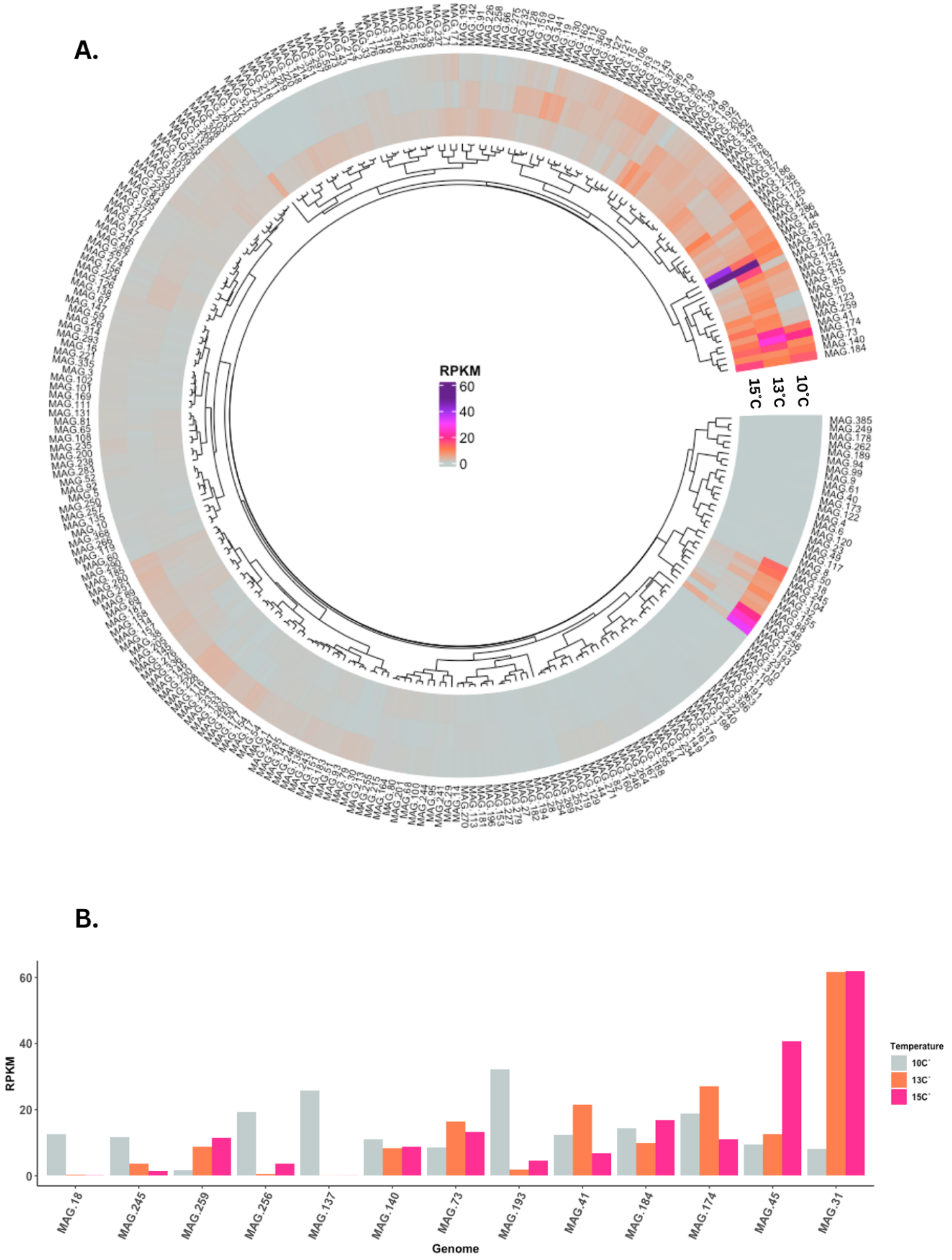

Figure 16: MAGs abundance across thermal conditions A. Circular heatmap of MAGs abundance (RPKM) on day 60 illustrates the distribution of MAGs across different thermal treatments (10C˚,13 C ˚,15 C ˚); **B.** Bar chart of the most variants MAG RPKM between the three thermal conditions.

Functional analysis of the metagenomic samples

We functionally annotated 1,780,113 ORFs to 7363 KOs. We analyzed the samples based on their normalized KO compositions across environmental conditions and time points. Although the KO compositions exhibited differences between the two temporal groups on days 1 and 60, these differences were not statistically significant (PERMANOVA p-value = 0.5). Therefore, we proceeded with the analysis using data from day 60 samples to determine the influence of thermal conditions on coral microbiome function after the incubation period. We performed a SIMPER analysis to identify potential KOs that differed significantly in abundance between the 10 °C, 13 ˚C, and 15 °C samples. The results identified 454 KO pathways that showed a significant difference (*p*-value < 0.05), including 26 KOs, which were found to contribute to five enriched (*q*-value < 0.05) (Figure 17; Supplementary Table 13).

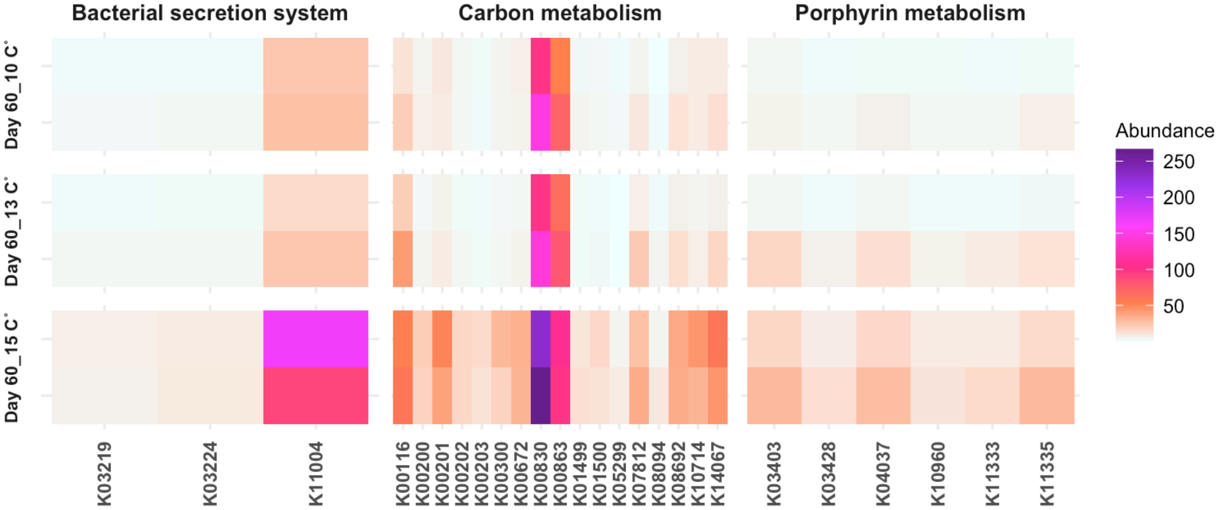

Figure 17: The Enriched KEGG pathways identified based on SIMPER analysis between 10C˚, 13 ˚C, and 15 °C on day 60 show a potential increase in gene abundance highlighting the increase in gene abundance of metabolic pathways: bacterial secretion system, porphyrin metabolism, and carbon metabolism.

These five metabolic pathways are related to three categories: the bacterial secretion system, porphyrin metabolism, and carbon metabolism. The bacterial secretion system includes three KOs: K03219 - type III secretion protein, K03224 - ATP synthase in type III secretion protein, and K11004 - ATP-binding cassette, hemolysin transporter (T1SS), which had the highest abundance. Moreover, the Porphyrin metabolism pathways include K03403 - magnesium chelatase subunit H, K03428 - magnesium-protoporphyrin O-methyltransferase, K04037 - light-independent protochlorophyllide reductase subunit L, K10960 - geranylgeranyl-bacteriochlorophyllide a reductase, K11333(chlorophyllide a reductase subunit X), and K11335 - chlorophyllide a reductase subunit Z.

Furthermore, 17 KOs were found to be related to carbon metabolism. Some of these KOs are related to methane metabolism, such as K00680 - formylmethanofuran--tetrahydromethanopterin N-formyltransferase, K00201 - formylmethanofuran dehydrogenase subunit B (*fwdB, fmdB*), K07812- trimethylamine-N-oxide reductase cytochrome c (*torZ*), K00300 - methylenetetrahydrofolate/ methylenetetrahydromethanopterin dehydrogenase (*mtdAI*), K08692 - malate-CoA ligase subunit alpha (*mtkB*), and K00830 - alanine-glyoxylate transaminase (*AGTX*) (Figure 17). Other KOs include K00116, malate dehydrogenase, which is related to carbon metabolism, and K01500 - methenyltetrahydrofolate cyclohydrolase, which is related to the carbon fixation pathway.

Additionally, some of these KOs, which have been identified by SIMPER analysis, were found to be part of the KEGG modules of formaldehyde assimilation (serine pathway), such as K00830, K08692, and K14067. Therefore, we investigated the presence of all functional genes related to the mentioned module. Interestingly, we found a complete formaldehyde assimilation (serine pathway) module in our data (Supplementary Figure 8).

Given the significant findings in our analysis of KOs pathways, particularly in carbon metabolism, we decided to delve deeper into the functional aspects of carbohydrate metabolism by investigating the carbohydrate-active enzymes (CAZymes) database. This analysis aimed to uncover the functional capabilities related to carbohydrate degradation and elucidate the metabolic adaptations of the microbiome to environmental stressors. The SIMPER analysis of the annotated CAZy showed an increase in the abundance of some Glycoside Hydrolase families such as β-1,6-

glucosidase (GH30), Mannosyl-glycoprotein endo-β-N-acetylglucosaminidase (GH85), β-D-arabinofuranosidase (GH116), and α-amylase (GH119) (Supplementary Figure 9, Supplementary Table 14). These enzymes are involved in the breakdown of complex carbohydrates into simpler sugars.

Furthermore, given the previously noted increase in Rhodobacterales MAGs, we suspect this increase might have an influence on the nitrogen cycle genes within the coral microbiome. Therefore, we investigated functional gene abundance related to the nitrogen cycle, such as dissimilatory/assimilatory nitrate reduction to ammonium (DNRA/ANRA), (*nap, nas, nar, nrf*), denitrification (*nir*, *nor*, *nos*), nitrogen fixation (*nif*, *vnf*), and nitrification (*amo*, *hao*) (Supplementary Figure 10, Supplementary Table 15). These functions showed an increased abundance with increasing temperature on day 60 (K-W *p*-value = 0.012) (Figure 18). There was almost no change in the nitrification genes. Also, one gene (*nifD*) showed higher abundance in the control temperature of 10˚C than in thermal stress conditions. Interestingly, there was a decrease in the abundance of most of these genes at 13 ˚C compared to the 10C˚ and 15 ˚C except for nitrogen fixation genes (*nifH, vnfH, nifK*) that showed an increase with the thermal stress. In contrast, most nitrogen cycle genes had the highest abundance at 15˚C with thermal stress such as dissimilatory/assimilatory nitrate reduction (*narG*, *napA* and *B*, and *nas*), denitrification genes (*nirK*, *norB*, and *nosZ*), and nitrogen fixation genes (*nifH, vnfH, nifK*) (Figure 18).

Moreover, we investigated the taxonomy of the ORFs annotated to key nitrogen genes. Most of the ORFs related to dissimilatory/assimilatory nitrate reduction to ammonium (*nap,nas,nar,nrf*), denitrification (*nir*,*nor*,*nos*), and nitrogen fixation (*nif*,*vnf*) were taxonomically annotated to Alpha and Gamma-proteobacteria. In contrast, nitrification (*amo*,*hao*) genes were mostly annotated to Gamma-proteobacteria (Figure 19). Most of the Alphaproteobacteria taxa belong to the orders Rhodobacterales Rhizobiales, while most Gammaproteobacteria belong to Pseudomonadales, and Enterobacterales.

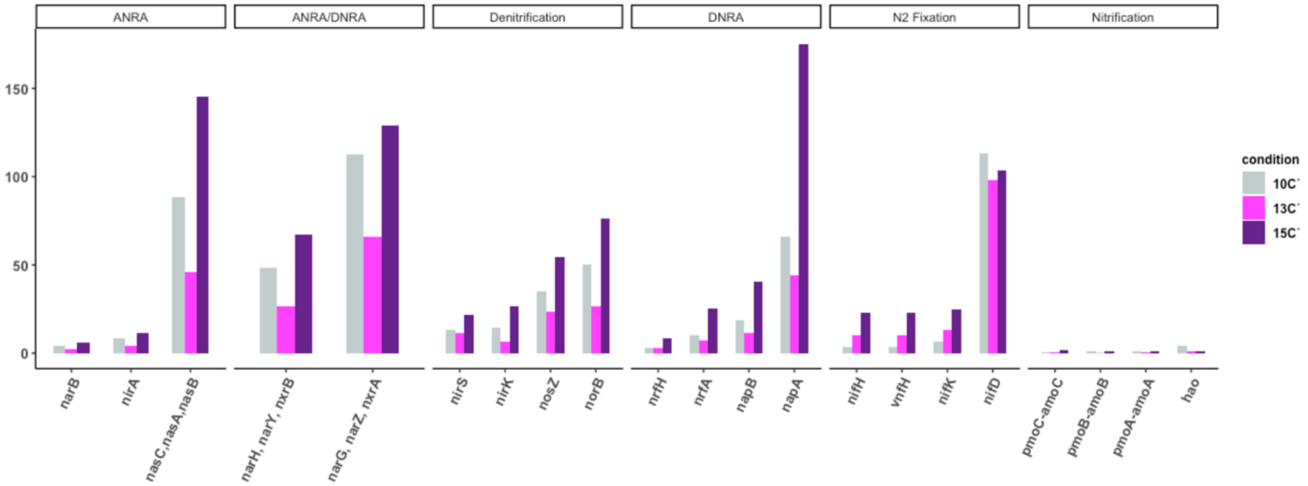

Figure 18: Nitrogen cycle genes abundance bar plot across thermal conditions on Day 60. It showed an abundance increase with the prolonged temperature increase in some genes related to dissimilatory/assimilatory nitrate reduction to ammonium (ANRA, DNRA), denitrification, and nitrogen. The y-axis represents the gene abundance and the x-axis represents genes.

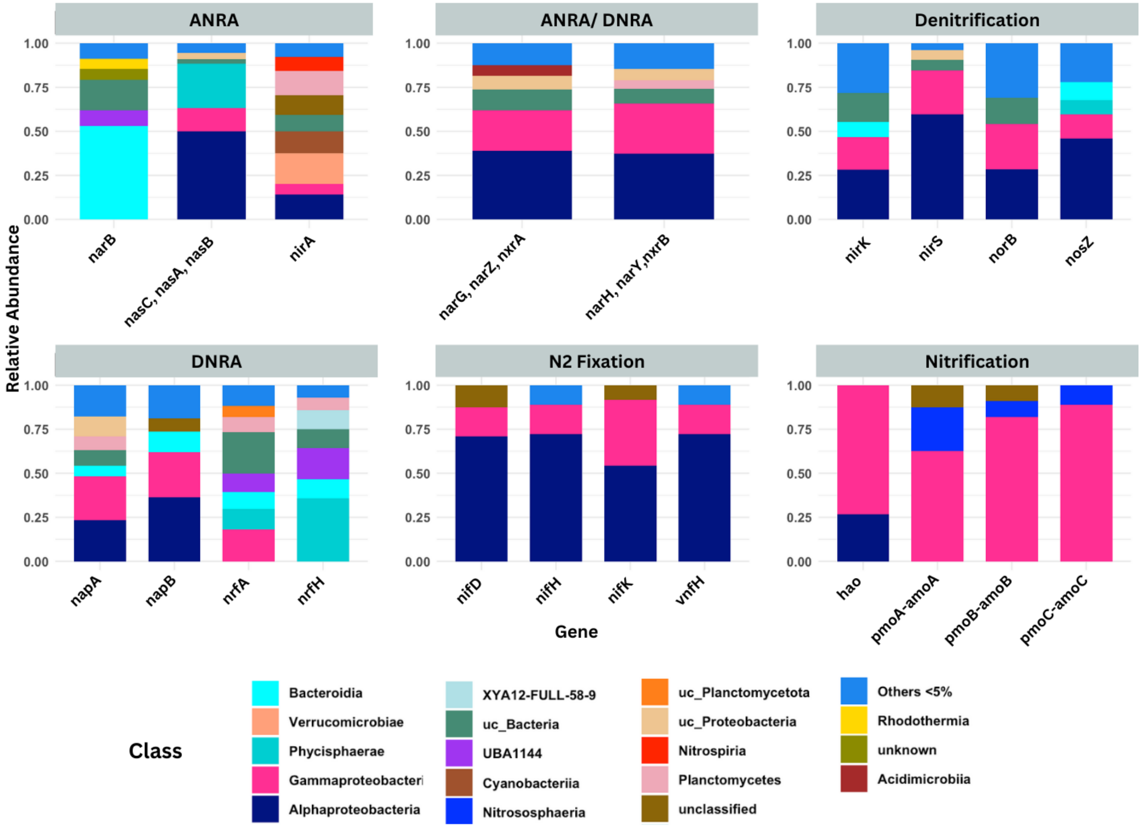

Figure 19: Relative abundance of nitrogen ORFs taxonomy at the class level. Each plot represents a nitrogen cycle pathway with the responsible key genes. The category (Others <5%) represents taxa that have been assigned to less than 5% of ORFs.

3.2.4. MAGs functional profiling

We further investigated the potential contribution of MAGs to previously identified KEGG functions. Many MAGs participated in carbon metabolism and bacterial secretion systems (Figure 20). Interestingly, none of the MAGs contained genes annotated with any of the KO pathways related to porphyrin metabolism. However, we found 19 MAGs belonging to nine orders, including KOs related to the secretion system. K03219 (T3SS) was found in two MAGs belonging to two orders, Geminicoccales (MAG.223) and Pseudomonadales (MAG.70). Additionally, K03224 (T3SS) was found in five MAGs belonging to four orders: Pseudomonadales (MAG.70), Chlamydiales (MAG.170), Rhodobacterales (MAG.227, MAG.360), and Geminicoccales (MAG.223). All displayed higher abundance with increasing temperature (Supplementary Figure 11). Furthermore, K11004 (T1SS) was found in 14 MAGs belonging to seven orders: Pseudomonadales, Minwuiales, Chromatiales, Rhizobiales, Sphingomonadales, HK1 (Gammaproteobacteria), and Competibacterales (Supplementary Table 16).

We identified MAGs that included KEGGs related to carbon metabolism pathways, such as K00116 - malate dehydrogenase, which was found in 15 MAGs belonging to five orders, including Pseudomonadales, Flavobacteriales, Chitinophagales, Rhodobacterales, and Opitutales. Furthermore, KOs related to methane metabolism were found in MAGs. For example, K00830 - alanine-glyoxylate transaminase (*AGTX)* was found in most MAGs, except for MAGs belonging to the orders Flavobacteriales and Chitinophagales. The K00863 - triose/dihydroxyacetone kinase (*DAK, TKFC*) was found in 17 MAGs belonging to Rhodobacterales, Sneathiellales, Rhizobiales, and J057 (Class: Bacteroidia). Interestingly, K08094 - 6-phospho-3-hexuloisomerase (*hxlB*) was found in one MAG from Promineofilales. Another KO, K08692, was found in 13 MAGs belonging to UBA4486 (Class: Gammaproteobacteria), Rhizobiales, Ga0077536 (Class: Gammaproteobacteria), Rhodobacterales, and Kiloniellales. Finally, the K14067 - malate-CoA ligase subunit beta (*mtkA*) - was also found in 13 MAGs belonging to UBA4486, Rhizobiales, Ga0077536, Rhodobacterales, and Kiloniellales (Figure 20).

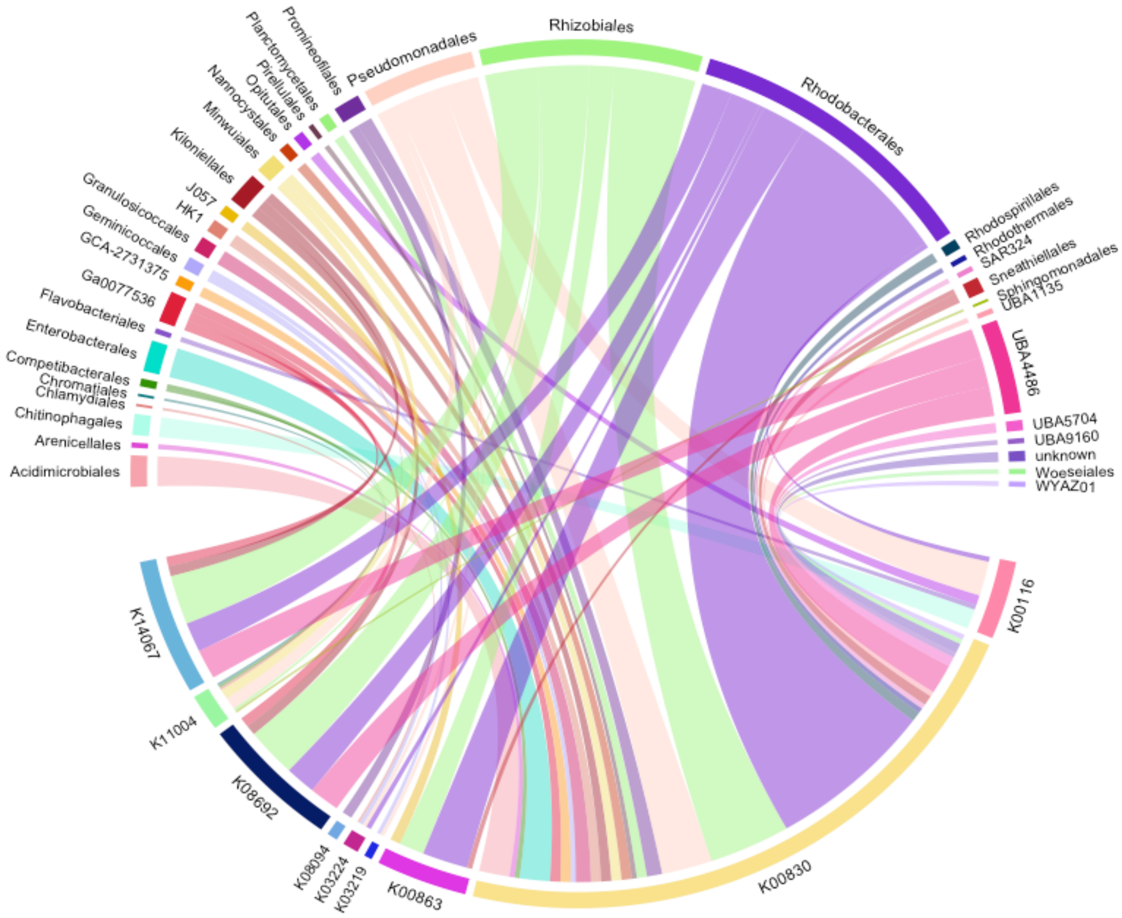

Figure 20: Chord diagram of MAGs that participate in functions related to carbon metabolism and the bacterial secretion system. This shows that the majority of MAGs contribute to formaldehyde assimilation (K00830, K08692, and K14067). Interestingly, some MAG orders, i.e., Pseudomonadales and Geminicoccales included K11004 (T1SS), K03219 (T3SS), K03224 (T3SS), and Rhodobacterales included K03224 (T3SS) in their genomes, indicating their potential pathogenicity.

We identified 211 MAGs belonging to 54 bacterial orders that could be involved in the nitrogen cycle processes (Supplementary Figure 12). Many MAGs were found to have denitrification genes (*nirK, nirS, norB, nosZ*). However, three MAGs belonging to Rhodobacterales showed the full suite of denitrification genes; these are MAG.73 (genus *Mangrovicoccus*), MAG.140 (species Ruegeria *meonggei*), and MAG.184 (genus *Sedimentitalea*) (Figure 21). Intriguingly, the *nrfH* and *nrfA* genes, which are essential for dissimilatory nitrate reduction to ammonium (DNRA), were widely distributed across our

MAGs. Similarly, the Dissimilatory/Assimilatory NO3- to NO2- genes (*narB* and *nas*) were broadly distributed, except for the *nirA* gene, which was only found in four MAGs: three from Opitutales (MAG.43, MAG.126, MAG.141) and one from Rhizobiales (MAG.176). Furthermore, Rhodobacterales, genus *Mangrovicoccus* (MAG.31,41,73), showed nitrogen fixation genes, especially *nifH*, *nifK,* and *nifD.* However, only Rhodobacterales (MAG.31) and UBA4486 (MAG.45) increased with increasing temperatures (Figure 21).

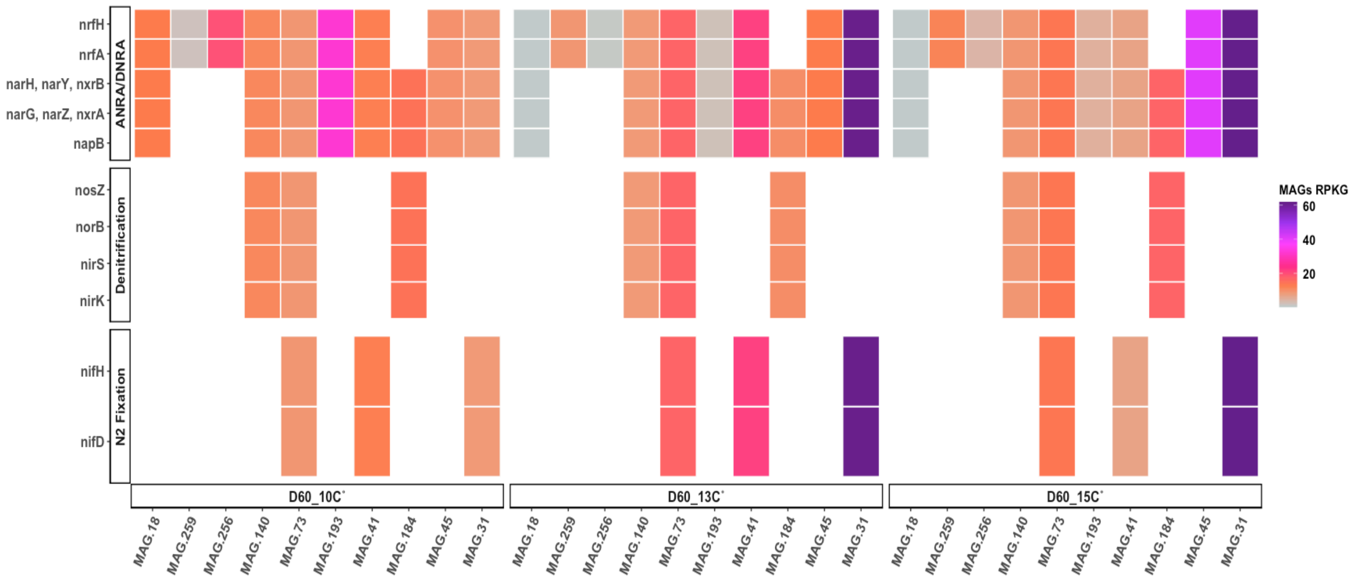

Figure 21: Heat map displaying the most abundant MAGs containing nitrogen cycle genes and their relative abundance across three thermal conditions. The data indicate that Rhodobacterales, genus *Mangrovicoccus* (MAG.31,41,73), possess a complete set of denitrification genes. Also, It shows the increasing abundance of *Mangrovicoccus* (MAG.31) and UBA4486 (MAG.45).

4. DISCUSSIONS

4.1. Eunicella metagenomes and gene composition structure

In previous research, it has been reported that dinoflagellates exhibit a wide range of genome sizes, up to 245×10^6 kbp containing 87,688 protein-coding and 92,013 total genes (Hou & Lin, 2009). In the case of *Symbiodinium*, it has been reported to have ~ 42,000 protein-coding genes and ~19 exons per gene (Shoguchi et al., 2013a). We have predicted a high number (151264 genes) of *Symbiodinium* genes, which could be because we are predicting exons with the tool Metaeuk. Also, gene fragmentation could have inflated the number of *Symbiodinium* genes.

Moreover, we found that the coral microbiome is richer and more diverse in shallow samples, which implies that depth might influence the microbiome. At the functional level, there was no significant influence of depth on the functional composition of the prokaryotic community in both shallow and mesophotic samples. This suggests that while microbial diversity varies with depth, the core functional capabilities of the microbiome remain stable across different depths.

4.2. The changes in E. singularis microbiome with depth

Based on the mTAGs SSU-rRNA taxonomic annotation, *Symbiodinium* was found more abundant in shallow *Eunicella singularis* compared to mesophotic colonies. In contrast, prokaryotic sequences were dominant in mesophotic samples, particularly by Alphaproteobacteria and Gammaproteobacteria. Additionally, the Gamma-proteobacterial genera *Endozoicomonas* and *Bermanella* were the most abundant at both depths. *Endozoicomonas* exhibits a broad distribution in marine environments across different depths and ecosystems (Neave et al., 2016b), forming associations with various Cnidaria species (Hochart et al., 2023) including Gorgonian corals (Tignat-Perrier et al., 2022). It is assumed that *Endozoicomonas* is involved in coral nutrient acquisition by participating in host-associated protein and carbohydrate transport and cycling, and structuring of the coral microbiome through the inhibition of pathogen proliferation using different mechanisms like the production of quorum-sensing antimicrobial compounds (Neave et al., 2016c; Tignat-Perrier et al., 2022). Despite their recognized mutualistic association with coral hosts, *Endozoicomonas* may adopt diverse roles, potentially residing within coral cells as commensals, parasites, or even pathogens (Pogoreutz & Ziegler, 2024).

Little is known about the role of *Bermanella* in the coral microbiome. One species belonging to this genus has been described, *Bermanella marisrubri*, which has been isolated from the Red Sea and described as a heterotrophic, marine, strictly aerobic, motile bacterium (Pinhassi et al., 2009). In addition, genomic evidence from *Bermanella* suggests a possible role in bioremediation and oil degradation by initiating *n*-alkane breakdown for other bacterial taxa, such as Spongiiabcteraceae, to carry out secondary *n*-alkane breakdown and beta-oxidization (Ribicic et al., 2018). This process suggests that *Bermanella*'s ability to utilize hydrocarbons as a carbon source may benefit corals by facilitating the degradation of organic matter or aiding in the mitigation of hydrocarbon pollutants in their environment. This capability could contribute to enhancing coral health and resilience. In addition, we could identify other families of Alpha- and Gamma-proteobacteria that are frequently found in corals, such as Saccharospirillaceae, Flavobacteriaceae, and Sphingomonadaceae (Delgadillo-Ordoñez et al., 2022). We identified the Sphingomonadaceae genus *Sphingomonas* as a shallow specialist taxon in our dataset. Members of this family have been proposed to be putative coral pathogens (Rosales et al., 2019).

We identified rare (less abundant) taxa from two genera in the phyla Firmicutes, *Mycoplasma*, and *Spiroplasma*. This phylum is assumed to include mutualistic or commensal microorganisms in temperate and deep-sea gorgonian species as well as in cold-water scleractinian corals (Meyer et al., 2019b; Tandon, Chiou, et al., 2022b; van de Water et al., 2017). It is also assumed to be involved in the assimilation and dissimilation of sulfur reduction (Yang et al., 2019). The genus *Mycoplasma* was observed in all samples and is commonly found in gorgonians (Gray et al., 2011; Holm & Heidelberg, 2016) and cold-water scleractinians (Kellogg et al., 2009; Neulinger et al., 2009).

However, its precise functional role in corals and cnidarians remains unknown (Samuel A. Vohsen et al., 2022). Interestingly, we identified *Spiroplasma,* which is known for its capacity to protect the host against pathogens (Ballinger & Perlman, 2019), as a shallow depth-specialized taxon in our *Eunicella* samples. It is believed to confer protection against fungi through the production of unique toxins (Ballinger & Perlman, 2019). This suggests its potential role in coral resilience against pathogens.

Certain bacterial taxa were strongly associated with the depth. For instance, BD1-7 genus (family Spongiiabcteraceae) was more prevalent in our mesophotic samples. This is consistent with its identification in the microbiomes of the mesophotic black corals *Antipathella subpinnata* and *Eunicella cavolini* at a depth of approximately 60 m (van de Water et al., 2020). It has also been recognized as a core member of the microbiome of *Eunicella singularis* (van de Water, Voolstra, et al., 2018). In addition, Spongiiabcteraceae has been reported to be associated with the degradation of mono- and polycyclic aromatics (Ribicic et al., 2018).

Despite its low abundance, the genus *Thalassolituus* (family Saccharospirillaceae) was predominantly found in mesophotic *E. singularis*. It is assumed to be involved in the carbon and nitrogen cycles by utilizing acetate and C7-C20 aliphatic hydrocarbons for carbon, as well as ammonia and nitrate for nitrogen (Satomi & Fujii, 2014). It has also been identified among associated bacteria in the endemic reef coral *Mussismilia braziliensis* (Reis et al., 2009). However, we are unaware of previous studies that have addressed the presence of *Thalassolituus* in the *Eunicella* microbiome. Similarly, *Aquimarina* (family Flavobacteriaceae) was identified as a mesophotic specialist taxon. Keller-Costa et al. (Keller-Costa et al., 2016) successfully isolated *Aquimarina* sp. strain EL33 from *Eunicella labiata* and obtained a nearly complete genome sequence. Analyses of the *Aquimarina* genome have revealed its potential roles in nutrient acquisition, utilization, and defense (Keller-Costa et al., 2016). This finding offers valuable insights into the functional contribution of this bacterium to the holobiont. In addition to nutrient cycling, it has been suggested that it might inhibit pathogenic bacteria by producing exoenzymes, organic compounds, and bacteriocin (Suantika, 2013).

Generally, the taxonomic analysis of *E. singularis* revealed an absence of *Symbiodinium* with increasing depth, signaling a shift in microbiome composition. While the dominant bacterial species remained consistent, variation in the bacterial community was primarily observed among rare bacterial members (less abundant), with certain taxa showing depth specificity. In addition, the bacterial taxa identified as mesophotic depth specialists are assumed to be capable of using different carbon sources, such as aromatic and hydrocarbon compounds (Ribicic et al., 2018), implying their metabolic versatility and adaptability to unique environmental conditions.

4.3. ***Impact of depth on E. singularis microbiome functions***

Overall, we could not find differences in the metabolic pathways between *Symbiodinium* and the associated prokaryotic community at either depth. However, the photosynthesis pathway (ko00195) was found only in the shallow sample microbiome. This can be attributed to the absence of endosymbiotic algae in the mesophotic samples coupled with insufficient light enrichment at lower depths. Furthermore, differences in the abundance of certain functional genes related to energy and amino acid metabolism were detected. For instance, the ribulose-bisphosphate carboxylase large chain (RuBisCO large chain – *rbcL, cbbL*), which is related to carbon fixation in photosynthetic organisms, is prevalent in the shallow *E. Singularis* microbiome. Furthermore, many *Symbiodinium* ORFs encoding RuBisCO were present. This could be because *Symbiodinium* may have multiple copies of RuBisCO genes (Shoguchi et al., 2018), and also due to the prediction of different exons from the same gene as well as due to the presence of fragmented genes. Moreover, the prokaryotic community in the shallow *E. Singularis* microbiome exhibited high carbon fixation gene numbers. This suggests a relevant role of prokaryotes in providing fixed carbon to the coral. Until recently, only *Symbiodinium* was considered responsible for carbon fixation in coral holobionts (Robbins et al., 2019b). This could also explain the presence of autotrophic prokaryotic MAG *Phormidesmiaceae* (Cyanobacteria) in the microbiome.

Moreover, dinoflagellates can hold multiple distinct copies of a single gene (Shoguchi et al., 2013b). This might explain the high number of ORFs that encode DNA methylation, particularly DNA (cytosine-5)-methyltransferase (K00558, K17398). DNA (cytosine-5)-methyltransferase is known to regulate gene expression and DNA maintenance (Moore et al., 2013). One potential explanation for the abundance of these enzymes in shallow samples could be the nature of the endosymbiotic relationship between *Symbiodinium* and coral hosts. Although *Symbiodinium* may adjust its gene expression in response to coral functions (Mohamed et al., 2016), the specific mechanisms underlying this process remain unclear. Therefore, although DNA methylation likely contributes to these regulatory mechanisms, further research is needed to unravel the full extent of how *Symbiodinium* and corals interact and influence each other's gene expression and physiological processes.

We further explored how the prokaryotic microbiome might contribute to enhancing the access of corals to energy. The increased abundance of some pathways, such as cytochrome c oxidase, in the mesophotic community suggests higher energy production. This increase in energy production could lead to higher microbial activity, which may support coral health and resilience by providing additional energy sources and facilitating metabolic processes crucial for survival in mesophotic environments. In addition, the mesophotic community showed a higher enrichment of some lipid metabolism functions, especially acyl-CoA oxidase. This allows fatty acids to be used as carbon sources (S. Kim & Kim, 2018) for energy production by the prokaryotic community. In addition, the higher abundance of genes related to carbohydrate metabolism, such as UDP-glucuronate decarboxylase, could indicate higher biosynthesis of nucleotide sugars, such as UDP-xylose (Moriarity et al., 2002), which serves as a key precursor for the synthesis of diverse glycan structures and is essential for bacterial growth (Bontemps et al., 2003) and interaction with the host (Banahene et al., 2022). This might be a possible mechanism by which the prokaryotic community can colonize and evade the host immune-like responses or contribute to the host response to pathogens (Lee et al., 2022).

Moreover, the mesophotic community showed a higher abundance of genes related to amino acid metabolism such as γ-glutamyltranspeptidase (GGT). This implies that the prokaryotic community uses GGT to degrade glutathione for amino acid utilization and as a nitrogen source. It can also be a virulence factor in some pathogenic gram-negative bacteria (Saini et al., 2021). In addition, the enriched steroid degradation pathway in the mesophotic prokaryotic community implies their capacity to use organic compounds such as steroids as carbon sources. Furthermore, the existence of Pinene, camphor, and geraniol degradation functional genes gives the assumption of the capability of the prokaryotic community to use aromatic hydrocarbons as a carbon source (Bhuvaneswari, 2013), and their ability to degrade antibiotics. This observation suggests that the prokaryotic community associated with mesophotic *Eunicella Singularis* may have a distinct capacity to utilize various carbon sources from their environment.

Figure 22. Main metabolic activities of shallow-water and mesophotic microbial communities associated with *E. singularis*. In shallow waters, the microbiome, particularly *Symbiodinium*, uses photosynthesis as a source of carbon (left panel). In contrast, the mesophotic microbiome exhibited different metabolic pathways related to carbon metabolism, including steroid and aromatic hydrocarbon degradation, reflecting their adaptation to deeper, lower-light environments (right panel).

In summary, our analysis revealed remarkable similarities in the metabolic pathways between *Symbiodinium* and the associated prokaryotic community across both shallow and mesophotic waters, except for the exclusive presence of the photosynthetic pathway in the shallow samples due to the presence of *Symbiodinium*, alongside specific autotrophic prokaryotes. In turn, the mesophotic community displayed an increase in gene abundance related to energy production and the utilization of diverse carbon sources, including fatty acids, steroids, and hydrocarbon compounds.

4.4. ***Exploring the Functional Potential of Microbial Taxa in the Eunicella singularis Microbiome***

Our MAGs indicate domination of Endozoicomondaceae in the *E. Singularis* microbiome across depth, which is further supported by the mTAGs classification. Interestingly, functional annotation of these MAGs allowed us to delve deeper into their metabolic potential, focusing on the shared prokaryotic metabolic pathways that varied across depths, such as carbohydrate metabolism, oxidative phosphorylation, cofactor and vitamin metabolism, and secretion systems. While glycolysis and gluconeogenesis were widespread among MAGs, oxidative phosphorylation genes were less common, with notable findings in specific taxa. For instance, NADH-quinone oxidoreductase genes have been exclusively identified in MAG.22 (Sphingomonas), highlighting its potential role in energy production. Moreover, the presence of cytochrome cbb3-type in MAG.22 (Sphingomonas) MAG.17 and MAG.25993 (Endozoicomonadaceae) suggests adaptations to varying oxygen levels (Lunak & Noel, 2015).

Cofactor and vitamin metabolism genes were detected in a subset of MAGs, including Phormidesmiaceae, Pseudomonadales, and Sphingomonadales, indicating their importance in microbial growth and metabolism. Vitamin B plays a central metabolic role in marine bacteria and is important for nutrient uptake (Sañudo-Wilhelmy et al., 2014). We detected a variety of vitamin B biosynthesis pathways in MAGs, including pantothenate (B_5), pyridoxal (B_6), biotin (B_7), and cobalamin (B_{12}). For example, MAGs from the genera DT-91 (Order Pseudomonadales) and SIO4C1 (Order Phormidesmiaceae) were found to encode genes responsible for vitamin B_{12} biosynthesis.

It is an important vitamin for corals and its symbiont *Symbiodinium* because both lack cobalamin biosynthesis capability (Villela et al., 2023), which is required for methionine synthesis in coral hosts (Robbins et al., 2019b). This implies a potential role of both Pseudomonadales and Phormidesmiaceae in supporting corals with B_{12}.

Moreover, some taxa showed potential for the biosynthesis of pantothenate (B_5), such as Endozoicomonadaceae MAGs and GCA-001730085. Vitamin B_5 has been suggested to play a role in energy generation as a precursor of coenzyme A, in addition to its use by commensal bacteria to enhance the protective activity against pathogens (Yoshii et al., 2019). However, its precise role in coral microbiome remains unknown. In addition, many MAGs were found to contribute to B_7 biosynthesis, which is essential for bacterial metabolism, particularly in processes such as gluconeogenesis and fatty acid synthesis (Wienhausen et al., 2022). Although biotin biosynthesis in bacteria involves multiple steps, comprehensive studies on marine bacteria are required to fully understand biotin metabolism in marine environments (Wienhausen et al., 2022).

Additionally, the presence of type II and III secretion systems in three MAGs (DT-91, Endozoicomonas, and Sphingomonas) indicated their possible role in pathogenesis. The type II secretion system is a multiprotein system that translocates substances through the outer bacterial membrane, including virulence factors, enzymes, and effectors (Ghosal et al., 2019). TSS III functions as an injectisome, allowing these bacteria to manipulate targeted cells and facilitate their transport across their membranes (Milne-Davies et al., 2021). Sphingomonas was previously identified as a putative coral pathogen which explains the presence of these virulence factors in the genome. However, *Endozicomonas* is recognized as a coral symbiont, but lately, the nature of this relationship has been questioned (Pogoreutz & Ziegler, 2024). One possible explanation is that *Endoziocomoans* may have an "accidental" pathogenic mode. To illustrate, the T3SS present in accidental pathogens serves as a fitness element, enhancing survival and interaction in benign associations with primary hosts, while acting as a virulence factor in accidental hosts. These pathogens may reside harmlessly in the hosts but can cause damage when encountering accidental hosts, although infection typically does not facilitate pathogen spread (Puhar & Sansonetti, 2014).

4.5. The impact of thermal stress on D. pertusum microbiome

The increase in ocean temperature threatens mesophotic habitats, resulting in a decline in coral populations and affecting the diversity of benthic communities (Castellan et al., 2022). Organisms such as *D. pertusum* are especially vulnerable to these changes because of their susceptibility to disturbance and slow recovery rates, which exacerbate the effects of climate change on coral ecosystems (Clark et al., 2016). Despite these challenges, the current literature on the microbiome of cold-water corals (CWC) remains limited, underscoring the pressing need for more comprehensive investigations. Therefore, understanding the response of the coral microbiome to such challenges is crucial (Epstein, Smith, et al., 2019; Tang et al., 2019). Our study addresses this gap and provides evidence that prolonged exposure to elevated water temperatures affects the functional capabilities of *the D. pertusum* microbiome. Furthermore, our findings suggest that temperature plays an important role in shaping the genetic and metabolic landscapes of the *D. pertusum* microbiome, potentially influencing its nitrogen cycle, carbon metabolism, and pathogenicity.

The gradual increase in some carbon metabolism genes observed during prolonged exposure to elevated temperatures (+3 °C and +5 °C) suggests heightened energy (Dean et al., 2018). This increase in functional genes related to formaldehyde assimilation (serine pathway) may facilitate the production of various one-carbon compounds (C1) that serve as metabolic intermediates for energy generation. These C1 substrates, such as formaldehyde and methanol, are assimilated by methylotrophs via formaldehyde assimilation pathways (T. Wu et al., 2023), which are integral to methanol metabolism (N. H. Chen et al., 2016). Therefore, the presence of a formaldehyde assimilation module in the genomes of some Gammaproteobacteria, such as

Rhodobacterales and Rhizobiales, suggests their potential for methylotrophy. The formaldehyde assimilation pathways are rarely discussed in the context of coral microbiomes, making these findings noteworthy and potentially indicative of unique metabolic capabilities within the microbial community. Such findings could offer new insights into how coral-associated microbes adapt to and mitigate environmental stressors. Moreover, this highlights the metabolic adaptability of these bacterial taxa, specifically Rhodobacterales and Rhizobiales, allowing them to efficiently utilize diverse carbon sources for growth and metabolism in thermally stressed microbiomes.

Additionally, coral mucus is known to be a complex mixture of proteins, lipids, and carbohydrates (Wright et al., 2019), mainly composed of C6 sugars (glucose, mannose, and galactose), deoxysugars (fucose and rhamnose), amino sugars (N-acetyl glucosamine), and C5 sugars (xylose) in the CWC (Wild et al., 2010). These carbohydrates are considered rich energy sources for the microbiome (Hadaidi et al., 2019). The increase in abundance that has been found in some carbohydrate degradation enzymes with increasing temperature such as β-1,6-Glucosidase, Mannosyl-glycoprotein Endo-β-N-Acetylglucosaminidase, β-D-Arabinofuranosidase, and α-Amylase might reflect the heightened energy uptake through carbohydrate by microbiome to cope with the changing environmental conditions (De Beul et al., 2021). Consequently, this increase in degrading enzymes in the coral microbiome may accelerate the decomposition of the mucus layer of stressed corals, which affects coral health. These enzymes may facilitate specific biochemical processes or reactions related to carbohydrate degradation or modification in response to the stress caused by elevated temperatures. This particular adaptation implies the microbiome's ability to respond dynamically to fluctuating energy requirements in its environment (Pei et al., 2022).

4.5.1. *Temperature-Induced Pathogenic Bacteria and Secretion Systems in the D. pertusum Microbiome*

The increase in temperature may lead to an increase in pathogenic bacteria in the *D. pertusum* microbiome. A recent study by Chemel et al., 2024, has shed light on the escalation of pathogenic activity in *the D. pertusum* microbiome under prolonged thermal stress (15 °C). They identified potentially pathogenic ASVs, including those belonging to *Myxococcaceae*, *Vibrionaceae*, *Alteromonadaceae*, UBA4486 (Gammaproteobacteria), and Puniceispirillales. We detected an increase in the mTAGs abundance of Vibrionales with increasing temperature on day 60 (13 °C and 15 °C), which further supports their results. Furthermore, our investigation revealed an increase in functional genes related to bacterial secretion systems T1SS and T3SS with rising water temperatures, suggesting a potential induction of pathogenic activity, as reported by Chemel et al., 2024. The T3SS functions as an injectisome, enabling bacteria to manipulate host cells and facilitating the transport of macromolecules across membranes (Milne-Davies et al., 2021). The presence of T3SS-related genes was detected in genomes of Rhodobacterales, Pseudomonadales, Chlamydiales, and Geminicoccales. These taxa exhibit increased abundance under thermal stress and have been implicated in stony coral tissue loss (Rosales et al., 2020). Notably, Rhodobacterales were present in the control temperature (10˚C) and increased in abundance with temperature treatments (13, and 15 °C), suggesting their potential as opportunistic bacteria. Notably, this study is the first to report Geminicoccales in the *D. pertusum* microbiome, with the genome encoding both components of T3SS, indicating their potential as cold-water coral pathogens.

Moreover, the type-I bacterial secretion ATP-binding cassette, a hemolysin transporter, was found to be more abundant than T3SS in our analysis and was encoded in many MAGs, including Minwuiales, Rhizobiales, and Sphingomonadales. The T1SS component is an exporter of various substrates, including RTX toxins and bacteriocins, through the cellular membranes (Kanonenberg et al., 2019). Therefore, it can be found in both pathogenic and non-pathogenic bacteria. However, toxin production usually occurs under stressful conditions, such as high water temperatures, and is used for self-immunity and to inhibit or eliminate closely related species for survival (Smits et al., 2020). The Minwuiales is a marine bacterial order belonging to Alphaproteobacteria (Sun et al., 2018), and we could not find any reports of this order in the coral microbiome. The presence of T1SS suggests its potential as a coral pathogen. In addition, members of the order Sphingomonadales have been described as putative coral pathogens (Rosales et al., 2019). Similarly, Rhizobiales is a potential coral pathogen and has been reported in Stony Coral Tissue Loss Disease (Rosales et al., 2020), which suggests the use of T1SS for pathogenicity.

4.5.2. *Impact of Thermal Stress on Nitrogen cycling in D. pertusum Microbiome*

The coral microbiome hosts a diverse array of nitrifying and denitrifying bacteria, which are crucial for transforming nitrogen-related waste into non-toxic compounds (Boilard et al., 2020; Kimes et al., 2010; Rädecker et al., 2015). Moreover, these bacteria are important for supplying organic nitrogen to the host, especially under low-nitrogen conditions (Boilard et al., 2020). In particular, diazotrophic communities are key players in nitrogen cycling, providing diazotrophically derived nitrogen (DDN) to the host (Benavides et al., 2017). Therefore, understanding the implications of disturbances in microbial nitrogen cycling on coral health is essential for understanding ecosystem responses to environmental changes. In the case of *D. pertusum*, meticulous regulation of nitrogen balance helps mitigate nitrogen loss by recycling nitrogen through the microbiome, thus minimizing the impact of high ammonium excretion rates in mucus (Middelburg et al., 2015b). However, disturbances in the regulation of nitrogen cycling may lead to nitrogen influx (M. Li et al., 2023), excessive ammonia stimulation, and nitrogen loss (Tilstra et al., 2019). This could increase the vulnerability of corals to thermal stress (Fernandes de Barros Marangoni et al., 2020) and diseases (Rädecker et al., 2015). In addition, D. pertusum appears to release dissolved inorganic nitrogen (DIN) and nutrient-rich mucus into the surrounding water (Middelburg et al., 2015b). This nutrient release might provide a rich source of nutrients, promoting the growth and activity of nitrogen-cycling microbial taxa such as Dadabacteriales, Rhodobacterales, and Rhodospirillales (D'Angelo et al., 2023; Rubio-Portillo et al., 2016).

We could identify various nitrogen metabolism pathways in our metagenomic samples such as dissimilatory NO_3-/NO_2- to ammonium (DNRA), assimilatory NO_3-/NO_2- pathways (ANRA), denitrification, and nitrification. Some of these pathways require anoxic conditions (low concentrations or absence of oxygen) such as reduction to ammonium and denitrification. Although they required anaerobic conditions, the presence of these pathways in the coral microbiome is not surprising (Babbin et al., 2021) and has been reported in the coral microbiome. Similar to different biological systems with micro-anaerobic sites that exist in aquatic environments such as cyanobacterial and algal aggregates (Klawonn et al., 2015), marine snow particles, and sediments (Fennel et al., 2009), the principle that biological oxygen consumption exceeds physical aeration through slow diffusion can be found in coral colonies due to their mucus production (Babbin et al., 2021). This mucus not only slows the diffusion of oxygen from the surrounding seawater but also serves as a carbon source that stimulates aerobic heterotrophy, further depleting oxygen levels (Wild et al., 2004). As a result, the thicker the mucus layer, the greater the potential for anaerobic processes to occur even when bulk oxygen concentrations remain relatively high (Dalsgaard et al., 2014).

Despite the diversity of the nitrogen metabolism genes identified, the most abundant genes belonged to the dissimilatory and assimilatory NO_3- to NO_2- pathways (DNR, ANR), such as *nap, nar, and nas*, which are indicators of DNR and ANR, suggesting an increase in nitrogen assimilation (Figure 25A). This implies a potential increase in nitrate respiration activity and energy synthesis/ATP synthesis, where nitrate is used as an electron acceptor in low concentrations or absence of oxygen (Ziv-El & Rittmann, 2009). This could facilitate the anaerobic respiration allowing the microbial community to thrive in low-oxygen or variable oxygen environments. Also, it has been found that coral constantly releases inorganic nitrogen, such as nitrite and nitrate (Middelburg et al., 2015b), which prokaryotes can use for nitrate respiration. However, the increase in the *narG* gene, which is involved in the DNR pathway, suggests higher nitrate reduction. This process can potentially lead to nitrogen loss (Asamoto et al., 2021) because the produced nitrite can be further reduced to gaseous forms of nitrogen, such as nitrous oxide (N_2O) or nitrogen gas (N_2). Alternatively, other microbes can also utilize this nitrite, potentially enhancing microbial biomass (Peng et al., 2015).

Notably, the presence of nitrite ammonification genes *nrfH* and *nrfA* in most MAGs (Figure 25C) and their increase in abundance with thermal stress suggest higher prokaryotic nitrite ammonification by using NO_2- directly for respiration and producing ammonium as a byproduct. The nitrite ammonification process forms part of the DNRA pathway which is assumed to be beneficial for coral fitness by increasing the availability of DIN through ammonium formation (Babbin et al., 2021) and reducing the impact of thermal stress in case of elevated temperature (Fernandes de Barros Marangoni et al., 2020). Additionally, nitrogen assimilation, in normal condition, is essential for *D. pertusum* survival in resource-depleted dark environment (Middelburg et al., 2015b) and could provide *D. pertusum* with nitrogen for the maintenance of coral metabolism under stressful conditions (Béraud et al., 2013). However, excessive nitrogen availability may create more favorable conditions for certain taxa that can thrive in nitrogen-rich environments the stressed coral microenvironment. This shift could lead to an imbalance in the coral microbiome and potentially disrupt essential microbial interactions, thereby altering the microbiome (Xiang et al., 2022). It could also cause metabolic stress in corals by increasing the phosphorus limitation and imbalance of the N:P stoichiometry, which may lead to diseases and mortality (Lapointe et al., 2019).

Moreover, the presence of nitrogen fixation genes, such as vnf and nif, in our dataset and MAGs belonging to Rhodobacterales (genus Mangrovicoccus), which showed a significant increase with thermal stress, indicates their ability to use different metal cofactors. For instance, FeMo-co is used in molybdenum-nitrogenase (Mo-nitrogenase) and FeV-co in vanadium-nitrogenase (V-nitrogenase). Mo-nitrogenase is the most active and commonly expressed nitrogenase enzyme at ambient temperatures, whereas V-nitrogenase is typically produced only under molybdenum-deficient conditions. This implies a potential role in supplying the coral with DIN through the fixation of atmospheric N_2. It has been proposed that during thermal stress events, corals may enhance the population and activity of diazotrophs [95], which can increase the available DIN for the coral host (Babbin et al., 2021). This may explain the increased abundance of *Mangrovicoccus* observed under thermal stress.

Surprisingly, the nitrification genes *amo* and *hao* were found in our dataset at low abundance and were not affected by prolonged thermal conditions (Figure 25A). Despite the expected presence of nitrification genes in our MAGs, their low abundance suggests a limited nitrification process. In contrast, denitrification, a microbial process that converts nitrate (NO_3^-) to nitrogen gas (N_2) or nitrous oxide (N_2O), is common in coral microbiomes (Glaze et al., 2022). This process is assumed to occur in anoxic microniches within *D. pertusum* mucus or the gastric cavity (Middelburg et al., 2015b) and helps maintain bioavailable nitrogen levels while reducing surplus excretion (Tilstra et al., 2021). Unlike tropical corals, where denitrification is of limited functional importance and denitrifiers likely respond opportunistically to inorganic nitrogen availability, it is a ubiquitous process in the D. *pertusum* microbiome, occurring regardless of physiology and habitat (Glaze et al., 2022).

Interestingly, in the thermally stressed D. *pertusum* microbiome, the abundance of denitrification genes increased compared to those involved in DNRA and N2 fixation (Figure 25A). The rise in genes such as *nor*, which contributes to N_2O production, and *nos*, which converts N_2O to N_2, suggests that the microbiome may respond to thermal stress by actively engaging in denitrification. This response results in the loss of fixed nitrogen from the system, potentially as a strategy to prevent nitrogen overload and maintain a balanced nitrogen cycle under stress conditions. Importantly, Middelburg et al. (2015) have provided insights into the role of prokaryotes in nitrogen production and consumption in D. *pertusum*, but further research is needed to quantify the exact levels of nitrogen produced by prokaryotic symbionts and corals under prolonged thermal stress conditions. Understanding these dynamics is crucial for assessing how thermal stress impacts the nitrogen cycle within coral microbiomes.

Interestingly, several MAGs that increased under thermal stress, particularly those of the genus Mangrovicoccus, demonstrated a potential capacity for denitrification by possessing a full suite of denitrification genes (Figure 25C). This is significant because Rhodobacteriales, which have been previously linked to denitrification processes (Middelburg et al., 2015b), were also prevalent, suggesting a crucial role for this genus in the denitrification process. Although denitrifiers play a beneficial role in balancing nitrogen levels, an increase in denitrification activity can lead to greater loss of fixed nitrogen, thereby reducing the availability of dissolved inorganic nitrogen (DIN) for corals (Tilstra et al., 2019). These findings indicate that denitrification activity in the microbiome may be higher compared to DIN production through dissimilatory nitrate reduction to ammonium (DNRA) or atmospheric nitrogen fixation. This situation is concerning because thermally stressed D. *pertusum* corals have been shown to reduce their energy reserves, such as lipids and proteins, redirecting their energy intake towards survival rather than growth (Chapron et al., 2021). Consequently, the increased loss of fixed nitrogen due to heightened denitrification under thermal stress could further strain the coral's already limited energy resources. However, further investigations are required to quantify the amount of fixed nitrogen loss under thermal stress in comparison to DIN production and nitrogen fixation. Additionally, measuring the expression levels of denitrification genes is essential to confirm these findings and provide a more comprehensive understanding of microbial dynamics under thermal stress.

Altogether, our study revealed that increasing temperatures significantly impact the microbiome structure of D. *pertusum* at both taxonomic and functional levels. Metagenomic analyses supported previous research showing the dominance of Rhodobacterales under thermal stress. Moreover, our analyses indicated a shift in metabolic capacity towards methylotrophic bacteria, which may destabilize the microbiome and promote the growth of opportunistic pathogenic organisms. Indeed, we found an increase in pathogenic marker genes and some MAGs that possess these markers within the D. *pertusum* microbiome as temperature increased. Additionally, we observed a variation in gene abundance associated with diazotrophic activity, including denitrification and nitrification, which could disrupt the nitrogen cycle balance between the coral and its microbiome, potentially increasing susceptibility to diseases and mortality. Together, these findings underscore the influence of increasing environmental temperature on the taxonomic and functional structure of the microbiome. However, further research is required to investigate the gene expression profiles associated with formaldehyde assimilation, denitrification, and nitrification. Examining the expression levels of these metabolic pathways would provide deeper insights into their activity and regulation, contributing to a more comprehensive understanding of their roles in the microbiome's response to environmental stressors such as temperature increases.

5. CONCLUSIONS AND FUTURE PERSPECTIVES

5.1. ***The coral microbiome***

The symbiotic relationship between corals and their microbial partners is fundamental to the health and resilience of coral ecosystems. Corals provide a range of microenvironments that support unique microbial communities, which in turn supply essential nutrients, energy, and antibiotics to their coral hosts. Despite ongoing research on factors influencing coral microbiome acquisition, such as coral age, taxonomy, and environmental changes, conclusive data remain elusive, necessitating further investigation. The symbiotic relationship between corals and their microbial partners is fundamental to the health and resilience of coral ecosystems. Corals provide a range of microenvironments that support unique microbial communities, which in turn supply essential nutrients, energy, and antibiotics to their coral hosts. Despite ongoing research on factors influencing coral microbiome acquisition, such as coral age, taxonomy, and environmental changes, conclusive data remain elusive, necessitating further investigation. Advances in -omic technologies hold promise for understanding the intricate dynamics within coral-microbe communities. Metagenomic analysis can identify critical genes and species that respond to various stressors and their impact on stress resilience. Additionally, metatranscriptomics can reveal actively expressed genes within the microbiome, shedding light on key pathways in microbial community interactions with coral hosts. However, challenges persist, such as low microbial DNA density, the presence of genes with unknown functions (particularly among eukaryotes), and limitations in the comprehensiveness and accuracy of available databases. These limitations can hinder the identification and functional annotation of microbial genes, making it difficult to fully understand microbial roles and interactions. To enhance comparability across studies, the adoption of standardized protocols for model coral species has been proposed, enabling the creation of harmonized multi-omics datasets. Such standardization would facilitate more accurate cross-study comparisons and contribute to a more cohesive understanding of coral-microbe interactions.

5.2. ***The Depth influences Eunicella singularis microbiome***

Eunicella, a soft gorgonian coral species commonly found in the Mediterranean Sea, possesses a microbiome that exhibits changes in taxonomic composition and function with depth. In shallow coral samples, the microbial community was predominantly composed of *Symbiodinium*, which explains the prevalence of photosynthesis and carbon fixation genes. In addition, some bacterial taxa, such as *Spiroplasma*, showed shallow depth preference. In contrast, the mesophotic *Eunicella* samples showed a higher prevalence of prokaryotes, such as *Thalassolituus,* BD1-7 clade*,* and *Aquimarina*. Moreover, the mesophotic microbiome showed a higher abundance of metabolic pathways related to carbon metabolism, suggesting its ability to adapt to various alternative sources of carbon. In addition, it showed a higher gene abundance related to cofactors and energy metabolism, suggesting higher microbial activity. These findings shed light on the poorly understood aspects of coral-bacterial symbiosis and highlight potential pathways for further research.

5.3. ***The impact of the thermal stress on D. pertusum microbiome***

To ensure deep-ocean sustainability, addressing the implications of climate change is imperative (Chapron et al., 2021; Dodds et al., 2007; Gori et al., 2014; Naumann et al., 2014). The relationship between corals and microorganisms is crucial for resilience and ecosystem health. However, the manifold effects of climate change on coral holobionts, including cold-water corals, remain inadequately understood (Chapron et al., 2021). Our investigation sheds light on the functional responses of the *D. pertusum* microbiome to extended thermal stress, revealing augmentation in specific metabolic pathways, particularly the carbon, nitrogen, and secretion systems. These findings suggest that microbial responses are adapting to utilize diverse forms of nitrogen and carbon as alternative energy sources. This indicates a potential shift in the microbiome community, with a possible increase in methylotrophs and denitrifiers. In addition, an increase in water temperature could incentivize pathogenic activity and enhance the thriving of opportunistic pathogens, such as Rhodobacterales. Although relevant in characterizing gene abundances, our research did not encompass the active expression of these genes. The future application of meta-transcriptomic and other -omics methodologies offers a promising avenue for a more profound understanding of the functionality of the *D. pertusum* microbiome. These insights are invaluable for forecasting future scenarios and advancing the conservation of benthic communities, which is crucial for mitigating the impact of thermal stress.

*5.4. **Future Perspectives***

5.4.1. The Nature of Endozoicomonas-Coral symbiosis

The coral microbiome field is highly dynamic, emphasizing the need to explore the symbiotic relationships between coral hosts and their diverse symbionts. The symbiotic relationship between corals and endosymbiotic dinoflagellates is well established in symbiotic corals. In contrast, prokaryote-coral symbiosis is ubiquitous across all coral types, underscoring its broad ecological significance. As previously described (Section 4.4.), the importance of this relationship still has many aspects that remain to be discovered. For example, *Endozoicomonas* has been widely identified as a coral symbiont bacterium. Recently, advances in metagenomic tools and the availability of Endozoicomonas genomes have led to a reassessment of the nature of this relationship. Metagenomic evidence, including genome size, insertion sequence (IS) expansion, pseudogenization, and the presence of eukaryotic-like proteins (ELPs) such as TPRs and ARPs, as well as secretion systems, suggests the potential for different types of symbiosis, such as commensalism, parasitism, or opportunistic pathogenesis.

In certain instances, the genome size of Endozoicomonas can be notably large, surpassing 7Mb, particularly in coral isolates (Pogoreutz et al., 2022). Large bacterial genomes often reflect significant selection pressures, exemplifying a prokaryotic strategy to accommodate diverse environmental challenges through expanded metabolic and regulatory capabilities. This suggests that *Endozoicomonas* may adopt an opportunistic lifestyle that extends beyond a strict host-associated setting. (Pogoreutz & Ziegler, 2024). Ding et al. (Ding et al., 2016) delineated various degrees of coral host specificity within *Endozoicomonas*. They identified *Endozoicomonas montiporae* as a potentially host-restricted facultative endosymbiont characterized by signs of genomic insertion sequence (IS) expansion and pseudogenization. The expansion of IS elements often indicates adaptation to a new niche or specialization towards a specific lifestyle, which can include mutualism, parasitism, or pathogenesis (Siguier et al., 2014).

One potential way to address this is to investigate the genomes of different coral species. Comparing the different genomes at the phylogenetic and metabolic levels could open doors to understanding the different possible roles of each *Endoziocomonas* taxon in each coral host. It is possible that some coral species may benefit from this symbiosis more than others. However, it has been suggested that coral- *Endoziocomonas* symbiosis has a species-specific nature (Hochart et al., 2023). Yet the specific role of these taxa needs further research , studying the genomic insertion expansion and how the coral host communicates with the specific *Endoziocomonas*.

5.4.2. Other microbiome taxa

Some other microbial taxa, such as Firmicutes, were found to be dominant along with *Endoziocomonas* in shallow-water gorgonian species from the Caribbean. However, we could not detect domination of Firmicutes in the Gorgonian *Eunicilla Singularis* from the Mediterranean Sea, which raises the question of whether this relationship is more influenced by the geographical distribution of the coral's phylogenetic type. In contrast, the microbial taxon of the genus *Bermanella* was found to be dominant along with *Endoziocomonas* in the mesophotic *Eunicella Singularis* microbiome. However, the role of *Bermanella* in the coral microbiome remains poorly understood. To date, only one species belonging to this genus has been described, and its specific role remains unclear. *Bermanella* has been suggested to participate in hydrocarbon degradation, which could indicate a specialized environmental niche.

5.4.3. The impact of thermal stress on CWC microbial nitrogen

During analysis of thermal stress impact on the cold-water coral D. *pertusum* microbiome, we observed an increase in denitrification genes, potentially indicating heightened fixed nitrogen loss. Concurrently, Rhodobacterales MAGs, notably *Mangrovicoccus*, showed an increase, suggesting potential diazotrophic activity. This implies corals may enhance diazotrophs to mitigate excessive nitrogen loss. Further investigation is needed to quantify N2 loss under thermal stress compared to DIN production and nitrogen fixation. Additionally, exploring gene expression profiles related to formaldehyde assimilation, denitrification, and nitrification will provide deeper insights into their activity and regulation, enhancing understanding of their roles in microbiome responses to environmental stressors like temperature increases.

6. Supplementary Figures and Tables

6.1. Supplementary Figures

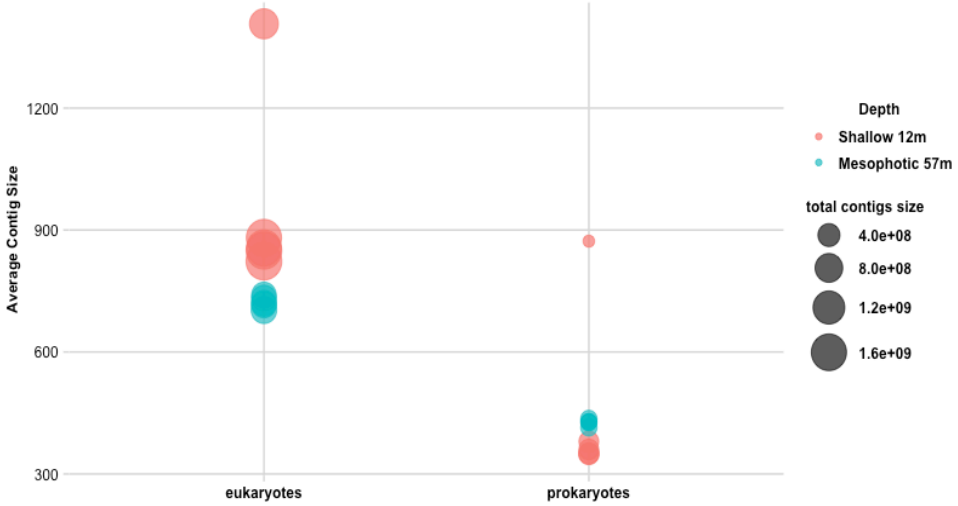

Supplementary Figure 1. Comparison of eukaryotic and prokaryotic contig sizes in shallow and mesophotic coral samples. Shallow metagenomes featured larger eukaryotic contigs, whereas mesophotic metagenomes exhibited slightly larger prokaryotic contigs than those in shallow samples.

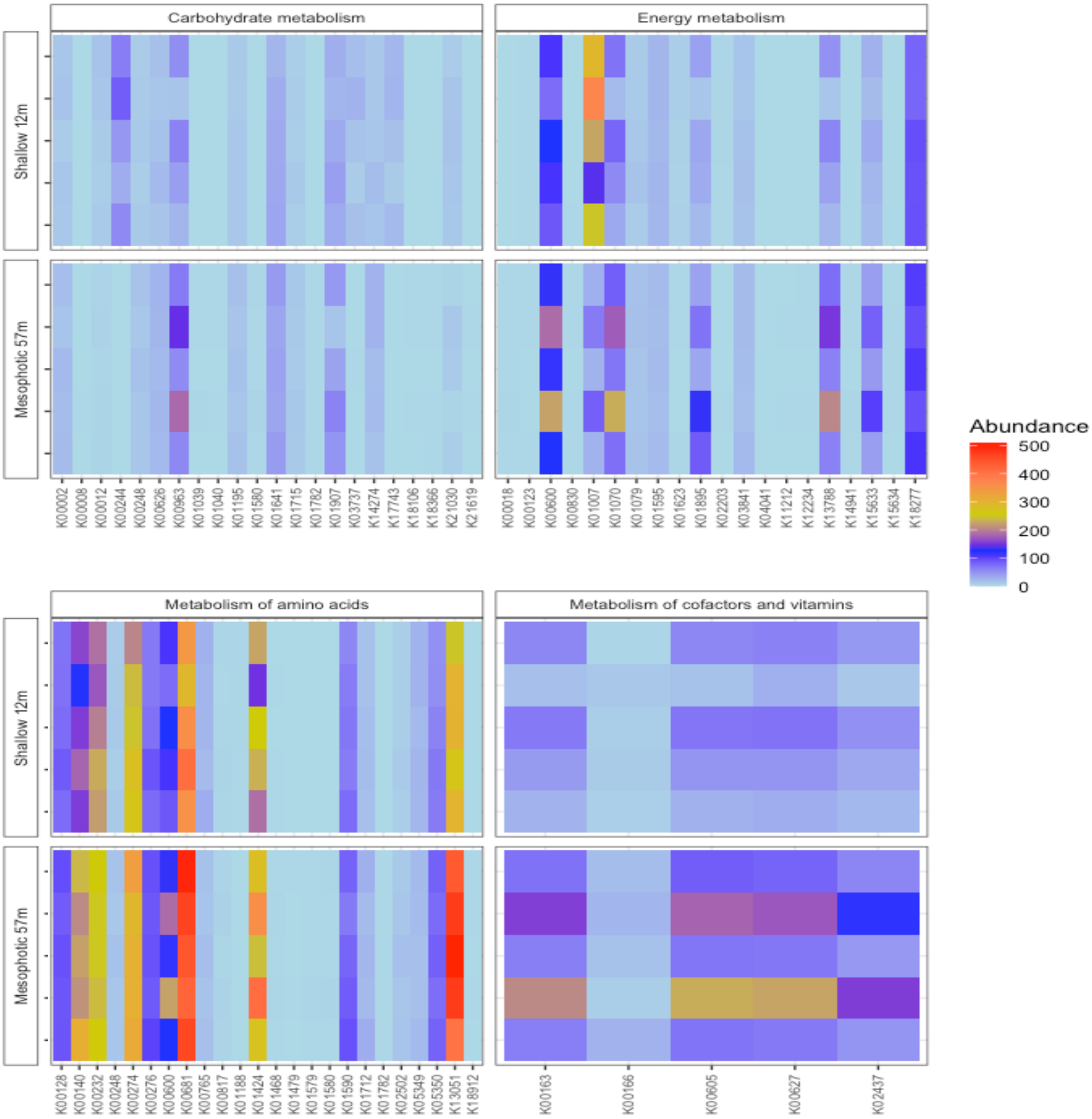

Supplementary Figure 2. Enrichment analysis of prokaryotic KEGG pathways in four metabolic categories: carbohydrate metabolism, energy metabolism, amino acid metabolism, and cofactor and vitamin metabolism between the shallow and mesophotic samples.

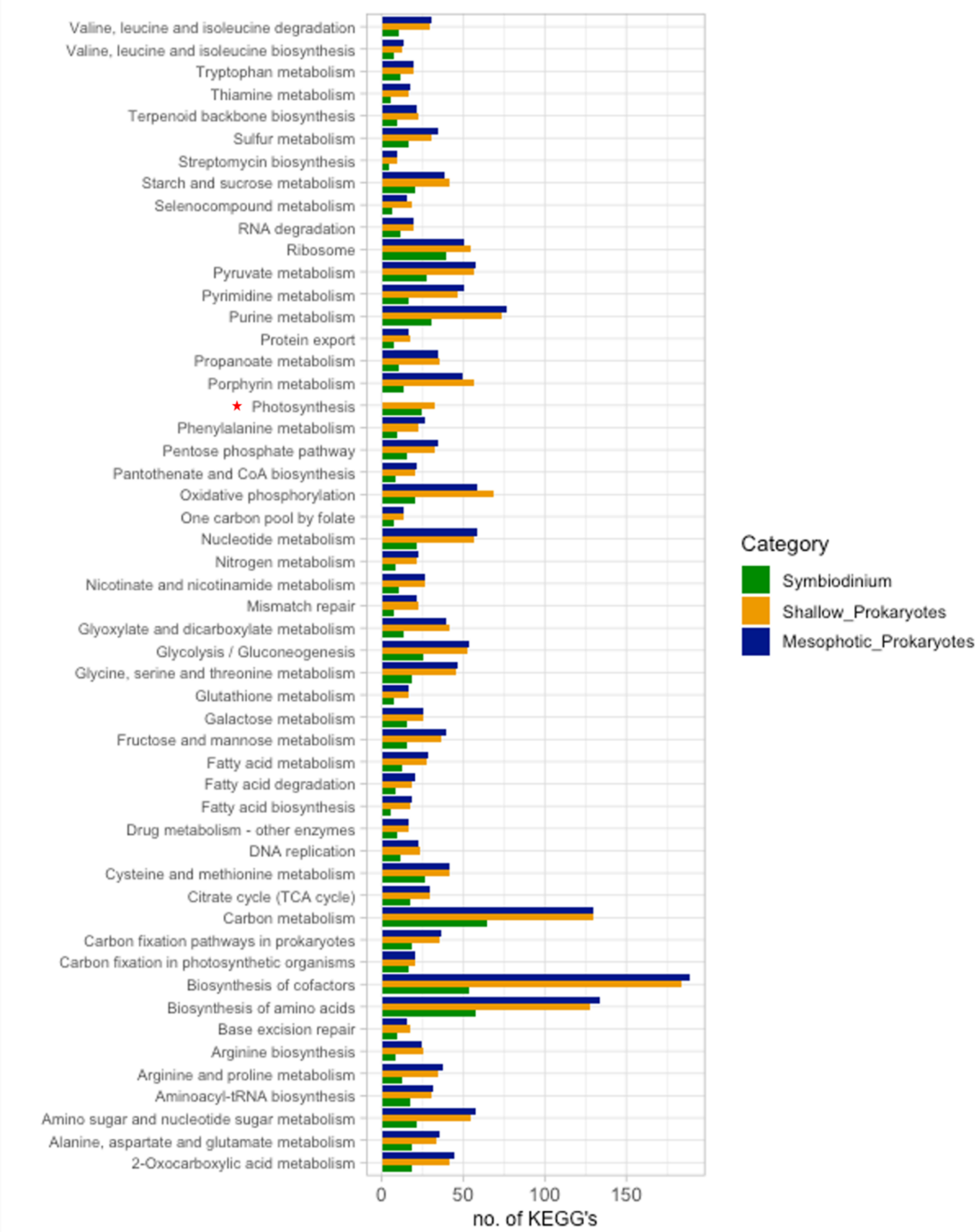

Supplementary Figure 3. Shared enriched KEGG pathways between *Symbiodinium* and the prokaryotic community in the *Eunicella* microbiome. The photosynthesis pathway (marked with a star) was only found in shallow communities. However, the mesophotic microbiome showed more KEGGs related to the metabolism of cofactors, vitamins, and amino acid biosynthesis.

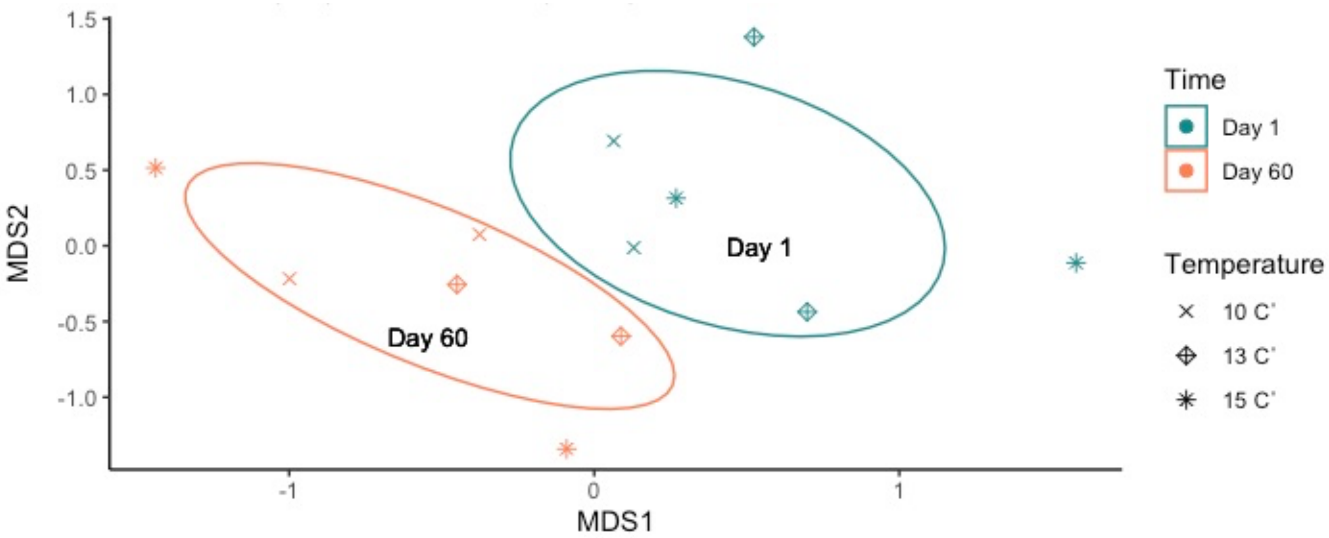

Supplementary Figure 4: Non-metric multidimensional scaling (NMDS) based on Bray-Curtis dissimilarities among the prokaryotic gene compositions of *D. pertusum* samples. Two clusters of prokaryotic genes were observed at the experiment's start (day 1) and end (day 60) at 10°C, 13°C, and 15°C.

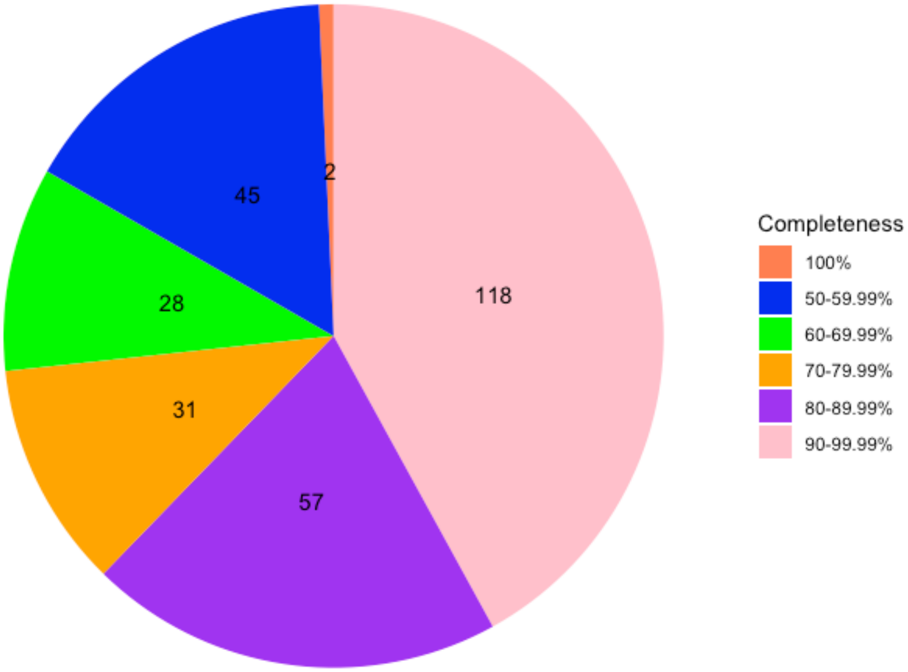

Supplementary Figure 5: Completeness of 281 MAGs and their quantities in the replicated set.

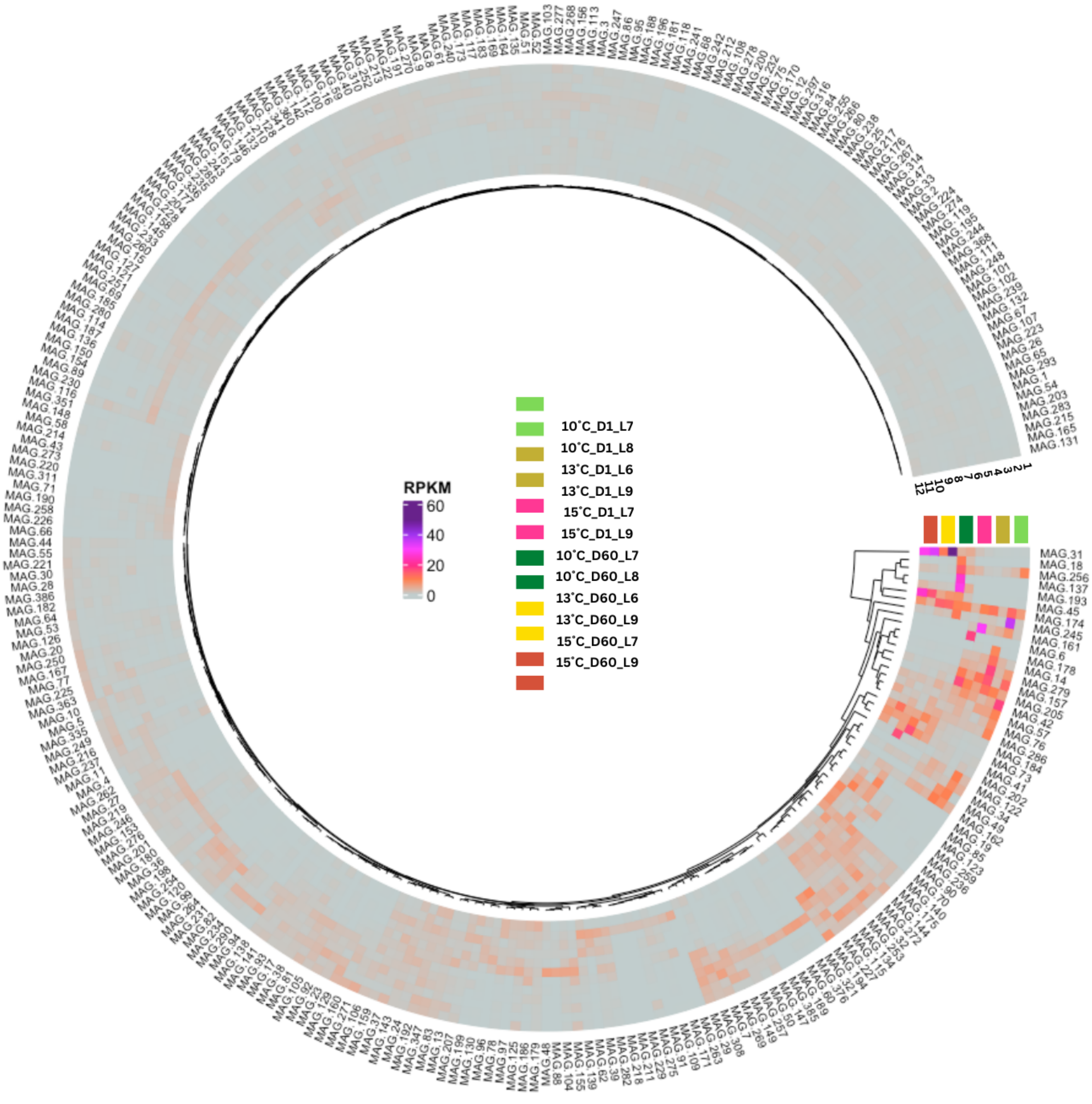

Supplementary Figure 6: Circular heatmap of MAGs abundance (RPKM) for the samples across different thermal conditions (10C˚,13C˚,15C˚) clustered based on Euclidean dissimilatory distance.

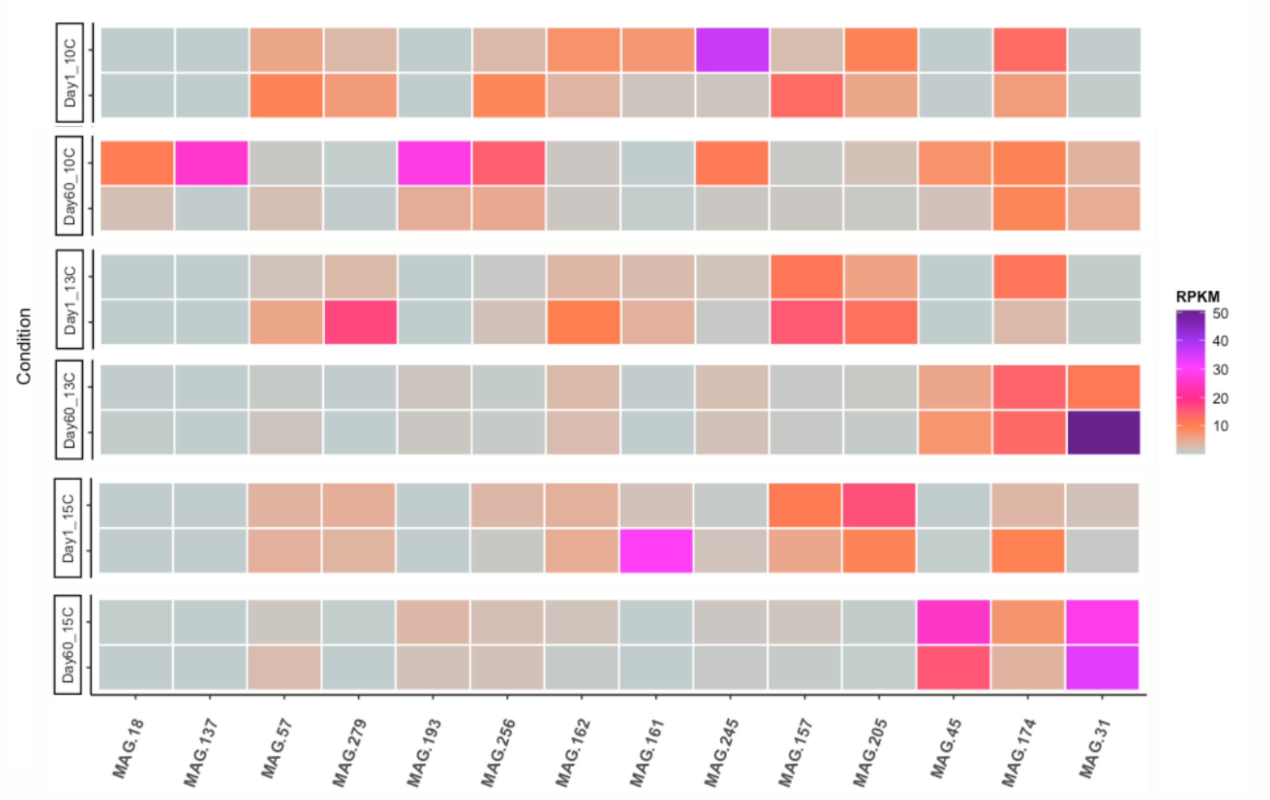

Supplementary Figure 7: Heatmap of the most variants MAG RPKM between the two temporal groups under three thermal conditions.

Supplementary Figure 8: Complete formaldehyde assimilation (serine pathway) module genes showed an increase in gene abundance with increased temperature (p-value < 0.05).

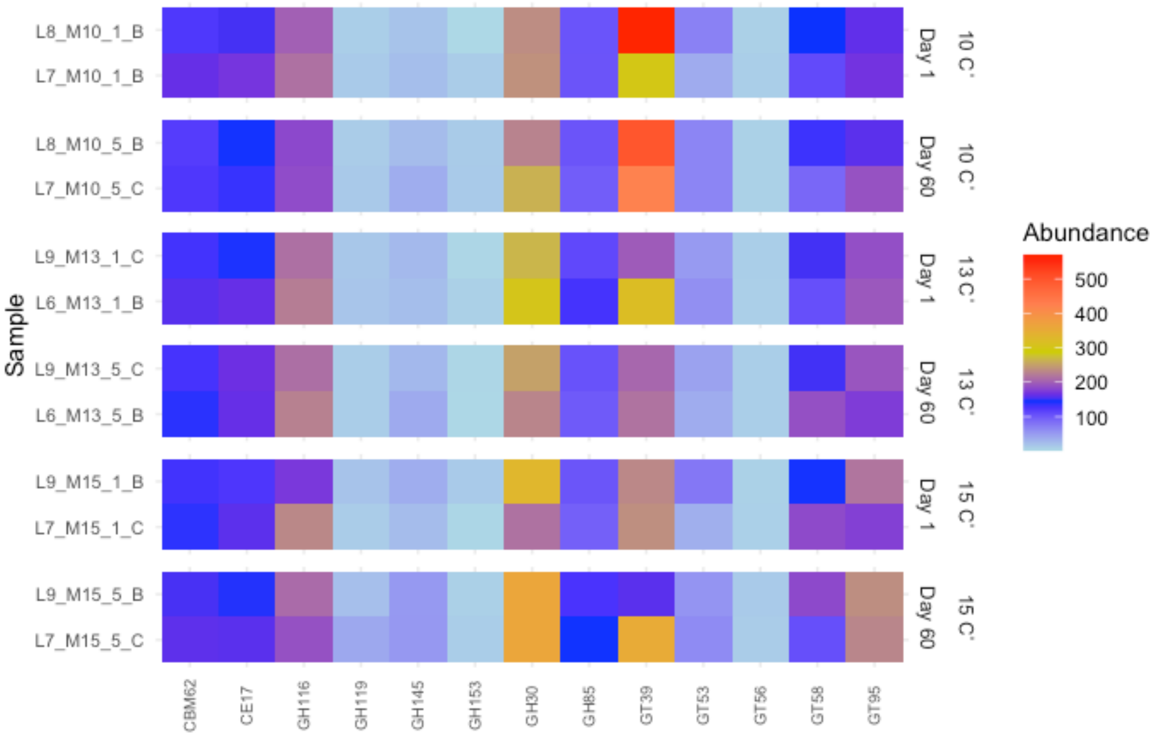

Supplementary Figure 9: Significant variation in CAZy enzymes between 10C°, 13C°, and 15C based on SIMPER analysis results (p-value < 0.05) with relative abundance. It shows increasing in abundance in Glycoside Hydrolase family enzymes such as GH30 and GH116

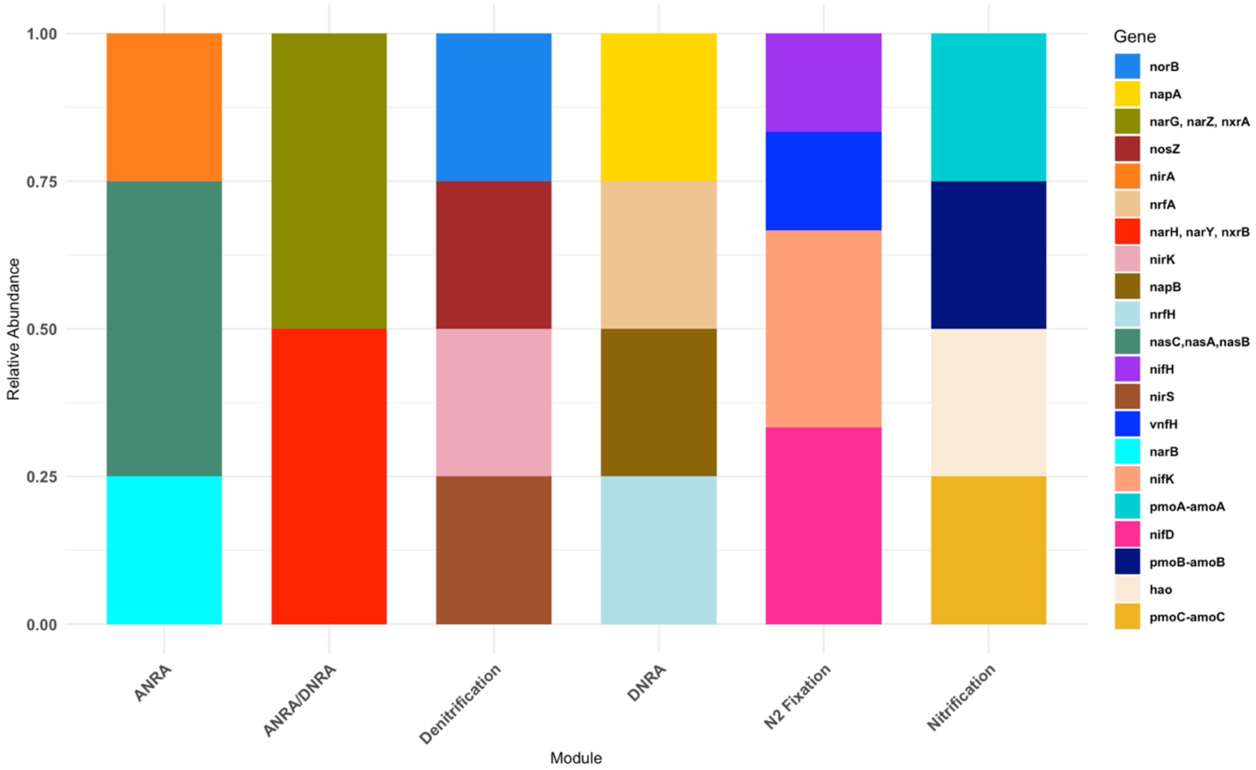

Supplementary Figure 10: Bar plots represent the nitrogen genes relative abundance in each nitrogen cycle pathway.

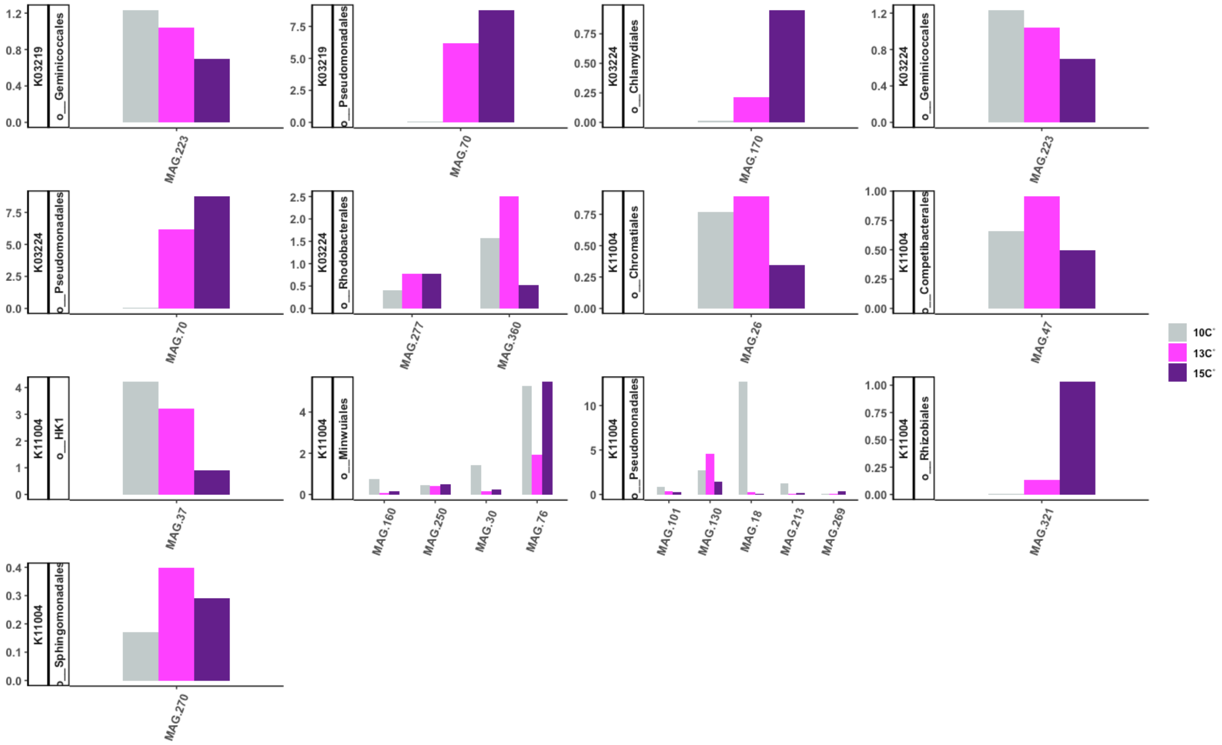

Supplementary Figure 11: Bar plots displaying the RPKM abundance of MAGs associated with secretion systems across different treatments on Day 60. K03219 (T3SS) was detected in Geminicoccales and Pseudomonadales. K03224 (T3SS) was present in Pseudomonadales, Chlamydiales, Rhodobacterales, and Geminicoccales, and its abundance increased with temperature. K11004 (T1SS) was identified in 14 MAGs across seven orders, including Pseudomonadales, Minwuiales, Chromatiales, Rhizobiales, Sphingomonadales, HK1 (Class: Gammaproteobacteria), and Competibacterales.

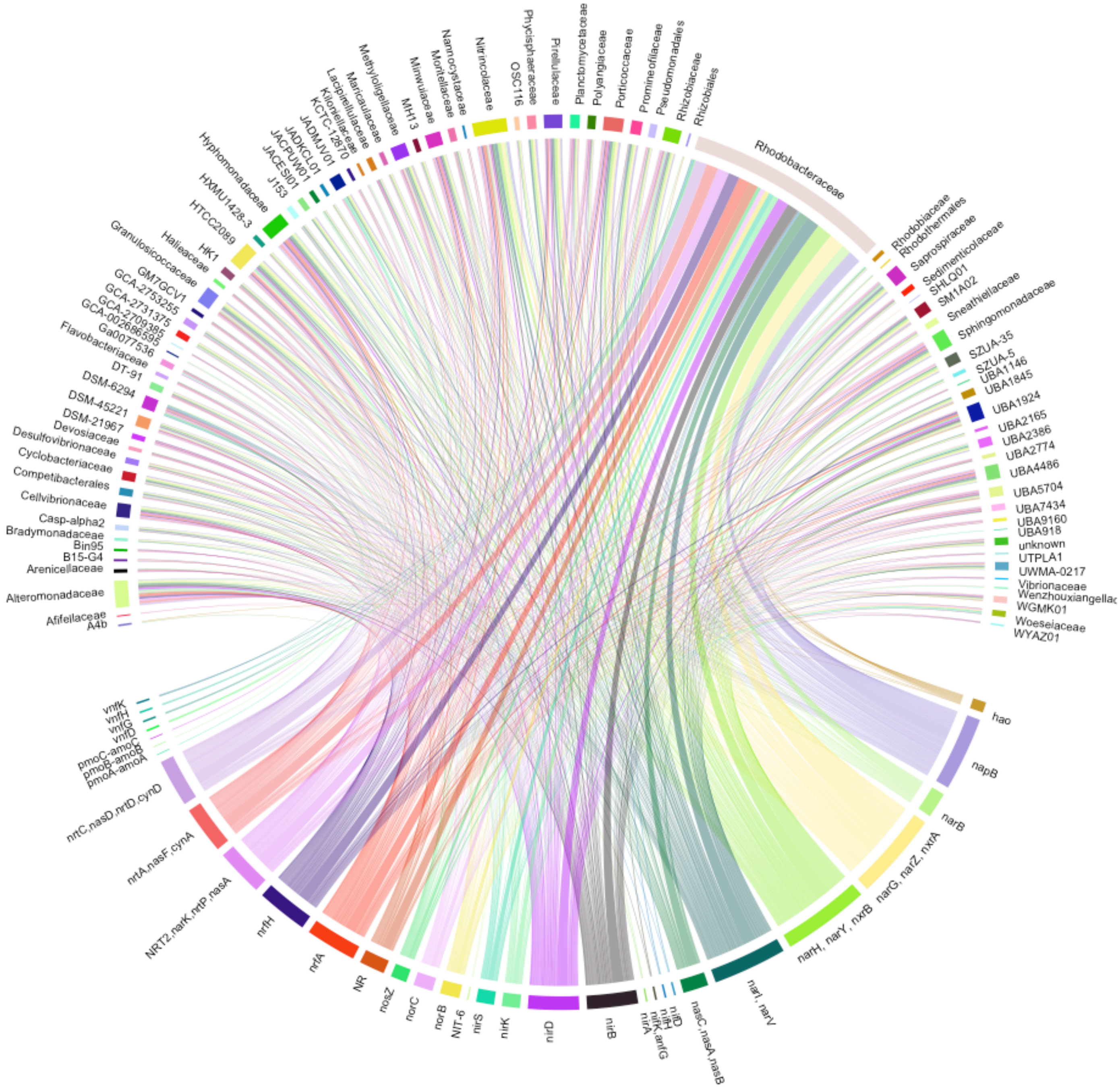

Supplementary Figure 12: Chord diagram illustrating MAGs involved in nitrogen cycle functions. The majority of MAGs belong to Rhodobacterales, Pseudomonadales, and Rhizobiales, encoding a significant number of functional genes within their genomes, highlighting their crucial roles in nitrogen cycling.

6.2. *Supplementary Tables*

Supplementary Table 1: Contig Information (Eukaryotic and Prokaryotic): Number, Average Size (bp), and Total Contigs Size (bp) per Sample from different depths.

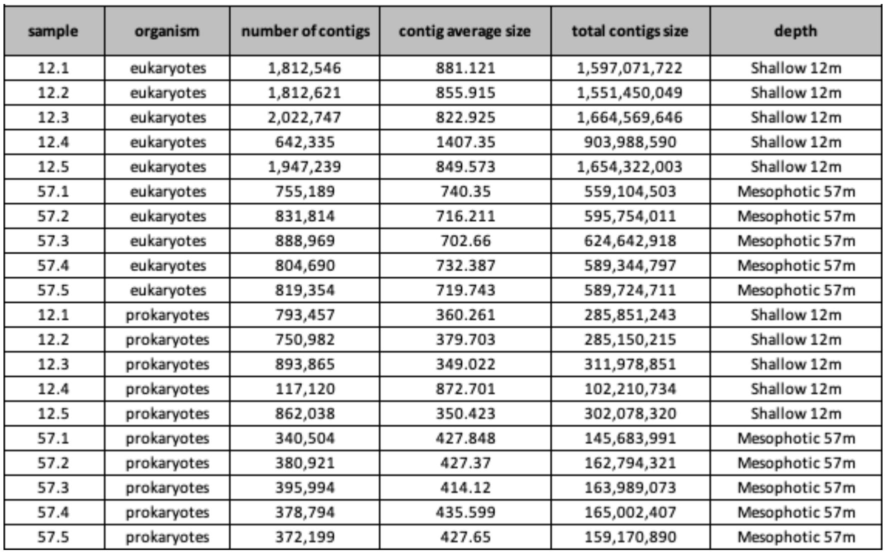

sample	organism	number of contigs	contig average size	total contigs size	depth
12.1	eukaryotes	1,812,546	881.121	1,597,071,722	Shallow 12m
12.2	eukaryotes	1,812,621	855.915	1,551,450,049	Shallow 12m
12.3	eukaryotes	2,022,747	822.925	1,664,569,646	Shallow 12m
12.4	eukaryotes	642,335	1407.35	903,988,590	Shallow 12m
12.5	eukaryotes	1,947,239	849.573	1,654,322,003	Shallow 12m
57.1	eukaryotes	755,189	740.35	559,104,503	Mesophotic 57m
57.2	eukaryotes	831,814	716.211	595,754,011	Mesophotic 57m
57.3	eukaryotes	888,969	702.66	624,642,918	Mesophotic 57m
57.4	eukaryotes	804,690	732.387	589,344,797	Mesophotic 57m
57.5	eukaryotes	819,354	719.743	589,724,711	Mesophotic 57m
12.1	prokaryotes	793,457	360.261	285,851,243	Shallow 12m
12.2	prokaryotes	750,982	379.703	285,150,215	Shallow 12m
12.3	prokaryotes	893,865	349.022	311,978,851	Shallow 12m
12.4	prokaryotes	117,120	872.701	102,210,734	Shallow 12m
12.5	prokaryotes	862,038	350.423	302,078,320	Shallow 12m
57.1	prokaryotes	340,504	427.848	145,683,991	Mesophotic 57m
57.2	prokaryotes	380,921	427.37	162,794,321	Mesophotic 57m
57.3	prokaryotes	395,994	414.12	163,989,073	Mesophotic 57m
57.4	prokaryotes	378,794	435.599	165,002,407	Mesophotic 57m
57.5	prokaryotes	372,199	427.65	159,170,890	Mesophotic 57m

Supplementary Table 2: Relative abundance and taxonomic classification of rRNA mTAGs for the most abundant taxa

phylum	class	order	family	genus	12.1	12.2	12.3	12.4	12.5	57.1	57.2	57.3	57.4	57.5	57.4	57.5
Proteobacteria	Gammaproteobacteria	Oceanospirillales	Endozoicomonadaceae	Endozoicomonas	61.61%	75.94%	80.52%	39.85%	72.06%	96.10%	96.89%	96.84%	96.76%	95.92%	96.76%	95.92%
Dinoflagellata	Dinophyceae	Suessiales	Symbiodiniaceae	Symbiodinium	36.62%	20.66%	17.24%	59.06%	25.33%	0.04%	0.11%	0.22%	0.02%	0.18%	0.02%	0.18%
Proteobacteria	Gammaproteobacteria	Oceanospirillales	Saccharospirillaceae	Bermanella	1.53%	2.11%	1.85%	0.98%	1.68%	2.39%	2.29%	2.23%	2.32%	2.26%	2.32%	2.26%
Proteobacteria	Gammaproteobacteria	Cellvibrionales	Spongiibacteraceae	BD1-7clade	0.01%	0.00%	0.05%	0.05%	0.03%	0.42%	0.58%	0.49%	0.36%	0.83%	0.36%	0.83%
Proteobacteria	Alphaproteobacteria	Sphingomonadales	Sphingomonadaceae	Sphingomonas	0.00%	1.14%	0.25%	0.00%	0.54%	0.84%	0.00%	0.00%	0.29%	0.65%	0.29%	0.65%
Proteobacteria	Gammaproteobacteria	Cellvibrionales	Halieaceae	Halioglobus	0.05%	0.08%	0.05%	0.04%	0.06%	0.06%	0.06%	0.05%	0.08%	0.07%	0.08%	0.07%
Firmicutes	Bacilli	Mycoplasmatales	Mycoplasmataceae	Mycoplasma	0.03%	0.06%	0.04%	0.00%	0.05%	0.07%	0.04%	0.06%	0.03%	0.03%	0.03%	0.03%
Firmicutes	Bacilli	Entomoplasmatales	Spiroplasmataceae	Spiroplasma	0.14%	0.00%	0.00%	0.03%	0.23%	0.00%	0.00%	0.00%	0.00%	0.00%	0.00%	0.00%
Proteobacteria	Gammaproteobacteria	Oceanospirillales	Saccharospirillaceae	Thalassolituus	0.01%	0.01%	0.00%	0.00%	0.00%	0.03%	0.03%	0.05%	0.06%	0.06%	0.06%	0.06%
Bacteroidota	Bacteroidia	Flavobacteriales	Flavobacteriaceae	Aquimarina	0.00%	0.00%	0.00%	0.00%	0.01%	0.05%	0.00%	0.06%	0.09%	0.00%	0.09%	0.00%

Supplementary Table 3: Microbial niche breadth results based on levins.Bn threshold(Bn), where the taxa above (Levins. Bn > 0.9, p-value => 0.05) are considered generalists and the taxa below (Levins. Bn < 0.5, p-value < 0.05) are considered specialists. The adjusted p-values (P.adj) control for multiple comparisons. P.adj < 0.05, indicating significant differences in niche breadth measures, whereas P.adj > 0.05, suggesting no significance. Below LOQ (limit of quantification) indicates whether taxa were falsely identified as generalists or specialists. If y means a high probability of false identification and If N means a low probability of false identification.

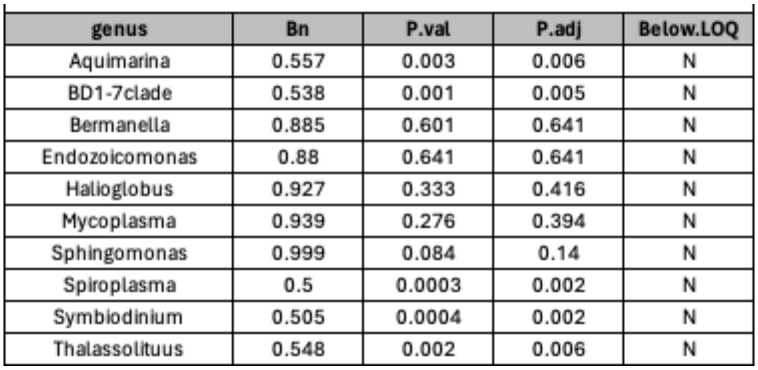

genus	Bn	P.val	P.adj	Below.LOQ
Aquimarina	0.557	0.003	0.006	N
BD1-7clade	0.538	0.001	0.005	N
Bermanella	0.885	0.601	0.641	N
Endozoicomonas	0.88	0.641	0.641	N
Halioglobus	0.927	0.333	0.416	N
Mycoplasma	0.939	0.276	0.394	N
Sphingomonas	0.999	0.084	0.14	N
Spiroplasma	0.5	0.0003	0.002	N
Symbiodinium	0.505	0.0004	0.002	N
Thalassolituus	0.548	0.002	0.006	N

Supplementary Table 4: Description of KEGG Pathways Showing Significant Differences (q-value < 0.05) Based on SIMPER Analyses (Contrast Shallow - Mesophotic) in Symbiodinium and Prokaryotic Communities

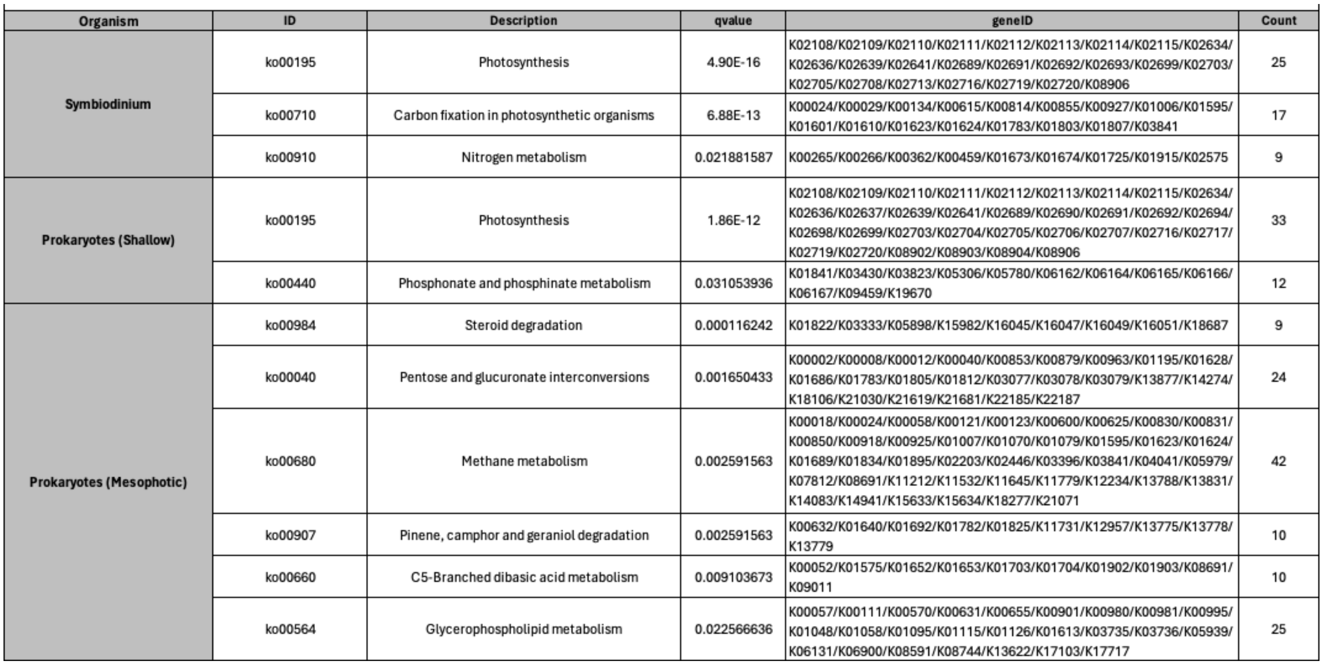

Organism	ID	Description	qvalue	geneID	Count
Symbiodinium	ko00195	Photosynthesis	4.90E-16	K02108/K02109/K02110/K02111/K02112/K02113/K02114/K02115/K02634/K02636/K02639/K02641/K02689/K02691/K02692/K02693/K02699/K02703/K02705/K02708/K02713/K02716/K02719/K02720/K08906	25
	ko00710	Carbon fixation in photosynthetic organisms	6.88E-13	K00024/K00029/K00134/K00615/K00814/K00855/K00927/K01006/K01595/K01601/K01610/K01623/K01624/K01783/K01803/K01807/K03841	17
	ko00910	Nitrogen metabolism	0.021881587	K00265/K00266/K00362/K00459/K01673/K01674/K01725/K01915/K02575	9
Prokaryotes (Shallow)	ko00195	Photosynthesis	1.86E-12	K02108/K02109/K02110/K02111/K02112/K02113/K02114/K02115/K02634/K02636/K02637/K02639/K02641/K02689/K02690/K02691/K02692/K02694/K02698/K02699/K02703/K02704/K02705/K02706/K02707/K02716/K02717/K02719/K02720/K08902/K08903/K08904/K08906	33
	ko00440	Phosphonate and phosphinate metabolism	0.031053936	K01841/K03430/K03823/K05306/K05780/K06162/K06164/K06165/K06166/K06167/K09459/K19670	12
Prokaryotes (Mesophotic)	ko00984	Steroid degradation	0.000116242	K01822/K03333/K05898/K15982/K16045/K16047/K16049/K16051/K18687	9
	ko00040	Pentose and glucuronate interconversions	0.001650433	K00002/K00008/K00012/K00040/K00853/K00879/K00963/K01195/K01628/K01686/K01783/K01805/K01812/K03077/K03078/K03079/K13877/K14274/K18106/K21030/K21619/K21681/K22185/K22187	24
	ko00680	Methane metabolism	0.002591563	K00018/K00024/K00058/K00121/K00123/K00600/K00625/K00830/K00831/K00850/K00918/K00925/K01007/K01070/K01079/K01595/K01623/K01624/K01689/K01834/K01895/K02203/K02446/K03396/K03841/K04041/K05979/K07812/K08691/K11212/K11532/K11645/K11779/K12234/K13788/K13831/K14083/K14941/K15633/K15634/K18277/K21071	42
	ko00907	Pinene, camphor and geraniol degradation	0.002591563	K00632/K01640/K01692/K01782/K01825/K11731/K12957/K13775/K13778/K13779	10
	ko00660	C5-Branched dibasic acid metabolism	0.009103673	K00052/K01575/K01652/K01653/K01703/K01704/K01902/K01903/K08691/K09011	10
	ko00564	Glycerophospholipid metabolism	0.022566636	K00057/K00111/K00570/K00631/K00655/K00901/K00980/K00981/K00995/K01048/K01058/K01095/K01115/K01126/K01613/K03735/K03736/K05939/K06131/K06900/K08591/K08744/K13622/K17103/K17717	25

Supplementary Table 5: Shared KEGG Pathways and KO's among prokaryotes in shallow and mesophotic communities.

Cycle	Pathway	KO
Central metabolism	Gluconeogenesis, oxaloacetate => fructose-6P	K02446/K01689/K11645/K03841/K01834/K01596/K01610/K15633/K01623/K15635/K00927/K00150/K00134/K01624/K01803/K03841/K01623/K01834/K15633/K01624/K01689/K01610/K11532/K01803/K02446/K00927/K00134/K11532/K03841/K15633/K01803/K01624/K02446/K00927/K01623/K00134/K01834/K01689/K01610/K15635/K01623/K01624/K01596/K01803/K01689/K00134/K03841/K00927/K01834/K02446/K15633/K01610/K03841/K01624/K01623/K01689/K00927/K01610/K01803/K02446/K01834/K00134/K11532/K15633/K01623/K01803/K03841/K01624/K15633/K01689/K00134/K00927/K11532/K02446/K01834/K01610/K01624/K01623/K01803/K03841/K00927/K15633/K01834/K01689/K01610/K00134/K02446/K01624/K01803/K01623/K04041/K15635/K02446/K01596/K15633/K01610/K00134/K01689/K00927/K01623/K02446/K01624/K15633/K01803/K03841/K00134/K11532/K00927/K01834/K01689/K01610/K01623/K01624/K00927/K03841/K01803/K00134/K11532/K02446/K01689/K15633/K01610/K04041/K01834
Central metabolism	Glycolysis (Embden-Meyerhof pathway), glucose => pyruvate	K00134/K01689/K00150/K00927/K00873/K00844/K01624/K00845/K00886/K01810/K01803/K00850/K15635/K15633/K01834/K01623/K11645/K00873/K01624/K00927/K00134/K01689/K01803/K15633/K01834/K00850/K01810/K00844/K01623/K00134/K00873/K01803/K15633/K01689/K01624/K01810/K00927/K00850/K01834/K01623/K00844/K01803/K15633/K00134/K01689/K00873/K15635/K01624/K00850/K00927/K01810/K01834/K00844/K01623/K01803/K01624/K15633/K01834/K00873/K00927/K01689/K00134/K00844/K00850/K01810/K01623/K01834/K00927/K15633/K00134/K01624/K00873/K01810/K01689/K01803/K00850/K01623/K00844/K15633/K01624/K01803/K01810/K01834/K00134/K00850/K00927/K00844/K00873/K00886/K01623/K01689/K01623/K15633/K01624/K01810/K00134/K00850/K00927/K00844/K01803/K15635/K00873/K01689/K01810/K00850/K01623/K01834/K00134/K15633/K01624/K00844/K00927/K00873/K01689/K01803/K00844/K00927/K01834/K00134/K01623/K00873/K15633/K01624/K01810/K01803/K00850/K01689
Oxidative phosphorylation	Cytochrome c oxidase, cbb3-type	K00404/K00405/K00407/K00406/K00404/K00405/K00406/K00407/K00406/K00405/K00404/K00407/K00406/K00407/K00404/K00405/K00406/K00404/K00405/K00407/K00406/K00407/K00404/K00405/K00405/K00406/K00407/K00404/K00404/K00407/K00405/K00406/K00404/K00406/K00407/K00405/K00405/K00407/K00404/K00406
Oxidative phosphorylation	Cytochrome c oxidase, prokaryotes	K02274/K02275/K02276/K02277/K02275/K02276/K02274/K02275/K02274/K02276/K02274/K02275/K02276/K02277/K02274/K02275/K02276/K02275/K02274/K02276/K02275/K02276/K02274/K02277/K02275/K02276/K02274/K02276/K02274/K02275/K02275/K02276/K02274
Oxidative phosphorylation	NADH-quinone oxidoreductase	K00341/K00343/K00339/K00335/K00334/K00338/K00340/K00330/K00337/K00341/K00333/K00342/K00332/K00335/K00339/K00336/K00340/K00330/K00343/K00331/K00334/K00337/K00338/K00341/K00332/K00340/K00335/K00339/K00336/K00333/K00342/K00331/K00330/K00334/K00338/K00343/K00337/K00341/K00339/K00340/K00330/K00337/K00343/K00342/K00340/K00341/K00335/K00331/K00339/K00334/K00332/K00330/K00343/K00336/K00333/K00337/K00338/K00342/K00340/K00331/K00337/K00332/K00335/K00341/K00338/K00339/K00336/K00330/K00334/K00333/K00343/K00339/K00340/K00341/K00343/K00337/K00330/K00339/K00340/K00337/K00330/K00343/K00341/K00331/K00343/K00342/K00330/K00332/K00335/K00337/K00336/K00334/K00333/K00341/K00340/K00338/K00339/K00331/K00342/K00343/K00330/K00339/K00333/K00337/K00336/K00332/K00334/K00335/K00340/K00341/K00331/K00338
Secretion system	Sec-SRP	K03076/K03210/K03071/K03110/K03217/K03075/K03073/K03072/K03070/K03106/K03074/K03075/K03073/K03072/K03217/K03076/K03074/K03070/K03071/K03110/K03106/K03210/K03217/K03106/K03110/K03073/K03210/K03072/K03076/K03075/K03070/K03071/K03074/K03076/K03106/K03110/K03217/K03210/K03071/K03070/K03074/K03073/K03075/K03072/K03075/K03073/K03217/K03076/K03110/K03072/K03070/K03106/K03210/K03071/K03074/K03072/K03106/K03217/K03073/K03110/K03076/K03075/K03071/K03070/K03210/K03074/K03076/K03075/K03073/K03106/K03070/K12257/K03072/K03217/K03110/K03071/K03210/K03074/K03073/K03075/K03076/K03072/K03210/K03217/K03071/K03074/K03110/K03070/K03106/K03075/K03073/K03106/K03210/K03070/K03217/K03071/K03076/K03074/K03110/K03072/K03075/K03076/K03073/K03210/K03070/K03110/K03217/K03074/K03071/K03106/K03072
Secretion system	Twin arginine targeting	K03118/K03116/K03117/K03117/K03118/K03116/K03117/K03116/K03118/K03116/K03118/K03116/K03118/K03117/K03116/K03118/K03117/K03117/K03116/K03118/K03117/K03116/K03118/K03116/K03118/K03117/K03116/K03117/K03118
Secretion system	Type II Secretion	K02458/K02461/K02454/K02452/K02456/K02459/K02462/K02460/K02457/K02462/K02460/K02458/K02455/K02457/K02452/K02456/K02461/K02459/K02453/K02454/K02455/K02458/K02456/K02453/K02459/K02461/K02460/K02462/K02452/K02457/K02454/K02461/K02459/K02456/K02457/K02453/K02460/K02458/K02454/K02455/K02458/K02453/K02457/K02461/K02456/K02452/K02460/K02459/K02454/K02462/K02458/K02455/K02456/K02461/K02459/K02452/K02457/K02453/K02454/K02460/K02462/K02455/K02456/K02457/K02458/K02461/K02454/K02462/K02452/K02453/K02460/K02459/K02458/K02457/K02455/K02454/K02453/K02459/K02456/K02462/K02460/K02452/K02457/K02455/K02456/K02460/K02458/K02461/K02459/K02454/K02452/K02453/K02462/K02455/K02456/K02454/K02462/K02458/K02452/K02457/K02460/K02459/K02461/K02453
Secretion system	Type III Secretion	K03219/K03226/K03230/K03221/K03227/K04058/K03225/K03224/K03228/K03229/K03223/K04056/K03222/K03219/K03226/K03227/K03221/K03230/K03228/K03222/K04058/K03224/K04056/K03225/K03229/K03223/K04058/K03219/K04056/K03221/K03228/K03226/K03222/K03229/K03227/K03230/K03224/K03225/K03223/K03219/K03226/K04058/K03222/K03228/K03227/K04056/K03221/K03224/K03230/K03229/K03223/K03225/K03219/K03224/K04056/K03228/K03227/K03230/K03226/K03229/K03225/K03221/K03223/K04058/K03222/K03219/K03226/K04056/K03224/K03227/K03228/K04058/K03222/K03221/K03225/K03230/K03229/K03224/K04056/K04058/K03225/K03227/K03230/K03229/K03228/K03226/K03222/K03221/K03223/K04056/K03222/K04058/K03230/K03228/K03226/K03225/K03227/K03221/K03229/K03224/K03226/K03230/K04056/K03227/K04058/K03222/K03225/K03228/K03224/K03221/K03229/K03219/K04056/K03229/K03222/K04058/K03227/K03228/K03226/K03221/K03230/K03224/K03225

Supplementary Table 6: Description of the shared KOs between *Symbiodinium* (shallow) and prokaryotic (shallow and mesophotic) communities that showed significant variation in abundance of KOs (read counts per gene normalized by gene length and the geometric mean abundance of 10 selected single-copy genes) across depths.

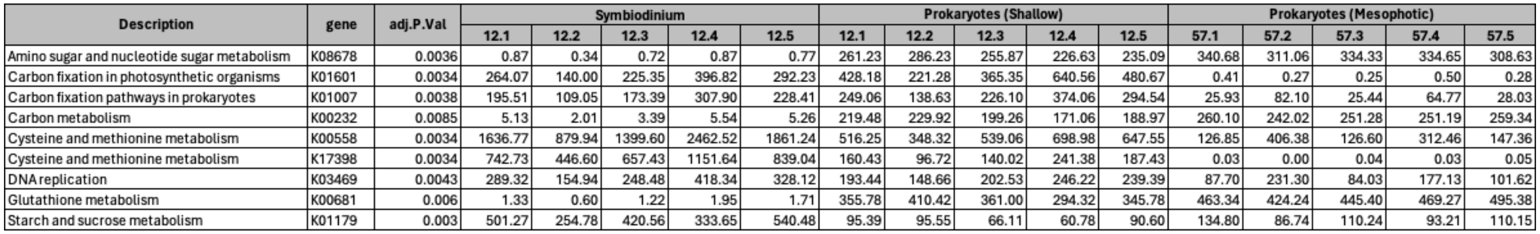

Description	gene	adj.P.Val	Symbiodinium					Prokaryotes (Shallow)					Prokaryotes (Mesophotic)				
			12.1	12.2	12.3	12.4	12.5	12.1	12.2	12.3	12.4	12.5	57.1	57.2	57.3	57.4	57.5
Amino sugar and nucleotide sugar metabolism	K08678	0.0036	0.87	0.34	0.72	0.87	0.77	261.23	286.23	255.87	226.63	235.09	340.68	311.06	334.33	334.65	308.63
Carbon fixation in photosynthetic organisms	K01601	0.0034	264.07	140.00	225.35	396.82	292.23	428.18	221.28	365.35	640.56	480.67	0.41	0.27	0.25	0.50	0.28
Carbon fixation pathways in prokaryotes	K01007	0.0038	195.51	109.05	173.39	307.90	228.41	249.06	138.63	226.10	374.06	294.54	25.93	82.10	25.44	64.77	28.03
Carbon metabolism	K00232	0.0085	5.13	2.01	3.39	5.54	5.26	219.48	229.92	199.26	171.06	188.97	260.10	242.02	251.28	251.19	259.34
Cysteine and methionine metabolism	K00558	0.0034	1636.77	879.94	1399.60	2462.52	1861.24	516.25	348.32	539.06	698.98	647.55	126.85	406.38	126.60	312.46	147.36
Cysteine and methionine metabolism	K17398	0.0034	742.73	446.60	657.43	1151.64	839.04	160.43	96.72	140.02	241.38	187.43	0.03	0.00	0.04	0.03	0.05
DNA replication	K03469	0.0043	289.32	154.94	248.48	418.34	328.12	193.44	148.66	202.53	246.22	239.39	87.70	231.30	84.03	177.13	101.62
Glutathione metabolism	K00681	0.006	1.33	0.60	1.22	1.95	1.71	355.78	410.42	361.00	294.32	345.78	463.34	424.24	445.40	469.27	495.38
Starch and sucrose metabolism	K01179	0.003	501.27	254.78	420.56	333.65	540.48	95.39	95.55	66.11	60.78	90.60	134.80	86.74	110.24	93.21	110.15

Supplementary Table 7: Summary of 15 De-replicated MAGs: GDBT taxonomic classification, completeness, quality, and abundance (RPKM) across samples from different depths

Genome	classification					Genome inforamtion				Mapped Reads Abundance (Reads Per Kilobase of genome and gigabase of metagenome; RPKM)									
	phylum	class	order	family	genus	completeness	GC	genome size	N50	12.1	12.2	12.3	12.4	12.5	57.1	57.2	57.3	57.4	57.5
MAG.2	Firmicutes	Bacilli	Mycoplasmatales	Mycoplasmataceae	Mycoplasmataceae	96.61	0.244	640089	231400	0.001	0.006	0.005	161.484	0.089	0.000	0.000	0.000	0.000	0.001
MAG.309811	GCA-001730085	GCA-001730085	GCA-001730085	GCA-001730086	GCA-001730087	95.85	0.31	1920058	53933	2.461	0.008	0.001	3.942	0.010	0.001	0.000	1.349	0.000	0.001
MAG.13	Firmicutes	Bacilli	Mycoplasmatales	Metamycoplasmataceae	DT-68	66.28	0.322	940850	5261	18.665	7.625	5.025	8.004	6.964	8.229	3.989	11.534	5.046	9.564
MAG.332111	Cyanobacteria	Cyanobacteria	Phormidesmiales	Phormidesmiaceae	SIO4C1	95.18	0.51	5919946	37874	5.928	0.000	0.000	0.000	0.000	0.000	0.000	0.000	0.000	0.000
MAG.25993	Proteobacteria	Gammaproteobacteria	Pseudomonadales	Endozoicomonadaceae	Endozoicomonadaceae	90.55	0.3	2547593	3913	273.317	335.751	344.668	193.105	319.282	359.912	379.658	371.984	377.000	358.219
MAG.8	Firmicutes	Bacilli	Mycoplasmatales	UBA3375	UBA3376	91.76	0.288	551729	11975	0.000	0.000	0.000	0.000	0.000	0.000	0.000	0.000	0.000	2.512
MAG.16	Firmicutes	Bacilli	Mycoplasmatales	VBWQ01	Spiroplasma_D	81.04	0.238	1068866	6516	1.236	0.000	0.000	0.192	2.367	0.000	0.000	0.000	0.000	0.000
MAG.12	Proteobacteria	Gammaproteobacteria	Pseudomonadales	DT-91	DT-91	97.83	0.404	4135921	25626	0.094	0.046	0.151	0.520	0.204	2.675	3.693	3.099	2.440	4.713
MAG.15	Spirochaetota	Spirochaetia	WTKD01	WTKD02	WTKD03	82.8	0.313	1800028	9038	0.400	0.119	0.125	0.866	0.066	0.163	0.729	1.306	0.096	0.136
MAG.10	Firmicutes	Bacilli	Mycoplasmatales	MT37	Spiroplasma_C	71.92	0.27	442759	38731	11.438	8.509	4.330	10.927	5.340	10.601	4.251	11.295	9.904	16.103
MAG.22	Proteobacteria	Alphaproteobacteria	Sphingomonadales	Sphingomonadaceae	Sphingomonas	99.65	0.675	3884718	315802	0.032	14.653	3.496	0.022	9.054	12.919	0.046	0.051	4.360	10.565
MAG.220783	Proteobacteria	Alphaproteobacteria	Alphaproteobacteria	Alphaproteobacteria	Alphaproteobacteria	70.8	0.37	1124719	2327	0.005	0.009	0.007	0.006	0.008	0.007	0.003	0.014	0.007	1.630
MAG.14	Firmicutes	Bacilli	Mycoplasmatales	Metamycoplasmataceae	Metamycoplasmataceae	88.53	0.213	710164	10028	0.000	0.852	2.943	0.002	6.029	5.595	5.607	12.357	2.485	1.034
MAG.302726	Bacteroidota	Bacteroidia	Flavobacteriales	Ichthyobacteriaceae	Ichthyobacteriaceae	69.46	0.4	1421504	2561	0.281	0.047	0.049	0.004	0.034	0.127	0.707	0.111	0.002	0.009
MAG.17	Proteobacteria	Gammaproteobacteria	Pseudomonadales	Endozoicomonadaceae	Endozoicomonas	94.44	0.459	3805921	16936	1.197	0.372	0.311	1.614	0.328	0.632	0.282	1.141	0.133	1.093

Supplementary Table 8: KO's found in MAGs related to different metabolic functions, i.e., carbon cycle, vitamin production, and secretion systems.

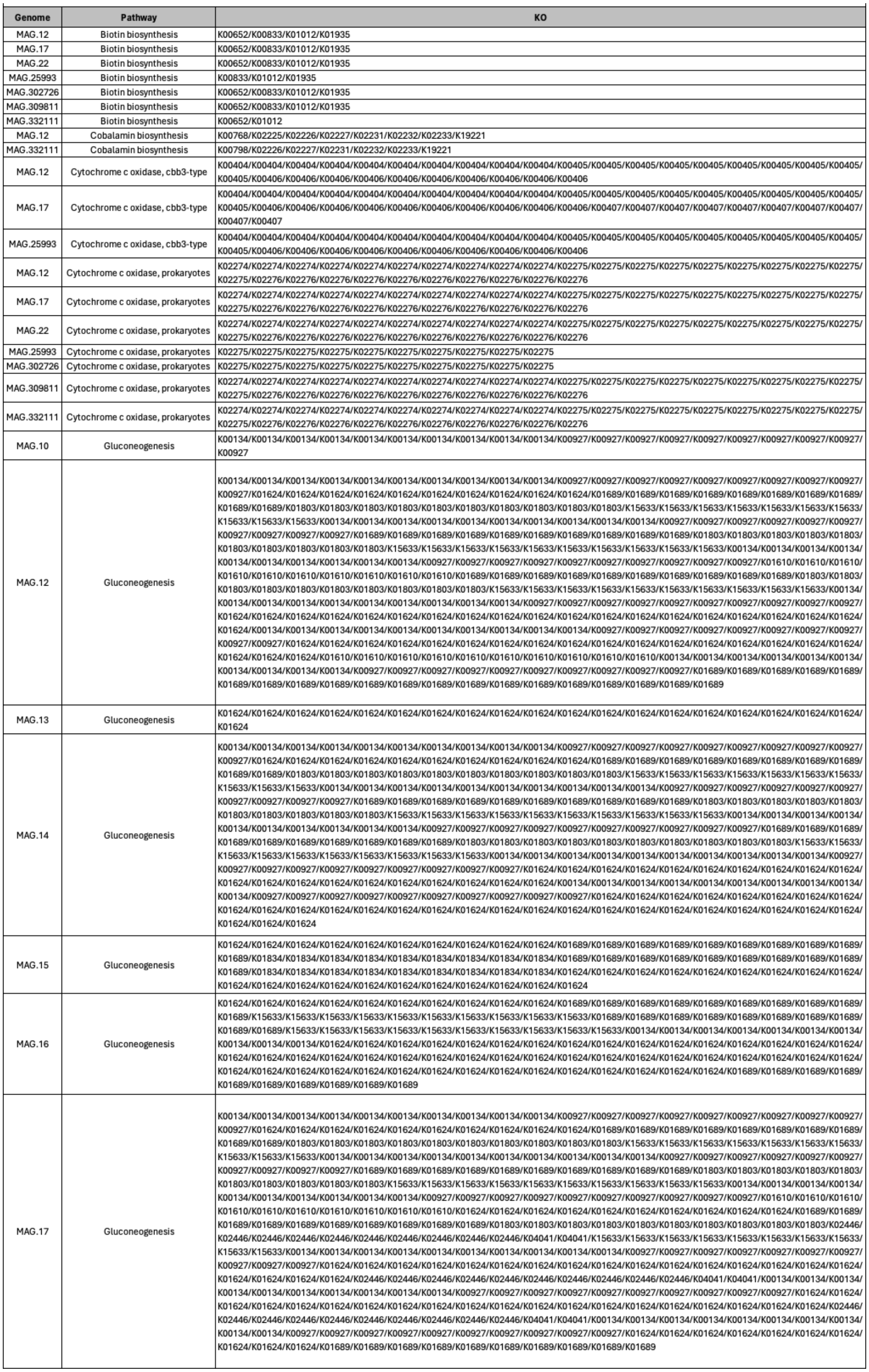

Genome	Pathway	KO
MAG.12	Biotin biosynthesis	K00652/K00833/K01012/K01935
MAG.17	Biotin biosynthesis	K00652/K00833/K01012/K01935
MAG.22	Biotin biosynthesis	K00652/K00833/K01012/K01935
MAG.25993	Biotin biosynthesis	K00833/K01012/K01935
MAG.302726	Biotin biosynthesis	K00652/K00833/K01012/K01935
MAG.309811	Biotin biosynthesis	K00652/K00833/K01012/K01935
MAG.332111	Biotin biosynthesis	K00652/K01012
MAG.12	Cobalamin biosynthesis	K00768/K02225/K02226/K02227/K02231/K02232/K02233/K19221
MAG.332111	Cobalamin biosynthesis	K00798/K02226/K02227/K02231/K02232/K02233/K19221
MAG.12	Cytochrome c oxidase, cbb3-type	K00404/K00404/K00404/K00404/K00404/K00404/K00404/K00404/K00404/K00404/K00405/K00405/K00405/K00405/K00405/K00405/K00405/K00405/K00405/K00405/K00406/K00406/K00406/K00406/K00406/K00406/K00406/K00406/K00406/K00406
MAG.17	Cytochrome c oxidase, cbb3-type	K00404/K00404/K00404/K00404/K00404/K00404/K00404/K00404/K00404/K00404/K00405/K00405/K00405/K00405/K00405/K00405/K00405/K00405/K00405/K00405/K00406/K00406/K00406/K00406/K00406/K00406/K00406/K00406/K00406/K00406/K00407/K00407/K00407/K00407/K00407/K00407/K00407/K00407/K00407/K00407
MAG.25993	Cytochrome c oxidase, cbb3-type	K00404/K00404/K00404/K00404/K00404/K00404/K00404/K00404/K00404/K00404/K00405/K00405/K00405/K00405/K00405/K00405/K00405/K00405/K00405/K00405/K00406/K00406/K00406/K00406/K00406/K00406/K00406/K00406/K00406/K00406
MAG.12	Cytochrome c oxidase, prokaryotes	K02274/K02274/K02274/K02274/K02274/K02274/K02274/K02274/K02274/K02274/K02275/K02275/K02275/K02275/K02275/K02275/K02275/K02275/K02275/K02275/K02276/K02276/K02276/K02276/K02276/K02276/K02276/K02276/K02276/K02276
MAG.17	Cytochrome c oxidase, prokaryotes	K02274/K02274/K02274/K02274/K02274/K02274/K02274/K02274/K02274/K02274/K02275/K02275/K02275/K02275/K02275/K02275/K02275/K02275/K02275/K02275/K02276/K02276/K02276/K02276/K02276/K02276/K02276/K02276/K02276/K02276
MAG.22	Cytochrome c oxidase, prokaryotes	K02274/K02274/K02274/K02274/K02274/K02274/K02274/K02274/K02274/K02274/K02275/K02275/K02275/K02275/K02275/K02275/K02275/K02275/K02275/K02275/K02276/K02276/K02276/K02276/K02276/K02276/K02276/K02276/K02276/K02276
MAG.25993	Cytochrome c oxidase, prokaryotes	K02275/K02275/K02275/K02275/K02275/K02275/K02275/K02275/K02275/K02275
MAG.302726	Cytochrome c oxidase, prokaryotes	K02275/K02275/K02275/K02275/K02275/K02275/K02275/K02275/K02275/K02275
MAG.309811	Cytochrome c oxidase, prokaryotes	K02274/K02274/K02274/K02274/K02274/K02274/K02274/K02274/K02274/K02274/K02275/K02275/K02275/K02275/K02275/K02275/K02275/K02275/K02275/K02275/K02276/K02276/K02276/K02276/K02276/K02276/K02276/K02276/K02276/K02276
MAG.332111	Cytochrome c oxidase, prokaryotes	K02274/K02274/K02274/K02274/K02274/K02274/K02274/K02274/K02274/K02274/K02275/K02275/K02275/K02275/K02275/K02275/K02275/K02275/K02275/K02275/K02276/K02276/K02276/K02276/K02276/K02276/K02276/K02276/K02276/K02276
MAG.10	Gluconeogenesis	K00134/K00134/K00134/K00134/K00134/K00134/K00134/K00134/K00134/K00134/K00927/K00927/K00927/K00927/K00927/K00927/K00927/K00927/K00927/K00927
MAG.12	Gluconeogenesis	K00134/K00134/K00134/K00134/K00134/K00134/K00134/K00134/K00134/K00134/K00927/K00927/K00927/K00927/K00927/K00927/K00927/K00927/K00927/K00927/K01624/K01624/K01624/K01624/K01624/K01624/K01624/K01624/K01624/K01624/K01689/K01689/K01689/K01689/K01689/K01689/K01689/K01689/K01689/K01689/K01803/K01803/K01803/K01803/K01803/K01803/K01803/K01803/K01803/K01803/K15633/K15633/K15633/K15633/K15633/K15633/K15633/K15633/K15633/K15633/K00134/K00134/K00134/K00134/K00134/K00134/K00134/K00134/K00134/K00134/K00927/K00927/K00927/K00927/K00927/K00927/K00927/K00927/K00927/K00927/K01689/K01689/K01689/K01689/K01689/K01689/K01689/K01689/K01689/K01689/K01803/K01803/K01803/K01803/K01803/K01803/K01803/K01803/K01803/K01803/K15633/K15633/K15633/K15633/K15633/K15633/K15633/K15633/K15633/K15633/K00134/K00134/K00134/K00134/K00134/K00134/K00134/K00134/K00134/K00134/K00927/K00927/K00927/K00927/K00927/K00927/K00927/K00927/K00927/K00927/K01610/K01610/K01610/K01610/K01610/K01610/K01610/K01610/K01610/K01610/K01689/K01689/K01689/K01689/K01689/K01689/K01689/K01689/K01689/K01689/K01803/K01803/K01803/K01803/K01803/K01803/K01803/K01803/K01803/K01803/K15633/K15633/K15633/K15633/K15633/K15633/K15633/K15633/K15633/K15633/K00134/K00134/K00134/K00134/K00134/K00134/K00134/K00134/K00134/K00134/K00927/K00927/K00927/K00927/K00927/K00927/K00927/K00927/K00927/K00927/K01624/K00134/K00134/K00134/K00134/K00134/K00134/K00134/K00134/K00134/K00134/K00927/K00927/K00927/K00927/K00927/K00927/K00927/K00927/K00927/K00927/K01624/K01610/K01610/K01610/K01610/K01610/K01610/K01610/K01610/K01610/K01610/K00134/K00134/K00134/K00134/K00134/K00134/K00134/K00134/K00134/K00134/K00927/K00927/K00927/K00927/K00927/K00927/K00927/K00927/K00927/K00927/K01689
MAG.13	Gluconeogenesis	K01624/K01624/K01624/K01624/K01624/K01624/K01624/K01624/K01624/K01624/K01624/K01624/K01624/K01624/K01624/K01624/K01624/K01624/K01624/K01624
MAG.14	Gluconeogenesis	K00134/K00134/K00134/K00134/K00134/K00134/K00134/K00134/K00134/K00134/K00927/K00927/K00927/K00927/K00927/K00927/K00927/K00927/K00927/K00927/K01624/K01624/K01624/K01624/K01624/K01624/K01624/K01624/K01624/K01624/K01689/K01689/K01689/K01689/K01689/K01689/K01689/K01689/K01689/K01689/K01803/K01803/K01803/K01803/K01803/K01803/K01803/K01803/K01803/K01803/K15633/K15633/K15633/K15633/K15633/K15633/K15633/K15633/K15633/K15633/K00134/K00134/K00134/K00134/K00134/K00134/K00134/K00134/K00134/K00134/K00927/K00927/K00927/K00927/K00927/K00927/K00927/K00927/K00927/K00927/K01689/K01689/K01689/K01689/K01689/K01689/K01689/K01689/K01689/K01689/K01803/K01803/K01803/K01803/K01803/K01803/K01803/K01803/K01803/K01803/K15633/K15633/K15633/K15633/K15633/K15633/K15633/K15633/K15633/K15633/K00134/K00134/K00134/K00134/K00134/K00134/K00134/K00134/K00134/K00134/K00927/K00927/K00927/K00927/K00927/K00927/K00927/K00927/K00927/K00927/K01689/K01689/K01689/K01689/K01689/K01689/K01689/K01689/K01689/K01689/K01803/K01803/K01803/K01803/K01803/K01803/K01803/K01803/K01803/K01803/K15633/K15633/K15633/K15633/K15633/K15633/K15633/K15633/K15633/K15633/K00134/K00134/K00134/K00134/K00134/K00134/K00134/K00134/K00134/K00134/K00927/K00927/K00927/K00927/K00927/K00927/K00927/K00927/K00927/K00927/K01624/K00134/K00134/K00134/K00134/K00134/K00134/K00134/K00134/K00134/K00134/K00927/K00927/K00927/K00927/K00927/K00927/K00927/K00927/K00927/K00927/K01624
MAG.15	Gluconeogenesis	K01624/K01624/K01624/K01624/K01624/K01624/K01624/K01624/K01624/K01624/K01689/K01689/K01689/K01689/K01689/K01689/K01689/K01689/K01689/K01689/K01834/K01834/K01834/K01834/K01834/K01834/K01834/K01834/K01834/K01689/K01689/K01689/K01689/K01689/K01689/K01689/K01689/K01689/K01689/K01834/K01834/K01834/K01834/K01834/K01834/K01834/K01834/K01834/K01624
MAG.16	Gluconeogenesis	K01624/K01624/K01624/K01624/K01624/K01624/K01624/K01624/K01624/K01624/K01689/K01689/K01689/K01689/K01689/K01689/K01689/K01689/K01689/K01689/K15633/K15633/K15633/K15633/K15633/K15633/K15633/K15633/K15633/K15633/K01689/K01689/K01689/K01689/K01689/K01689/K01689/K01689/K01689/K01689/K15633/K15633/K15633/K15633/K15633/K15633/K15633/K15633/K15633/K15633/K00134/K00134/K00134/K00134/K00134/K00134/K00134/K00134/K00134/K00134/K01624/K01689/K01689/K01689/K01689/K01689/K01689/K01689/K01689/K01689/K01689
MAG.17	Gluconeogenesis	K00134/K00134/K00134/K00134/K00134/K00134/K00134/K00134/K00134/K00134/K00927/K00927/K00927/K00927/K00927/K00927/K00927/K00927/K00927/K00927/K01624/K01624/K01624/K01624/K01624/K01624/K01624/K01624/K01624/K01624/K01689/K01689/K01689/K01689/K01689/K01689/K01689/K01689/K01689/K01689/K01803/K01803/K01803/K01803/K01803/K01803/K01803/K01803/K01803/K01803/K15633/K15633/K15633/K15633/K15633/K15633/K15633/K15633/K15633/K15633/K00134/K00134/K00134/K00134/K00134/K00134/K00134/K00134/K00134/K00134/K00927/K00927/K00927/K00927/K00927/K00927/K00927/K00927/K00927/K00927/K01689/K01689/K01689/K01689/K01689/K01689/K01689/K01689/K01689/K01689/K01803/K01803/K01803/K01803/K01803/K01803/K01803/K01803/K01803/K01803/K15633/K15633/K15633/K15633/K15633/K15633/K15633/K15633/K15633/K15633/K00134/K00134/K00134/K00134/K00134/K00134/K00134/K00134/K00134/K00134/K00927/K00927/K00927/K00927/K00927/K00927/K00927/K00927/K00927/K00927/K01610/K01610/K01610/K01610/K01610/K01610/K01610/K01610/K01610/K01610/K01624/K01624/K01624/K01624/K01624/K01624/K01624/K01624/K01624/K01624/K01689/K01689/K01689/K01689/K01689/K01689/K01689/K01689/K01689/K01689/K01803/K01803/K01803/K01803/K01803/K01803/K01803/K01803/K01803/K01803/K02446/K02446/K02446/K02446/K02446/K02446/K02446/K02446/K02446/K02446/K04041/K04041/K15633/K15633/K15633/K15633/K15633/K15633/K15633/K15633/K15633/K15633/K00134/K00134/K00134/K00134/K00134/K00134/K00134/K00134/K00134/K00134/K00927/K00927/K00927/K00927/K00927/K00927/K00927/K00927/K00927/K00927/K01624/K02446/K02446/K02446/K02446/K02446/K02446/K02446/K02446/K02446/K02446/K04041/K04041/K00134/K00134/K00134/K00134/K00134/K00134/K00134/K00134/K00134/K00134/K00927/K00927/K00927/K00927/K00927/K00927/K00927/K00927/K00927/K00927/K01624/K02446/K02446/K02446/K02446/K02446/K02446/K02446/K02446/K02446/K02446/K04041/K04041/K00134/K00134/K00134/K00134/K00134/K00134/K00134/K00134/K00134/K00134/K00927/K00927/K00927/K00927/K00927/K00927/K00927/K00927/K00927/K00927/K01624/K01624/K01624/K01624/K01624/K01624/K01624/K01624/K01624/K01624/K01689/K01689/K01689/K01689/K01689/K01689/K01689/K01689/K01689/K01689

MAG.2	Gluconeogenesis	K00134/K00134/K00134/K00134/K00134/K00134/K00134/K00134/K00134/K00134/K00927/K00927/K00927/K00927/K00927/K00927/K00927/K00927/K00927/K00927/K01624/K01624/K01624/K01624/K01624/K01624/K01624/K01624/K01624/K01624/K01689/K01689/K01689/K01689/K01689/K01689/K01689/K01689/K01689/K01689/K01803/K01803/K01803/K01803/K01803/K01803/K01803/K01803/K01803/K01803/K15633/K15633/K15633/K15633/K15633/K15633/K15633/K15633/K15633/K15633/K00134/K00134/K00134/K00134/K00134/K00134/K00134/K00134/K00134/K00134/K00927/K00927/K00927/K00927/K00927/K00927/K00927/K00927/K00927/K00927/K01689/K01689/K01689/K01689/K01689/K01689/K01689/K01689/K01689/K01689/K01803/K01803/K01803/K01803/K01803/K01803/K01803/K01803/K01803/K01803/K15633/K15633/K15633/K15633/K15633/K15633/K15633/K15633/K15633/K15633/K00134/K00134/K00134/K00134/K00134/K00134/K00134/K00134/K00134/K00134/K00927/K00927/K00927/K00927/K00927/K00927/K00927/K00927/K00927/K00927/K01689/K01689/K01689/K01689/K01689/K01689/K01689/K01689/K01689/K01689/K01803/K01803/K01803/K01803/K01803/K01803/K01803/K01803/K01803/K01803/K15633/K15633/K15633/K15633/K15633/K15633/K15633/K15633/K15633/K15633/K00134/K00134/K00134/K00134/K00134/K00134/K00134/K00134/K00134/K00134/K00927/K00927/K00927/K00927/K00927/K00927/K00927/K00927/K00927/K00927/K01624/K00134/K00134/K00134/K00134/K00134/K00134/K00134/K00134/K00134/K00134/K00927/K00927/K00927/K00927/K00927/K00927/K00927/K00927/K00927/K00927/K01624
MAG.22	Gluconeogenesis	K00134/K00134/K00134/K00134/K00134/K00134/K00134/K00134/K00134/K00134/K00927/K00927/K00927/K00927/K00927/K00927/K00927/K00927/K00927/K00927/K01623/K01623/K01623/K01623/K01623/K01623/K01623/K01623/K01623/K01689/K01689/K01689/K01689/K01689/K01689/K01689/K01689/K01689/K01689/K01689/K01803/K01803/K01803/K01803/K01803/K01803/K01803/K01803/K01803/K01803/K01834/K01834/K01834/K01834/K01834/K01834/K01834/K01834/K01834/K00134/K00134/K00134/K00134/K00134/K00134/K00134/K00134/K00134/K00134/K00927/K00927/K00927/K00927/K00927/K00927/K00927/K00927/K00927/K00927/K01689/K01689/K01689/K01689/K01689/K01689/K01689/K01689/K01689/K01689/K01803/K01803/K01803/K01803/K01803/K01803/K01803/K01803/K01803/K01803/K01834/K01834/K01834/K01834/K01834/K01834/K01834/K01834/K01834/K00134/K00134/K00134/K00134/K00134/K00134/K00134/K00134/K00134/K00134/K00927/K00927/K00927/K00927/K00927/K00927/K00927/K00927/K00927/K00927/K01610/K01610/K01610/K01610/K01610/K01610/K01610/K01610/K01610/K01610/K01623/K01623/K01623/K01623/K01623/K01623/K01623/K01623/K01623/K01623/K01689/K01689/K01689/K01689/K01689/K01689/K01689/K01689/K01689/K01689/K01803/K01803/K01803/K01803/K01803/K01803/K01803/K01803/K01803/K01803/K01834/K01834/K01834/K01834/K01834/K01834/K01834/K01834/K01834/K03841/K03841/K03841/K03841/K03841/K03841/K03841/K03841/K03841/K11532/K11532/K11532/K11532/K11532/K11532/K00134/K00134/K00134/K00134/K00134/K00134/K00134/K00134/K00134/K00134/K00927/K00927/K00927/K00927/K00927/K00927/K00927/K00927/K00927/K00927/K01623/K03841/K03841/K03841/K03841/K03841/K03841/K03841/K03841/K03841/K11532/K11532/K11532/K11532/K11532/K11532/K11532/K11532/K11532/K11532/K11532/K11532/K00134/K00134/K00134/K00134/K00134/K00134/K00134/K00134/K00134/K00134/K00927/K00927/K00927/K00927/K00927/K00927/K00927/K00927/K00927/K00927/K01623/K03841/K03841/K03841/K03841/K03841/K03841/K03841/K03841/K03841/K11532/K11532/K11532/K11532/K11532/K11532/K11532/K11532/K11532/K11532/K11532/K11532/K01610/K01610/K01610/K01610/K01610/K01610/K01610/K01610/K01610/K01610/K00134/K00134/K00134/K00134/K00134/K00134/K00134/K00134/K00134/K00134/K00927/K00927/K00927/K00927/K00927/K00927/K00927/K00927/K00927/K00927/K01689/K01689/K01689/K01689/K01689/K01689/K01689/K01689/K01689/K01689/K00134/K00134/K00134/K00134/K00134/K00134/K00134/K00134/K00134/K00134/K00927/K00927/K00927/K00927/K00927/K00927/K00927/K00927/K00927/K00927
MAG.220783	Gluconeogenesis	K00134/K00134/K00134/K00134/K00134/K00134/K00134/K00134/K00134/K00134/K00927/K00927/K00927/K00927/K00927/K00927/K00927/K00927/K00927/K00927/K01689/K01689/K01689/K01689/K01689/K01689/K01689/K01689/K01689/K01689/K01803/K01803/K01803/K01803/K01803/K01803/K01803/K01803/K01803/K01803/K15633/K15633/K15633/K15633/K15633/K15633/K15633/K15633/K15633/K15633/K00134/K00134/K00134/K00134/K00134/K00134/K00134/K00134/K00134/K00134/K00927/K00927/K00927/K00927/K00927/K00927/K00927/K00927/K00927/K00927/K01689/K01689/K01689/K01689/K01689/K01689/K01689/K01689/K01689/K01689/K01803/K01803/K01803/K01803/K01803/K01803/K01803/K01803/K01803/K01803/K15633/K15633/K15633/K15633/K15633/K15633/K15633/K15633/K15633/K15633/K00134/K00134/K00134/K00134/K00134/K00134/K00134/K00134/K00134/K00134/K00927/K00927/K00927/K00927/K00927/K00927/K00927/K00927/K00927/K00927
MAG.25993	Gluconeogenesis	K01624/K01624/K01624/K01624/K01624/K01624/K01624/K01624/K01624/K01624/K01689/K01689/K01689/K01689/K01689/K01689/K01689/K01689/K01689/K01689/K01803/K01803/K01803/K01803/K01803/K01803/K01803/K01803/K01803/K15633/K15633/K15633/K15633/K15633/K15633/K15633/K15633/K15633/K15633/K15633/K01689/K01689/K01689/K01689/K01689/K01689/K01689/K01689/K01689/K01689/K01803/K01803/K01803/K01803/K01803/K01803/K01803/K01803/K01803/K01803/K15633/K15633/K15633/K15633/K15633/K15633/K15633/K15633/K15633/K15633/K00927/K00927/K00927/K00927/K00927/K00927/K00927/K00927/K00927/K00927/K01610/K01610/K01610/K01610/K01610/K01610/K01610/K01610/K01610/K01610/K01689/K01689/K01689/K01689/K01689/K01689/K01689/K01689/K01689/K01689/K01803/K01803/K01803/K01803/K01803/K01803/K01803/K01803/K01803/K01803/K15633/K15633/K15633/K15633/K15633/K15633/K15633/K15633/K15633/K15633/K01624/K01624/K01624/K01624/K01624/K01624/K01624/K01624/K01624/K01624/K01689/K01689/K01689/K01689/K01689/K01689/K01689/K01689/K01689/K01689
MAG.302726	Gluconeogenesis	K01624/K01624/K01624/K01624/K01624/K01624/K01624/K01624/K01624/K01624/K01689/K01689/K01689/K01689/K01689/K01689/K01689/K01689/K01689/K01689/K01803/K01803/K01803/K01803/K01803/K01803/K01803/K01803/K01803/K15633/K15633/K15633/K15633/K15633/K15633/K15633/K15633/K15633/K15633/K15633/K01689/K01689/K01689/K01689/K01689/K01689/K01689/K01689/K01689/K01689/K01803/K01803/K01803/K01803/K01803/K01803/K01803/K01803/K01803/K01803/K15633/K15633/K15633/K15633/K15633/K15633/K15633/K15633/K15633/K15633/K00134/K00134/K00134/K00134/K00134/K00134/K00134/K00134/K00134/K00134/K01610/K01610/K01610/K01610/K01610/K01610/K01610/K01610/K01610/K01610/K01624/K01624/K01624/K01624/K01624/K01624/K01624/K01624/K01624/K01624/K01689/K01689/K01689/K01689/K01689/K01689/K01689/K01689/K01689/K01689/K01803/K01803/K01803/K01803/K01803/K01803/K01803/K01803/K01803/K01803/K03841/K03841/K03841/K03841/K03841/K03841/K03841/K03841/K03841/K15633/K15633/K15633/K15633/K15633/K15633/K15633/K15633/K15633/K15633/K00134/K00134/K00134/K00134/K00134/K00134/K00134/K00134/K00134/K00134/K01624/K03841/K03841/K03841/K03841/K03841/K03841/K03841/K03841/K03841/K01624/K03841/K03841/K03841/K03841/K03841/K03841/K03841/K03841/K03841/K01624/K01624/K01624/K01624/K01624/K01624/K01624/K01624/K01624/K01624/K03841/K03841/K03841/K03841/K03841/K03841/K03841/K03841/K03841
MAG.309811	Gluconeogenesis	K00134/K00134/K00134/K00134/K00134/K00134/K00134/K00134/K00134/K00134/K00927/K00927/K00927/K00927/K00927/K00927/K00927/K00927/K00927/K00927/K01624/K01624/K01624/K01624/K01624/K01624/K01624/K01624/K01624/K01624/K01689/K01689/K01689/K01689/K01689/K01689/K01689/K01689/K01689/K01689/K01803/K01803/K01803/K01803/K01803/K01803/K01803/K01803/K01803/K01803/K01834/K01834/K01834/K01834/K01834/K01834/K01834/K01834/K01834/K15635/K15635/K15635/K00134/K00134/K00134/K00134/K00134/K00134/K00134/K00134/K00134/K00134/K00927/K00927/K00927/K00927/K00927/K00927/K00927/K00927/K00927/K00927/K01689/K01689/K01689/K01689/K01689/K01689/K01689/K01689/K01689/K01689/K01803/K01803/K01803/K01803/K01803/K01803/K01803/K01803/K01803/K01803/K01834/K01834/K01834/K01834/K01834/K01834/K01834/K01834/K01834/K15635/K15635/K15635/K00134/K00134/K00134/K00134/K00134/K00134/K00134/K00134/K00134/K00134/K00927/K00927/K00927/K00927/K00927/K00927/K00927/K00927/K00927/K00927/K01596/K01596/K01596/K01689/K01689/K01689/K01689/K01689/K01689/K01689/K01689/K01689/K01689/K01803/K01803/K01803/K01803/K01803/K01803/K01803/K01803/K01803/K01803/K01834/K01834/K01834/K01834/K01834/K01834/K01834/K01834/K01834/K15635/K15635/K15635/K00134/K00134/K00134/K00134/K00134/K00134/K00134/K00134/K00134/K00134/K00927/K00927/K00927/K00927/K00927/K00927/K00927/K00927/K00927/K00927/K01624/K00134/K00134/K00134/K00134/K00134/K00134/K00134/K00134/K00134/K00134/K00927/K00927/K00927/K00927/K00927/K00927/K00927/K00927/K00927/K00927/K01624/K01689/K01689/K01689/K01689/K01689/K01689/K01689/K01689/K01689/K01689
MAG.332111	Gluconeogenesis	K00134/K00134/K00134/K00134/K00134/K00134/K00134/K00134/K00134/K00134/K00150/K00927/K00927/K00927/K00927/K00927/K00927/K00927/K00927/K00927/K00927/K01624/K01624/K01624/K01624/K01624/K01624/K01624/K01624/K01624/K01624/K01689/K01689/K01689/K01689/K01689/K01689/K01689/K01689/K01689/K01689/K01803/K01803/K01803/K01803/K01803/K01803/K01803/K01803/K01803/K01803/K11645/K15633/K15633/K15633/K15633/K15633/K15633/K15633/K15633/K15633/K15633/K00134/K00134/K00134/K00134/K00134/K00134/K00134/K00134/K00134/K00134/K00150/K00927/K00927/K00927/K00927/K00927/K00927/K00927/K00927/K00927/K00927/K01689/K01689/K01689/K01689/K01689/K01689/K01689/K01689/K01689/K01689/K01803/K01803/K01803/K01803/K01803/K01803/K01803/K01803/K01803/K01803/K15633/K15633/K15633/K15633/K15633/K15633/K15633/K15633/K15633/K15633/K00134/K00134/K00134/K00134/K00134/K00134/K00134/K00134/K00134/K00134/K00150/K00927/K00927/K00927/K00927/K00927/K00927/K00927/K00927/K00927/K00927/K01610/K01610/K01610/K01610/K01610/K01610/K01610/K01610/K01610/K01610/K01624/K01624/K01624/K01624/K01624/K01624/K01624/K01624/K01624/K01624/K01689/K01689/K01689/K01689/K01689/K01689/K01689/K01689/K01689/K01689/K01803/K01803/K01803/K01803/K01803/K01803/K01803/K01803/K01803/K01803/K03841/K03841/K03841/K03841/K03841/K03841/K03841/K03841/K03841/K11532/K11532/K11532/K11532/K11532/K11532/K11645/K15633/K15633/K15633/K15633/K15633/K15633/K15633/K15633/K15633/K15633/K00134/K00134/K00134/K00134/K00134/K00134/K00134/K00134/K00134/K00134/K00150/K00927/K00927/K00927/K00927/K00927/K00927/K00927/K00927/K00927/K00927/K01624/K03841/K03841/K03841/K03841/K03841/K03841/K03841/K03841/K03841/K11532/K11532/K11532/K11532/K11532/K11532/K11532/K11532/K11532/K11532/K11532/K11532/K00134/K00134/K00134/K00134/K00134/K00134/K00134/K00134/K00134/K00134/K00150/K00927/K00927/K00927/K00927/K00927/K00927/K00927/K00927/K00927/K00927/K01624/K03841/K03841/K03841/K03841/K03841/K03841/K03841/K03841/K03841/K11532/K11532/K11532/K11532/K11532/K11532/K11532/K11532/K11532/K11532/K11532/K11532/K01610/K01610/K01610/K01610/K01610/K01610/K01610/K01610/K01610/K01610/K00134/K00134/K00134/K00134/K00134/K00134/K00134/K00134/K00134/K00134/K00927/K00927/K00927/K00927/K00927/K00927/K00927/K00927/K00927/K00927/K01624/K01624/K01624/K01624/K01624/K01624/K01624/K01624/K01624/K01624/K03841/K03841/K03841/K03841/K03841/K03841/K03841/K03841/K03841/K01689
MAG.8	Gluconeogenesis	K01624/K01624/K01624/K01624/K01624/K01624/K01624/K01624/K01624/K01624/K01689/K01689/K01689/K01689/K01689/K01689/K01689/K01689/K01689/K01689/K01803/K01803/K01803/K01803/K01803/K01803/K01803/K01803/K01803/K01689/K01689/K01689/K01689/K01689/K01689/K01689/K01689/K01689/K01689/K01689/K01803/K01803/K01803/K01803/K01803/K01803/K01803/K01803/K01803/K01803/K00927/K00927/K00927/K00927/K00927/K00927/K00927/K00927/K00927/K00927/K01624

MAG.10	Glycolysis	K00134/K00134/K00134/K00134/K00134/K00134/K00134/K00134/K00134/K00134/K00927/K00927/K00927/K00927/K00927/K00927/K00927/K00927/K00927/K00927
MAG.12	Glycolysis	K00134/K00134/K00134/K00134/K00134/K00134/K00134/K00134/K00134/K00134/K00873/K00873/K00873/K00873/K00873/K00873/K00873/K00873/K00873/K00873/K00927/K00927/K00927/K00927/K00927/K00927/K00927/K00927/K00927/K00927/K01624/K01624/K01624/K01624/K01624/K01624/K01624/K01624/K01624/K01624/K01689/K01689/K01689/K01689/K01689/K01689/K01689/K01689/K01689/K01689/K01803/K01803/K01803/K01803/K01803/K01803/K01803/K01803/K01803/K01803/K01810/K01810/K01810/K01810/K01810/K01810/K01810/K01810/K01810/K01810/K15633/K15633/K15633/K15633/K15633/K15633/K15633/K15633/K15633/K15633/K00134/K00134/K00134/K00134/K00134/K00134/K00134/K00134/K00134/K00134/K00873/K00873/K00873/K00873/K00873/K00873/K00873/K00873/K00873/K00873/K00927/K00927/K00927/K00927/K00927/K00927/K00927/K00927/K00927/K00927/K01689/K01689/K01689/K01689/K01689/K01689/K01689/K01689/K01689/K01689/K01803/K01803/K01803/K01803/K01803/K01803/K01803/K01803/K01803/K01803/K15633/K15633/K15633/K15633/K15633/K15633/K15633/K15633/K15633/K15633/K00134/K00134/K00134/K00134/K00134/K00134/K00134/K00134/K00134/K00134/K00927/K00927/K00927/K00927/K00927/K00927/K00927/K00927/K00927/K00927/K01689/K01689/K01689/K01689/K01689/K01689/K01689/K01689/K01689/K01689/K01803/K01803/K01803/K01803/K01803/K01803/K01803/K01803/K01803/K01803/K15633/K15633/K15633/K15633/K15633/K15633/K15633/K15633/K15633/K15633/K01810/K01810/K01810/K01810/K01810/K01810/K01810/K01810/K01810/K01810/K00873/K00134/K00134/K00134/K00134/K00134/K00134/K00134/K00134/K00134/K00134/K00927/K00927/K00927/K00927/K00927/K00927/K00927/K00927/K00927/K00927/K01624/K00134/K00134/K00134/K00134/K00134/K00134/K00134/K00134/K00134/K00134/K00927/K00927/K00927/K00927/K00927/K00927/K00927/K00927/K00927/K00927/K01624/K00134/K00134/K00134/K00134/K00134/K00134/K00134/K00134/K00134/K00134/K00927/K00927/K00927/K00927/K00927/K00927/K00927/K00927/K00927/K00927/K01689
MAG.13	Glycolysis	K01624/K01624/K01624/K01624/K01624/K01624/K01624/K01624/K01624/K01624/K01624/K01624/K01624/K01624/K01624/K01624/K01624/K01624/K01624/K01624
MAG.14	Glycolysis	K00134/K00134/K00134/K00134/K00134/K00134/K00134/K00134/K00134/K00134/K00850/K00850/K00850/K00850/K00850/K00850/K00850/K00850/K00850/K00850/K00873/K00873/K00873/K00873/K00873/K00873/K00873/K00873/K00873/K00873/K00927/K00927/K00927/K00927/K00927/K00927/K00927/K00927/K00927/K00927/K01624/K01624/K01624/K01624/K01624/K01624/K01624/K01624/K01624/K01624/K01689/K01689/K01689/K01689/K01689/K01689/K01689/K01689/K01689/K01689/K01803/K01803/K01803/K01803/K01803/K01803/K01803/K01803/K01803/K01803/K01810/K01810/K01810/K01810/K01810/K01810/K01810/K01810/K01810/K01810/K15633/K15633/K15633/K15633/K15633/K15633/K15633/K15633/K15633/K15633/K00134/K00134/K00134/K00134/K00134/K00134/K00134/K00134/K00134/K00134/K00873/K00873/K00873/K00873/K00873/K00873/K00873/K00873/K00873/K00873/K00927/K00927/K00927/K00927/K00927/K00927/K00927/K00927/K00927/K00927/K01689/K01689/K01689/K01689/K01689/K01689/K01689/K01689/K01689/K01689/K01803/K01803/K01803/K01803/K01803/K01803/K01803/K01803/K01803/K01803/K15633/K15633/K15633/K15633/K15633/K15633/K15633/K15633/K15633/K15633/K00134/K00134/K00134/K00134/K00134/K00134/K00134/K00134/K00134/K00134/K00927/K00927/K00927/K00927/K00927/K00927/K00927/K00927/K00927/K00927/K01689/K01689/K01689/K01689/K01689/K01689/K01689/K01689/K01689/K01689/K01803/K01803/K01803/K01803/K01803/K01803/K01803/K01803/K01803/K01803/K15633/K15633/K15633/K15633/K15633/K15633/K15633/K15633/K15633/K15633/K01810/K01810/K01810/K01810/K01810/K01810/K01810/K01810/K01810/K01810/K00873/K00134/K00134/K00134/K00134/K00134/K00134/K00134/K00134/K00134/K00134/K00927/K00927/K00927/K00927/K00927/K00927/K00927/K00927/K00927/K00927/K01624/K00134/K00134/K00134/K00134/K00134/K00134/K00134/K00134/K00134/K00134/K00927/K00927/K00927/K00927/K00927/K00927/K00927/K00927/K00927/K00927/K01624/K00850/K00850/K00850/K00850/K00850/K00850/K00850/K00850/K00850/K00850/K01624/K01624/K01624/K01624/K01624/K01624/K01624/K01624/K01624/K01624
MAG.15	Glycolysis	K00845/K00873/K00873/K00873/K00873/K00873/K00873/K00873/K00873/K00873/K00873/K01624/K01624/K01624/K01624/K01624/K01624/K01624/K01624/K01624/K01624/K01689/K01689/K01689/K01689/K01689/K01689/K01689/K01689/K01689/K01689/K01810/K01810/K01810/K01810/K01810/K01810/K01810/K01810/K01810/K01810/K01834/K01834/K01834/K01834/K01834/K01834/K01834/K01834/K01834/K00873/K00873/K00873/K00873/K00873/K00873/K00873/K00873/K00873/K00873/K01689/K01689/K01689/K01689/K01689/K01689/K01689/K01689/K01689/K01689/K01834/K01834/K01834/K01834/K01834/K01834/K01834/K01834/K01834/K01810/K01810/K01810/K01810/K01810/K01810/K01810/K01810/K01810/K01810/K00873/K01624/K00845
MAG.16	Glycolysis	K00850/K00850/K00850/K00850/K00850/K00850/K00850/K00850/K00850/K00850/K00873/K00873/K00873/K00873/K00873/K00873/K00873/K00873/K00873/K00873/K01624/K01624/K01624/K01624/K01624/K01624/K01624/K01624/K01624/K01624/K01689/K01689/K01689/K01689/K01689/K01689/K01689/K01689/K01689/K01689/K01810/K01810/K01810/K01810/K01810/K01810/K01810/K01810/K01810/K01810/K15633/K15633/K15633/K15633/K15633/K15633/K15633/K15633/K15633/K15633/K00873/K00873/K00873/K00873/K00873/K00873/K00873/K00873/K00873/K00873/K01689/K01689/K01689/K01689/K01689/K01689/K01689/K01689/K01689/K01689/K15633/K15633/K15633/K15633/K15633/K15633/K15633/K15633/K15633/K15633/K00873/K00134/K00134/K00134/K00134/K00134/K00134/K00134/K00134/K00134/K00134/K01624/K00850/K00850/K00850/K00850/K00850/K00850/K00850/K00850/K00850/K00850/K01624/K01624/K01624/K01624/K01624/K01624/K01624/K01624/K01624/K01624/K01689/K01689/K01689/K01689/K01689/K01689/K01689/K01689/K01689/K01689
MAG.17	Glycolysis	K00134/K00134/K00134/K00134/K00134/K00134/K00134/K00134/K00134/K00134/K00850/K00850/K00850/K00850/K00850/K00850/K00850/K00850/K00850/K00850/K00873/K00873/K00873/K00873/K00873/K00873/K00873/K00873/K00873/K00873/K00927/K00927/K00927/K00927/K00927/K00927/K00927/K00927/K00927/K00927/K01624/K01624/K01624/K01624/K01624/K01624/K01624/K01624/K01624/K01624/K01689/K01689/K01689/K01689/K01689/K01689/K01689/K01689/K01689/K01689/K01803/K01803/K01803/K01803/K01803/K01803/K01803/K01803/K01803/K01803/K01810/K01810/K01810/K01810/K01810/K01810/K01810/K01810/K01810/K01810/K15633/K15633/K15633/K15633/K15633/K15633/K15633/K15633/K15633/K15633/K00134/K00134/K00134/K00134/K00134/K00134/K00134/K00134/K00134/K00134/K00873/K00873/K00873/K00873/K00873/K00873/K00873/K00873/K00873/K00873/K00927/K00927/K00927/K00927/K00927/K00927/K00927/K00927/K00927/K00927/K01689/K01689/K01689/K01689/K01689/K01689/K01689/K01689/K01689/K01689/K01803/K01803/K01803/K01803/K01803/K01803/K01803/K01803/K01803/K01803/K15633/K15633/K15633/K15633/K15633/K15633/K15633/K15633/K15633/K15633/K00134/K00134/K00134/K00134/K00134/K00134/K00134/K00134/K00134/K00134/K00927/K00927/K00927/K00927/K00927/K00927/K00927/K00927/K00927/K00927/K01624/K01624/K01624/K01624/K01624/K01624/K01624/K01624/K01624/K01624/K01689/K01689/K01689/K01689/K01689/K01689/K01689/K01689/K01689/K01689/K01803/K01803/K01803/K01803/K01803/K01803/K01803/K01803/K01803/K01803/K15633/K15633/K15633/K15633/K15633/K15633/K15633/K15633/K15633/K15633/K01810/K01810/K01810/K01810/K01810/K01810/K01810/K01810/K01810/K01810/K00873/K00134/K00134/K00134/K00134/K00134/K00134/K00134/K00134/K00134/K00134/K00927/K00927/K00927/K00927/K00927/K00927/K00927/K00927/K00927/K00927/K01624/K00134/K00134/K00134/K00134/K00134/K00134/K00134/K00134/K00134/K00134/K00927/K00927/K00927/K00927/K00927/K00927/K00927/K00927/K00927/K00927/K01624/K00134/K00134/K00134/K00134/K00134/K00134/K00134/K00134/K00134/K00134/K00927/K00927/K00927/K00927/K00927/K00927/K00927/K00927/K00927/K00927/K00850/K00850/K00850/K00850/K00850/K00850/K00850/K00850/K00850/K00850/K01624/K01624/K01624/K01624/K01624/K01624/K01624/K01624/K01624/K01624/K01689/K01689/K01689/K01689/K01689/K01689/K01689/K01689/K01689/K01689
MAG.2	Glycolysis	K00134/K00134/K00134/K00134/K00134/K00134/K00134/K00134/K00134/K00134/K00845/K00850/K00850/K00850/K00850/K00850/K00850/K00850/K00850/K00850/K00850/K00873/K00873/K00873/K00873/K00873/K00873/K00873/K00873/K00873/K00873/K00927/K00927/K00927/K00927/K00927/K00927/K00927/K00927/K00927/K00927/K01624/K01624/K01624/K01624/K01624/K01624/K01624/K01624/K01624/K01624/K01689/K01689/K01689/K01689/K01689/K01689/K01689/K01689/K01689/K01689/K01803/K01803/K01803/K01803/K01803/K01803/K01803/K01803/K01803/K01803/K01810/K01810/K01810/K01810/K01810/K01810/K01810/K01810/K01810/K01810/K15633/K15633/K15633/K15633/K15633/K15633/K15633/K15633/K15633/K15633/K00134/K00134/K00134/K00134/K00134/K00134/K00134/K00134/K00134/K00134/K00873/K00873/K00873/K00873/K00873/K00873/K00873/K00873/K00873/K00873/K00927/K00927/K00927/K00927/K00927/K00927/K00927/K00927/K00927/K00927/K01689/K01689/K01689/K01689/K01689/K01689/K01689/K01689/K01689/K01689/K01803/K01803/K01803/K01803/K01803/K01803/K01803/K01803/K01803/K01803/K15633/K15633/K15633/K15633/K15633/K15633/K15633/K15633/K15633/K15633/K00134/K00134/K00134/K00134/K00134/K00134/K00134/K00134/K00134/K00134/K00927/K00927/K00927/K00927/K00927/K00927/K00927/K00927/K00927/K00927/K01689/K01689/K01689/K01689/K01689/K01689/K01689/K01689/K01689/K01689/K01803/K01803/K01803/K01803/K01803/K01803/K01803/K01803/K01803/K01803/K15633/K15633/K15633/K15633/K15633/K15633/K15633/K15633/K15633/K15633/K01810/K01810/K01810/K01810/K01810/K01810/K01810/K01810/K01810/K01810/K00873/K00134/K00134/K00134/K00134/K00134/K00134/K00134/K00134/K00134/K00134/K00927/K00927/K00927/K00927/K00927/K00927/K00927/K00927/K00927/K00927/K01624/K00134/K00134/K00134/K00134/K00134/K00134/K00134/K00134/K00134/K00134/K00927/K00927/K00927/K00927/K00927/K00927/K00927/K00927/K00927/K00927/K01624/K00850/K00850/K00850/K00850/K00850/K00850/K00850/K00850/K00850/K00850/K01624/K01624/K01624/K01624/K01624/K01624/K01624/K01624/K01624/K01624/K00845

MAG.22	Glycolysis	K00134/K00134/K00134/K00134/K00134/K00134/K00134/K00134/K00134/K00134/K00845/K00873/K00873/K00873/K00873/K00873/K00873/K00873/K00873/K00873/K00873/K00927/K00927/K00927/K00927/K00927/K00927/K00927/K00927/K00927/K00927/K01623/K01623/K01623/K01623/K01623/K01623/K01623/K01623/K01623/K01623/K01689/K01689/K01689/K01689/K01689/K01689/K01689/K01689/K01689/K01689/K01803/K01803/K01803/K01803/K01803/K01803/K01803/K01803/K01803/K01803/K01810/K01810/K01810/K01810/K01810/K01810/K01810/K01810/K01810/K01810/K01834/K01834/K01834/K01834/K01834/K01834/K01834/K01834/K01834/K00134/K00134/K00134/K00134/K00134/K00134/K00134/K00134/K00134/K00134/K00873/K00873/K00873/K00873/K00873/K00873/K00873/K00873/K00873/K00873/K00927/K00927/K00927/K00927/K00927/K00927/K00927/K00927/K00927/K00927/K01689/K01689/K01689/K01689/K01689/K01689/K01689/K01689/K01689/K01689/K01803/K01803/K01803/K01803/K01803/K01803/K01803/K01803/K01803/K01803/K01834/K01834/K01834/K01834/K01834/K01834/K01834/K01834/K01834/K00134/K00134/K00134/K00134/K00134/K00134/K00134/K00134/K00134/K00134/K00927/K00927/K00927/K00927/K00927/K00927/K00927/K00927/K00927/K00927/K01623/K01623/K01623/K01623/K01623/K01623/K01623/K01623/K01623/K01623/K01689/K01689/K01689/K01689/K01689/K01689/K01689/K01689/K01689/K01689/K01803/K01803/K01803/K01803/K01803/K01803/K01803/K01803/K01803/K01803/K01834/K01834/K01834/K01834/K01834/K01834/K01834/K01834/K01834/K01810/K01810/K01810/K01810/K01810/K01810/K01810/K01810/K01810/K01810/K00873/K00134/K00134/K00134/K00134/K00134/K00134/K00134/K00134/K00134/K00134/K00927/K00927/K00927/K00927/K00927/K00927/K00927/K00927/K00927/K00927/K01623/K00134/K00134/K00134/K00134/K00134/K00134/K00134/K00134/K00134/K00134/K00927/K00927/K00927/K00927/K00927/K00927/K00927/K00927/K00927/K00927/K01623/K00134/K00134/K00134/K00134/K00134/K00134/K00134/K00134/K00134/K00134/K00927/K00927/K00927/K00927/K00927/K00927/K00927/K00927/K00927/K00927/K01689/K01689/K01689/K01689/K01689/K01689/K01689/K01689/K01689/K01689/K00845/K00134/K00134/K00134/K00134/K00134/K00134/K00134/K00134/K00134/K00134/K00927/K00927/K00927/K00927/K00927/K00927/K00927/K00927/K00927/K00927
MAG.220783	Glycolysis	K00134/K00134/K00134/K00134/K00134/K00134/K00134/K00134/K00134/K00134/K00927/K00927/K00927/K00927/K00927/K00927/K00927/K00927/K00927/K00927/K01689/K01689/K01689/K01689/K01689/K01689/K01689/K01689/K01689/K01689/K01803/K01803/K01803/K01803/K01803/K01803/K01803/K01803/K01803/K01803/K15633/K15633/K15633/K15633/K15633/K15633/K15633/K15633/K15633/K15633/K00134/K00134/K00134/K00134/K00134/K00134/K00134/K00134/K00134/K00134/K00927/K00927/K00927/K00927/K00927/K00927/K00927/K00927/K00927/K00927/K01689/K01689/K01689/K01689/K01689/K01689/K01689/K01689/K01689/K01689/K01803/K01803/K01803/K01803/K01803/K01803/K01803/K01803/K01803/K01803/K15633/K15633/K15633/K15633/K15633/K15633/K15633/K15633/K15633/K15633/K00134/K00134/K00134/K00134/K00134/K00134/K00134/K00134/K00134/K00134/K00927/K00927/K00927/K00927/K00927/K00927/K00927/K00927/K00927/K00927
MAG.25993	Glycolysis	K00850/K00850/K00850/K00850/K00850/K00850/K00850/K00850/K00850/K00850/K01624/K01624/K01624/K01624/K01624/K01624/K01624/K01624/K01624/K01624/K01689/K01689/K01689/K01689/K01689/K01689/K01689/K01689/K01689/K01689/K01803/K01803/K01803/K01803/K01803/K01803/K01803/K01803/K01803/K01803/K01810/K01810/K01810/K01810/K01810/K01810/K01810/K01810/K01810/K01810/K15633/K15633/K15633/K15633/K15633/K15633/K15633/K15633/K15633/K15633/K01689/K01689/K01689/K01689/K01689/K01689/K01689/K01689/K01689/K01689/K01803/K01803/K01803/K01803/K01803/K01803/K01803/K01803/K01803/K01803/K15633/K15633/K15633/K15633/K15633/K15633/K15633/K15633/K15633/K15633/K00927/K00927/K00927/K00927/K00927/K00927/K00927/K00927/K00927/K00927/K01689/K01689/K01689/K01689/K01689/K01689/K01689/K01689/K01689/K01689/K01803/K01803/K01803/K01803/K01803/K01803/K01803/K01803/K01803/K01803/K15633/K15633/K15633/K15633/K15633/K15633/K15633/K15633/K15633/K15633/K00850/K00850/K00850/K00850/K00850/K00850/K00850/K00850/K00850/K00850/K01624/K01624/K01624/K01624/K01624/K01624/K01624/K01624/K01624/K01624/K01689/K01689/K01689/K01689/K01689/K01689/K01689/K01689/K01689/K01689
MAG.302726	Glycolysis	K00873/K00873/K00873/K00873/K00873/K00873/K00873/K00873/K00873/K00873/K01624/K01624/K01624/K01624/K01624/K01624/K01624/K01624/K01624/K01624/K01689/K01689/K01689/K01689/K01689/K01689/K01689/K01689/K01689/K01689/K01803/K01803/K01803/K01803/K01803/K01803/K01803/K01803/K01803/K01803/K15633/K15633/K15633/K15633/K15633/K15633/K15633/K15633/K15633/K15633/K00873/K00873/K00873/K00873/K00873/K00873/K00873/K00873/K00873/K00873/K01689/K01689/K01689/K01689/K01689/K01689/K01689/K01689/K01689/K01689/K01803/K01803/K01803/K01803/K01803/K01803/K01803/K01803/K01803/K01803/K15633/K15633/K15633/K15633/K15633/K15633/K15633/K15633/K15633/K15633/K00134/K00134/K00134/K00134/K00134/K00134/K00134/K00134/K00134/K00134/K01624/K01624/K01624/K01624/K01624/K01624/K01624/K01624/K01624/K01624/K01689/K01689/K01689/K01689/K01689/K01689/K01689/K01689/K01689/K01689/K01803/K01803/K01803/K01803/K01803/K01803/K01803/K01803/K01803/K01803/K15633/K15633/K15633/K15633/K15633/K15633/K15633/K15633/K15633/K15633/K00873/K00134/K00134/K00134/K00134/K00134/K00134/K00134/K00134/K00134/K00134/K01624
MAG.309811	Glycolysis	K00134/K00134/K00134/K00134/K00134/K00134/K00134/K00134/K00134/K00134/K00845/K00850/K00850/K00850/K00850/K00850/K00850/K00850/K00850/K00850/K00850/K00873/K00873/K00873/K00873/K00873/K00873/K00873/K00873/K00873/K00873/K00927/K00927/K00927/K00927/K00927/K00927/K00927/K00927/K00927/K00927/K01624/K01624/K01624/K01624/K01624/K01624/K01624/K01624/K01624/K01624/K01689/K01689/K01689/K01689/K01689/K01689/K01689/K01689/K01689/K01689/K01803/K01803/K01803/K01803/K01803/K01803/K01803/K01803/K01803/K01803/K01810/K01810/K01810/K01810/K01810/K01810/K01810/K01810/K01810/K01810/K01834/K01834/K01834/K01834/K01834/K01834/K01834/K01834/K01834/K15635/K15635/K15635/K00134/K00134/K00134/K00134/K00134/K00134/K00134/K00134/K00134/K00134/K00873/K00873/K00873/K00873/K00873/K00873/K00873/K00873/K00873/K00873/K00927/K00927/K00927/K00927/K00927/K00927/K00927/K00927/K00927/K00927/K01689/K01689/K01689/K01689/K01689/K01689/K01689/K01689/K01689/K01689/K01803/K01803/K01803/K01803/K01803/K01803/K01803/K01803/K01803/K01803/K01834/K01834/K01834/K01834/K01834/K01834/K01834/K01834/K01834/K15635/K15635/K15635/K00134/K00134/K00134/K00134/K00134/K00134/K00134/K00134/K00134/K00134/K00927/K00927/K00927/K00927/K00927/K00927/K00927/K00927/K00927/K00927/K01689/K01689/K01689/K01689/K01689/K01689/K01689/K01689/K01689/K01689/K01803/K01803/K01803/K01803/K01803/K01803/K01803/K01803/K01803/K01803/K01834/K01834/K01834/K01834/K01834/K01834/K01834/K01834/K01834/K15635/K15635/K15635/K01810/K01810/K01810/K01810/K01810/K01810/K01810/K01810/K01810/K01810/K00873/K00134/K00134/K00134/K00134/K00134/K00134/K00134/K00134/K00134/K00134/K00927/K00927/K00927/K00927/K00927/K00927/K00927/K00927/K00927/K00927/K01624/K00134/K00134/K00134/K00134/K00134/K00134/K00134/K00134/K00134/K00134/K00927/K00927/K00927/K00927/K00927/K00927/K00927/K00927/K00927/K00927/K01624/K00850/K00850/K00850/K00850/K00850/K00850/K00850/K00850/K00850/K00850/K01624/K01624/K01624/K01624/K01624/K01624/K01624/K01624/K01624/K01624/K01689/K01689/K01689/K01689/K01689/K01689/K01689/K01689/K01689/K01689/K00845
MAG.332111	Glycolysis	K00134/K00134/K00134/K00134/K00134/K00134/K00134/K00134/K00134/K00134/K00150/K00845/K00873/K00873/K00873/K00873/K00873/K00873/K00873/K00873/K00873/K00873/K00886/K00886/K00927/K00927/K00927/K00927/K00927/K00927/K00927/K00927/K00927/K00927/K01624/K01624/K01624/K01624/K01624/K01624/K01624/K01624/K01624/K01624/K01689/K01689/K01689/K01689/K01689/K01689/K01689/K01689/K01689/K01689/K01803/K01803/K01803/K01803/K01803/K01803/K01803/K01803/K01803/K01803/K01810/K01810/K01810/K01810/K01810/K01810/K01810/K01810/K01810/K01810/K11645/K15633/K15633/K15633/K15633/K15633/K15633/K15633/K15633/K15633/K15633/K00134/K00134/K00134/K00134/K00134/K00134/K00134/K00134/K00134/K00134/K00150/K00873/K00873/K00873/K00873/K00873/K00873/K00873/K00873/K00873/K00873/K00927/K00927/K00927/K00927/K00927/K00927/K00927/K00927/K00927/K00927/K01689/K01689/K01689/K01689/K01689/K01689/K01689/K01689/K01689/K01689/K01803/K01803/K01803/K01803/K01803/K01803/K01803/K01803/K01803/K01803/K15633/K15633/K15633/K15633/K15633/K15633/K15633/K15633/K15633/K15633/K00134/K00134/K00134/K00134/K00134/K00134/K00134/K00134/K00134/K00134/K00150/K00927/K00927/K00927/K00927/K00927/K00927/K00927/K00927/K00927/K00927/K01624/K01624/K01624/K01624/K01624/K01624/K01624/K01624/K01624/K01624/K01689/K01689/K01689/K01689/K01689/K01689/K01689/K01689/K01689/K01689/K01803/K01803/K01803/K01803/K01803/K01803/K01803/K01803/K01803/K01803/K11645/K15633/K15633/K15633/K15633/K15633/K15633/K15633/K15633/K15633/K15633/K01810/K01810/K01810/K01810/K01810/K01810/K01810/K01810/K01810/K01810/K00873/K00134/K00134/K00134/K00134/K00134/K00134/K00134/K00134/K00134/K00134/K00150/K00927/K00927/K00927/K00927/K00927/K00927/K00927/K00927/K00927/K00927/K01624/K00134/K00134/K00134/K00134/K00134/K00134/K00134/K00134/K00134/K00134/K00150/K00927/K00927/K00927/K00927/K00927/K00927/K00927/K00927/K00927/K00927/K01624/K00134/K00134/K00134/K00134/K00134/K00134/K00134/K00134/K00134/K00134/K00927/K00927/K00927/K00927/K00927/K00927/K00927/K00927/K00927/K00927/K01624/K01624/K01624/K01624/K01624/K01624/K01624/K01624/K01624/K01624/K01689/K00845/K00886/K00886
MAG.8	Glycolysis	K00850/K00850/K00850/K00850/K00850/K00850/K00850/K00850/K00850/K00850/K00873/K00873/K00873/K00873/K00873/K00873/K00873/K00873/K00873/K00873/K01624/K01624/K01624/K01624/K01624/K01624/K01624/K01624/K01624/K01624/K01689/K01689/K01689/K01689/K01689/K01689/K01689/K01689/K01689/K01689/K01803/K01803/K01803/K01803/K01803/K01803/K01803/K01803/K01803/K01803/K01810/K01810/K01810/K01810/K01810/K01810/K01810/K01810/K01810/K01810/K00873/K00873/K00873/K00873/K00873/K00873/K00873/K00873/K00873/K00873/K01689/K01689/K01689/K01689/K01689/K01689/K01689/K01689/K01689/K01689/K01803/K01803/K01803/K01803/K01803/K01803/K01803/K01803/K01803/K01803/K01810/K01810/K01810/K01810/K01810/K01810/K01810/K01810/K01810/K01810/K00873/K00927/K00927/K00927/K00927/K00927/K00927/K00927/K00927/K00927/K00927/K01624/K00850/K00850/K00850/K00850/K00850/K00850/K00850/K00850/K00850/K00850/K01624/K01624/K01624/K01624/K01624/K01624/K01624/K01624/K01624/K01624

MAG.17	Menaquinone biosynthesis	K01661/K01911/K02548/K02549/K02551/K02552/K03183/K08680/K19222
MAG.302726	Menaquinone biosynthesis	K01661/K01911/K02548/K03183
MAG.309811	Menaquinone biosynthesis	K01661/K01911/K02548/K02549/K02551/K02552/K03183/K08680/K12073
MAG.332111	Menaquinone biosynthesis	K01661/K01911/K02548/K02549/K02551/K02552/K03183/K08680/K12073
MAG.22	NADH-quinone oxidoreductase	K00330/K00330/K00330/K00330/K00330/K00330/K00330/K00330/K00330/K00330/K00332/K00332/K00332/K00332/K00332/K00332/K00333/K00333/K00333/K00333/K00333/K00333/K00334/K00334/K00334/K00334/K00334/K00334/K00334/K00335/K00335/K00335/K00335/K00335/K00335/K00335/K00336/K00336/K00336/K00336/K00336/K00336/K00337/K00337/K00337/K00337/K00337/K00337/K00337/K00337/K00337/K00337/K00338/K00338/K00338/K00338/K00338/K00338/K00338/K00339/K00339/K00339/K00339/K00339/K00339/K00339/K00339/K00339/K00339/K00340/K00340/K00340/K00340/K00340/K00340/K00340/K00340/K00340/K00340/K00341/K00341/K00341/K00341/K00341/K00341/K00341/K00341/K00341/K00341/K00342/K00342/K00342/K00342/K00342/K00342/K00343/K00343/K00343/K00343/K00343/K00343/K00343/K00343/K00343/K00343
MAG.12	Pantothenate biosynthesis	K00077/K00606/K00826/K01579/K01918
MAG.17	Pantothenate biosynthesis	K00077/K00606/K00826/K01918
MAG.22	Pantothenate biosynthesis	K00606/K00826/K01918
MAG.309811	Pantothenate biosynthesis	K00606/K00826/K01579/K01918
MAG.332111	Photosystem II (psbABCDEF)	K02703/K02703/K02703/K02703/K02703/K02703/K02703/K02703/K02703/K02703/K02704/K02704/K02704/K02704/K02704/K02707/K02708
MAG.12	Pyridoxal biosynthesis	K00097/K00275/K00831/K03472/K03473/K03474
MAG.15	Pyridoxal biosynthesis	K00097/K00275/K00831
MAG.17	Pyridoxal biosynthesis	K00097/K00275/K00831/K03472/K03473/K03474
MAG.22	Pyridoxal biosynthesis	K00097/K00275/K00831/K03474
MAG.25993	Pyridoxal biosynthesis	K00097/K00275/K00831/K03472
MAG.302726	Pyridoxal biosynthesis	K00097/K00275/K00831/K03474
MAG.309811	Pyridoxal biosynthesis	K00097/K00275/K00831/K03474
MAG.332111	Pyridoxal biosynthesis	K00097/K00275/K03474
MAG.12	Sec-SRP	K03070/K03070/K03070/K03070/K03070/K03070/K03070/K03070/K03070/K03070/K03072/K03072/K03072/K03072/K03072/K03072/K03072/K03072/K03072/K03072/K03073/K03073/K03073/K03073/K03073/K03073/K03073/K03073/K03073/K03073/K03074/K03074/K03074/K03074/K03074/K03074/K03074/K03074/K03074/K03074/K03075/K03075/K03075/K03075/K03075/K03075/K03075/K03075/K03075/K03075/K03076/K03076/K03076/K03076/K03076/K03076/K03076/K03076/K03076/K03076/K03110/K03110/K03110/K03110/K03110/K03110/K03110/K03110/K03110/K03110/K03210/K03210/K03210/K03210/K03210/K03210/K03210/K03210/K03210/K03210/K03217/K03217/K03217/K03217/K03217/K03217/K03217/K03217/K03217/K03217
MAG.13	Sec-SRP	K03070/K03070/K03070/K03070/K03070/K03070/K03070/K03070/K03070/K03070/K03075/K03075/K03075/K03075/K03075/K03075/K03075/K03075/K03075/K03075/K03110/K03110/K03110/K03110/K03110/K03110/K03110/K03110/K03110/K03110/K03217/K03217/K03217/K03217/K03217/K03217/K03217/K03217/K03217/K03217
MAG.14	Sec-SRP	K03070/K03070/K03070/K03070/K03070/K03070/K03070/K03070/K03070/K03070/K03075/K03075/K03075/K03075/K03075/K03075/K03075/K03075/K03075/K03075/K03076/K03076/K03076/K03076/K03076/K03076/K03076/K03076/K03076/K03076/K03110/K03110/K03110/K03110/K03110/K03110/K03110/K03110/K03110/K03110/K03217/K03217/K03217/K03217/K03217/K03217/K03217/K03217/K03217/K03217/K12257
MAG.15	Sec-SRP	K03070/K03070/K03070/K03070/K03070/K03070/K03070/K03070/K03070/K03070/K03072/K03072/K03072/K03072/K03072/K03072/K03072/K03072/K03072/K03072/K03073/K03073/K03073/K03073/K03073/K03073/K03073/K03073/K03073/K03073/K03074/K03074/K03074/K03074/K03074/K03074/K03074/K03074/K03074/K03074/K03076/K03076/K03076/K03076/K03076/K03076/K03076/K03076/K03076/K03076/K03110/K03110/K03110/K03110/K03110/K03110/K03110/K03110/K03110/K03110/K03210/K03210/K03210/K03210/K03210/K03210/K03210/K03210/K03210/K03210/K03217/K03217/K03217/K03217/K03217/K03217/K03217/K03217/K03217/K03217
MAG.17	Sec-SRP	K03070/K03070/K03070/K03070/K03070/K03070/K03070/K03070/K03070/K03070/K03072/K03072/K03072/K03072/K03072/K03072/K03072/K03072/K03072/K03072/K03073/K03073/K03073/K03073/K03073/K03073/K03073/K03073/K03073/K03073/K03074/K03074/K03074/K03074/K03074/K03074/K03074/K03074/K03074/K03074/K03075/K03075/K03075/K03075/K03075/K03075/K03075/K03075/K03075/K03075/K03076/K03076/K03076/K03076/K03076/K03076/K03076/K03076/K03076/K03076/K03110/K03110/K03110/K03110/K03110/K03110/K03110/K03110/K03110/K03110/K03210/K03210/K03210/K03210/K03210/K03210/K03210/K03210/K03210/K03210/K03217/K03217/K03217/K03217/K03217/K03217/K03217/K03217/K03217/K03217
MAG.2	Sec-SRP	K03070/K03070/K03070/K03070/K03070/K03070/K03070/K03070/K03070/K03070/K03075/K03075/K03075/K03075/K03075/K03075/K03075/K03075/K03075/K03075/K03076/K03076/K03076/K03076/K03076/K03076/K03076/K03076/K03076/K03076/K03110/K03110/K03110/K03110/K03110/K03110/K03110/K03110/K03110/K03110/K03217/K03217/K03217/K03217/K03217/K03217/K03217/K03217/K03217/K03217
MAG.22	Sec-SRP	K03070/K03070/K03070/K03070/K03070/K03070/K03070/K03070/K03070/K03070/K03072/K03072/K03072/K03072/K03072/K03072/K03072/K03072/K03072/K03072/K03073/K03073/K03073/K03073/K03073/K03073/K03073/K03073/K03073/K03073/K03074/K03074/K03074/K03074/K03074/K03074/K03074/K03074/K03074/K03074/K03075/K03075/K03075/K03075/K03075/K03075/K03075/K03075/K03075/K03075/K03076/K03076/K03076/K03076/K03076/K03076/K03076/K03076/K03076/K03076/K03110/K03110/K03110/K03110/K03110/K03110/K03110/K03110/K03110/K03110/K03210/K03210/K03210/K03210/K03210/K03210/K03210/K03210/K03210/K03210/K03217/K03217/K03217/K03217/K03217/K03217/K03217/K03217/K03217/K03217
MAG.25993	Sec-SRP	K03070/K03070/K03070/K03070/K03070/K03070/K03070/K03070/K03070/K03070/K03073/K03073/K03073/K03073/K03073/K03073/K03073/K03073/K03073/K03073/K03075/K03075/K03075/K03075/K03075/K03075/K03075/K03075/K03075/K03075/K03076/K03076/K03076/K03076/K03076/K03076/K03076/K03076/K03076/K03076/K03110/K03110/K03110/K03110/K03110/K03110/K03110/K03110/K03110/K03110/K03210/K03210/K03210/K03210/K03210/K03210/K03210/K03210/K03210/K03210/K03217/K03217/K03217/K03217/K03217/K03217/K03217/K03217/K03217/K03217
MAG.302726	Sec-SRP	K03070/K03070/K03070/K03070/K03070/K03070/K03070/K03070/K03070/K03070/K03075/K03075/K03075/K03075/K03075/K03075/K03075/K03075/K03075/K03075/K03110/K03110/K03110/K03110/K03110/K03110/K03110/K03110/K03110/K03110/K12257
MAG.309811	Sec-SRP	K03070/K03070/K03070/K03070/K03070/K03070/K03070/K03070/K03070/K03070/K03072/K03072/K03072/K03072/K03072/K03072/K03072/K03072/K03072/K03072/K03074/K03074/K03074/K03074/K03074/K03074/K03074/K03074/K03074/K03074/K03076/K03076/K03076/K03076/K03076/K03076/K03076/K03076/K03076/K03076/K03110/K03110/K03110/K03110/K03110/K03110/K03110/K03110/K03110/K03110/K03210/K03210/K03210/K03210/K03210/K03210/K03210/K03210/K03210/K03210/K03217/K03217/K03217/K03217/K03217/K03217/K03217/K03217/K03217/K03217
MAG.332111	Sec-SRP	K03070/K03070/K03070/K03070/K03070/K03070/K03070/K03070/K03070/K03070/K03072/K03072/K03072/K03072/K03072/K03072/K03072/K03072/K03072/K03072/K03073/K03073/K03073/K03073/K03073/K03073/K03073/K03073/K03073/K03073/K03074/K03074/K03074/K03074/K03074/K03074/K03074/K03074/K03074/K03074/K03075/K03075/K03075/K03075/K03075/K03075/K03075/K03075/K03075/K03075/K03076/K03076/K03076/K03076/K03076/K03076/K03076/K03076/K03076/K03076/K03110/K03110/K03110/K03110/K03110/K03110/K03110/K03110/K03110/K03110/K03217/K03217/K03217/K03217/K03217/K03217/K03217/K03217/K03217/K03217
MAG.8	Sec-SRP	K03070/K03070/K03070/K03070/K03070/K03070/K03070/K03070/K03070/K03070/K03076/K03076/K03076/K03076/K03076/K03076/K03076/K03076/K03076/K03076/K03110/K03110/K03110/K03110/K03110/K03110/K03110/K03110/K03110/K03110/K12257
MAG.12	Succinate	K01610/K01610/K01610/K01610/K01610/K01610/K01610/K01610/K01610/K01610/K00024/K00024/K00024/K00024/K00024/K00024/K00024/K00024/K00024/K00024/K01676/K01676/K01676/K01676/K01676/K01676/K01676/K01676/K01676/K01679/K01679/K01679/K01679/K01679/K01679/K01679/K00024/K00024/K00024/K00024/K00024/K00024/K00024/K00024/K00024/K00024/K01676/K01676/K01676/K01676/K01676/K01676/K01676/K01676/K01676/K01679/K01679/K01679/K01679/K01679/K01679/K01679/K00024/K01595/K01610/K01610/K01610/K01610/K01610/K01610/K01610/K01610/K01610/K01610/K01595/K01595/K01595/K01595/K01595/K01595/K01595/K01595/K01595/K01595/K00024/K00024/K00024/K00024/K00024/K00024/K00024/K00024/K00024/K00024/K01595/K01595/K01595/K01595/K01595/K01595/K01595/K01595/K01595/K01595/K01676/K01676/K01676/K01676/K01676/K01676/K01676/K01676/K01676/K01679/K01679/K01679/K01679/K01679/K01679/K01679/K00024/K00024/K00024/K00024/K00024/K00024/K00024/K00024/K00024/K00024/K01595/K01595/K01595/K01595/K01595/K01595/K01595/K01595/K01595/K01595/K00024/K00024/K00024/K00024/K00024/K00024/K00024/K00024/K00024/K00024/K01595/K01595/K01595/K01595/K01595/K01595/K01595/K01595/K01595/K01595/K01676/K01676/K01676/K01676/K01676/K01676/K01676/K01676/K01676
MAG.15	Succinate	K00024/K00024/K00024/K00024/K00024/K00024/K00024/K00024/K00024/K00024/K01679/K01679/K01679/K01679/K01679/K01679/K01679/K00024
MAG.17	Succinate	K01610/K01610/K01610/K01610/K01610/K01610/K01610/K01610/K01610/K01610/K00024/K00024/K00024/K00024/K00024/K00024/K00024/K00024/K00024/K00024/K00244/K00245/K01676/K01676/K01676/K01676/K01676/K01676/K01676/K01679/K01679/K01679/K01679/K01679/K01679/K01679/K01679/K01679/K00024/K00024/K00024/K00024/K00024/K00024/K00024/K00024/K00024/K00024/K00244/K00245/K01676/K01676/K01676/K01676/K01676/K01676/K01676/K01676/K01676/K01679/K01679/K01679/K01679/K01679/K01679/K01679/K00024/K00024/K00024/K00024/K00024/K00024/K00024/K00024/K00024/K00024/K00244/K00245/K00247/K00247/K00247/K00247/K00247/K00024/K00244/K00245/K01676/K01676/K01676/K01676/K01676/K01676/K01676/K01676/K01676/K01679/K01679/K01679/K01679/K01679/K01679/K01679

MAG.22	Succinate	K01610/K01610/K01610/K01610/K01610/K01610/K01610/K01610/K01610/K01610/K00024/K00024/K00024/K00024/K00024/K00024/K00024/K00024/K00024/K00024/K01676/K01676/K01676/K01676/K01676/K01676/K01676/K01676/K01676/K01679/K01679/K01679/K01679/K01679/K01679/K01679/K00024/K00024/K00024/K00024/K00024/K00024/K00024/K00024/K00024/K00024/K01676/K01676/K01676/K01676/K01676/K01676/K01676/K01676/K01676/K01679/K01679/K01679/K01679/K01679/K01679/K01679/K00024/K01595/K01610/K01610/K01610/K01610/K01610/K01610/K01610/K01610/K01610/K01610/K01595/K01595/K01595/K01595/K01595/K01595/K01595/K01595/K01595/K01595/K00024/K00024/K00024/K00024/K00024/K00024/K00024/K00024/K00024/K00024/K01595/K01595/K01595/K01595/K01595/K01595/K01595/K01595/K01595/K01595/K01676/K01676/K01676/K01676/K01676/K01676/K01676/K01676/K01676/K01679/K01679/K01679/K01679/K01679/K01679/K01679
MAG.220783	Succinate	K00024/K00024/K00024/K00024/K00024/K00024/K00024/K00024/K00024/K00024
MAG.25993	Succinate	K01610/K01610/K01610/K01610/K01610/K01610/K01610/K01610/K01610/K01610/K00024
MAG.302726	Succinate	K01610/K01610/K01610/K01610/K01610/K01610/K01610/K01610/K01610/K01610/K00024/K00024/K00024/K00024/K00024/K00024/K00024/K00024/K00024/K00024/K01679/K01679/K01679/K01679/K01679/K01679/K01679/K00024/K00024/K00024/K00024/K00024/K00024/K00024/K00024/K00024/K00024/K01679/K01679/K01679/K01679/K01679/K01679/K01679/K00024/K01679/K01679/K01679/K01679/K01679/K01679/K01679
MAG.309811	Succinate	K01596/K01596/K01596/K00024/K00024/K00024/K00024/K00024/K00024/K00024/K00024/K00024/K00024/K01676/K01676/K01676/K01676/K01676/K01676/K01676/K01676/K01676/K00024/K00024/K00024/K00024/K00024/K00024/K00024/K00024/K00024/K00024/K01676/K01676/K01676/K01676/K01676/K01676/K01676/K01676/K01676/K00024/K01595/K00024/K00024/K00024/K00024/K00024/K00024/K00024/K00024/K00024/K00024/K01595/K01595/K01595/K01595/K01595/K01595/K01595/K01595/K01595/K01595/K01676/K01676/K01676/K01676/K01676/K01676/K01676/K01676/K01676
MAG.332111	Succinate	K01610/K01610/K01610/K01610/K01610/K01610/K01610/K01610/K01610/K01610/K00024/K01595/K01610/K01610/K01610/K01610/K01610/K01610/K01610/K01610/K01610/K01610/K00024/K00024/K00024/K00024/K00024/K00024/K00024/K00024/K00024/K00024/K01595/K01595/K01595/K01595/K01595/K01595/K01595/K01595/K01595/K01595/K00024/K00024/K00024/K00024/K00024/K00024/K00024/K00024/K00024/K00024/K01595/K01595/K01595/K01595/K01595/K01595/K01595/K01595/K01595/K01595
MAG.12	Twin arginine targeting	K03116/K03116/K03116/K03116/K03116/K03116/K03116/K03116/K03116/K03116/K03118/K03118/K03118/K03118/K03118/K03118/K03118/K03118/K03118/K03118
MAG.17	Twin arginine targeting	K03116/K03116/K03116/K03116/K03116/K03116/K03116/K03116/K03116/K03116/K03118/K03118/K03118/K03118/K03118/K03118/K03118/K03118/K03118/K03118
MAG.22	Twin arginine targeting	K03116/K03116/K03116/K03116/K03116/K03116/K03116/K03116/K03116/K03116/K03118/K03118/K03118/K03118/K03118/K03118/K03118/K03118/K03118/K03118
MAG.220783	Twin arginine targeting	K03118/K03118/K03118/K03118/K03118/K03118/K03118/K03118/K03118/K03118
MAG.25993	Twin arginine targeting	K03116/K03116/K03116/K03116/K03116/K03116/K03116/K03116/K03116/K03116/K03118/K03118/K03118/K03118/K03118/K03118/K03118/K03118/K03118/K03118
MAG.302726	Twin arginine targeting	K03116/K03116/K03116/K03116/K03116/K03116/K03116/K03116/K03116/K03116
MAG.309811	Twin arginine targeting	K03118/K03118/K03118/K03118/K03118/K03118/K03118/K03118/K03118/K03118
MAG.332111	Twin arginine targeting	K03116/K03116/K03116/K03116/K03116/K03116/K03116/K03116/K03116/K03116/K03118/K03118/K03118/K03118/K03118/K03118/K03118/K03118/K03118/K03118
MAG.12	Type II Secretion	K02452/K02452/K02452/K02452/K02452/K02452/K02452/K02452/K02452/K02453/K02453/K02453/K02453/K02453/K02453/K02453/K02453/K02453/K02454/K02454/K02454/K02454/K02454/K02454/K02454/K02454/K02454/K02454/K02455/K02455/K02455/K02455/K02455/K02455/K02455/K02455/K02456/K02456/K02456/K02456/K02456/K02456/K02456/K02456/K02456/K02456/K02457/K02457/K02457/K02457/K02457/K02457/K02457/K02457/K02457/K02457/K02460/K02460/K02460/K02460/K02460/K02460/K02460/K02460/K02460/K02460/K02462/K02462/K02462/K02462/K02462/K02462/K02462/K02462/K02462
MAG.17	Type II Secretion	K02452/K02452/K02452/K02452/K02452/K02452/K02452/K02452/K02452/K02453/K02453/K02453/K02453/K02453/K02453/K02453/K02453/K02453/K02454/K02454/K02454/K02454/K02454/K02454/K02454/K02454/K02454/K02454/K02455/K02455/K02455/K02455/K02455/K02455/K02455/K02455/K02456/K02456/K02456/K02456/K02456/K02456/K02456/K02456/K02456/K02456/K02457/K02457/K02457/K02457/K02457/K02457/K02457/K02457/K02457/K02457/K02458/K02458/K02458/K02458/K02458/K02458/K02458/K02458/K02458/K02458/K02459/K02459/K02459/K02459/K02459/K02459/K02459/K02459/K02459/K02459/K02460/K02460/K02460/K02460/K02460/K02460/K02460/K02460/K02460/K02460/K02461/K02461/K02461/K02461/K02461/K02461/K02461/K02461/K02461
MAG.22	Type II Secretion	K02452/K02452/K02452/K02452/K02452/K02452/K02452/K02452/K02452/K02453/K02453/K02453/K02453/K02453/K02453/K02453/K02453/K02453/K02454/K02454/K02454/K02454/K02454/K02454/K02454/K02454/K02454/K02454/K02455/K02455/K02455/K02455/K02455/K02455/K02455/K02455/K02456/K02456/K02456/K02456/K02456/K02456/K02456/K02456/K02456/K02456/K02457/K02457/K02457/K02457/K02457/K02457/K02457/K02457/K02457/K02457/K02458/K02458/K02458/K02458/K02458/K02458/K02458/K02458/K02458/K02458/K02460/K02460/K02460/K02460/K02460/K02460/K02460/K02460/K02460/K02460/K02461/K02461/K02461/K02461/K02461/K02461/K02461/K02461/K02461/K02462/K02462/K02462/K02462/K02462/K02462/K02462/K02462/K02462
MAG.17	Type III Secretion	K03219/K03219/K03219/K03219/K03219/K03219/K03219/K03222/K03222/K03222/K03222/K03222/K03222/K03222/K03222/K03222/K03222/K03224/K03224/K03224/K03224/K03224/K03224/K03224/K03224/K03224/K03224/K03226/K03226/K03226/K03226/K03226/K03226/K03226/K03226/K03226/K03226/K03227/K03227/K03227/K03227/K03227/K03227/K03227/K03227/K03227/K03227/K03228/K03228/K03228/K03228/K03228/K03228/K03228/K03228/K03228/K03228/K03229/K03229/K03229/K03229/K03229/K03229/K03229/K03229/K03229/K03229/K03230/K03230/K03230/K03230/K03230/K03230/K03230/K03230/K03230/K03230
MAG.25993	Type III Secretion	K03219/K03219/K03219/K03219/K03219/K03219/K03219/K03222/K03222/K03222/K03222/K03222/K03222/K03222/K03222/K03222/K03222/K03224/K03224/K03224/K03224/K03224/K03224/K03224/K03224/K03224/K03224/K03226/K03226/K03226/K03226/K03226/K03226/K03226/K03226/K03226/K03226/K03227/K03227/K03227/K03227/K03227/K03227/K03227/K03227/K03227/K03227/K03228/K03228/K03228/K03228/K03228/K03228/K03228/K03228/K03228/K03228/K03229/K03229/K03229/K03229/K03229/K03229/K03229/K03229/K03229/K03229/K03230/K03230/K03230/K03230/K03230/K03230/K03230/K03230/K03230/K03230

Supplementary Table 9: Contig Information (Eukaryotic and Prokaryotic) across the temporal groups under different thermal conditions showing total contigs size (bp) and the total contigs number per sample.

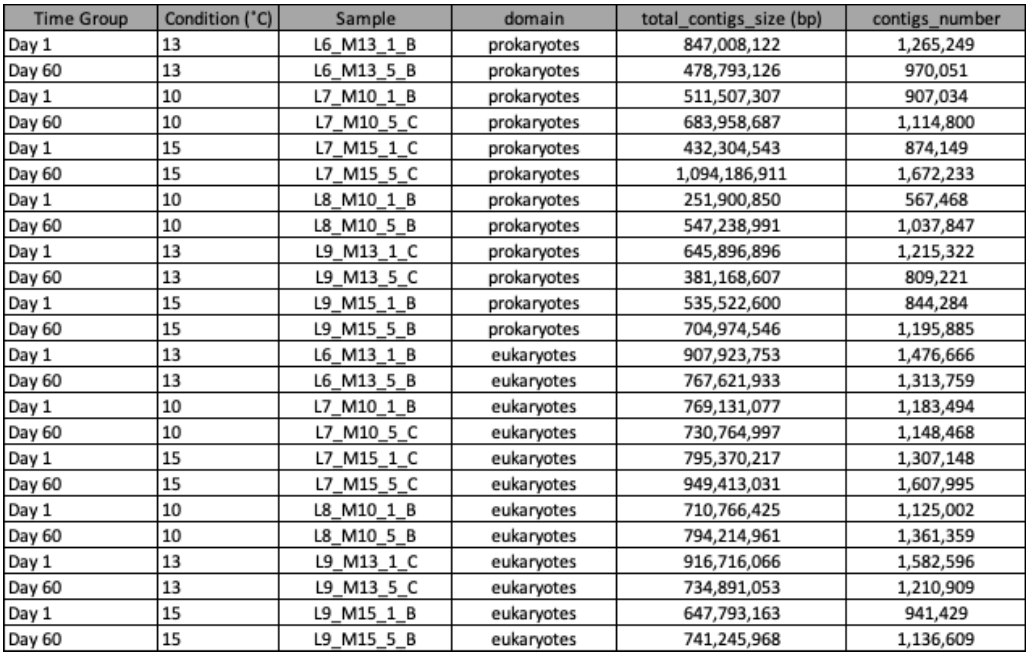

Time Group	Condition (˚C)	Sample	domain	total_contigs_size (bp)	contigs_number
Day 1	13	L6_M13_1_B	prokaryotes	847,008,122	1,265,249
Day 60	13	L6_M13_5_B	prokaryotes	478,793,126	970,051
Day 1	10	L7_M10_1_B	prokaryotes	511,507,307	907,034
Day 60	10	L7_M10_5_C	prokaryotes	683,958,687	1,114,800
Day 1	15	L7_M15_1_C	prokaryotes	432,304,543	874,149
Day 60	15	L7_M15_5_C	prokaryotes	1,094,186,911	1,672,233
Day 1	10	L8_M10_1_B	prokaryotes	251,900,850	567,468
Day 60	10	L8_M10_5_B	prokaryotes	547,238,991	1,037,847
Day 1	13	L9_M13_1_C	prokaryotes	645,896,896	1,215,322
Day 60	13	L9_M13_5_C	prokaryotes	381,168,607	809,221
Day 1	15	L9_M15_1_B	prokaryotes	535,522,600	844,284
Day 60	15	L9_M15_5_B	prokaryotes	704,974,546	1,195,885
Day 1	13	L6_M13_1_B	eukaryotes	907,923,753	1,476,666
Day 60	13	L6_M13_5_B	eukaryotes	767,621,933	1,313,759
Day 1	10	L7_M10_1_B	eukaryotes	769,131,077	1,183,494
Day 60	10	L7_M10_5_C	eukaryotes	730,764,997	1,148,468
Day 1	15	L7_M15_1_C	eukaryotes	795,370,217	1,307,148
Day 60	15	L7_M15_5_C	eukaryotes	949,413,031	1,607,995
Day 1	10	L8_M10_1_B	eukaryotes	710,766,425	1,125,002
Day 60	10	L8_M10_5_B	eukaryotes	794,214,961	1,361,359
Day 1	13	L9_M13_1_C	eukaryotes	916,716,066	1,582,596
Day 60	13	L9_M13_5_C	eukaryotes	734,891,053	1,210,909
Day 1	15	L9_M15_1_B	eukaryotes	647,793,163	941,429
Day 60	15	L9_M15_5_B	eukaryotes	741,245,968	1,136,609

Supplementary Table 10: Relative Abundance Table of *D. pertusum* Microbiome (Order-Level Taxonomy) at the Start and End of the Experiment Under Different Thermal Conditions

taxonomy			Day 1						Day 60					
			10˚ C		13˚ C		15˚ C		10˚ C		13˚ C		15˚ C	
phylum	class	order	L7_M10_1_B	L8_M10_1_B	L6_M13_1_B	L9_M13_1_C	L7_M15_1_C	L9_M15_1_B	L7_M10_5_C	L8_M10_5_B	L6_M13_5_B	L9_M13_5_C	L7_M15_5_C	L9_M15_5_B
WPS-2	unknown	unknown	0.39%	0.04%	0.06%	0.13%	0.11%	0.17%	0.41%	0.12%	0.05%	0.06%	0.04%	0.06%
Verrucomicrobiota	Verrucomicrobiae	Verrucomicrobiales	0.10%	0.19%	0.09%	0.10%	0.16%	0.36%	0.17%	0.01%	0.25%	0.42%	0.14%	0.04%
Verrucomicrobiota	Verrucomicrobiae	Pedosphaerales	0.02%	0.00%	0.00%	0.05%	0.01%	0.01%	0.03%	0.08%	0.03%	0.02%	0.00%	0.00%
Verrucomicrobiota	Verrucomicrobiae	Opitutales	0.38%	0.15%	0.10%	0.15%	0.12%	0.16%	0.78%	0.12%	0.12%	1.19%	0.14%	0.46%
Verrucomicrobiota	Verrucomicrobiae	Chthoniobacterales	0.00%	0.00%	0.00%	0.03%	0.00%	0.00%	0.00%	0.00%	0.00%	0.00%	0.00%	0.00%
Verrucomicrobiota	Omnitrophia	Omnitrophales	0.00%	0.00%	0.00%	0.07%	0.01%	0.00%	0.00%	0.07%	0.00%	0.00%	0.00%	0.01%
Verrucomicrobiota	Lentisphaeria	Victivallales	0.00%	0.00%	0.00%	0.02%	0.01%	0.01%	0.00%	0.00%	0.00%	0.00%	0.00%	0.00%
Verrucomicrobiota	Lentisphaeria	P.palmC41	0.00%	0.08%	0.00%	5.08%	0.00%	0.01%	0.02%	0.00%	0.00%	0.00%	0.01%	0.09%
Verrucomicrobiota	Lentisphaeria	Lentisphaerales	0.00%	0.00%	0.00%	0.23%	0.02%	0.00%	0.00%	0.01%	0.12%	0.03%	0.00%	0.03%
Verrucomicrobiota	Kiritimatiellae	WCHB1-41	0.00%	0.00%	0.00%	0.02%	0.00%	0.00%	0.00%	0.00%	0.00%	0.00%	0.00%	0.00%
Verrucomicrobiota	Chlamydiae	Chlamydiales	0.03%	0.00%	0.07%	0.01%	0.13%	0.18%	0.27%	0.16%	0.27%	0.23%	0.23%	0.22%
Sumerlaeota	Sumerlaeia	Sumerlaeales	0.03%	0.00%	0.00%	0.05%	0.00%	0.00%	0.00%	0.00%	0.00%	0.00%	0.00%	0.00%
Spirochaetota	Leptospirae	Leptospirales	0.01%	0.00%	0.01%	0.01%	0.00%	0.01%	0.05%	0.14%	0.19%	0.35%	0.03%	0.06%
SAR324cladeMarinegroupB	unknown	unknown	0.00%	0.00%	0.01%	0.28%	0.00%	0.02%	0.00%	0.00%	0.01%	0.00%	0.02%	0.05%
Proteobacteria	Gammaproteobacteria	unknown	0.01%	0.00%	0.00%	0.01%	0.00%	0.00%	0.00%	0.00%	0.00%	0.00%	0.00%	0.00%
Proteobacteria	Gammaproteobacteria	uncultured	0.06%	0.00%	0.02%	0.03%	0.03%	0.01%	0.02%	0.02%	0.09%	0.10%	0.31%	0.23%
Proteobacteria	Gammaproteobacteria	sediment-surface35	0.00%	0.00%	0.00%	0.01%	0.00%	0.00%	0.10%	0.00%	0.00%	0.00%	0.00%	0.00%
Proteobacteria	Gammaproteobacteria	Xanthomonadales	0.04%	0.00%	0.02%	0.01%	0.00%	0.00%	0.01%	0.00%	0.01%	0.00%	0.00%	0.03%
Proteobacteria	Gammaproteobacteria	Vibrionales	7.27%	14.73%	26.11%	20.26%	4.58%	5.65%	2.45%	0.53%	0.46%	7.41%	2.93%	2.43%
Proteobacteria	Gammaproteobacteria	UBA4486	0.03%	0.00%	0.01%	0.01%	0.00%	0.01%	0.33%	0.56%	0.33%	0.20%	0.23%	0.48%
Proteobacteria	Gammaproteobacteria	UBA10353marinegroup	0.12%	0.00%	0.01%	0.03%	0.00%	0.03%	0.01%	0.04%	0.00%	0.05%	0.01%	0.00%
Proteobacteria	Gammaproteobacteria	Thiotrichales	0.00%	0.00%	0.04%	0.00%	0.02%	0.10%	0.13%	0.22%	0.03%	0.01%	0.07%	0.11%
Proteobacteria	Gammaproteobacteria	Thiomicrospirales	0.02%	0.04%	0.02%	0.01%	0.00%	0.01%	0.03%	0.00%	0.10%	0.00%	0.01%	0.07%
Proteobacteria	Gammaproteobacteria	Thiohalorhabdales	0.00%	0.00%	0.00%	0.00%	0.00%	0.00%	0.01%	0.02%	0.00%	0.00%	0.00%	0.00%
Proteobacteria	Gammaproteobacteria	Tenderiales	0.00%	0.00%	0.00%	0.00%	0.00%	0.00%	0.02%	0.01%	0.00%	0.04%	0.01%	0.00%
Proteobacteria	Gammaproteobacteria	Steroidobacterales	0.26%	0.00%	0.03%	0.43%	0.25%	0.36%	0.34%	0.02%	0.07%	0.58%	0.12%	0.07%
Proteobacteria	Gammaproteobacteria	Salinisphaerales	0.00%	0.00%	0.00%	0.01%	0.00%	0.00%	0.00%	0.09%	0.00%	0.00%	0.07%	0.00%
Proteobacteria	Gammaproteobacteria	SZB50	0.06%	0.00%	0.00%	0.01%	0.00%	0.01%	0.43%	0.05%	0.07%	0.29%	0.06%	0.00%
Proteobacteria	Gammaproteobacteria	SS1-B-07-19	0.01%	0.00%	0.00%	0.00%	0.00%	0.00%	0.02%	0.04%	0.12%	0.28%	0.09%	0.20%
Proteobacteria	Gammaproteobacteria	SAR86clade	0.00%	0.00%	0.00%	0.00%	0.00%	0.00%	0.00%	0.01%	0.00%	0.00%	0.02%	0.00%
Proteobacteria	Gammaproteobacteria	Pseudomonadales	0.04%	0.14%	0.13%	0.03%	0.05%	0.04%	0.01%	0.02%	0.00%	0.09%	0.03%	0.01%
Proteobacteria	Gammaproteobacteria	Piscirickettsiales	0.03%	0.05%	0.00%	0.00%	0.00%	0.09%	0.00%	0.00%	0.00%	0.00%	0.01%	0.00%
Proteobacteria	Gammaproteobacteria	Oceanospirillales	6.56%	28.96%	19.28%	6.24%	26.39%	9.28%	5.23%	3.72%	5.00%	6.61%	0.82%	1.43%
Proteobacteria	Gammaproteobacteria	OM182clade	0.13%	0.12%	0.02%	0.04%	0.21%	0.10%	0.34%	0.17%	0.19%	0.44%	0.27%	0.57%
Proteobacteria	Gammaproteobacteria	Nitrosococcales	0.76%	0.15%	0.17%	0.30%	0.07%	0.10%	0.65%	0.29%	0.17%	0.63%	0.21%	0.14%
Proteobacteria	Gammaproteobacteria	Milano-WF1B-44	0.01%	0.02%	0.00%	0.00%	0.01%	0.00%	0.03%	0.00%	0.03%	0.02%	0.20%	0.65%
Proteobacteria	Gammaproteobacteria	Methylococcales	0.09%	0.01%	0.00%	0.00%	0.02%	0.02%	0.05%	0.07%	0.05%	0.11%	0.02%	0.02%
Proteobacteria	Gammaproteobacteria	MBAE14	0.23%	0.00%	0.02%	0.10%	0.04%	0.06%	0.01%	0.01%	0.00%	0.00%	0.00%	0.01%
Proteobacteria	Gammaproteobacteria	Legionellales	0.03%	0.00%	0.02%	0.03%	0.04%	0.01%	0.08%	0.00%	0.05%	0.09%	0.15%	0.15%
Proteobacteria	Gammaproteobacteria	KI89Aclade	0.12%	0.09%	0.04%	0.01%	0.02%	0.02%	0.20%	0.56%	0.18%	0.03%	0.08%	0.01%
Proteobacteria	Gammaproteobacteria	JTB23	0.60%	0.03%	0.03%	0.22%	0.09%	0.09%	0.50%	1.76%	2.27%	1.06%	2.57%	5.62%
Proteobacteria	Gammaproteobacteria	HgCo23	0.00%	0.00%	0.00%	0.00%	0.00%	0.00%	0.03%	0.09%	0.05%	0.11%	0.28%	0.65%
Proteobacteria	Gammaproteobacteria	HOC36	0.02%	0.00%	0.00%	0.01%	0.02%	0.01%	0.02%	0.02%	0.01%	0.08%	0.01%	0.02%
Proteobacteria	Gammaproteobacteria	Granulosicoccales	0.09%	0.00%	0.01%	0.01%	0.01%	0.05%	0.06%	0.05%	0.00%	0.02%	0.13%	0.23%
Proteobacteria	Gammaproteobacteria	GammaproteobacteriaIncertaeSedi	0.30%	0.07%	0.12%	0.26%	0.17%	0.09%	2.45%	0.36%	0.38%	0.91%	0.26%	0.72%
Proteobacteria	Gammaproteobacteria	Ga0077536	0.10%	0.00%	0.02%	0.02%	0.11%	0.16%	0.71%	0.16%	0.12%	0.37%	0.25%	0.07%
Proteobacteria	Gammaproteobacteria	Francisellales	0.06%	0.00%	0.04%	0.00%	0.03%	0.03%	1.23%	0.06%	0.19%	1.55%	0.19%	0.07%
Proteobacteria	Gammaproteobacteria	F9P41300-M23	0.02%	0.00%	0.03%	0.00%	0.00%	0.00%	0.01%	0.02%	0.00%	0.00%	0.00%	0.00%
Proteobacteria	Gammaproteobacteria	Enterobacterales	0.15%	0.00%	0.02%	0.19%	0.05%	0.05%	0.06%	0.11%	0.05%	0.02%	0.01%	0.03%
Proteobacteria	Gammaproteobacteria	Ectothiorhodospirales	0.23%	0.14%	0.35%	0.04%	0.09%	0.67%	0.20%	0.10%	0.02%	0.04%	0.18%	0.13%
Proteobacteria	Gammaproteobacteria	EV818SWSAP88	0.01%	0.00%	0.00%	0.00%	0.00%	0.01%	0.00%	0.00%	0.00%	0.06%	0.00%	0.00%
Proteobacteria	Gammaproteobacteria	EPR3968-O8a-Bc78	0.00%	0.00%	0.00%	0.00%	0.00%	0.01%	0.00%	0.00%	0.00%	0.00%	0.03%	0.00%
Proteobacteria	Gammaproteobacteria	EC3	0.00%	0.00%	0.01%	0.01%	0.01%	0.00%	0.00%	0.00%	0.01%	0.00%	0.02%	0.03%
Proteobacteria	Gammaproteobacteria	Diplorickettsiales	0.02%	0.01%	0.01%	0.01%	0.00%	0.00%	0.02%	0.00%	0.00%	0.00%	0.01%	0.00%
Proteobacteria	Gammaproteobacteria	Coxiellales	0.63%	0.08%	0.38%	0.22%	0.14%	0.29%	0.05%	0.02%	2.07%	0.23%	0.47%	0.04%
Proteobacteria	Gammaproteobacteria	Chromatiales	0.02%	0.15%	0.04%	0.03%	0.27%	0.12%	0.48%	0.23%	0.33%	0.56%	0.23%	0.24%
Proteobacteria	Gammaproteobacteria	Cellvibrionales	10.35%	4.29%	3.14%	5.69%	2.06%	2.06%	4.64%	10.71%	6.04%	5.59%	1.20%	2.19%
Proteobacteria	Gammaproteobacteria	Cardiobacteriales	0.06%	0.00%	0.00%	0.00%	0.00%	0.00%	0.00%	0.00%	0.00%	0.00%	0.01%	0.00%
Proteobacteria	Gammaproteobacteria	Burkholderiales	0.03%	0.00%	0.00%	0.49%	0.02%	0.08%	0.16%	0.05%	0.10%	0.07%	0.09%	0.10%
Proteobacteria	Gammaproteobacteria	BD7-8	0.00%	0.00%	0.00%	0.00%	0.01%	0.01%	0.04%	0.00%	0.00%	0.00%	0.00%	0.01%
Proteobacteria	Gammaproteobacteria	B2M28	0.08%	0.00%	0.01%	0.02%	0.00%	0.01%	0.00%	0.00%	0.01%	0.00%	0.05%	0.02%
Proteobacteria	Gammaproteobacteria	Arenicellales	0.37%	0.18%	0.61%	0.27%	1.72%	0.89%	0.56%	0.06%	0.03%	0.25%	0.27%	0.39%
Proteobacteria	Gammaproteobacteria	Alteromonadales	15.17%	16.33%	14.94%	20.84%	24.67%	28.46%	3.77%	23.60%	1.94%	1.91%	11.43%	11.23%
Proteobacteria	Gammaproteobacteria	211ds20	0.00%	0.00%	0.00%	0.00%	0.00%	0.00%	0.00%	0.00%	0.02%	0.00%	0.02%	0.03%
Proteobacteria	Alphaproteobacteria	uncultured	0.05%	0.00%	0.09%	0.09%	0.01%	0.10%	0.87%	0.97%	1.48%	1.00%	0.42%	0.06%
Proteobacteria	Alphaproteobacteria	Zavarziniales	0.00%	0.00%	0.00%	0.00%	0.00%	0.00%	0.03%	0.01%	0.00%	0.00%	0.02%	0.00%
Proteobacteria	Alphaproteobacteria	Tistrellales	0.04%	0.00%	0.02%	0.09%	0.02%	0.02%	0.10%	0.04%	0.06%	0.04%	0.01%	0.03%
Proteobacteria	Alphaproteobacteria	Thalassobaculales	0.09%	0.00%	0.00%	0.25%	0.03%	0.06%	0.02%	0.02%	0.02%	0.03%	0.01%	0.03%
Proteobacteria	Alphaproteobacteria	Sphingomonadales	0.75%	0.15%	0.43%	0.12%	0.29%	0.38%	0.29%	0.12%	0.52%	0.16%	0.76%	0.89%
Proteobacteria	Alphaproteobacteria	Sneathiellales	1.40%	0.01%	0.05%	0.21%	0.20%	0.37%	1.02%	0.51%	0.98%	2.57%	0.20%	0.28%
Proteobacteria	Alphaproteobacteria	SAR11clade	0.01%	0.00%	0.01%	0.00%	0.00%	0.00%	0.00%	0.00%	0.00%	0.00%	0.00%	0.01%
Proteobacteria	Alphaproteobacteria	Rickettsiales	0.66%	0.26%	0.27%	0.39%	0.11%	0.12%	0.49%	0.39%	0.96%	0.96%	0.13%	0.27%
Proteobacteria	Alphaproteobacteria	Rhodospirillales	1.47%	0.18%	0.03%	0.38%	0.12%	0.08%	1.39%	0.38%	0.53%	3.29%	1.71%	6.86%
Proteobacteria	Alphaproteobacteria	Rhodobacterales	7.45%	8.27%	15.58%	5.40%	3.66%	5.34%	9.45%	28.23%	43.74%	9.11%	20.50%	15.35%
Proteobacteria	Alphaproteobacteria	Rhizobiales	4.76%	0.62%	0.68%	4.55%	2.19%	3.28%	6.21%	3.49%	4.69%	1.78%	5.57%	4.56%
Proteobacteria	Alphaproteobacteria	Puniceispirillales	0.08%	0.00%	0.03%	0.01%	0.07%	0.01%	0.02%	0.04%	0.04%	0.01%	0.03%	0.34%
Proteobacteria	Alphaproteobacteria	Parvibaculales	0.23%	0.30%	0.23%	0.11%	0.25%	0.17%	1.51%	1.15%	2.24%	2.42%	0.41%	0.41%
Proteobacteria	Alphaproteobacteria	Paracaedibacterales	0.00%	0.00%	0.00%	0.00%	0.00%	0.00%	0.03%	0.01%	0.01%	0.00%	0.01%	0.00%
Proteobacteria	Alphaproteobacteria	NRL2	5.57%	1.65%	0.78%	1.20%	0.57%	0.34%	0.98%	1.29%	0.10%	1.41%	0.45%	2.10%
Proteobacteria	Alphaproteobacteria	Micavibrionales	0.46%	0.28%	0.15%	0.30%	0.49%	1.21%	1.13%	0.07%	0.13%	0.28%	0.31%	0.38%
Proteobacteria	Alphaproteobacteria	Kordiimonadales	0.09%	0.13%	0.01%	0.15%	0.22%	0.08%	0.26%	0.21%	0.89%	0.76%	0.52%	1.58%
Proteobacteria	Alphaproteobacteria	Kiloniellales	1.38%	0.12%	0.03%	0.96%	0.58%	0.12%	0.89%	0.56%	0.41%	2.12%	0.07%	0.21%
Proteobacteria	Alphaproteobacteria	Elsterales	0.02%	0.00%	0.00%	0.02%	0.00%	0.00%	0.12%	0.01%	0.00%	0.00%	0.00%	0.00%
Proteobacteria	Alphaproteobacteria	Defluviicoccales	0.36%	0.00%	0.04%	0.32%	0.05%	0.24%	0.58%	0.25%	0.19%	0.05%	0.11%	0.03%
Proteobacteria	Alphaproteobacteria	Caulobacterales	1.22%	2.39%	4.44%	0.49%	1.43%	2.10%	1.27%	0.77%	0.87%	0.55%	1.20%	1.32%
Proteobacteria	Alphaproteobacteria	Caedibacterales	0.00%	0.00%	0.00%	0.00%	0.00%	0.01%	0.00%	0.00%	0.05%	0.00%	0.00%	0.00%
Proteobacteria	Alphaproteobacteria	Azospirillales	0.01%	0.00%	0.00%	0.01%	0.01%	0.03%	0.01%	0.01%	0.01%	0.00%	0.05%	0.07%
Proteobacteria	Alphaproteobacteria	Acetobacterales	0.00%	0.01%	0.01%	0.01%	0.00%	0.01%	0.00%	0.00%	0.00%	0.00%	0.00%	0.00%
Proteobacteria	Alphaproteobacteria	AT-s3-44	0.00%	0.00%	0.00%	0.00%	0.00%	0.01%	0.00%	0.00%	0.00%	0.00%	0.05%	0.00%
Planctomycetota	vadinHA49	unknown	0.00%	0.00%	0.00%	0.00%	0.01%	0.00%	0.05%	0.11%	0.10%	0.17%	0.01%	0.03%
Planctomycetota	Planctomycetes	Planctomycetales	0.96%	0.08%	0.08%	0.92%	0.08%	0.07%	0.46%	0.31%	0.72%	0.62%	0.18%	0.31%
Planctomycetota	Planctomycetes	Pirellulales	0.87%	0.21%	0.31%	0.90%	0.23%	0.40%	3.56%	0.31%	0.82%	4.11%	3.03%	2.49%
Planctomycetota	Planctomycetes	Gemmatales	0.00%	0.00%	0.00%	0.00%	0.00%	0.00%	0.00%	0.00%	0.03%	0.00%	0.01%	0.02%
Planctomycetota	Pla4lineage	unknown	0.09%	0.02%	0.01%	0.15%	0.10%	0.10%	0.14%	0.44%	0.41%	0.09%	0.09%	0.19%
Planctomycetota	Pla3lineage	unknown	0.04%	0.09%	0.02%	0.02%	0.03%	0.06%	0.05%	0.09%	0.09%	0.02%	0.19%	0.10%
Planctomycetota	Phycisphaerae	mle1-8	0.01%	0.00%	0.00%	0.00%	0.00%	0.00%	0.03%	0.00%	0.00%	0.00%	0.01%	0.00%
Planctomycetota	Phycisphaerae	S-70	0.00%	0.00%	0.00%	0.00%	0.00%	0.00%	0.01%	0.00%	0.01%	0.03%	0.05%	0.05%
Planctomycetota	Phycisphaerae	Pla1lineage	0.02%	0.08%	0.00%	0.01%	0.00%	0.00%	0.05%	0.01%	0.01%	0.00%	0.03%	0.02%
Planctomycetota	Phycisphaerae	Phycisphaerales	1.64%	0.32%	0.46%	1.37%	2.14%	2.35%	1.98%	0.29%	0.28%	2.87%	0.96%	1.57%
Planctomycetota	Phycisphaerae	CCM11a	0.05%	0.00%	0.01%	0.10%	0.01%	0.02%	0.17%	0.09%	0.06%	0.08%	0.20%	0.08%
Planctomycetota	Phycisphaerae	C86	0.01%	0.01%	0.00%	0.00%	0.00%	0.00%	0.05%	0.02%	0.00%	0.00%	0.01%	0.00%
Planctomycetota	OM190	unknown	0.69%	0.92%	1.09%	0.34%	2.29%	2.68%	2.60%	1.70%	0.81%	2.46%	0.89%	1.13%
Planctomycetota	BD7-11	unknown	0.62%	0.51%	0.03%	0.22%	0.12%	0.02%	0.07%	0.13%	0.09%	0.06%	0.01%	0.06%
Planctomycetota	028H05-P-BN-P5	unknown	0.05%	0.00%	0.01%	0.01%	0.01%	0.00%	0.33%	0.02%	0.03%	0.00%	0.03%	0.03%
Patescibacteria	Saccharimonadia	Saccharimonadales	0.01%	0.00%	0.00%	0.00%	0.00%	0.00%	0.00%	0.02%	0.12%	0.00%	0.07%	0.00%
Patescibacteria	Parcubacteria	CandidatusKaiserbacteria	0.12%	0.06%	0.09%	0.36%	0.09%	0.42%	0.61%	0.36%	0.89%	0.07%	0.18%	0.74%
Patescibacteria	Parcubacteria	CandidatusCampbellbacteria	0.00%	0.00%	0.00%	0.00%	0.00%	0.01%	0.01%	0.00%	0.01%	0.00%	0.01%	0.01%
Patescibacteria	Gracilibacteria	unknown	0.03%	0.04%	0.14%	0.03%	0.07%	0.09%	1.00%	0.04%	0.05%	0.06%	0.03%	0.05%
Patescibacteria	Gracilibacteria	JGI0000069-P22	0.00%	0.00%	0.00%	0.00%	0.04%	0.01%	0.06%	0.01%	0.01%	0.03%	0.02%	0.01%
Patescibacteria	Gracilibacteria	CandidatusPeribacteria	0.00%	0.00%	0.02%	0.00%	0.00%	0.00%	0.03%	0.00%	0.00%	0.07%	0.00%	0.01%
Patescibacteria	ABY1	CandidatusMagasanikbacteria	0.00%	0.00%	0.00%	0.00%	0.00%	0.00%	0.00%	0.02%	0.02%	0.00%	0.01%	0.00%
Nitrospirota	Nitrospiria	Nitrospirales	0.13%	0.00%	0.01%	0.59%	0.07%	0.03%	0.09%	0.19%	0.12%	0.51%	0.02%	0.04%
Nitrospinota	Nitrospinia	Nitrospinales	0.00%	0.00%	0.01%	0.49%	0.03%	0.00%	0.00%	0.00%	0.01%	0.37%	0.02%	0.04%
NB1-j	unknown	unknown	0.16%	0.02%	0.09%	0.23%	0.07%	0.08%	0.28%	1.23%	1.64%	1.03%	0.38%	0.63%
Myxococcota	bacteriap25	unknown	0.00%	0.02%	0.00%	0.05%	0.00%	0.11%	0.00%	0.02%	0.00%	0.00%	0.00%	0.00%
Myxococcota	Polyangia	Polyangiales	0.02%	0.00%	0.02%	0.02%	0.04%	0.19%	0.66%	0.23%	0.33%	0.38%	1.06%	1.06%
Myxococcota	Polyangia	Nannocystales	0.49%	0.00%	0.24%	0.10%	0.02%	0.14%	1.70%	0.49%	0.24%	0.74%	0.82%	0.70%
Myxococcota	Polyangia	Haliangiales	0.02%	0.00%	0.01%	0.05%	0.08%	0.11%	0.09%	0.02%	0.02%	0.00%	0.03%	0.10%
Myxococcota	Polyangia	Blfdi19	0.01%	0.00%	0.00%	0.01%	0.00%	0.00%	0.01%	0.07%	0.03%	0.00%	0.27%	0.04%
Myxococcota	Myxococcia	Myxococcales	0.06%	0.00%	0.01%	0.02%	0.03%	0.01%	0.18%	0.04%	0.03%	0.17%	0.10%	0.03%
MarinimicrobiaSAR406clade	unknown	unknown	0.03%	0.00%	0.00%	0.00%	0.03%	0.00%	0.00%	0.00%	0.00%	0.00%	0.00%	0.00%
MBNT15	unknown	unknown	0.03%	0.00%	0.00%	0.01%	0.01%	0.00%	0.12%	0.02%	0.00%	0.00%	0.01%	0.00%
Latescibacterota	unknown	unknown	0.01%	0.00%	0.01%	0.01%	0.00%	0.00%	0.01%	0.00%	0.03%	0.00%	0.02%	0.03%
Hydrogenedentes	Hydrogenedentia	Hydrogenedentiales	0.01%	0.05%	0.04%	0.03%	0.02%	0.03%	0.02%	0.02%	0.02%	0.02%	0.04%	0.04%
Gemmatimonadota	PAUC43fmarinebenthicgroup	unknown	0.00%	0.00%	0.00%	0.00%	0.00%	0.00%	0.03%	0.00%	0.05%	0.00%	0.00%	0.00%
Gemmatimonadota	BD2-11terrestrialgroup	unknown	0.00%	0.00%	0.00%	0.01%	0.00%	0.01%	0.04%	0.00%	0.00%	0.00%	0.00%	0.01%

Fusobacteriota	Fusobacteriia	Fusobacteriales	0.00%	0.00%	0.00%	2.21%	0.01%	0.00%	0.00%	0.00%	0.00%	0.00%	0.00%	0.01%
Firmicutes	Clostridia	Peptostreptococcales-Tissierellales	0.00%	0.00%	0.02%	0.81%	0.04%	0.01%	0.01%	0.00%	0.09%	0.02%	0.00%	0.40%
Firmicutes	Bacilli	Lactobacillales	0.00%	0.00%	0.00%	0.01%	0.00%	0.00%	0.00%	0.00%	0.00%	0.09%	0.00%	0.03%
Firmicutes	Bacilli	Bacillales	0.00%	0.00%	0.00%	0.03%	0.02%	0.01%	0.00%	0.02%	0.02%	0.00%	0.01%	0.04%
Entotheonellaeota	Entotheonellia	Entotheonellales	0.00%	0.00%	0.00%	0.00%	0.00%	0.02%	0.00%	0.00%	0.10%	0.00%	0.03%	0.00%
Desulfobacterota	uncultured	unknown	0.00%	0.00%	0.02%	0.01%	0.02%	0.01%	0.00%	0.00%	0.01%	0.09%	0.07%	0.05%
Desulfobacterota	Syntrophia	Syntrophales	0.00%	0.08%	0.00%	0.01%	0.00%	0.00%	0.00%	0.00%	0.00%	0.00%	0.00%	0.01%
Desulfobacterota	Desulfuromonadia	unknown	0.00%	0.00%	0.00%	0.00%	0.00%	0.00%	0.00%	0.05%	0.03%	0.00%	0.04%	0.00%
Desulfobacterota	Desulfuromonadia	PB19	0.03%	0.00%	0.01%	0.06%	0.02%	0.04%	1.53%	0.06%	0.02%	0.06%	0.12%	0.10%
Desulfobacterota	Desulfuromonadia	Bradymonadales	0.11%	0.00%	0.11%	0.11%	0.03%	0.10%	0.19%	0.08%	0.04%	0.04%	0.08%	0.07%
Desulfobacterota	Desulfovibrionia	Desulfovibrionales	0.00%	0.00%	0.00%	0.00%	0.00%	0.00%	0.82%	0.00%	0.00%	0.18%	4.96%	1.27%
Desulfobacterota	Desulfobulbia	Desulfobulbales	0.00%	0.00%	0.01%	0.01%	0.00%	0.00%	0.00%	0.02%	0.06%	0.00%	0.04%	0.00%
Desulfobacterota	Desulfobacteria	Desulfobacterales	0.06%	0.00%	0.00%	0.00%	0.00%	0.00%	0.02%	0.00%	0.00%	0.02%	0.00%	0.09%
Dependentiae	Babeliae	Babeliales	0.02%	0.00%	0.05%	0.00%	0.00%	0.05%	0.00%	0.00%	0.05%	0.06%	0.25%	0.01%
Dadabacteria	Dadabacteriia	Dadabacteriales	0.02%	0.00%	0.03%	0.02%	0.09%	0.15%	1.35%	0.11%	1.47%	3.73%	9.27%	2.77%
Cyanobacteria	Vampirivibrionia	Obscuribacterales	0.00%	0.00%	0.00%	0.02%	0.01%	0.00%	0.00%	0.01%	0.01%	0.00%	0.00%	0.03%
Cyanobacteria	Sericytochromatia	unknown	0.04%	0.00%	0.02%	0.01%	0.01%	0.17%	0.00%	0.00%	0.00%	0.00%	0.02%	0.00%
Cyanobacteria	Cyanobacteriia	Chloroplast	0.02%	0.03%	0.01%	0.03%	0.01%	0.01%	0.01%	0.09%	0.06%	0.13%	0.01%	0.05%
Chloroflexi	Dehalococcoidia	SAR202clade	0.00%	0.00%	0.00%	0.05%	0.00%	0.00%	0.00%	0.00%	0.00%	0.00%	0.00%	0.00%
Chloroflexi	Anaerolineae	SBR1031	0.14%	0.00%	0.04%	0.13%	0.04%	0.07%	1.80%	1.72%	1.09%	1.54%	0.29%	0.37%
Chloroflexi	Anaerolineae	Caldilineales	0.00%	0.00%	0.00%	0.00%	0.00%	0.00%	0.01%	0.00%	0.00%	0.00%	0.03%	0.00%
Chloroflexi	Anaerolineae	Ardenticatenales	0.18%	0.23%	0.10%	0.42%	0.07%	0.38%	2.29%	0.41%	0.32%	1.30%	1.68%	1.49%
Campilobacterota	Campylobacteria	Campylobacterales	1.51%	0.96%	0.20%	1.87%	0.56%	1.36%	0.04%	0.00%	0.06%	0.04%	0.56%	9.35%
Calditrichota	Calditrichia	Calditrichales	0.02%	0.00%	0.00%	0.00%	0.01%	0.01%	0.18%	0.02%	0.07%	0.23%	0.05%	0.03%
Bdellovibrionota	Oligoflexia	Oligoflexales	0.21%	0.44%	0.12%	0.01%	0.30%	0.49%	0.21%	0.01%	0.00%	0.00%	0.04%	0.06%
Bdellovibrionota	Bdellovibrionia	Bdellovibrionales	0.24%	0.15%	0.63%	0.14%	0.19%	0.25%	1.23%	0.24%	0.24%	0.82%	1.02%	1.58%
Bdellovibrionota	Bdellovibrionia	Bacteriovoracales	0.14%	0.34%	0.26%	0.11%	0.07%	0.07%	0.08%	0.16%	0.39%	0.09%	0.12%	0.25%
Bacteroidota	Rhodothermia	Rhodothermales	0.45%	0.00%	0.03%	0.08%	0.09%	0.30%	0.43%	0.27%	0.27%	0.05%	0.70%	0.39%
Bacteroidota	Rhodothermia	Balneolales	0.01%	0.00%	0.01%	0.01%	0.02%	0.00%	0.00%	0.00%	0.00%	0.00%	0.01%	0.01%
Bacteroidota	Kapabacteria	Kapabacteriales	0.00%	0.00%	0.00%	0.01%	0.03%	0.00%	0.00%	0.04%	0.05%	0.00%	0.01%	0.02%
Bacteroidota	Bacteroidia	Sphingobacteriales	0.01%	0.02%	0.04%	0.00%	0.08%	0.06%	0.01%	0.01%	0.01%	0.19%	0.00%	0.07%
Bacteroidota	Bacteroidia	ML602M-17	0.00%	0.00%	0.00%	0.00%	0.01%	0.00%	0.05%	0.00%	0.00%	0.00%	0.00%	0.02%
Bacteroidota	Bacteroidia	Flavobacteriales	13.03%	5.13%	2.70%	4.39%	15.94%	12.35%	3.19%	0.39%	0.56%	3.04%	1.94%	1.73%
Bacteroidota	Bacteroidia	Cytophagales	1.56%	0.40%	0.19%	1.06%	1.66%	4.93%	1.06%	3.51%	5.41%	1.52%	4.63%	3.67%
Bacteroidota	Bacteroidia	Chitinophagales	3.99%	8.86%	3.35%	3.66%	2.11%	5.57%	9.23%	2.88%	1.48%	2.74%	1.46%	1.19%
Bacteroidota	Bacteroidia	BacteroidetesVC2.1Bac22	0.00%	0.00%	0.00%	0.01%	0.08%	0.00%	0.04%	0.00%	0.00%	0.05%	0.02%	0.02%
Bacteroidota	Bacteroidia	Bacteroidales	0.21%	0.03%	0.00%	0.59%	0.00%	0.00%	0.02%	0.01%	0.01%	0.02%	0.01%	0.07%
Actinobacteriota	Thermoleophilia	Gaiellales	0.00%	0.00%	0.00%	0.00%	0.00%	0.00%	0.00%	0.00%	0.00%	0.03%	0.04%	0.05%
Actinobacteriota	Actinobacteria	Propionibacteriales	0.03%	0.02%	0.01%	0.03%	0.00%	0.01%	0.00%	0.04%	0.02%	0.07%	0.01%	0.00%
Actinobacteriota	Actinobacteria	Micrococcales	0.00%	0.09%	0.01%	0.01%	0.01%	0.00%	0.01%	0.00%	0.00%	0.00%	0.00%	0.02%
Actinobacteriota	Actinobacteria	Corynebacteriales	0.00%	0.00%	0.00%	0.00%	0.00%	0.02%	0.01%	0.01%	0.01%	0.00%	0.03%	0.09%
Actinobacteriota	Acidimicrobiia	Microtrichales	0.32%	0.11%	0.22%	0.16%	0.40%	2.56%	4.88%	0.24%	0.94%	2.67%	4.74%	0.17%
Actinobacteriota	Acidimicrobiia	IMCC26256	0.01%	0.00%	0.00%	0.00%	0.00%	0.00%	0.01%	0.00%	0.00%	0.00%	0.00%	0.04%
Actinobacteriota	Acidimicrobiia	Actinomarinales	0.01%	0.00%	0.00%	0.01%	0.02%	0.01%	0.03%	0.01%	0.03%	0.00%	0.00%	0.00%
Acidobacteriota	Vicinamibacteria	Subgroup9	0.00%	0.00%	0.01%	0.03%	0.00%	0.00%	0.02%	0.01%	0.02%	0.00%	0.00%	0.00%
Acidobacteriota	Vicinamibacteria	Subgroup17	0.00%	0.00%	0.00%	0.07%	0.00%	0.00%	0.00%	0.00%	0.00%	0.00%	0.00%	0.00%
Acidobacteriota	Thermoanaerobaculia	Thermoanaerobaculales	0.05%	0.06%	0.03%	0.07%	0.03%	0.03%	2.66%	0.02%	0.09%	8.32%	2.06%	0.16%
Acidobacteriota	Subgroup22	unknown	0.02%	0.00%	0.05%	0.02%	0.01%	0.01%	0.09%	0.09%	0.18%	0.04%	0.08%	0.01%
Acidobacteriota	Holophagae	Subgroup7	0.00%	0.00%	0.00%	0.03%	0.00%	0.00%	0.00%	0.00%	0.00%	0.00%	0.01%	0.00%
Acidobacteriota	Holophagae	Acanthopleuribacterales	0.02%	0.00%	0.06%	0.06%	0.04%	0.02%	0.05%	0.03%	0.08%	0.17%	0.20%	0.02%
Acidobacteriota	Blastocatellia	Blastocatellales	0.01%	0.00%	0.01%	0.01%	0.02%	0.00%	0.00%	0.04%	0.10%	0.00%	0.01%	0.01%
Acidobacteriota	Acidobacteriae	PAUC26f	0.00%	0.00%	0.00%	0.01%	0.01%	0.00%	0.04%	0.00%	0.00%	0.00%	0.00%	0.00%
Acetothermia	Acetothermiia	unknown	0.00%	0.00%	0.00%	0.01%	0.00%	0.00%	0.00%	0.00%	0.00%	0.00%	0.00%	0.01%
Nanoarchaeota	Nanoarchaeia	Woesearchaeales	0.04%	0.10%	0.00%	0.02%	0.00%	0.01%	0.00%	0.00%	0.00%	0.00%	0.00%	0.06%
Crenarchaeota	Nitrososphaeria	Nitrosopumilales	0.04%	0.10%	0.01%	0.32%	0.24%	0.06%	0.00%	0.01%	0.00%	0.05%	0.00%	0.22%

Supplementary Table 11: 281 de-replicated metagenome-assembled genomes (MAGs) information including taxonomy, completeness, and size

Genome	Classification	Completeness [%]	Contamination	GC	N50	Size [bp]
MAG.1	d__Bacteria;p__Bacteroidota;c__Bacteroidia;o__Cytophagales;f__Cyclobacteriaceae;g__UBA6059;s__	70.99	4.315	0.444	6152	4097614
MAG.10	d__Bacteria;p__Proteobacteria;c__Gammaproteobacteria;o__Pseudomonadales;f__Nitrincolaceae;g__Neptuniibacter;s__	79.52	2.238	0.446	6405	2713555
MAG.100	d__Bacteria;p__Proteobacteria;c__Gammaproteobacteria;o__Granulosicoccales;f__Granulosicoccaceae;g__;s__	83.48	4.401	0.532	8335	5368582
MAG.101	d__Bacteria;p__Proteobacteria;c__Gammaproteobacteria;o__Pseudomonadales;f__HTCC2089;g__;s__	54.45	1.666	0.538	4618	2929034
MAG.102	d__Bacteria;p__Proteobacteria;c__Gammaproteobacteria;o__Pseudomonadales;f__HTCC2089;g__UBA4582;s__	51.72	2.586	0.485	5190	4152802
MAG.103	d__Bacteria;p__Planctomycetota;c__Phycisphaerae;o__Phycisphaerales;f__UBA1924;g__UBA1926;s__	94.31	0	0.678	88311	3965039
MAG.104	d__Bacteria;p__Proteobacteria;c__Alphaproteobacteria;o__GCA-2731375;f__GCA-2731375;g__;s__	91.52	2.318	0.563	19318	5310489
MAG.105	d__Bacteria;p__Planctomycetota;c__Phycisphaerae;o__Phycisphaerales;f__UBA1924;g__UBA1924;s__	95.45	2.272	0.517	319647	2915416
MAG.106	d__Bacteria;p__Proteobacteria;c__Alphaproteobacteria;o__Rhodobacterales;f__Rhodobacteraceae;g__Litoreibacter;s__	98.08	1.204	0.565	132137	4506390
MAG.107	d__Bacteria;p__Planctomycetota;c__Phycisphaerae;o__Phycisphaerales;f__SM1A02;g__;s__	68.35	2.442	0.569	11277	2994732
MAG.108	d__Bacteria;p__Proteobacteria;c__Alphaproteobacteria;o__Rhizobiales;f__Rhodobiaceae;g__;s__	54.14	0.791	0.593	4215	4234061
MAG.109	d__Bacteria;p__Actinobacteriota;c__Acidimicrobiia;o__Acidimicrobiales;f__SZUA-35;g__CADEDH01;s__	80.9	3.418	0.666	48551	5898155
MAG.11	d__Bacteria;p__Proteobacteria;c__Gammaproteobacteria;o__Pseudomonadales;f__DSM-6294;g__Oceanobacter;s__	95.81	0.907	0.537	30656	4161600
MAG.111	d__Bacteria;p__Proteobacteria;c__Alphaproteobacteria;o__Micavibrionales;f__UBA2020;g__;s__	51.29	5.724	0.414	4000	988330
MAG.112	d__Bacteria;p__Myxococcota_A;c__UBA9160;o__UBA9160;f__;g__;s__	94.35	2.741	0.641	112605	7218910
MAG.113	d__Bacteria;p__Proteobacteria;c__Alphaproteobacteria;o__Rhodobacterales;f__Rhodobacteraceae;g__Cognatishimia;s__	55.25	0	0.539	4390	1764462
MAG.114	d__Bacteria;p__Planctomycetota;c__GCA-002687715;o__GCA-002687715;f__;g__;s__	50.07	3.056	0.594	3688	1707175
MAG.115	d__Bacteria;p__Eremiobacterota;c__Xenobia;o__Xenobiales;f__JADMJV01;g__;s__	76.95	4.629	0.534	9636	7845607
MAG.116	d__Bacteria;p__Bacteroidota;c__Bacteroidia;o__Chitinophagales;f__Saprospiraceae;g__;s__	99.5	1	0.366	128445	6348341
MAG.117	d__Bacteria;p__Proteobacteria;c__Alphaproteobacteria;o__Sphingomonadales;f__Sphingomonadaceae;g__Pontixanthobacter;s__	87.95	4.579	0.57	10600	2906456
MAG.118	d__Bacteria;p__Proteobacteria;c__Alphaproteobacteria;o__UBA8366;f__GCA-2696645;g__GCA-2696645;s__	51.57	0.996	0.572	4416	1871161
MAG.119	d__Bacteria;p__Proteobacteria;c__Alphaproteobacteria;o__Rhodobacterales;f__Rhodobacteraceae;g__Sulfitobacter;s__Sulfitobacter mediterraneus	81.47	1.395	0.582	6393	3092074
MAG.12	d__Bacteria;p__Dependentiae;c__Babeliae;o__Babeliales;f__RVW-14;g__;s__	63.57	2.197	0.377	5356	1060846
MAG.120	d__Bacteria;p__Proteobacteria;c__Alphaproteobacteria;o__Rhodobacterales;f__Rhodobacteraceae;g__Parasedimentitalea;s__Parasedimentitalea marina_A	99.16	0.844	0.542	181208	5208656
MAG.121	d__Bacteria;p__Proteobacteria;c__Alphaproteobacteria;o__Rhodobacterales;f__Rhodobacteraceae;g__Mangrovicoccus;s__	96.98	0.515	0.586	90627	4257309
MAG.122	d__Bacteria;p__Proteobacteria;c__Gammaproteobacteria;o__Pseudomonadales;f__UBA7434;g__;s__	94.87	0.555	0.413	101804	3556077
MAG.123	d__Bacteria;p__Desulfobacterota_D;c__UBA1144;o__;f__;g__;s__	82.28	4.201	0.383	10429	1928183
MAG.125	d__Bacteria;p__Myxococcota;c__Polyangia;o__Nannocystales;f__Nannocystaceae;g__;s__	95.64	4.516	0.65	697735	11138351
MAG.126	d__Bacteria;p__Verrucomicrobiota;c__Verrucomicrobiae;o__Opitutales;f__DSM-45221;g__BACL24;s__	96.62	2.252	0.494	26348	3156521
MAG.127	d__Bacteria;p__Proteobacteria;c__Alphaproteobacteria;o__Rhizobiales;f__OSC116;g__;s__	90.34	0.434	0.499	23547	3111790
MAG.128	d__Bacteria;p__Planctomycetota;c__PLA2;o__;f__;g__;s__	90.9	2.272	0.685	75810	7051079
MAG.129	d__Bacteria;p__Proteobacteria;c__Alphaproteobacteria;o__Caulobacterales;f__Maricaulaceae;g__Robiginitomaculum_A;s__	99.18	0.324	0.498	433006	3288981
MAG.13	d__Bacteria;p__Bacteroidota;c__Bacteroidia;o__Chitinophagales;f__Saprospiraceae;g__Lewinella_A;s__	82.25	1.1	0.509	7527	6020282
MAG.130	d__Bacteria;p__Proteobacteria;c__Gammaproteobacteria;o__Pseudomonadales;f__Cellvibrionaceae;g__Marinagarivorans;s__	98.51	1.199	0.458	99767	4798301
MAG.131	d__Bacteria;p__Planctomycetota;c__Phycisphaerae;o__Phycisphaerales;f__UBA1924;g__;s__	86.69	0	0.663	16444	2515481
MAG.132	d__Bacteria;p__Bacteroidota;c__Bacteroidia;o__Chitinophagales;f__Saprospiraceae;g__DT-111;s__	54.88	2.777	0.427	4432	5807677
MAG.133	d__Bacteria;p__Patescibacteria;c__Gracilibacteria;o__UBA4473;f__UBA4473;g__JAACPJ01;s__	69.74	2.849	0.437	14062	1250881
MAG.134	d__Bacteria;p__Proteobacteria;c__Alphaproteobacteria;o__Bin95;f__Bin95;g__VMCJ01;s__	56.11	0.594	0.646	4261	2760956
MAG.135	d__Bacteria;p__Actinobacteriota;c__Acidimicrobiia;o__Acidimicrobiales;f__SHLQ01;g__SHLQ01;s__	88.38	3.513	0.629	8931	4043431
MAG.136	d__Bacteria;p__Planctomycetota;c__UBA1135;o__UBA2386;f__UBA2386;g__JADJWQ01;s__	51.05	1.239	0.641	4378	2861618
MAG.137	d__Bacteria;p__Bacteroidota;c__Bacteroidia;o__Cytophagales;f__;g__;s__	55.35	0	0.369	15606	616463
MAG.138	d__Bacteria;p__Proteobacteria;c__Alphaproteobacteria;o__Caulobacterales;f__Hyphomonadaceae;g__UBA5336;s__	87.66	1.309	0.581	17873	2815569
MAG.139	d__Bacteria;p__Proteobacteria;c__Alphaproteobacteria;o__Rhizobiales;f__Rhizobiaceae;g__GCA-2401155;s__	97.15	0.432	0.48	50855	4437867
MAG.14	d__Bacteria;p__Proteobacteria;c__Gammaproteobacteria;o__Enterobacterales;f__Vibrionaceae;g__Vibrio;s__Vibrio splendidus	60.34	9.247	0.438	5190	3739722
MAG.140	d__Bacteria;p__Proteobacteria;c__Alphaproteobacteria;o__Rhodobacterales;f__Rhodobacteraceae;g__Ruegeria;s__Ruegeria meonggei	95.63	1.118	0.576	32081	4482110
MAG.141	d__Bacteria;p__Verrucomicrobiota;c__Verrucomicrobiae;o__Opitutales;f__DSM-45221;g__UBA7441;s__	100	0	0.516	339466	2827205
MAG.142	d__Bacteria;p__Planctomycetota;c__Phycisphaerae;o__Phycisphaerales;f__SM1A02;g__;s__	93.18	1.807	0.697	22293	4335923
MAG.143	d__Bacteria;p__Proteobacteria;c__Alphaproteobacteria;o__Caulobacterales;f__Hyphomonadaceae;g__Henriciella;s__	97.94	3.03	0.547	158779	3921363
MAG.144	d__Bacteria;p__Proteobacteria;c__Alphaproteobacteria;o__Caulobacterales;f__Hyphomonadaceae;g__Henriciella;s__	98.91	3.922	0.55	71029	4146604
MAG.145	d__Bacteria;p__Patescibacteria;c__Paceibacteria;o__UBA9983_A;f__UBA918;g__OLB19;s__	51.86	0	0.393	6052	617582
MAG.146	d__Bacteria;p__Proteobacteria;c__Alphaproteobacteria;o__GCA-2731375;f__GCA-2731375;g__;s__	88.62	1.304	0.559	11070	6549394
MAG.147	d__Bacteria;p__Planctomycetota;c__Planctomycetia;o__Planctomycetales;f__Planctomycetaceae;g__JABMPE01;s__	82.48	3.448	0.583	9055	10228853
MAG.148	d__Bacteria;p__Chlamydiota;c__Chlamydiia;o__Chlamydiales;f__GCA-2709385;g__;s__	62.71	0	0.387	4529	1094745
MAG.149	d__Bacteria;p__Proteobacteria;c__Gammaproteobacteria;o__Enterobacterales;f__Alteromonadaceae;g__Colwellia;s__	96.14	2.118	0.362	17524	4524466
MAG.15	d__Bacteria;p__Planctomycetota;c__Phycisphaerae;o__UBA1845;f__UBA1845;g__UBA1845;s__	95.45	2.272	0.558	371848	4873431
MAG.150	d__Bacteria;p__Sumerlaeota;c__Sumerlaeia;o__SLMS01;f__;g__;s__	54.52	0.029	0.483	4604	2070526
MAG.151	d__Bacteria;p__Proteobacteria;c__Alphaproteobacteria;o__Rhizobiales;f__HXMU1428-3;g__HXMU1428-3;s__	55.35	2.208	0.455	5045	1523401
MAG.153	d__Bacteria;p__Proteobacteria;c__Gammaproteobacteria;o__Pseudomonadales;f__Halieaceae;g__Congregibacter;s__	94.34	1.115	0.544	19634	2871557
MAG.154	d__Bacteria;p__Bdellovibrionota;c__Bdellovibrionia;o__Bdellovibrionales;f__;g__;s__	82.68	3.21	0.409	6266	2169211
MAG.155	d__Bacteria;p__Proteobacteria;c__Gammaproteobacteria;o__Granulosicoccales;f__Granulosicoccaceae;g__UBA7957;s__	96.03	6.785	0.459	196809	6526097
MAG.156	d__Bacteria;p__Proteobacteria;c__Alphaproteobacteria;o__Caulobacterales;f__Hyphomonadaceae;g__;s__	85.4	2.38	0.566	8371	2524260
MAG.157	d__Bacteria;p__Proteobacteria;c__Alphaproteobacteria;o__Rhodobacterales;f__Rhodobacteraceae;g__Actibacterium;s__	94.86	2.219	0.611	86167	3620077
MAG.158	d__Bacteria;p__Proteobacteria;c__Alphaproteobacteria;o__Micavibrionales;f__Micavibrionaceae;g__TMED27;s__	92.31	1.014	0.482	31481	1871309
MAG.159	d__Bacteria;p__Planctomycetota;c__Phycisphaerae;o__Phycisphaerales;f__UBA1924;g__;s__	96.02	0.51	0.612	129757	3009249
MAG.16	d__Bacteria;p__Proteobacteria;c__Alphaproteobacteria;o__Caulobacterales;f__Hyphomonadaceae;g__Henriciella;s__	92.39	1.418	0.569	44579	2815854
MAG.160	d__Bacteria;p__Proteobacteria;c__Alphaproteobacteria;o__Minwuiales;f__Minwuiaceae;g__Minwuia;s__	86.33	0.362	0.639	11768	3999996
MAG.161	d__Bacteria;p__Proteobacteria;c__Gammaproteobacteria;o__Pseudomonadales;f__Nitrincolaceae;g__Pontibacterium;s__	85.75	0.929	0.509	10721	3500245
MAG.162	d__Bacteria;p__Proteobacteria;c__Gammaproteobacteria;o__Pseudomonadales;f__Nitrincolaceae;g__Neptuniibacter;s__	91.72	0.214	0.46	51427	2852220
MAG.164	d__Bacteria;p__Proteobacteria;c__Alphaproteobacteria;o__Rhodobacterales;f__Rhodobacteraceae;g__Amylibacter;s__	63.2	0.455	0.465	5280	2154237
MAG.165	d__Bacteria;p__Planctomycetota;c__UBA1135;o__UBA2386;f__UBA2386;g__;s__	68.59	1.075	0.658	5660	5191195
MAG.167	d__Bacteria;p__Proteobacteria;c__Alphaproteobacteria;o__Micavibrionales;f__Micavibrionaceae;g__;s__	89.72	0.869	0.495	16409	1786896
MAG.169	d__Bacteria;p__Proteobacteria;c__Alphaproteobacteria;o__Rhodobacterales;f__Rhodobacteraceae;g__Pseudooceanicola_C;s__	97.32	1.478	0.62	19399	4304744
MAG.17	d__Bacteria;p__Planctomycetota;c__UBA1135;o__UBA1135;f__GCA-002686595;g__GCA-2862085;s__	95.69	0.537	0.638	66090	8923139
MAG.170	d__Bacteria;p__Chlamydiota;c__Chlamydiia;o__Chlamydiales;f__SLFE01;g__;s__	53.2	1.351	0.418	3923	969073
MAG.171	d__Bacteria;p__Bacteroidota;c__Bacteroidia;o__J057;f__JADKCL01;g__;s__	97.81	1.366	0.493	287329	9463275
MAG.173	d__Bacteria;p__Proteobacteria;c__Alphaproteobacteria;o__Sphingomonadales;f__Sphingomonadaceae;g__Pontixanthobacter;s__	80.2	2.73	0.552	10457	2260549
MAG.174	d__Bacteria;p__Bacteroidota;c__Bacteroidia;o__Cytophagales;f__;g__;s__	52.69	5.382	0.386	20932	701459
MAG.175	d__Bacteria;p__Actinobacteriota;c__Acidimicrobiia;o__Acidimicrobiales;f__SZUA-35;g__CADEDH01;s__	99.05	4.107	0.653	22347	6560164
MAG.176	d__Bacteria;p__Proteobacteria;c__Alphaproteobacteria;o__Rhizobiales;f__Methyloligellaceae;g__Methyloceanibacter;s__	95.33	1.104	0.61	27579	2916637
MAG.177	d__Bacteria;p__Chloroflexota;c__Anaerolineae;o__Promineofilales;f__Promineofilaceae;g__;s__	89.59	3.818	0.506	10679	7593054
MAG.178	d__Bacteria;p__Proteobacteria;c__Gammaproteobacteria;o__Enterobacterales;f__Alteromonadaceae;g__Pseudoalteromonas;s__	95.43	1.013	0.399	66416	3981841

MAG.179	d__Bacteria;p__Planctomycetota;c__Phycisphaerae;o__Phycisphaerales;f__UBA1924;g__REDD01;s__	92.8	2.272	0.672	171936	3144260
MAG.18	d__Bacteria;p__Proteobacteria;c__Gammaproteobacteria;o__Pseudomonadales;f__Porticoccaceae;g__Porticoccus;s__	98.14	0.925	0.441	231514	2402837
MAG.180	d__Bacteria;p__Proteobacteria;c__Alphaproteobacteria;o__Rhodobacterales;f__Rhodobacteraceae;g__Cognatishimia;s__	95.72	0.214	0.532	50191	3159778
MAG.181	d__Bacteria;p__Proteobacteria;c__Alphaproteobacteria;o__Rhizobiales;f__Rhizobiaceae;g__Ahrensia;s__	84.61	1.971	0.506	7714	3188336
MAG.182	d__Bacteria;p__Eremiobacterota;c__Xenobia;o__Xenobiales;f__JADMJV01;g__;s__	85.64	6.018	0.513	14284	6959212
MAG.183	d__Bacteria;p__Proteobacteria;c__Alphaproteobacteria;o__Rhodobacterales;f__Rhodobacteraceae;g__;s__	88.68	1.461	0.645	9049	4229825
MAG.184	d__Bacteria;p__Proteobacteria;c__Alphaproteobacteria;o__Rhodobacterales;f__Rhodobacteraceae;g__Sedimentitalea;s__	86.1	2.335	0.608	88544	3759964
MAG.185	d__Bacteria;p__Chloroflexota;c__Anaerolineae;o__Aggregatilineales;f__A4b;g__;s__	60.05	5.454	0.427	7588	5382503
MAG.186	d__Bacteria;p__Chloroflexota;c__Anaerolineae;o__Promineofilales;f__Promineofilaceae;g__WTJY01;s__	96.06	4.545	0.458	38076	9298964
MAG.187	d__Bacteria;p__Planctomycetota;c__UBA1135;o__UBA1135;f__GCA-002686595;g__;s__	96.77	1.075	0.612	24568	4080738
MAG.188	d__Bacteria;p__Planctomycetota;c__Phycisphaerae;o__Phycisphaerales;f__UBA1924;g__;s__	83.52	0.066	0.681	9754	2924240
MAG.189	d__Bacteria;p__Proteobacteria;c__Gammaproteobacteria;o__Woeseiales;f__Woeseiaceae;g__;s__	58.67	3.521	0.57	4825	3187947
MAG.19	d__Bacteria;p__Proteobacteria;c__Alphaproteobacteria;o__Paracaedibacterales;f__;g__;s__	92.47	0	0.358	53573	1606354
MAG.190	d__Bacteria;p__Planctomycetota;c__Phycisphaerae;o__Phycisphaerales;f__UBA1924;g__;s__	97.72	0	0.626	121107	3175198
MAG.191	d__Bacteria;p__Proteobacteria;c__Alphaproteobacteria;o__Rhodobacterales;f__Rhodobacteraceae;g__Marinovum;s__	89.98	0.998	0.599	11248	3962981
MAG.192	d__Bacteria;p__Planctomycetota;c__Phycisphaerae;o__Phycisphaerales;f__Phycisphaeraceae;g__;s__	93.54	1.988	0.653	26853	4359134
MAG.193	d__Bacteria;p__Proteobacteria;c__Gammaproteobacteria;o__Pseudomonadales;f__Porticoccaceae;g__Porticoccus;s__	72.49	3.395	0.433	8353	1995864
MAG.194	d__Bacteria;p__Proteobacteria;c__Gammaproteobacteria;o__Pseudomonadales;f__;g__;s__	98.56	1.131	0.497	211369	4754708
MAG.195	d__Bacteria;p__Proteobacteria;c__Gammaproteobacteria;o__Woeseiales;f__Woeseiaceae;g__UBA1847;s__	70.84	0	0.568	11344	2802047
MAG.196	d__Bacteria;p__Hydrogenedentota;c__Hydrogenedentia;o__Hydrogenedentiales;f__WGMK01;g__;s__	87.36	1.198	0.575	10181	4759649
MAG.198	d__Bacteria;p__Proteobacteria;c__Gammaproteobacteria;o__JABDGN01;f__JABDGN01;g__;s__	88.08	1.744	0.393	8212	1923199
MAG.199	d__Bacteria;p__Proteobacteria;c__Alphaproteobacteria;o__Caulobacterales;f__Hyphomonadaceae;g__;s__	97.55	2.976	0.564	34307	3288413
MAG.2	d__Bacteria;p__Proteobacteria;c__Alphaproteobacteria;o__Rhizobiales;f__Afifellaceae;g__;s__	50.94	1.204	0.546	4257	2500893
MAG.20	d__Bacteria;p__Proteobacteria;c__Alphaproteobacteria;o__Rhodospirillales;f__UBA2165;g__;s__	87.1	1.16	0.468	10670	3765314
MAG.200	d__Bacteria;p__Proteobacteria;c__Alphaproteobacteria;o__Sphingomonadales;f__Sphingomonadaceae;g__Parasphingorhabdus;s__	77.89	1.877	0.526	7209	2686240
MAG.201	d__Bacteria;p__Myxococcota;c__Bradymonadia;o__Bradymonadales;f__Bradymonadaceae;g__;s__	90.64	4.681	0.642	58869	9050246
MAG.202	d__Bacteria;p__Acidobacteriota;c__Thermoanaerobaculia;o__UBA5704;f__UBA5704;g__;s__	98.29	4.273	0.652	112953	9845739
MAG.203	d__Bacteria;p__Planctomycetota;c__Planctomycetia;o__Pirellulales;f__Pirellulaceae;g__;s__	96.48	3.448	0.54	23188	10289006
MAG.204	d__Bacteria;p__Proteobacteria;c__Gammaproteobacteria;o__Pseudomonadales;f__HTCC2089;g__UBA4421;s__	81.51	4.259	0.537	7502	4495332
MAG.205	d__Bacteria;p__Proteobacteria;c__Gammaproteobacteria;o__Enterobacterales;f__Alteromonadaceae;g__Paraglaciecola;s__Paraglaciecola chathamensis	98.54	1.122	0.443	54361	4828884
MAG.207	d__Bacteria;p__Planctomycetota;c__UBA8108;o__UBA1146;f__;g__;s__	97.84	3.405	0.616	167360	7880354
MAG.210	d__Bacteria;p__Proteobacteria;c__Gammaproteobacteria;o__Pseudomonadales;f__HTCC2089;g__UBA4582;s__	94.24	4.614	0.498	152426	5536602
MAG.211	d__Bacteria;p__Bacteroidota;c__Bacteroidia;o__Flavobacteriales;f__UBA10066;g__;s__	97.17	0.537	0.366	17422	3321607
MAG.212	d__Bacteria;p__Myxococcota;c__Polyangia;o__Polyangiales;f__Polyangiaceae;g__NIC37A-2;s__	53.07	0.668	0.597	4474	3868848
MAG.213	d__Bacteria;p__Proteobacteria;c__Gammaproteobacteria;o__Pseudomonadales;f__DSM-21967;g__Oceanicoccus;s__	98.26	2.29	0.466	37086	4055470
MAG.214	d__Bacteria;p__Proteobacteria;c__Alphaproteobacteria;o__Rhizobiales;f__MH13;g__MH13;s__	98.23	1.137	0.566	62077	3926594
MAG.215	d__Bacteria;p__Proteobacteria;c__Gammaproteobacteria;o__UWMA-0217;f__UWMA-0217;g__;s__	81.24	4.422	0.489	6399	3546941
MAG.216	d__Bacteria;p__Planctomycetota;c__Phycisphaerae;o__Phycisphaerales;f__Phycisphaeraceae;g__;s__	75	2.272	0.665	31771	3018270
MAG.217	d__Bacteria;p__Proteobacteria;c__Alphaproteobacteria;o__Rhizobiales;f__Rhizobiaceae;g__Ahrensia;s__	78.84	4.047	0.501	5815	3041618
MAG.218	d__Bacteria;p__Dependentiae;c__Babeliae;o__Babeliales;f__Vermiphilaceae;g__;s__	52.58	0	0.349	25467	870198
MAG.219	d__Bacteria;p__Proteobacteria;c__Gammaproteobacteria;o__Pseudomonadales;f__DSM-21967;g__;s__	100	0.432	0.458	165972	3147943
MAG.22	d__Bacteria;p__Planctomycetota;c__Phycisphaerae;o__Phycisphaerales;f__UBA1924;g__UBA1924;s__	88.17	1.136	0.509	16393	2766236
MAG.220	d__Bacteria;p__Patescibacteria;c__Paceibacteria;o__UBA9983_A;f__UBA918;g__OLB19;s__	56.62	1.255	0.396	6316	584872
MAG.221	d__Bacteria;p__Planctomycetota;c__B15-G4;o__B15-G4;f__B15-G4;g__;s__	93.75	1.136	0.668	55177	5058348
MAG.223	d__Bacteria;p__Proteobacteria;c__Alphaproteobacteria;o__Geminicoccales;f__Geminicoccaceae;g__CADEGR01;s__	94.65	2.503	0.571	14010	7227267
MAG.224	d__Bacteria;p__Planctomycetota;c__Planctomycetia;o__Pirellulales;f__Lacipirellulaceae;g__Aeoliella;s__	94.18	0.208	0.583	22639	4965952
MAG.225	d__Bacteria;p__Proteobacteria;c__Alphaproteobacteria;o__Sneathiellales;f__Sneathiellaceae;g__Sneathiella;s__	62.06	7.758	0.509	12104	3423313
MAG.226	d__Bacteria;p__Proteobacteria;c__Gammaproteobacteria;o__UBA4486;f__UBA4486;g__;s__	82.23	4.06	0.377	8575	1885996
MAG.227	d__Bacteria;p__Proteobacteria;c__Alphaproteobacteria;o__Rhodobacterales;f__Rhodobacteraceae;g__OMPR01;s__	66.06	7.534	0.554	6812	3687273
MAG.228	d__Bacteria;p__Patescibacteria;c__Paceibacteria;o__UBA9983_A;f__UBA918;g__OLB19;s__	62.71	2.564	0.435	131554	1042042
MAG.229	d__Bacteria;p__Desulfobacterota_I;c__Desulfovibrionia;o__Desulfovibrionales;f__Desulfovibrionaceae;g__Halodesulfovibrio;s__	97.04	0.065	0.449	43686	3719627
MAG.23	d__Bacteria;p__Proteobacteria;c__Alphaproteobacteria;o__Rhodobacterales;f__Rhodobacteraceae;g__Phaeobacter_A;s__	93.82	0.638	0.605	54010	4437349
MAG.230	d__Bacteria;p__Proteobacteria;c__Alphaproteobacteria;o__Rhodobacterales;f__Rhodobacteraceae;g__Fluviibacterium;s__	94.3	1.094	0.524	12986	3380286
MAG.231	d__Bacteria;p__Proteobacteria;c__Gammaproteobacteria;o__Arenicellales;f__Arenicellaceae;g__Arenicella;s__	96.42	0	0.446	25757	4698766
MAG.232	d__Bacteria;p__Proteobacteria;c__Gammaproteobacteria;o__Pseudomonadales;f__Porticoccaceae;g__LSUCC0057;s__	99.21	0.277	0.592	46714	2111063
MAG.233	d__Bacteria;p__Proteobacteria;c__Alphaproteobacteria;o__Rhizobiales;f__JACESI01;g__JACESI01;s__	71.7	0.344	0.475	8626	4263593
MAG.234	d__Bacteria;p__Proteobacteria;c__Gammaproteobacteria;o__Arenicellales;f__Arenicellaceae;g__Arenicella;s__	98.17	0	0.445	273240	4957047
MAG.235	d__Bacteria;p__Proteobacteria;c__Alphaproteobacteria;o__Micavibrionales;f__Micavibrionaceae;g__UBA1672;s__	75.26	0.681	0.437	8377	1653986
MAG.236	d__Bacteria;p__Proteobacteria;c__Gammaproteobacteria;o__Xanthomonadales;f__Wenzhouxiangellaceae;g__;s__	98.91	0.764	0.434	339403	4925501
MAG.237	d__Bacteria;p__Proteobacteria;c__Gammaproteobacteria;o__Pseudomonadales;f__Porticoccaceae;g__;s__	55.82	0.925	0.499	4697	1546096
MAG.238	d__Bacteria;p__Planctomycetota;c__Planctomycetia;o__Pirellulales;f__Pirellulaceae;g__;s__	72.27	2.873	0.533	7285	6664739
MAG.239	d__Bacteria;p__Myxococcota;c__Polyangia;o__Polyangiales;f__Polyangiaceae;g__NIC37A-2;s__	89.03	1.29	0.603	11515	6265828
MAG.24	d__Bacteria;p__Actinobacteriota;c__Acidimicrobiia;o__Acidimicrobiales;f__SHLQ01;g__SHLQ01;s__	97.43	1.282	0.618	112806	5170803
MAG.240	d__Bacteria;p__Eremiobacterota;c__Xenobia;o__Xenobiales;f__JADMJV01;g__;s__	79.98	3.935	0.52	10235	6410319
MAG.241	d__Bacteria;p__Proteobacteria;c__Alphaproteobacteria;o__Sphingomonadales;f__Sphingomonadaceae;g__Parasphingorhabdus;s__	69.15	0.195	0.494	6490	2553006
MAG.242	d__Bacteria;p__Planctomycetota;c__Phycisphaerae;o__UBA1845;f__UTPLA1;g__ECT2AJA-110-A;s__	50.93	0	0.547	4641	2853487
MAG.243	d__Bacteria;p__Chloroflexota;c__Anaerolineae;o__Promineofilales;f__Promineofilaceae;g__;s__	61.12	3.636	0.469	5647	5576440
MAG.244	d__Bacteria;p__Bacteroidota;c__Bacteroidia;o__Flavobacteriales;f__Flavobacteriaceae;g__Saonia;s__	52.22	0.917	0.383	4404	2690371
MAG.245	d__Bacteria;p__Firmicutes;c__Bacilli;o__Mycoplasmatales;f__Mycoplasmataceae;g__;s__	79.94	0.751	0.288	52409	618172
MAG.246	d__Bacteria;p__Proteobacteria;c__Alphaproteobacteria;o__Micavibrionales;f__Micavibrionaceae;g__UBA1672;s__	90.83	2.246	0.444	24177	2209244
MAG.247	d__Bacteria;p__Proteobacteria;c__Alphaproteobacteria;o__Rhizobiales;f__;g__;s__	67.47	1.766	0.545	5394	5558507
MAG.248	d__Bacteria;p__Proteobacteria;c__Gammaproteobacteria;o__Pseudomonadales;f__Pseudohongiellaceae;g__UBA9145;s__	55.02	1.556	0.497	4822	1807334
MAG.249	d__Bacteria;p__Dependentiae;c__Babeliae;o__Babeliales;f__JAHIUU01;g__;s__	52.41	3.475	0.46	10178	994623
MAG.25	d__Bacteria;p__Planctomycetota;c__Phycisphaerae;o__Phycisphaerales;f__SM1A02;g__;s__	76.49	7.489	0.591	10865	3428793
MAG.250	d__Bacteria;p__Proteobacteria;c__Alphaproteobacteria;o__Minwuiales;f__Minwuiaceae;g__;s__	96.59	0.217	0.561	164320	4416444
MAG.251	d__Bacteria;p__Myxococcota;c__Polyangia;o__Nannocystales;f__Nannocystaceae;g__;s__	95.75	5.483	0.661	218764	13295286
MAG.252	d__Bacteria;p__Proteobacteria;c__Gammaproteobacteria;o__Pseudomonadales;f__Cellvibrionaceae;g__Agaribacterium;s__	85.67	1.163	0.473	7631	2653267
MAG.253	d__Bacteria;p__Bacteroidota;c__Bacteroidia;o__CAILMK01;f__JACPUW01;g__;s__	73.2	1.202	0.427	6234	4695506
MAG.254	d__Bacteria;p__Proteobacteria;c__Gammaproteobacteria;o__Pseudomonadales;f__DT-91;g__;s__	99.25	1.203	0.451	111469	4264802
MAG.255	d__Bacteria;p__Actinobacteriota;c__Acidimicrobiia;o__Acidimicrobiales;f__SZUA-35;g__;s__	51.53	0	0.611	4515	3217816
MAG.256	d__Bacteria;p__Proteobacteria;c__Gammaproteobacteria;o__Enterobacterales;f__Alteromonadaceae;g__Glaciecola;s__	98.87	0.19	0.386	230320	4297241
MAG.257	d__Bacteria;p__Proteobacteria;c__Alphaproteobacteria;o__Rhodobacterales;f__Rhodobacteraceae;g__Sulfitobacter;s__	94.88	2.932	0.573	26410	4050190
MAG.258	d__Bacteria;p__Bacteroidota;c__Rhodothermia;o__Rhodothermales;f__;g__;s__	96.72	4.793	0.47	47323	7841084
MAG.259	d__Bacteria;p__Desulfobacterota_D;c__UBA1144;o__UBA2774;f__UBA2774;g__CR02bin9;s__	96.63	6.302	0.394	44586	2496860
MAG.26	d__Bacteria;p__Proteobacteria;c__Gammaproteobacteria;o__Chromatiales;f__Sedimenticolaceae;g__;s__	51.41	2.032	0.632	4300	2091238

MAG.260	d__Bacteria;p__Proteobacteria;c__Alphaproteobacteria;o__Caulobacterales;f__Hyphomonadaceae;g__;s__	76.53	1.623	0.538	6079	2152761
MAG.262	d__Bacteria;p__Proteobacteria;c__Gammaproteobacteria;o__Pseudomonadales;f__Cellvibrionaceae;g__Pseudomaricurvus;s__	97.27	0.215	0.484	33664	4437687
MAG.263	d__Bacteria;p__Acidobacteriota;c__Thermoanaerobaculia;o__UBA5704;f__UBA5704;g__;s__	97	3.846	0.587	67067	9465534
MAG.264	d__Bacteria;p__Proteobacteria;c__Gammaproteobacteria;o__Pseudomonadales;f__Nitrincolaceae;g__Pontibacterium;s__	96.7	3.075	0.542	42761	4537692
MAG.266	d__Bacteria;p__Actinobacteriota;c__Acidimicrobiia;o__Acidimicrobiales;f__SZUA-35;g__;s__	53.53	1.709	0.615	4634	4002378
MAG.267	d__Bacteria;p__Myxococcota;c__Polyangia;o__Polyangiales;f__SG8-38;g__;s__	62.93	2.903	0.616	4512	2847258
MAG.268	d__Bacteria;p__Proteobacteria;c__Alphaproteobacteria;o__Rhodobacterales;f__Rhodobacteraceae;g__;s__	86.43	1.597	0.606	132364	3273506
MAG.269	d__Bacteria;p__Proteobacteria;c__Gammaproteobacteria;o__Pseudomonadales;f__DSM-6294;g__Oceanobacter;s__	99.42	0.745	0.516	87862	4128156
MAG.27	d__Bacteria;p__Proteobacteria;c__Alphaproteobacteria;o__Rhodobacterales;f__Rhodobacteraceae;g__Donghicola;s__	97.72	1.06	0.602	169522	3281014
MAG.270	d__Bacteria;p__Proteobacteria;c__Alphaproteobacteria;o__Sphingomonadales;f__Sphingomonadaceae;g__Parasphingorhabdus;s__	92.97	0.93	0.511	22770	3422949
MAG.271	d__Bacteria;p__Proteobacteria;c__Alphaproteobacteria;o__Rhodobacterales;f__Rhodobacteraceae;g__NORP181;s__	93.15	2.728	0.576	20422	4020071
MAG.272	d__Bacteria;p__Proteobacteria;c__Gammaproteobacteria;o__Enterobacterales;f__Moritellaceae;g__Moritella;s__	55.17	0	0.422	5182	1994471
MAG.273	d__Bacteria;p__Proteobacteria;c__Gammaproteobacteria;o__Xanthomonadales;f__SZUA-5;g__SZUA-5;s__	56.97	2.282	0.584	4236	3196766
MAG.274	d__Bacteria;p__Desulfobacterota_D;c__UBA1144;o__RKRQ01;f__;g__;s__	94.18	4.201	0.392	18731	2134500
MAG.275	d__Bacteria;p__Bacteroidota;c__Bacteroidia;o__J057;f__JADKCL01;g__;s__	99.18	0.546	0.455	89622	9536463
MAG.276	d__Bacteria;p__Proteobacteria;c__Alphaproteobacteria;o__Caulobacterales;f__Hyphomonadaceae;g__;s__	99.35	0.162	0.592	185624	3137955
MAG.277	d__Bacteria;p__Proteobacteria;c__Alphaproteobacteria;o__Rhodobacterales;f__Rhodobacteraceae;g__Actibacterium;s__	95.45	0.707	0.567	86100	3078466
MAG.278	d__Bacteria;p__Chloroflexota;c__Anaerolineae;o__Aggregatilineales;f__A4b;g__;s__	83.98	1.363	0.47	9361	5266120
MAG.279	d__Bacteria;p__Proteobacteria;c__Gammaproteobacteria;o__Coxiellales;f__Coxiellaceae;g__;s__	97.43	1.162	0.451	179395	2230703
MAG.28	d__Bacteria;p__Planctomycetota;c__Phycisphaerae;o__Phycisphaerales;f__Phycisphaeraceae;g__;s__	83.58	9.157	0.655	14140	4274694
MAG.280	d__Bacteria;p__Proteobacteria;c__Alphaproteobacteria;o__Rhodobacterales;f__Rhodobacteraceae;g__Mangrovicoccus;s__	98.73	0.389	0.592	77028	4003063
MAG.282	d__Bacteria;p__Actinobacteriota;c__Acidimicrobiia;o__Acidimicrobiales;f__SZUA-35;g__;s__	71.71	3.846	0.603	10709	4225400
MAG.283	d__Bacteria;p__Planctomycetota;c__Planctomycetia;o__Pirellulales;f__Lacipirellulaceae;g__Bythopirellula;s__	52.76	6.896	0.545	5000	2542241
MAG.285	d__Bacteria;p__Proteobacteria;c__Alphaproteobacteria;o__;f__;g__;s__	65.61	0	0.377	4455	844873
MAG.286	d__Bacteria;p__Proteobacteria;c__Gammaproteobacteria;o__UBA4486;f__UBA4486;g__;s__	85.91	0.586	0.447	235474	2105365
MAG.29	d__Bacteria;p__Proteobacteria;c__Gammaproteobacteria;o__Enterobacterales;f__Alteromonadaceae;g__Pseudoalteromonas;s__Pseudoalteromonas atlantica	70.14	0.862	0.407	57702	4420223
MAG.290	d__Bacteria;p__Bacteroidota;c__Bacteroidia;o__Chitinophagales;f__Saprospiraceae;g__JAFMDF01;s__	84.24	4.95	0.356	16781	12388985
MAG.293	d__Bacteria;p__Proteobacteria;c__Alphaproteobacteria;o__Kiloniellales;f__J153;g__;s__	81.57	4.376	0.64	7136	6197378
MAG.297	d__Bacteria;p__Myxococcota;c__WYAZ01;o__WYAZ01;f__WYAZ01;g__;s__	90.44	6.039	0.601	8747	11943676
MAG.3	d__Bacteria;p__Planctomycetota;c__UBA1135;o__UBA2386;f__UBA2386;g__;s__	87.13	3.512	0.647	10352	8694236
MAG.30	d__Bacteria;p__Proteobacteria;c__Alphaproteobacteria;o__Minwuiales;f__Minwuiaceae;g__Minwuia;s__	86.39	0.413	0.639	11410	3622814
MAG.308	d__Bacteria;p__Proteobacteria;c__Alphaproteobacteria;o__Rhizobiales;f__Devosiaceae;g__JAHJQZ01;s__	78.17	1.482	0.541	8095	3104918
MAG.31	d__Bacteria;p__Proteobacteria;c__Alphaproteobacteria;o__Rhodobacterales;f__Rhodobacteraceae;g__Mangrovicoccus;s__	82.37	2.083	0.638	10166	4653998
MAG.310	d__Bacteria;p__Planctomycetota;c__Phycisphaerae;o__Phycisphaerales;f__Phycisphaeraceae;g__;s__	80.12	0	0.638	11536	4907440
MAG.311	d__Bacteria;p__Proteobacteria;c__Alphaproteobacteria;o__UBA1280;f__UBA6503;g__UBA6503;s__	71.79	1.12	0.468	5926	1136925
MAG.314	d__Bacteria;p__Proteobacteria;c__Gammaproteobacteria;o__Woeseiales;f__Woeseiaceae;g__;s__	73.27	8.223	0.531	4383	3686470
MAG.316	d__Bacteria;p__Planctomycetota;c__Planctomycetia;o__Pirellulales;f__Pirellulaceae;g__CAJQPP01;s__	94.04	2.352	0.493	11800	6446244
MAG.32	d__Bacteria;p__Proteobacteria;c__Alphaproteobacteria;o__GCA-2731375;f__GCA-2731375;g__;s__	78.82	2.127	0.535	9141	5288117
MAG.321	d__Bacteria;p__Proteobacteria;c__Alphaproteobacteria;o__Rhizobiales;f__Methyloligellaceae;g__;s__	98.39	1.506	0.581	40023	4513236
MAG.33	d__Bacteria;p__Proteobacteria;c__Alphaproteobacteria;o__Rhizobiales;f__Methyloligellaceae;g__;s__	83.58	3.514	0.573	7603	5252315
MAG.335	d__Bacteria;p__Proteobacteria;c__Gammaproteobacteria;o__Pseudomonadales;f__HTCC2089;g__UBA4582;s__	87.52	3.873	0.436	8289	4301856
MAG.336	d__Bacteria;p__Proteobacteria;c__Alphaproteobacteria;o__Rickettsiales;f__Rickettsiaceae;g__;s__	98.54	1.675	0.385	17279	1490383
MAG.34	d__Bacteria;p__Bacteroidota;c__Bacteroidia;o__Chitinophagales;f__Saprospiraceae;g__;s__	97.02	1.776	0.341	33872	8155405
MAG.341	d__Bacteria;p__Bacteroidota;c__Bacteroidia;o__Cytophagales;f__Cyclobacteriaceae;g__Reichenbachiella;s__	71.43	1.547	0.4	7153	3450805
MAG.347	d__Bacteria;p__Bdellovibrionota;c__Bdellovibrionia;o__Bdellovibrionales;f__;g__;s__	97.32	2.083	0.413	38531	3380686
MAG.351	d__Bacteria;p__Planctomycetota;c__Planctomycetia;o__Planctomycetales;f__Planctomycetaceae;g__Thalassoglobus;s__	95	1.212	0.503	22263	6434185
MAG.36	d__Bacteria;p__Proteobacteria;c__Alphaproteobacteria;o__Rhodobacterales;f__Rhodobacteraceae;g__Pikeienuella;s__	96.6	1.5	0.611	29928	4922375
MAG.360	d__Bacteria;p__Proteobacteria;c__Alphaproteobacteria;o__Rhodobacterales;f__Rhodobacteraceae;g__;s__	59.05	1.413	0.608	5524	3520603
MAG.363	d__Bacteria;p__Proteobacteria;c__Alphaproteobacteria;o__Rhodobacterales;f__Rhodobacteraceae;g__Ascidiaceihabitans;s__	51.1	1.326	0.551	4558	2242807
MAG.368	d__Bacteria;p__Proteobacteria;c__Alphaproteobacteria;o__Rhodobacterales;f__Rhodobacteraceae;g__;s__	52.57	1.038	0.613	4332	2886732
MAG.37	d__Bacteria;p__Proteobacteria;c__Gammaproteobacteria;o__HK1;f__HK1;g__WLWT01;s__	89.89	9.052	0.595	14965	6870859
MAG.376	d__Bacteria;p__SAR324;c__SAR324;o__SAR324;f__GCA-2753255;g__;s__	81.66	1.26	0.449	12096	8392057
MAG.38	d__Bacteria;p__Proteobacteria;c__Alphaproteobacteria;o__Rhodobacterales;f__Rhodobacteraceae;g__NORP181;s__	89.89	1.917	0.559	24644	3866463
MAG.385	d__Bacteria;p__Proteobacteria;c__Gammaproteobacteria;o__Enterobacterales;f__Alteromonadaceae;g__Algicola;s__	68.37	1.081	0.482	9337	7512438
MAG.386	d__Bacteria;p__Eremiobacterota;c__Xenobia;o__Xenobiales;f__JADMJV01;g__;s__	70.75	2.314	0.562	5918	7413940
MAG.39	d__Bacteria;p__Actinobacteriota;c__Acidimicrobiia;o__Acidimicrobiales;f__SZUA-35;g__CADEDH01;s__	77.14	1.282	0.66	13666	5506059
MAG.4	d__Bacteria;p__Proteobacteria;c__Gammaproteobacteria;o__Pseudomonadales;f__Nitrincolaceae;g__Rs1;s__	56.19	5.172	0.44	4677	3662165
MAG.40	d__Bacteria;p__Patescibacteria;c__Paceibacteria;o__UBA9983_A;f__UBA918;g__OLB19;s__	55.92	0	0.427	22693	589046
MAG.41	d__Bacteria;p__Proteobacteria;c__Alphaproteobacteria;o__Rhodobacterales;f__Rhodobacteraceae;g__Mangrovicoccus;s__	98.38	1.919	0.589	81245	4029020
MAG.42	d__Bacteria;p__Proteobacteria;c__Gammaproteobacteria;o__Pseudomonadales;f__UBA7434;g__UBA7434;s__	97.68	0	0.401	260745	3427796
MAG.43	d__Bacteria;p__Verrucomicrobiota;c__Verrucomicrobiae;o__Opitutales;f__KCTC-12870;g__Cerasicoccus;s__	58.49	0	0.544	4954	2555599
MAG.44	d__Bacteria;p__Proteobacteria;c__Gammaproteobacteria;o__Woeseiales;f__Woeseiaceae;g__UBA1844;s__	77.25	2.67	0.549	7509	3118912
MAG.45	d__Bacteria;p__Proteobacteria;c__Gammaproteobacteria;o__UBA4486;f__UBA4486;g__UBA7359;s__	95.77	3.028	0.397	108592	3384366
MAG.47	d__Bacteria;p__Proteobacteria;c__Gammaproteobacteria;o__Competibacterales;f__;g__;s__	72.98	3.23	0.582	5077	3286940
MAG.48	d__Bacteria;p__Proteobacteria;c__Alphaproteobacteria;o__Rhizobiales;f__JACESI01;g__JACESI01;s__	99.59	0	0.49	112995	3080087
MAG.49	d__Bacteria;p__Bacteroidota;c__Bacteroidia;o__Chitinophagales;f__Saprospiraceae;g__Aureispira;s__	98.51	0.742	0.348	48032	7131235
MAG.5	d__Bacteria;p__Patescibacteria;c__Paceibacteria;o__UBA9983_A;f__UBA918;g__OLB19;s__	69.25	1.88	0.434	9134	797846
MAG.50	d__Bacteria;p__Proteobacteria;c__Alphaproteobacteria;o__Rhodobacterales;f__Rhodobacteraceae;g__Cognatishimia;s__	96.02	0.382	0.565	121862	3346286
MAG.51	d__Bacteria;p__Proteobacteria;c__Alphaproteobacteria;o__Rhizobiales;f__HXMU1428-3;g__HXMU1428-3;s__	88.43	0.071	0.469	19290	2058922
MAG.52	d__Bacteria;p__Proteobacteria;c__Alphaproteobacteria;o__Caulobacterales;f__Hyphomonadaceae;g__UBA5336;s__	51.37	6.896	0.573	11736	2602051
MAG.53	d__Bacteria;p__Proteobacteria;c__Alphaproteobacteria;o__Sneathiellales;f__Sneathiellaceae;g__Sneathiella;s__	83.36	3.537	0.504	40881	4063481
MAG.54	d__Bacteria;p__Planctomycetota;c__Phycisphaerae;o__UBA1845;f__;g__;s__	82.34	0.103	0.61	13654	3829602
MAG.55	d__Bacteria;p__Proteobacteria;c__Gammaproteobacteria;o__Pseudomonadales;f__GM7GCV1;g__GM7GCV1;s__	61.25	0.37	0.472	4915	1529644
MAG.57	d__Bacteria;p__Bacteroidota;c__Bacteroidia;o__Flavobacteriales;f__Flavobacteriaceae;g__Dokdonia;s__	99.61	2.823	0.333	323014	5699336
MAG.58	d__Bacteria;p__Bacteroidota;c__Bacteroidia;o__Chitinophagales;f__Saprospiraceae;g__UBA1994;s__	68.33	1.364	0.355	6260	5968938
MAG.59	d__Bacteria;p__Proteobacteria;c__Alphaproteobacteria;o__Micavibrionales;f__Micavibrionaceae;g__UBA1672;s__	90.76	1.231	0.436	106006	2108142
MAG.6	d__Bacteria;p__Bacteroidota;c__Bacteroidia;o__Cytophagales;f__;g__;s__	56.95	0.364	0.407	15343	2327918
MAG.60	d__Bacteria;p__Bacteroidota;c__Bacteroidia;o__Chitinophagales;f__Saprospiraceae;g__;s__	99	2.227	0.42	47835	9584424
MAG.61	d__Bacteria;p__Proteobacteria;c__Gammaproteobacteria;o__Coxiellales;f__Coxiellaceae;g__CACHNP01;s__	60.61	0.581	0.382	5386	1289074
MAG.62	d__Bacteria;p__Bacteroidota;c__Bacteroidia;o__J057;f__JADKCL01;g__;s__	99.45	3.278	0.47	253295	10960494
MAG.64	d__Bacteria;p__Proteobacteria;c__Alphaproteobacteria;o__Rhizobiales;f__Rhizobiaceae;g__SZUA-100;s__	74.63	1.874	0.471	5695	3164594
MAG.65	d__Bacteria;p__Proteobacteria;c__Gammaproteobacteria;o__Ga0077536;f__Ga0077536;g__UBA11873;s__	88.98	4.366	0.483	9387	4578784
MAG.66	d__Bacteria;p__Proteobacteria;c__Alphaproteobacteria;o__Rhodobacterales;f__Rhodobacteraceae;g__Cognatishimia;s__	82.86	1.863	0.518	8493	2695642

MAG.67	d__Bacteria;p__Planctomycetota;c__Planctomycetia;o__Pirellulales;f__Pirellulaceae;g__;s__	84.27	3.583	0.535	8017	9117239
MAG.68	d__Bacteria;p__Bacteroidota;c__Bacteroidia;o__Chitinophagales;f__Saprospiraceae;g__Lewinella_A;s__	64.78	0	0.499	5162	4268961
MAG.69	d__Bacteria;p__Proteobacteria;c__Alphaproteobacteria;o__Rhodobacterales;f__Rhodobacteraceae;g__Roseovarius;s__Roseovarius aestuarii	75.05	2.999	0.583	6475	3331526
MAG.7	d__Bacteria;p__Proteobacteria;c__Alphaproteobacteria;o__Caulobacterales;f__Maricaulaceae;g__Litorimonas;s__	99.4	0.108	0.557	422854	2951684
MAG.70	d__Bacteria;p__Proteobacteria;c__Gammaproteobacteria;o__Pseudomonadales;f__DSM-21967;g__;s__	83.8	0.431	0.448	34100	2384237
MAG.71	d__Bacteria;p__Planctomycetota;c__Phycisphaerae;o__Phycisphaerales;f__UBA1924;g__;s__	97.72	0	0.662	116501	3607309
MAG.73	d__Bacteria;p__Proteobacteria;c__Alphaproteobacteria;o__Rhodobacterales;f__Rhodobacteraceae;g__Mangrovicoccus;s__	94.48	3.752	0.644	32857	4326134
MAG.75	d__Bacteria;p__Chloroflexota;c__Anaerolineae;o__Promineofilales;f__Promineofilaceae;g__WTJY01;s__	66.07	4.09	0.465	4858	6152347
MAG.76	d__Bacteria;p__Proteobacteria;c__Alphaproteobacteria;o__Minwuiales;f__Minwuiaceae;g__Minwuia;s__	85.04	0.884	0.621	8288	3254837
MAG.77	d__Bacteria;p__Proteobacteria;c__Alphaproteobacteria;o__Kiloniellales;f__Kiloniellaceae;g__Kiloniella;s__	58.95	6.739	0.473	4146	3390810
MAG.78	d__Bacteria;p__Proteobacteria;c__Alphaproteobacteria;o__Rhodobacterales;f__Rhodobacteraceae;g__Pikeienuella;s__	98.8	0	0.579	149221	4045166
MAG.79	d__Bacteria;p__Proteobacteria;c__Alphaproteobacteria;o__Rhodobacterales;f__Rhodobacteraceae;g__Phaeobacter_A;s__	69.5	1.198	0.575	5954	3673762
MAG.8	d__Bacteria;p__Proteobacteria;c__Alphaproteobacteria;o__Caulobacterales;f__Maricaulaceae;g__JACOMS01;s__	61.88	0.865	0.505	5313	2181973
MAG.80	d__Bacteria;p__Proteobacteria;c__Alphaproteobacteria;o__Rhodobacterales;f__Rhodobacteraceae;g__Roseovarius;s__	59.54	1.355	0.595	4714	2665801
MAG.81	d__Bacteria;p__Proteobacteria;c__Alphaproteobacteria;o__Caulobacterales;f__Hyphomonadaceae;g__Hyphomonas;s__	99.35	0.162	0.527	1730696	3225234
MAG.82	d__Bacteria;p__Proteobacteria;c__Alphaproteobacteria;o__Rhodobacterales;f__Rhodobacteraceae;g__Phaeobacter_A;s__	95.93	0.503	0.566	25239	4208693
MAG.83	d__Bacteria;p__Proteobacteria;c__Alphaproteobacteria;o__Rhodobacterales;f__Rhodobacteraceae;g__Sulfitobacter;s__	93.41	1.581	0.562	15519	5306022
MAG.84	d__Bacteria;p__Bacteroidota;c__Bacteroidia;o__Cytophagales;f__Cyclobacteriaceae;g__;s__	63.25	2.013	0.387	5008	2180407
MAG.85	d__Bacteria;p__Proteobacteria;c__Gammaproteobacteria;o__Coxiellales;f__Coxiellaceae;g__;s__	81.1	1.744	0.435	9944	1373449
MAG.86	d__Bacteria;p__Planctomycetota;c__Planctomycetia;o__Pirellulales;f__Pirellulaceae;g__Mariniblastus;s__	59.15	1.78	0.476	5504	5895881
MAG.88	d__Bacteria;p__Proteobacteria;c__Alphaproteobacteria;o__Caulobacterales;f__Hyphomonadaceae;g__;s__	99.35	1.244	0.586	145431	3465726
MAG.89	d__Bacteria;p__Bacteroidota;c__Bacteroidia;o__Cytophagales;f__Cyclobacteriaceae;g__;s__	92.85	3.928	0.401	16709	7156625
MAG.9	d__Bacteria;p__Proteobacteria;c__Alphaproteobacteria;o__Rhodobacterales;f__Rhodobacteraceae;g__Sulfitobacter;s__	55.4	3.448	0.531	5593	2960578
MAG.90	d__Bacteria;p__Proteobacteria;c__Alphaproteobacteria;o__Rhodospirillales;f__Casp-alpha2;g__UBA4479;s__	64.13	4.31	0.509	10432	3543106
MAG.91	d__Bacteria;p__Desulfobacterota_D;c__UBA1144;o__;f__;g__;s__	65.55	1.89	0.38	6682	1374608
MAG.92	d__Bacteria;p__Proteobacteria;c__Alphaproteobacteria;o__Sphingomonadales;f__Sphingomonadaceae;g__Parasphingorhabdus;s__	98.71	1.717	0.513	176312	3466348
MAG.93	d__Bacteria;p__Proteobacteria;c__Alphaproteobacteria;o__Rhodobacterales;f__Rhodobacteraceae;g__Roseicyclus;s__	98.23	1.397	0.606	88480	4298927
MAG.94	d__Bacteria;p__Proteobacteria;c__Gammaproteobacteria;o__Enterobacterales;f__Alteromonadaceae;g__Pseudoalteromonas;s__Pseudoalteromonas arabiensis	96.32	2.94	0.409	65467	4429469
MAG.95	d__Bacteria;p__Planctomycetota;c__Phycisphaerae;o__Phycisphaerales;f__UBA1924;g__REDD01;s__	74.13	6.25	0.654	6569	2664471
MAG.96	d__Bacteria;p__Proteobacteria;c__Gammaproteobacteria;o__Pseudomonadales;f__Porticoccaceae;g__Porticoccus;s__	50.86	0	0.438	6566	1708192
MAG.97	d__Bacteria;p__Proteobacteria;c__Alphaproteobacteria;o__Rhodobacterales;f__Rhodobacteraceae;g__Fluviibacterium;s__	98.16	0.6	0.59	206853	3680815
MAG.99	d__Bacteria;p__Proteobacteria;c__Gammaproteobacteria;o__Enterobacterales;f__Alteromonadaceae;g__Alteromonas;s__Alteromonas naphthalenivorans	73.96	0.982	0.437	11738	3389615

Supplementary Table 12: 281 MAGs Abundance in Reads per Kilobase per Million (RPKM) in metagenomic Ssamples, showing differences in abundance across temporal groups and thermal conditions

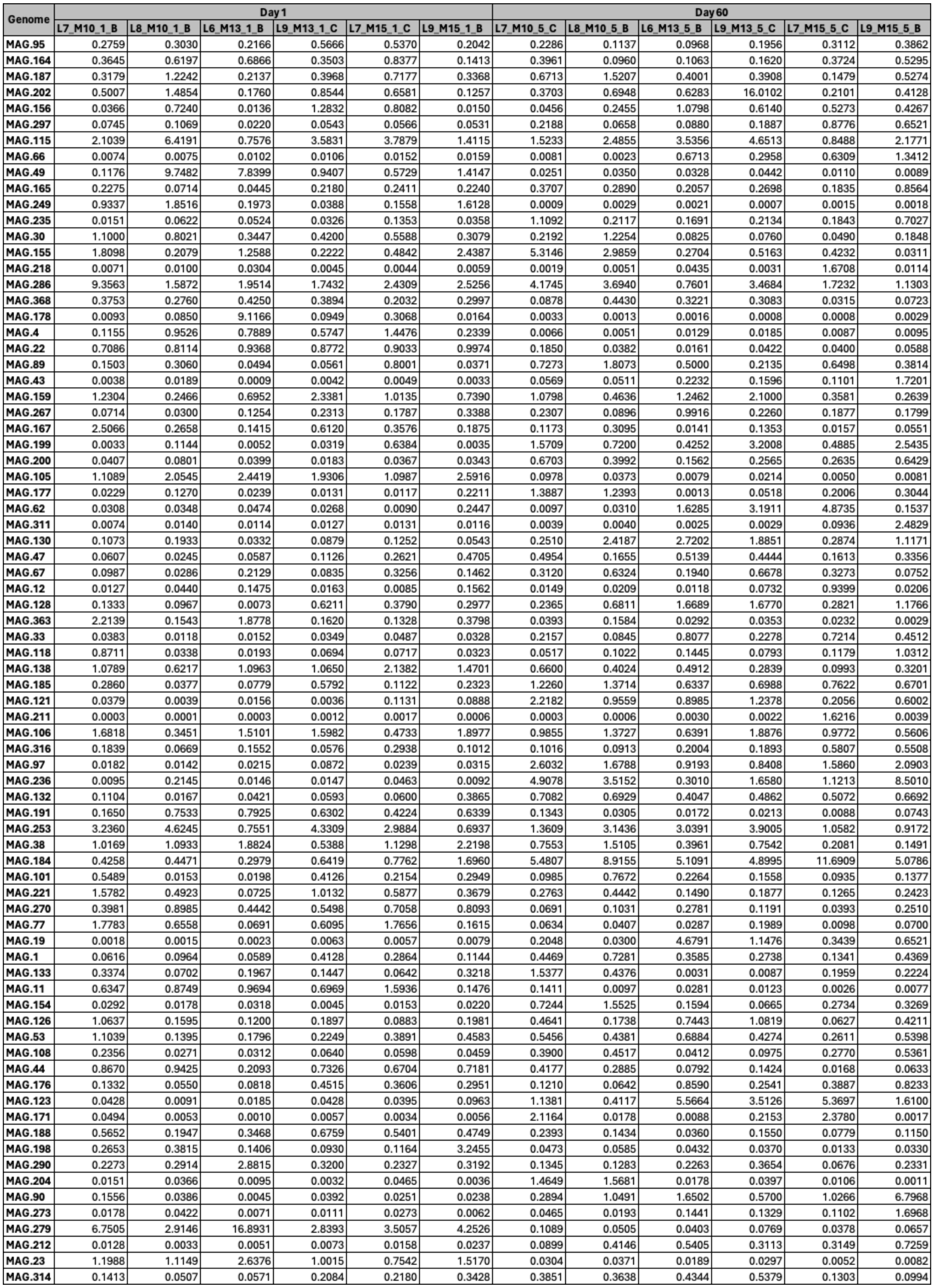

Genome	Day 1						Day 60					
	L7_M10_1_B	L8_M10_1_B	L6_M13_1_B	L9_M13_1_C	L7_M15_1_C	L9_M15_1_B	L7_M10_5_C	L8_M10_5_B	L6_M13_5_B	L9_M13_5_C	L7_M15_5_C	L9_M15_5_B
MAG.95	0.2759	0.3030	0.2166	0.5666	0.5370	0.2042	0.2286	0.1137	0.0968	0.1956	0.3112	0.3862
MAG.164	0.3645	0.6197	0.6866	0.3503	0.8377	0.1413	0.3961	0.0960	0.1063	0.1620	0.3724	0.5295
MAG.187	0.3179	1.2242	0.2137	0.3968	0.7177	0.3368	0.6713	1.5207	0.4001	0.3908	0.1479	0.5274
MAG.202	0.5007	1.4854	0.1760	0.8544	0.6581	0.1257	0.3703	0.6948	0.6283	16.0102	0.2101	0.4128
MAG.156	0.0366	0.7240	0.0136	1.2832	0.8082	0.0150	0.0456	0.2455	1.0798	0.6140	0.5273	0.4267
MAG.297	0.0745	0.1069	0.0220	0.0543	0.0566	0.0531	0.2188	0.0658	0.0880	0.1887	0.8776	0.6521
MAG.115	2.1039	6.4191	0.7576	3.5831	3.7879	1.4115	1.5233	2.4855	3.5356	4.6513	0.8488	2.1771
MAG.66	0.0074	0.0075	0.0102	0.0106	0.0152	0.0159	0.0081	0.0023	0.6713	0.2958	0.6309	1.3412
MAG.49	0.1176	9.7482	7.8399	0.9407	0.5729	1.4147	0.0251	0.0350	0.0328	0.0442	0.0110	0.0089
MAG.165	0.2275	0.0714	0.0445	0.2180	0.2411	0.2240	0.3707	0.2890	0.2057	0.2698	0.1835	0.8564
MAG.249	0.9337	1.8516	0.1973	0.0388	0.1558	1.6128	0.0009	0.0029	0.0021	0.0007	0.0015	0.0018
MAG.235	0.0151	0.0622	0.0524	0.0326	0.1353	0.0358	1.1092	0.2117	0.1691	0.2134	0.1843	0.7027
MAG.30	1.1000	0.8021	0.3447	0.4200	0.5588	0.3079	0.2192	1.2254	0.0825	0.0760	0.0490	0.1848
MAG.155	1.8098	0.2079	1.2588	0.2222	0.4842	2.4387	5.3146	2.9859	0.2704	0.5163	0.4232	0.0311
MAG.218	0.0071	0.0100	0.0304	0.0045	0.0044	0.0059	0.0019	0.0051	0.0435	0.0031	1.6708	0.0114
MAG.286	9.3563	1.5872	1.9514	1.7432	2.4309	2.5256	4.1745	3.6940	0.7601	3.4684	1.7232	1.1303
MAG.368	0.3753	0.2760	0.4250	0.3894	0.2032	0.2997	0.0878	0.4430	0.3221	0.3083	0.0315	0.0723
MAG.178	0.0093	0.0850	9.1166	0.0949	0.3068	0.0164	0.0033	0.0013	0.0016	0.0008	0.0008	0.0029
MAG.4	0.1155	0.9526	0.7889	0.5747	1.4476	0.2339	0.0066	0.0051	0.0129	0.0185	0.0087	0.0095
MAG.22	0.7086	0.8114	0.9368	0.8772	0.9033	0.9974	0.1850	0.0382	0.0161	0.0422	0.0400	0.0588
MAG.89	0.1503	0.3060	0.0494	0.0561	0.8001	0.0371	0.7273	1.8073	0.5000	0.2135	0.6498	0.3814
MAG.43	0.0038	0.0189	0.0009	0.0042	0.0049	0.0033	0.0569	0.0511	0.2232	0.1596	0.1101	1.7201
MAG.159	1.2304	0.2466	0.6952	2.3381	1.0135	0.7390	1.0798	0.4636	1.2462	2.1000	0.3581	0.2639
MAG.267	0.0714	0.0300	0.1254	0.2313	0.1787	0.3388	0.2307	0.0896	0.9916	0.2260	0.1877	0.1799
MAG.167	2.5066	0.2658	0.1415	0.6120	0.3576	0.1875	0.1173	0.3095	0.0141	0.1353	0.0157	0.0551
MAG.199	0.0033	0.1144	0.0052	0.0319	0.6384	0.0035	1.5709	0.7200	0.4252	3.2008	0.4885	2.5435
MAG.200	0.0407	0.0801	0.0399	0.0183	0.0367	0.0343	0.6703	0.3992	0.1562	0.2565	0.2635	0.6429
MAG.105	1.1089	2.0545	2.4419	1.9306	1.0987	2.5916	0.0978	0.0373	0.0079	0.0214	0.0050	0.0081
MAG.177	0.0229	0.1270	0.0239	0.0131	0.0117	0.2211	1.3887	1.2393	0.0013	0.0518	0.2006	0.3044
MAG.62	0.0308	0.0348	0.0474	0.0268	0.0090	0.2447	0.0097	0.0310	1.6285	3.1911	4.8735	0.1537
MAG.311	0.0074	0.0140	0.0114	0.0127	0.0131	0.0116	0.0039	0.0040	0.0025	0.0029	0.0936	2.4829
MAG.130	0.1073	0.1933	0.0332	0.0879	0.1252	0.0543	0.2510	2.4187	2.7202	1.8851	0.2874	1.1171
MAG.47	0.0607	0.0245	0.0587	0.1126	0.2621	0.4705	0.4954	0.1655	0.5139	0.4444	0.1613	0.3356
MAG.67	0.0987	0.0286	0.2129	0.0835	0.3256	0.1462	0.3120	0.6324	0.1940	0.6678	0.3273	0.0752
MAG.12	0.0127	0.0440	0.1475	0.0163	0.0085	0.1562	0.0149	0.0209	0.0118	0.0732	0.9399	0.0206
MAG.128	0.1333	0.0967	0.0073	0.6211	0.3790	0.2977	0.2365	0.6811	1.6689	1.6770	0.2821	1.1766
MAG.363	2.2139	0.1543	1.8778	0.1620	0.1328	0.3798	0.0393	0.1584	0.0292	0.0353	0.0232	0.0029
MAG.33	0.0383	0.0118	0.0152	0.0349	0.0487	0.0328	0.2157	0.0845	0.8077	0.2278	0.7214	0.4512
MAG.118	0.8711	0.0338	0.0193	0.0694	0.0717	0.0323	0.0517	0.1022	0.1445	0.0793	0.1179	1.0312
MAG.138	1.0789	0.6217	1.0963	1.0650	2.1382	1.4701	0.6600	0.4024	0.4912	0.2839	0.0993	0.3201
MAG.185	0.2860	0.0377	0.0779	0.5792	0.1122	0.2323	1.2260	1.3714	0.6337	0.6988	0.7622	0.6701
MAG.121	0.0379	0.0039	0.0156	0.0036	0.1131	0.0888	2.2182	0.9559	0.8985	1.2378	0.2056	0.6002
MAG.211	0.0003	0.0001	0.0003	0.0012	0.0017	0.0006	0.0003	0.0006	0.0030	0.0022	1.6216	0.0039
MAG.106	1.6818	0.3451	1.5101	1.5982	0.4733	1.8977	0.9855	1.3727	0.6391	1.8876	0.9772	0.5606
MAG.316	0.1839	0.0669	0.1552	0.0576	0.2938	0.1012	0.1016	0.0913	0.2004	0.1893	0.5807	0.5508
MAG.97	0.0182	0.0142	0.0215	0.0872	0.0239	0.0315	2.6032	1.6788	0.9193	0.8408	1.5860	2.0903
MAG.236	0.0095	0.2145	0.0146	0.0147	0.0463	0.0092	4.9078	3.5152	0.3010	1.6580	1.1213	8.5010
MAG.132	0.1104	0.0167	0.0421	0.0593	0.0600	0.3865	0.7082	0.6929	0.4047	0.4862	0.5072	0.6692
MAG.191	0.1650	0.7533	0.7925	0.6302	0.4224	0.6339	0.1343	0.0305	0.0172	0.0213	0.0088	0.0743
MAG.253	3.2360	4.6245	0.7551	4.3309	2.9884	0.6937	1.3609	3.1436	3.0391	3.9005	1.0582	0.9172
MAG.38	1.0169	1.0933	1.8824	0.5388	1.1298	2.2198	0.7553	1.5105	0.3961	0.7542	0.2081	0.1491
MAG.184	0.4258	0.4471	0.2979	0.6419	0.7762	1.6960	5.4807	8.9155	5.1091	4.8995	11.6909	5.0786
MAG.101	0.5489	0.0153	0.0198	0.4126	0.2154	0.2949	0.0985	0.7672	0.2264	0.1558	0.0935	0.1377
MAG.221	1.5782	0.4923	0.0725	1.0132	0.5877	0.3679	0.2763	0.4442	0.1490	0.1877	0.1265	0.2423
MAG.270	0.3981	0.8985	0.4442	0.5498	0.7058	0.8093	0.0691	0.1031	0.2781	0.1191	0.0393	0.2510
MAG.77	1.7783	0.6558	0.0691	0.6095	1.7656	0.1615	0.0634	0.0407	0.0287	0.1989	0.0098	0.0700
MAG.19	0.0018	0.0015	0.0023	0.0063	0.0057	0.0079	0.2048	0.0300	4.6791	1.1476	0.3439	0.6521
MAG.1	0.0616	0.0964	0.0589	0.4128	0.2864	0.1144	0.4469	0.7281	0.3585	0.2738	0.1341	0.4369
MAG.133	0.3374	0.0702	0.1967	0.1447	0.0642	0.3218	1.5377	0.4376	0.0031	0.0087	0.1959	0.2224
MAG.11	0.6347	0.8749	0.9694	0.6969	1.5936	0.1476	0.1411	0.0097	0.0281	0.0123	0.0026	0.0077
MAG.154	0.0292	0.0178	0.0318	0.0045	0.0153	0.0220	0.7244	1.5525	0.1594	0.0665	0.2734	0.3269
MAG.126	1.0637	0.1595	0.1200	0.1897	0.0883	0.1981	0.4641	0.1738	0.7443	1.0819	0.0627	0.4211
MAG.53	1.1039	0.1395	0.1796	0.2249	0.3891	0.4583	0.5456	0.4381	0.6884	0.4274	0.2611	0.5398
MAG.108	0.2356	0.0271	0.0312	0.0640	0.0598	0.0459	0.3900	0.4517	0.0412	0.0975	0.2770	0.5361
MAG.44	0.8670	0.9425	0.2093	0.7326	0.6704	0.7181	0.4177	0.2885	0.0792	0.1424	0.0168	0.0633
MAG.176	0.1332	0.0550	0.0818	0.4515	0.3606	0.2951	0.1210	0.0642	0.8590	0.2541	0.3887	0.8233
MAG.123	0.0428	0.0091	0.0185	0.0428	0.0395	0.0963	1.1381	0.4117	5.5664	3.5126	5.3697	1.6100
MAG.171	0.0494	0.0053	0.0010	0.0057	0.0034	0.0056	2.1164	0.0178	0.0088	0.2153	2.3780	0.0017
MAG.188	0.5652	0.1947	0.3468	0.6759	0.5401	0.4749	0.2393	0.1434	0.0360	0.1550	0.0779	0.1150
MAG.198	0.2653	0.3815	0.1406	0.0930	0.1164	3.2455	0.0473	0.0585	0.0432	0.0370	0.0133	0.0330
MAG.290	0.2273	0.2914	2.8815	0.3200	0.2327	0.3192	0.1345	0.1283	0.2263	0.3654	0.0676	0.2331
MAG.204	0.0151	0.0366	0.0095	0.0032	0.0465	0.0036	1.4649	1.5681	0.0178	0.0397	0.0106	0.0011
MAG.90	0.1556	0.0386	0.0045	0.0392	0.0251	0.0238	0.2894	1.0491	1.6502	0.5700	1.0266	6.7968
MAG.273	0.0178	0.0422	0.0071	0.0111	0.0273	0.0062	0.0465	0.0193	0.1441	0.1329	0.1102	1.6968
MAG.279	6.7505	2.9146	16.8931	2.8393	3.5057	4.2526	0.1089	0.0505	0.0403	0.0769	0.0378	0.0657
MAG.212	0.0128	0.0033	0.0051	0.0073	0.0158	0.0237	0.0899	0.4146	0.5405	0.3113	0.3149	0.7259
MAG.23	1.1988	1.1149	2.6376	1.0015	0.7542	1.5170	0.0304	0.0371	0.0189	0.0297	0.0052	0.0082
MAG.314	0.1413	0.0507	0.0571	0.2084	0.2180	0.3428	0.3851	0.3638	0.4344	0.5379	0.1303	0.0994

MAG.233	0.0072	0.0211	0.0083	0.0031	0.0696	0.0062	2.4297	0.2846	0.1122	0.1953	0.0463	0.0023
MAG.179	0.4777	0.4260	0.4362	0.9008	0.6253	0.6705	1.0149	0.5703	0.4294	1.0260	1.4003	3.6452
MAG.65	0.1081	0.0151	0.0389	0.0174	0.0249	0.0521	0.5798	0.2154	0.1659	0.5751	0.6619	0.1965
MAG.347	2.1430	2.5224	0.3201	1.4855	1.0088	0.4483	1.2668	1.1222	1.4446	2.0619	1.3367	2.7554
MAG.260	0.0053	0.1055	0.0023	0.0050	0.1537	0.0014	1.8070	0.0916	0.0042	0.0033	0.3306	0.0031
MAG.103	0.3934	0.1121	0.1489	1.3567	0.5789	0.3278	0.7061	0.2809	0.1210	1.0230	0.2096	0.7656
MAG.16	0.3724	0.2502	0.4877	0.6741	0.4085	1.0723	0.5747	0.2346	0.2330	0.4509	0.1749	0.1009
MAG.220	0.0074	0.0144	0.0014	0.0057	0.0048	0.0025	0.0535	0.0286	0.1042	0.0200	0.1774	2.0683
MAG.134	1.6643	5.4716	0.5998	2.5686	2.3921	0.7715	1.5929	2.4806	2.4380	3.4689	0.7379	2.8563
MAG.57	9.5960	5.4908	5.4892	1.4260	3.9502	3.5744	2.1646	0.8298	1.0821	0.4555	2.3715	1.0546
MAG.219	1.1940	0.7602	1.0485	0.9040	0.5027	2.6721	0.2001	0.4037	0.1624	0.1792	0.0359	0.0285
MAG.143	0.8534	0.8674	2.1275	0.9191	1.3554	2.3650	2.4843	1.5370	1.1306	1.3055	0.6205	1.7756
MAG.240	0.7164	0.6038	0.8558	0.1707	0.2332	0.5604	0.1378	0.0913	0.0419	0.0740	0.0264	0.0705
MAG.112	0.2731	0.2417	0.3147	0.4156	0.7765	0.5270	0.8928	0.7449	1.1020	0.7303	0.5301	0.2577
MAG.120	0.3793	0.8879	0.9317	2.7045	3.9899	1.0962	0.0223	0.0055	0.0247	0.0219	0.0040	0.0140
MAG.31	0.1688	0.0956	0.1898	0.2030	0.5462	1.5064	4.5583	3.6155	50.6505	11.0516	33.4694	28.4760
MAG.243	0.0241	0.0089	0.0115	0.0066	0.0157	0.0582	1.0546	0.2136	0.1157	0.1034	0.5133	0.0919
MAG.248	0.8491	0.1478	0.0289	0.0695	0.0530	0.0648	0.3653	0.6638	0.3654	0.2540	0.1218	0.1322
MAG.264	0.7027	1.4660	2.4107	2.4495	2.7030	0.9051	0.2171	0.1687	0.0193	0.0668	0.0384	0.0559
MAG.186	0.0891	0.0121	0.1196	0.7613	0.0581	3.1325	2.0520	0.8459	0.3445	1.5698	1.1023	2.8082
MAG.225	2.3562	0.2570	0.4757	0.5377	0.9060	1.7105	0.4039	0.5278	0.6324	0.7652	0.4070	0.7556
MAG.376	0.0391	0.1989	0.0131	6.1337	0.0647	0.0203	0.0287	0.0480	0.0497	0.0826	0.0145	0.0279
MAG.151	0.0575	0.1624	0.1555	0.0617	0.0768	0.1317	0.8750	0.2226	0.1161	0.1176	0.4570	0.2680
MAG.213	0.7045	0.7137	0.4171	0.6756	0.7926	1.8272	0.3829	0.8327	0.0539	0.0499	0.0394	0.0924
MAG.114	0.4660	0.8892	0.2724	0.5019	0.6418	0.1559	0.7207	1.0739	0.5632	0.7102	0.2464	0.8089
MAG.173	0.3186	0.4918	0.9599	0.2486	0.4400	0.7681	0.0164	0.0080	0.0082	0.0053	0.0048	0.0135
MAG.226	0.1073	0.1618	0.0283	0.0182	0.1280	0.2702	0.1294	0.0239	0.6758	0.0186	1.1429	1.6556
MAG.20	1.6449	0.1802	0.0220	0.4886	0.3085	0.1148	0.0638	0.5806	0.4683	0.6194	0.0394	0.8515
MAG.224	0.1241	0.0694	0.2318	0.2306	0.1660	0.2512	0.3970	0.2418	1.0856	0.6880	0.6126	0.1320
MAG.251	0.7551	0.1574	0.4693	0.0992	0.1841	0.5003	1.3205	1.4837	0.1722	0.7817	0.4123	0.6000
MAG.157	12.7741	2.2772	15.0737	11.2470	5.3369	10.6549	0.9235	0.7266	0.5404	0.5885	0.2902	1.1653
MAG.129	3.1053	3.7180	2.5499	0.2678	1.2307	1.5510	0.3460	0.1869	0.1072	0.1477	0.0264	0.0650
MAG.229	0.0020	0.0008	0.0006	0.0026	0.0011	0.0010	0.0332	0.0006	0.0013	0.0109	1.9078	0.2151
MAG.96	0.0268	0.0213	0.0045	0.0114	0.0262	0.0110	1.3993	3.6728	1.5913	0.9917	0.6284	0.4808
MAG.58	0.4313	0.1149	0.1173	0.0528	0.1027	0.0289	0.0825	0.1624	0.3074	0.1106	0.0911	1.4497
MAG.153	0.9847	0.5082	1.3462	1.0221	1.6784	2.9060	0.1398	0.0514	0.1164	0.1524	0.1052	0.1191
MAG.189	0.0020	0.0006	0.0004	3.3032	0.0028	0.0013	0.0008	0.0006	0.0012	0.0103	0.0005	0.0052
MAG.201	0.4098	0.5120	1.0507	0.3516	0.3824	2.4508	0.4139	0.0781	0.0267	0.0532	0.3009	0.4829
MAG.195	0.6881	0.0504	0.0823	0.2599	0.1978	0.2559	0.4224	0.0930	0.1663	0.5216	0.5021	0.2932
MAG.137	0.0242	0.0038	0.0212	0.0028	0.0045	0.0030	0.0822	25.6958	0.0276	0.0037	0.0117	0.0244
MAG.239	0.0196	0.0535	0.0084	0.0058	0.0283	0.0212	0.6872	0.5046	0.7649	0.5462	0.4232	0.3304
MAG.158	0.0297	0.0806	0.0126	0.1094	0.0454	0.0644	1.6714	0.0967	0.5923	0.6548	0.3480	0.7934
MAG.272	1.6299	4.2910	2.1373	6.6836	4.7157	3.0837	3.4392	3.2549	3.5472	4.9736	0.6943	1.7059
MAG.116	0.7167	0.3992	1.5050	0.7617	0.4136	0.6400	0.6876	2.3913	0.4202	0.2031	0.2125	0.1555
MAG.29	2.4756	2.9495	4.6351	3.8986	3.5231	3.8628	0.0676	0.1028	0.0045	0.0433	0.0047	0.5349
MAG.81	2.3270	0.8010	2.0676	1.3420	1.9648	2.6317	0.5658	0.1879	0.1585	0.2620	0.0778	0.7412
MAG.139	0.2150	0.1614	0.2183	0.1927	0.4107	0.5135	1.1086	0.4592	3.2409	1.4648	5.3357	1.1343
MAG.181	0.2562	0.3878	0.4776	1.0014	0.7568	0.5593	0.1073	0.0590	0.2918	0.1142	0.0845	0.1185
MAG.215	0.1454	0.1598	0.1106	0.4346	0.2286	0.4118	0.3912	0.1010	0.1476	0.2376	0.2622	0.4668
MAG.92	1.8229	0.8173	3.6339	0.9578	1.3434	1.6252	0.3096	0.0864	0.2550	0.2232	0.0906	0.4714
MAG.27	0.2805	1.3221	1.5016	1.5770	1.7768	0.3178	0.1428	0.0212	0.0758	0.0358	0.0416	0.0592
MAG.119	0.3865	0.0849	0.3346	0.1593	0.1987	0.1375	0.1665	0.0594	0.2577	0.3136	0.2481	0.4208
MAG.308	1.7268	1.8436	2.7125	4.9610	2.0108	3.5466	0.7097	0.1409	0.2493	0.5677	0.1362	1.0422
MAG.217	0.2270	0.1422	0.2538	0.5425	0.2738	0.3541	0.1185	0.0473	0.4327	0.2586	0.2288	0.7136
MAG.336	0.2900	0.0321	0.7722	0.1971	0.3566	0.3708	1.4914	0.3738	0.0078	0.7607	0.0571	0.0062
MAG.3	0.7592	0.3446	0.0163	1.1059	0.3478	0.2209	0.2513	0.5445	0.1961	0.1426	0.0971	0.3413
MAG.223	0.1370	0.0742	0.1832	0.0759	0.1788	0.2852	0.7905	0.4437	0.4139	0.6269	0.6505	0.0470
MAG.84	0.1435	0.2126	0.0248	0.1216	0.1660	0.0541	0.3166	0.3168	0.5666	0.1866	0.6414	0.1229
MAG.39	0.2362	0.3740	0.3126	0.2996	0.3188	0.6454	2.2682	0.5076	2.1275	1.1648	4.3162	0.2079
MAG.183	0.6837	0.0384	0.5773	0.3075	0.5331	0.2627	0.8975	0.1650	0.0777	0.2234	0.1991	0.2995
MAG.335	1.0347	1.7371	0.1373	0.1463	0.4271	0.2124	0.1990	0.5320	0.1711	0.1812	0.0617	0.2005
MAG.117	0.6832	0.1359	0.8566	0.2572	0.5331	0.8176	0.0304	0.0087	0.0122	0.0278	0.0155	0.0367
MAG.113	0.0778	0.1066	0.1259	0.8476	1.3781	0.2364	0.2233	0.0087	0.1911	0.2046	0.1183	0.0624
MAG.310	0.7080	0.2258	0.4177	0.5469	1.1927	1.5652	0.0976	0.0412	0.0113	0.0430	0.0167	0.0251
MAG.269	0.4544	3.9966	2.6772	3.5177	4.0975	0.1692	0.0205	0.0053	0.0063	0.0531	0.0052	0.3345
MAG.205	5.4251	9.6474	12.0381	5.8905	9.5501	16.1948	0.5963	1.7191	0.3101	0.6522	0.0719	0.1396
MAG.275	0.1617	1.3139	0.0223	0.0530	0.2572	0.2225	0.1461	0.2362	0.4525	0.0941	1.8709	0.0357
MAG.91	0.0324	0.0268	0.0111	0.0307	0.0262	0.0382	0.5573	0.2466	1.2475	0.8896	1.5384	0.3564
MAG.196	0.3173	0.4076	0.2481	0.9320	0.7364	0.5585	0.1596	0.0741	0.0544	0.2089	0.0701	0.2100
MAG.147	1.4459	0.9635	0.1601	2.4129	0.5959	0.1804	0.2682	0.3830	0.2950	0.4901	0.0934	0.1693
MAG.107	0.0847	0.0751	0.3978	0.3161	0.2793	0.2503	0.4337	0.2237	0.3515	0.7503	0.3044	0.2423
MAG.247	0.3448	0.6144	0.1501	0.9100	0.6370	0.1447	0.3786	0.9013	0.3453	0.3927	0.1087	0.2708
MAG.203	0.1442	0.4402	0.1632	0.2988	0.3707	0.2988	0.5620	0.4317	0.4586	0.3223	0.5173	0.7750
MAG.266	0.0273	0.0329	0.0475	0.0380	0.0411	0.2596	0.3462	0.0750	0.3636	0.2849	0.6191	0.0140
MAG.78	0.2349	0.1817	0.3233	0.0883	0.0781	0.3593	3.2880	0.9229	0.9772	0.1723	3.0530	3.0327
MAG.54	0.2335	0.0467	0.1639	0.3588	0.3437	0.2226	0.7441	0.5183	0.1794	0.3472	0.1959	0.3120
MAG.59	0.3099	0.3930	0.4355	0.6006	0.4908	1.3445	0.3696	0.1858	0.6492	0.0982	0.2275	0.1549
MAG.169	1.0230	0.2269	0.4025	0.3249	0.5980	0.4735	0.5507	0.2560	0.0536	0.2076	0.1629	0.1167
MAG.268	0.8817	0.3833	0.8420	1.2683	0.6403	1.1882	0.5167	0.4908	0.3243	0.3787	0.4314	0.6414
MAG.150	0.0643	0.1939	0.0050	0.0155	0.1221	0.0173	0.0726	1.6767	0.1350	0.1351	0.0758	0.4851

MAG.102	0.7811	0.1649	0.0255	0.3491	0.2870	0.0963	0.1571	0.6451	0.1525	0.2610	0.0457	0.2573
MAG.244	0.2335	0.2968	0.3329	0.0557	0.0673	0.1506	0.1368	0.3254	0.0121	0.0714	0.3335	0.0767
MAG.193	0.0192	0.0068	0.0037	0.0235	0.0071	0.0164	4.3547	27.8465	0.8521	1.0819	1.5862	3.0089
MAG.13	0.5629	1.8731	0.2674	0.6542	0.7778	0.2346	3.1924	0.6967	0.8010	1.0689	0.2197	0.4667
MAG.93	0.7596	1.0486	1.9487	0.8475	0.9687	1.1052	1.0486	0.5461	0.0319	0.0127	0.0557	0.0573
MAG.280	0.1070	0.0496	0.0476	0.1793	0.0613	0.0402	0.7050	1.5050	0.9910	0.5183	0.3450	0.6977
MAG.40	0.5347	0.4137	0.5643	0.6141	0.6766	1.4152	0.0315	0.0149	0.0084	0.0093	0.0044	0.0101
MAG.122	2.6019	10.0488	0.4679	2.8635	4.1481	1.1423	0.0074	0.0234	0.0072	0.0085	0.0060	0.0086
MAG.274	0.1779	0.0406	0.0861	0.2520	0.2016	0.3656	0.5612	0.2381	1.0684	0.6837	0.6068	0.3998
MAG.68	0.1089	0.0038	0.2392	0.7186	0.0361	0.0233	0.0680	0.2523	0.0543	0.0361	0.1495	0.6499
MAG.256	9.2436	2.9033	1.5085	0.5352	0.8110	3.0163	4.9241	14.4734	0.4315	0.1963	1.6206	2.0032
MAG.259	0.0627	0.0135	0.0289	0.0780	0.0646	0.1278	1.1132	0.5146	5.6021	3.1161	9.4022	2.0911
MAG.48	0.0137	0.0171	0.0224	0.0026	0.1839	0.0039	5.9479	0.2108	0.4821	0.2580	0.8178	0.8308
MAG.36	0.9005	0.9944	1.0469	0.4986	1.0523	2.2659	0.5723	0.4417	0.0664	0.1486	0.3873	0.8644
MAG.32	1.2509	6.7961	1.2564	1.3960	1.8017	0.9159	1.9298	4.3718	1.3887	2.5949	0.4236	0.5393
MAG.385	0.0207	0.0035	0.0013	4.0935	0.0031	0.0010	0.0090	0.0023	0.0012	0.0052	0.0013	0.0014
MAG.34	4.0295	8.1218	1.3920	1.9217	3.6600	2.6565	0.6703	1.2441	1.1170	1.4478	0.3431	0.5280
MAG.255	0.0277	0.0111	0.0577	0.0115	0.0167	0.2047	0.3622	0.1014	0.2153	0.1657	0.6421	0.1309
MAG.41	0.7441	0.4934	0.2150	0.7962	1.2400	0.9725	4.9759	7.3209	15.7434	5.7157	0.7366	6.0066
MAG.50	0.2807	0.7327	1.1386	3.3455	0.7082	0.2601	0.0319	0.0054	0.0223	0.0464	0.0118	0.0287
MAG.145	0.0021	0.0019	0.0017	0.0044	0.0042	0.0062	1.2520	0.5186	0.9994	0.2758	0.0440	0.1376
MAG.25	0.1454	0.1390	0.6521	0.4275	0.4578	0.4257	0.5144	0.2516	0.3438	0.8434	0.5995	0.7607
MAG.80	0.0954	0.0345	0.0176	0.0252	0.0431	0.0557	0.3550	0.2626	0.1389	0.0907	0.6383	0.1183
MAG.76	7.8391	2.5481	0.4940	1.7731	3.5576	1.6262	1.2356	4.0304	0.5110	1.4100	0.8579	4.5997
MAG.194	7.0868	1.0072	2.6869	1.4317	4.6808	6.6739	0.0642	0.0903	0.0655	0.1134	0.0094	0.1571
MAG.9	0.2851	0.3852	0.9620	0.3792	0.5179	0.2616	0.0271	0.0143	0.0009	0.0015	0.0007	0.0015
MAG.190	0.2217	0.0723	0.1444	0.1668	0.2417	0.1554	0.2751	0.1383	0.5779	0.8535	0.6949	1.5773
MAG.125	1.6402	0.0765	0.5596	0.2677	0.4150	0.9121	4.2849	2.2155	0.4523	1.3280	1.4059	2.1591
MAG.148	0.0764	0.1203	0.2374	0.0549	0.0453	0.0884	0.0928	0.0580	0.1772	0.1571	0.5346	1.5365
MAG.141	1.4312	0.6290	0.5597	0.8363	1.1623	1.7077	0.5313	0.6893	0.3042	0.2364	0.0511	0.1428
MAG.321	0.0009	0.0012	0.0006	5.0950	0.0018	0.0010	0.0015	0.0007	0.0009	0.1310	0.0010	1.0281
MAG.360	0.2385	0.0509	0.2365	0.1903	0.2129	0.4569	1.3319	0.2475	2.1455	0.3662	0.3016	0.2286
MAG.180	0.4342	0.4820	0.4998	0.2437	0.2869	2.0269	0.2056	0.0724	0.0617	0.2691	0.0818	1.0966
MAG.82	0.1431	0.9328	3.2568	0.7565	1.2858	0.9383	0.2027	0.4039	0.0498	0.0472	0.0095	0.0099
MAG.42	17.0415	4.5653	2.7727	5.2276	7.6154	4.3274	2.2234	3.8305	1.2557	2.2146	1.7072	2.6429
MAG.73	0.2513	0.2417	0.1275	0.3796	0.6923	1.1737	5.6304	3.0248	10.4683	5.8822	6.0576	7.2229
MAG.170	0.0095	0.0346	0.0015	0.0032	0.0114	0.0064	0.0101	0.0053	0.2125	0.0033	0.9484	0.0034
MAG.14	1.1679	3.2322	12.0617	3.5464	2.2223	2.0257	0.1062	0.1558	0.1192	0.2439	0.1528	0.0934
MAG.104	0.2740	0.0527	0.7668	0.4976	0.6259	0.6853	5.3558	1.3990	0.5384	1.4232	0.8173	0.2607
MAG.17	0.8738	0.7441	1.2524	0.8394	0.5747	1.0346	0.6702	0.6598	0.1653	0.3978	0.1118	0.5247
MAG.83	1.5467	1.7007	0.9170	1.1769	1.1454	0.7360	1.8945	1.5656	0.5640	1.1023	0.2828	0.4672
MAG.69	0.2468	0.1741	0.0717	0.2357	0.4874	0.2418	1.2776	0.9364	0.2354	0.3013	0.5448	0.4757
MAG.55	0.8388	0.6235	0.2288	0.4251	0.2796	0.3043	0.1404	0.2178	0.1270	0.0757	0.0158	0.0141
MAG.263	0.0029	0.0155	0.0010	0.0012	0.0030	0.0058	0.0170	0.0127	0.0549	0.0439	4.4314	0.0049
MAG.28	1.4345	0.3279	0.6349	0.1955	0.3184	0.6179	0.1202	0.1056	0.0162	0.0821	0.0635	0.1583
MAG.245	1.1423	36.2520	0.5740	1.4192	1.4489	0.4498	0.8653	10.9043	1.5492	2.1136	0.4984	0.9753
MAG.88	0.0039	0.0018	0.0011	0.0025	0.0067	0.0010	5.1342	0.0224	0.5357	0.5155	0.2562	0.0100
MAG.135	0.2991	0.2544	0.4788	0.1935	0.5950	0.7954	0.2582	0.1328	0.1591	0.2318	0.2347	0.0260
MAG.228	0.2958	0.2217	0.5792	0.0590	0.1478	0.2030	1.9312	1.3347	0.0731	0.0741	0.1374	0.0896
MAG.37	2.8355	0.3167	0.8407	0.8060	1.2828	0.9389	1.3886	2.8162	0.7755	2.4467	0.4896	0.4061
MAG.242	0.0358	0.0064	0.0216	0.0504	0.0313	0.0232	0.2609	0.2055	0.1452	0.3497	0.2630	0.8925
MAG.75	0.0335	0.0188	0.0080	0.0080	0.0091	0.0041	0.0147	0.0141	0.0073	0.0249	0.9583	0.2651
MAG.341	0.3294	1.2474	0.1695	0.2720	0.4058	0.1483	0.3050	1.0698	2.2190	0.8594	0.5079	0.5146
MAG.111	0.3780	0.6079	0.3342	0.2754	0.2192	0.2454	0.2722	0.3952	0.1174	0.1559	0.0619	0.2240
MAG.283	0.1583	0.0766	0.0972	0.3032	0.1488	0.1912	0.2928	0.2249	0.2137	0.2656	0.3372	0.3480
MAG.161	1.1504	7.1628	3.9272	2.5360	29.5361	1.6199	0.0600	0.0419	0.0479	0.0798	0.0116	0.0420
MAG.160	3.3218	0.4604	0.3221	2.2673	1.8344	0.4863	0.5611	0.1977	0.0151	0.0433	0.0227	0.1152
MAG.162	3.4594	7.9407	10.1431	3.1461	4.5292	4.0026	0.9479	0.9790	2.3799	2.7195	0.3773	1.4054
MAG.277	1.3562	0.3552	0.6721	1.3703	0.6453	0.8456	0.3415	0.0659	0.4445	0.3387	0.3134	0.4545
MAG.127	0.2376	0.1456	0.1426	0.5836	0.3756	0.1227	2.0230	0.3880	0.8677	1.2194	0.7348	0.1994
MAG.278	0.0703	0.0044	0.0047	0.0366	0.0613	0.0405	0.5646	0.1790	0.2494	0.2287	0.4888	0.6845
MAG.18	0.0062	0.0051	0.0033	0.0066	0.0066	0.0024	2.0063	10.6376	0.2083	0.0812	0.0257	0.0528
MAG.231	0.0853	0.1202	0.6883	0.1592	4.1841	0.1059	0.0043	0.0891	0.0042	0.0046	0.0795	0.0102
MAG.8	0.3545	0.2986	0.8594	0.3041	0.1134	0.3148	0.0142	0.0020	0.0102	0.0541	0.0304	0.0140
MAG.174	6.6163	12.8420	2.7643	11.4886	9.8146	3.1995	9.3045	9.6271	13.1610	13.8437	3.5450	7.5286
MAG.232	0.0004	0.0006	0.0006	0.0012	0.0014	0.0008	0.4468	0.0622	0.3331	0.5777	1.0951	0.7531
MAG.175	0.5513	2.1566	0.7165	0.3955	0.7216	2.3003	4.8303	1.6189	2.8931	2.2513	6.3544	0.2262
MAG.207	0.9812	0.4962	0.1507	0.4514	0.4740	0.2926	0.9556	2.3850	0.7752	2.9997	1.8435	1.3520
MAG.86	0.4041	0.5508	0.3380	0.4207	0.6524	0.5266	0.2653	0.3274	0.5017	0.6785	0.2857	0.1559
MAG.293	0.2923	0.1431	0.0853	0.6117	0.5099	0.2934	0.3833	0.4161	0.4529	0.3450	0.0825	0.2031
MAG.61	0.5803	0.1394	0.8485	0.3695	0.1034	0.2949	0.0171	0.0212	0.0013	0.0080	0.0023	0.0064
MAG.144	3.6804	1.0084	2.2047	1.6849	2.5777	3.1218	4.4261	2.9813	3.0780	1.7179	2.5362	1.5019
MAG.52	0.3078	0.2233	0.4642	0.4520	0.6288	0.7125	0.5457	0.3039	0.2575	0.2447	0.1415	0.4396
MAG.252	0.6179	1.0670	0.1644	0.7296	0.5913	1.4762	0.1250	0.4666	0.1521	0.1610	0.0598	0.0613
MAG.15	0.2399	0.1143	0.2284	0.4892	0.5095	0.2629	1.5221	0.6978	0.8010	1.3123	0.9680	0.6316
MAG.70	0.0049	0.0172	0.0253	0.0138	0.0177	0.0183	0.0038	0.0719	5.6197	0.5826	1.3919	7.3898
MAG.271	4.2951	0.4127	0.8639	1.0246	0.5725	0.4608	0.3757	0.2570	0.0184	0.1056	0.0471	0.0178
MAG.45	0.0767	0.0481	0.0396	0.0423	0.0500	0.0288	1.6473	7.8898	7.4118	5.2018	15.5082	25.2971
MAG.254	1.0172	0.1970	1.6357	2.4373	2.9943	1.5061	0.0161	0.0668	0.0064	0.1060	0.0081	0.2124
MAG.276	1.0229	0.6403	0.7356	0.6381	0.5508	3.1075	1.0356	0.5235	0.5260	0.5493	0.2872	0.1463

MAG.24	0.7799	0.4897	1.0739	0.5732	0.9262	2.7798	1.1607	0.6742	1.2387	2.2102	2.1254	0.5133
MAG.351	0.0912	0.0163	0.0210	0.1617	0.0422	0.0625	0.1656	0.0795	0.2381	0.2660	0.4719	1.6536
MAG.7	2.1417	0.9300	5.9796	3.5199	1.4380	0.9329	0.0850	0.0087	0.0618	0.0362	0.0219	0.0204
MAG.99	0.5954	1.5383	0.9907	1.6719	2.9879	2.0643	0.0537	0.0129	0.0038	0.0056	0.0010	0.0029
MAG.230	0.0090	0.0097	0.0049	0.0167	0.0183	0.0125	0.5302	2.6944	0.0435	0.0430	0.1289	0.4002
MAG.146	0.1351	0.0406	0.1651	0.0594	0.2714	0.2558	1.2745	0.5788	0.2197	0.3243	0.1568	0.0212
MAG.149	0.4589	3.3771	0.7276	2.4515	1.8176	0.3774	0.0363	0.0923	0.0793	0.0899	0.0274	0.0226
MAG.227	1.7557	1.5923	5.3984	1.9617	3.3245	8.4993	0.1144	0.1343	0.0871	0.1745	0.0511	0.0858
MAG.262	0.1504	0.3196	1.3380	1.2217	0.8772	0.1500	0.0046	0.0048	0.0049	0.0139	0.0021	0.0063
MAG.100	0.0775	0.1647	0.1107	0.1278	0.1500	1.3823	0.5500	0.0509	0.0634	0.1270	0.1650	0.3064
MAG.10	0.9135	1.5295	0.2642	1.3562	0.7868	1.2504	0.1863	0.1436	0.1682	0.3394	0.1657	0.2033
MAG.237	0.6535	1.7402	0.1761	0.3225	1.4787	0.6297	0.6319	0.3402	0.0892	0.2396	0.2879	1.7092
MAG.2	0.0290	0.0515	0.0139	0.0589	0.0838	0.0746	0.1624	0.1231	0.9898	0.1964	0.3433	0.5887
MAG.234	0.2494	0.7916	3.4081	0.3340	0.8172	0.7608	0.0771	0.1422	0.0653	0.1232	0.0192	0.0305
MAG.386	1.1434	0.4277	0.3873	0.3060	0.2992	0.4344	0.1275	0.0755	0.0148	0.0751	0.0176	0.0594
MAG.238	0.0613	0.0211	0.1141	0.1638	0.1019	0.1488	0.3034	0.3235	0.1897	0.2618	0.5934	0.0919
MAG.241	0.9928	0.1091	0.1977	0.1504	0.1703	0.1781	0.0781	0.0555	0.1920	0.0846	0.1635	0.4938
MAG.257	0.7772	0.7846	0.9631	2.7471	1.2317	0.7028	0.2193	0.1670	0.2240	0.2081	0.0454	0.2189
MAG.109	0.0591	0.0326	0.1090	0.0507	0.0888	0.1802	0.7513	0.1873	0.7543	0.4481	1.7532	0.0689
MAG.94	0.0706	0.1870	4.3389	0.0966	0.8024	1.3728	0.0022	0.0019	0.0038	0.0094	0.0013	0.0076
MAG.258	0.0815	0.0053	0.0925	0.0060	0.0637	0.0382	0.5729	0.1560	0.4484	0.5295	1.1357	1.8081
MAG.285	0.0620	0.0047	0.0228	0.0105	0.0188	0.2236	0.6854	0.5282	0.1593	0.1877	0.3051	0.0723
MAG.140	0.7091	2.2719	1.5854	1.9972	2.5704	2.4483	4.4417	6.5214	3.8478	4.5525	3.2825	5.5194
MAG.246	0.5254	1.3430	0.6748	1.4001	0.7933	2.6037	0.2573	0.1553	0.0359	0.0764	0.0332	0.1132
MAG.131	0.3280	0.1717	0.2116	0.2868	0.4237	0.1139	0.4906	0.2639	0.0943	0.2715	0.3142	0.6436
MAG.6	0.0131	0.0355	0.0720	0.0165	0.0415	17.1468	0.0117	0.0194	0.0114	0.0154	0.0052	0.0138
MAG.210	0.4984	0.0989	0.0445	0.4111	0.5736	0.1997	0.3388	0.6061	1.1732	1.9870	0.3693	0.5414
MAG.60	0.1017	0.3201	0.0396	5.7175	0.1618	0.0357	0.1011	0.1701	0.2949	0.3905	0.1795	0.1048
MAG.216	1.0520	2.5043	0.2902	1.0094	1.6976	0.9651	0.4155	0.3285	0.2644	0.7817	0.0970	0.5385
MAG.282	0.1642	0.1218	0.3607	0.1760	0.1811	1.2599	2.0028	0.4235	1.5899	1.0854	3.2197	0.1349
MAG.26	0.0803	0.0676	0.0879	0.0594	0.1323	0.2028	0.5953	0.1739	0.3585	0.5369	0.2981	0.0488
MAG.182	0.9821	0.2773	0.8190	0.1848	0.7242	0.3377	0.1002	0.0315	0.0312	0.0753	0.0193	0.0924
MAG.136	0.0592	0.1744	0.0613	0.0109	0.3565	0.0841	0.1978	1.3132	0.1479	0.3956	0.0928	0.1952
MAG.85	0.0013	0.0010	0.0066	0.0004	0.0012	0.0024	0.0008	0.0002	8.9868	0.0213	3.4009	0.0067
MAG.250	2.4673	0.6107	0.2598	1.0489	0.6520	0.3915	0.2424	0.2193	0.0786	0.3250	0.0479	0.4456
MAG.79	0.1017	0.3704	0.5763	0.1348	0.1321	0.1306	1.1342	0.4576	0.0539	0.0228	0.0103	0.0093
MAG.142	0.0184	0.0384	0.1351	0.1062	0.2362	0.0914	0.4311	0.2890	1.4478	0.7128	0.7698	0.9523
MAG.51	0.1966	0.1820	0.3732	0.2651	0.5007	0.4886	0.8474	0.1977	0.0515	0.0992	0.2482	0.2704
MAG.214	0.1120	0.0498	0.1810	0.9713	0.2972	0.0962	0.1712	0.0427	0.2156	0.2878	0.1729	1.9213
MAG.5	0.2448	1.2979	0.3134	0.6114	0.3909	1.0576	0.2348	0.1658	0.1995	0.2647	0.1917	0.3478
MAG.192	1.7727	2.7855	0.8525	2.3413	1.7487	1.6895	1.2361	1.6411	1.3666	2.7197	0.6417	2.5666
MAG.71	0.1326	0.0130	0.0173	0.3736	0.1546	0.0608	0.4632	0.9169	0.3187	0.6021	0.4141	1.9982
MAG.64	1.8157	0.0912	0.2750	0.1590	0.3695	0.1804	0.1103	0.0584	0.0441	0.2278	0.0147	0.0369

Supplementary Table 13: KEGG pathways showed significant enrichment differences based on SIMPER analyses (Contrast 10˚C - 15˚C; q-value <0.05) on day 60. The geneID column represents the KO’s related to each metabolic pathway and the counts column represents the number of KO’s found related to each pathway.

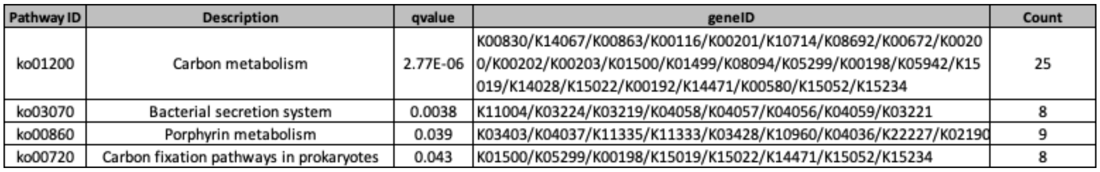

Pathway ID	Description	qvalue	geneID	Count
ko01200	Carbon metabolism	2.77E-06	K00830/K14067/K00863/K00116/K00201/K10714/K08692/K00672/K00200/K00202/K00203/K01500/K01499/K08094/K05299/K00198/K05942/K15019/K14028/K15022/K00192/K14471/K00580/K15052/K15234	25
ko03070	Bacterial secretion system	0.0038	K11004/K03224/K03219/K04058/K04057/K04056/K04059/K03221	8
ko00860	Porphyrin metabolism	0.039	K03403/K04037/K11335/K11333/K03428/K10960/K04036/K22227/K02190	9
ko00720	Carbon fixation pathways in prokaryotes	0.043	K01500/K05299/K00198/K15019/K15022/K14471/K15052/K15234	8

Supplementary Table 14: Significant variation in CAZy enzymes between 10C˚, 13C˚, and 15°C based on SIMPER analysis results using relative abundance

CAZy	L6_M13_5_B	L7_M10_5_C	L8_M10_5_B	L9_M13_5_C	L6_M13_1_B	L7_M10_1_B	L7_M15_1_C	L7_M15_5_C	L8_M10_1_B	L9_M13_1_C	L9_M15_1_B	L9_M15_5_B
CE17	161.33792	132.694067	141.35794	164.141206	161.630999	168.442939	157.747519	156.895449	151.460769	140.085435	122.206772	145.72852
GT58	187.497974	87.716053	130.329393	150.501239	105.261185	108.636392	183.061396	105.613474	144.049969	150.736754	141.121829	181.971696
GH153	2.377923	12.172587	11.55123	2.707362	7.348787	10.964677	3.226409	10.063654	1.468955	2.910265	11.906438	7.449074
GT39	214.093822	423.250035	498.024165	204.668115	318.411213	297.912517	236.251575	352.618486	569.436702	195.729151	230.634833	157.090636
GH116	224.915042	183.943964	181.463782	210.731593	222.341263	212.166006	230.475183	187.996216	199.200434	211.715739	170.4432	207.737166
GT53	35.002446	65.560319	65.207367	42.987171	57.42271	35.641723	32.995465	60.81868	68.639193	48.878329	75.910572	54.10403
GH119	10.216789	12.777232	10.313757	10.131562	15.901818	11.887589	10.328185	38.361983	8.824418	14.203397	17.246994	20.56275
CBM62	136.568336	121.546721	118.044827	126.398385	156.420059	161.362512	136.098555	158.337905	120.678546	127.66876	128.189715	151.965255
GT95	173.051874	189.034509	157.336538	191.261793	192.970345	166.857773	175.753881	228.745333	159.336376	186.282792	215.39125	235.732776
GH30	228.49053	263.230783	226.759944	250.422817	301.982602	238.106381	213.126592	363.391439	234.222688	266.82741	331.202046	361.86022
GH145	36.494501	34.515194	23.09502	25.818041	21.526093	21.174624	23.211805	50.411334	17.663565	25.476696	34.645915	49.878941
GT56	9.225062	7.091712	7.092844	9.401078	8.461005	8.855728	7.577778	10.494828	7.22723	9.300486	7.145795	12.049223
GH85	97.438646	95.296198	101.760903	103.689648	126.679723	101.801294	93.270357	141.749676	102.05532	110.506806	101.059044	124.279227

Supplementary Table 15: Abundance of Nitrogen Genes in Metagenomic Samples on Day 60 and their possible involvement in different nitrogen cycle pathway such as Assimilatory Nitrate Reduction to Ammonium (ANRA), Dissimilatory Nitrate Reduction to Ammonium (DNRA), Denitrification, nitrification, and nitrogen fixation

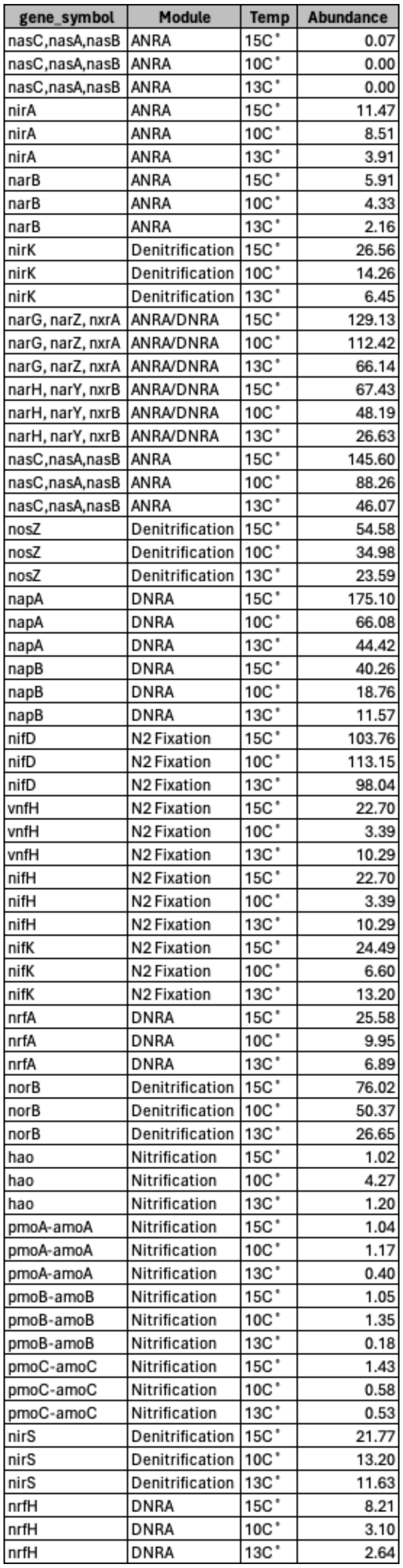

gene_symbol	Module	Temp	Abundance
nasC,nasA,nasB	ANRA	15C°	0.07
nasC,nasA,nasB	ANRA	10C°	0.00
nasC,nasA,nasB	ANRA	13C°	0.00
nirA	ANRA	15C°	11.47
nirA	ANRA	10C°	8.51
nirA	ANRA	13C°	3.91
narB	ANRA	15C°	5.91
narB	ANRA	10C°	4.33
narB	ANRA	13C°	2.16
nirK	Denitrification	15C°	26.56
nirK	Denitrification	10C°	14.26
nirK	Denitrification	13C°	6.45
narG, narZ, nxrA	ANRA/DNRA	15C°	129.13
narG, narZ, nxrA	ANRA/DNRA	10C°	112.42
narG, narZ, nxrA	ANRA/DNRA	13C°	66.14
narH, narY, nxrB	ANRA/DNRA	15C°	67.43
narH, narY, nxrB	ANRA/DNRA	10C°	48.19
narH, narY, nxrB	ANRA/DNRA	13C°	26.63
nasC,nasA,nasB	ANRA	15C°	145.60
nasC,nasA,nasB	ANRA	10C°	88.26
nasC,nasA,nasB	ANRA	13C°	46.07
nosZ	Denitrification	15C°	54.58
nosZ	Denitrification	10C°	34.98
nosZ	Denitrification	13C°	23.59
napA	DNRA	15C°	175.10
napA	DNRA	10C°	66.08
napA	DNRA	13C°	44.42
napB	DNRA	15C°	40.26
napB	DNRA	10C°	18.76
napB	DNRA	13C°	11.57
nifD	N2 Fixation	15C°	103.76
nifD	N2 Fixation	10C°	113.15
nifD	N2 Fixation	13C°	98.04
vnfH	N2 Fixation	15C°	22.70
vnfH	N2 Fixation	10C°	3.39
vnfH	N2 Fixation	13C°	10.29
nifH	N2 Fixation	15C°	22.70
nifH	N2 Fixation	10C°	3.39
nifH	N2 Fixation	13C°	10.29
nifK	N2 Fixation	15C°	24.49
nifK	N2 Fixation	10C°	6.60
nifK	N2 Fixation	13C°	13.20
nrfA	DNRA	15C°	25.58
nrfA	DNRA	10C°	9.95
nrfA	DNRA	13C°	6.89
norB	Denitrification	15C°	76.02
norB	Denitrification	10C°	50.37
norB	Denitrification	13C°	26.65
hao	Nitrification	15C°	1.02
hao	Nitrification	10C°	4.27
hao	Nitrification	13C°	1.20
pmoA-amoA	Nitrification	15C°	1.04
pmoA-amoA	Nitrification	10C°	1.17
pmoA-amoA	Nitrification	13C°	0.40
pmoB-amoB	Nitrification	15C°	1.05
pmoB-amoB	Nitrification	10C°	1.35
pmoB-amoB	Nitrification	13C°	0.18
pmoC-amoC	Nitrification	15C°	1.43
pmoC-amoC	Nitrification	10C°	0.58
pmoC-amoC	Nitrification	13C°	0.53
nirS	Denitrification	15C°	21.77
nirS	Denitrification	10C°	13.20
nirS	Denitrification	13C°	11.63
nrfH	DNRA	15C°	8.21
nrfH	DNRA	10C°	3.10
nrfH	DNRA	13C°	2.64

Supplementary Table 16: MAGs Associated with Secretion System functions Identified by SIMPER analysis on Day 60, Including their taxonomy at the order level and abundance in RPKM.

genome	gene	order	10C°	13C°	15C°
MAG.101	K11004	o__Pseudomonadales	0.87	0.38	0.23
MAG.130	K11004	o__Pseudomonadales	2.67	4.61	1.40
MAG.160	K11004	o__Minwuiales	0.76	0.06	0.14
MAG.170	K03224	o__Chlamydiales	0.02	0.22	0.95
MAG.18	K11004	o__Pseudomonadales	12.64	0.29	0.08
MAG.213	K11004	o__Pseudomonadales	1.22	0.10	0.13
MAG.223	K03224	o__Geminicoccales	1.23	1.04	0.70
MAG.223	K03219	o__Geminicoccales	1.23	1.04	0.70
MAG.250	K11004	o__Minwuiales	0.46	0.40	0.49
MAG.26	K11004	o__Chromatiales	0.77	0.90	0.35
MAG.269	K11004	o__Pseudomonadales	0.03	0.06	0.34
MAG.270	K11004	o__Sphingomonadales	0.17	0.40	0.29
MAG.277	K03224	o__Rhodobacterales	0.41	0.78	0.77
MAG.30	K11004	o__Minwuiales	1.44	0.16	0.23
MAG.321	K11004	o__Rhizobiales	0.00	0.13	1.03
MAG.360	K03224	o__Rhodobacterales	1.58	2.51	0.53
MAG.37	K11004	o__HK1	4.20	3.22	0.90
MAG.47	K11004	o__Competibacterales	0.66	0.96	0.50
MAG.70	K03224	o__Pseudomonadales	0.08	6.20	8.78
MAG.70	K03219	o__Pseudomonadales	0.08	6.20	8.78
MAG.76	K11004	o__Minwuiales	5.27	1.92	5.46

Appendix

CAMA: coral-associated microbial aggregates.

Symbiocytes: Gastrodermal specialized cells that hold the endosymbiotic algae.

CWC: Cold water corals

Holobionts: The collective genetic composition of organisms that coexist with corals

Metabarcoding: The process of DNA/RNA barcoding, or eDNA/eRNA barcoding, enabling simultaneous identification of multiple taxa within a single sample.

Metagenomics: The study of the genetic material (DNA or RNA) isolated from all organisms present in a complex sample, aimed at understanding both the diversity (structure) and functional capabilities (function) of the microbial community.

Metatranscriptomic: The study involving the extraction and analysis of mRNA from a metagenomic sample (metatranscriptome), providing insights into the regulatory mechanisms and expression profiles of complex microbial communities within the environment.

Metaproteomic: The study of all proteins that are expressed at specific times by organisms within an ecosystem.

ELPs: Eukaryotic-like proteins

RPKM (Reads Per Kilobase per Million): A measurement used to normalize read counts by the length of the genomic region and the total number of sequencing reads.

KEGG (Kyoto Encyclopedia of Genes and Genomes): A bioinformatics database linking genomic data to biological pathways, enhancing understanding of biological systems and their environmental interactions.

KEGG Pathway: Molecular entities like genes, proteins, and small molecules, along with their interactions, operate within cellular processes or broader biological pathways.

KEGG module: Functional units within a pathway that execute specific biological functions.

CAZy: Database of Carbohydrate-Active enzymes (CAZymes)

References

Aeby, G. S., Howells, E., Work, T., Abrego, D., Williams, G. J., Wedding, L. M., Caldwell, J. M., Moritsch, M., & Burt, J. A. (2020). Localized outbreaks of coral disease on Arabian reefs are linked to extreme temperatures and environmental stressors. *Coral Reefs*, *39*(3), 829–846. https://doi.org/10.1007/s00338-020-01928-4

Aeby, G. S., Ushijima, B., Campbell, J. E., Jones, S., Williams, G. J., Meyer, J. L., Häse, C., & Paul, V. J. (2019). Pathogenesis of a Tissue Loss Disease Affecting Multiple Species of Corals Along the Florida Reef Tract. *Frontiers in Marine Science*, *6*. https://doi.org/10.3389/fmars.2019.00678

Agostini, S., Suzuki, Y., Higuchi, T., Casareto, B. E., Yoshinaga, K., Nakano, Y., & Fujimura, H. (2012). Biological and chemical characteristics of the coral gastric cavity. *Coral Reefs*, *31*(1), 147–156. https://doi.org/10.1007/s00338-011-0831-6

Aguiar-Pulido, V., Huang, W., Suarez-Ulloa, V., Cickovski, T., Mathee, K., & Narasimhan, G. (2016). Metagenomics, Metatranscriptomics, and Metabolomics Approaches for Microbiome Analysis. *Evolutionary Bioinformatics*, *12s1*, EBO.S36436. https://doi.org/10.4137/EBO.S36436

Ainsworth, T. D., Fordyce, A. J., & Camp, E. F. (2017). The Other Microeukaryotes of the Coral Reef Microbiome. *Trends in Microbiology*, *25*(12), 980–991. https://doi.org/10.1016/j.tim.2017.06.007

Ainsworth, T. D., Hoegh-Guldberg, O., Heron, S. F., Skirving, W. J., & Leggat, W. (2008). Early cellular changes are indicators of pre-bleaching thermal stress in the coral host. *Journal of Experimental Marine Biology and Ecology*, *364*(2), 63–71. https://doi.org/10.1016/j.jembe.2008.06.032

Ainsworth, T. D., Thurber, R. V., & Gates, R. D. (2010). The future of coral reefs: a microbial perspective. *Trends in Ecology & Evolution*, *25*(4), 233–240. https://doi.org/10.1016/j.tree.2009.11.001

Alker, A. P., Smith, G. W., & Kim, K. (2001). Characterization of Aspergillus sydowii (Thom et Church), a fungal pathogen of Caribbean sea fan corals. *Hydrobiologia*, *460*(1/3), 105–111. https://doi.org/10.1023/A:1013145524136

Alneberg, J., Bjarnason, B. S., de Bruijn, I., Schirmer, M., Quick, J., Ijaz, U. Z., Loman, N. J., Andersson, A. F., & Quince, C. (2013). *CONCOCT: Clustering cONtigs on COverage and ComposiTion*.

Alvarez-Filip, L., González-Barrios, F. J., Pérez-Cervantes, E., Molina-Hernández, A., & Estrada-Saldívar, N. (2022). Stony coral tissue loss disease decimated Caribbean coral populations and reshaped reef functionality. *Communications Biology*, *5*(1), 440. https://doi.org/10.1038/s42003-022-03398-6

Anders, S., Pyl, P. T., & Huber, W. (2015). HTSeq—a Python framework to work with high-throughput sequencing data. *Bioinformatics*, *31*(2), 166–169. https://doi.org/10.1093/bioinformatics/btu638

Andersson, E. R., Day, R. D., Loewenstein, J. M., Woodley, C. M., & Schock, T. B. (2019). Evaluation of Sample Preparation Methods for the Analysis of Reef-Building Corals Using ^{1}H-NMR-Based Metabolomics. *Metabolites*, *9*(2). https://doi.org/10.3390/metabo9020032

Apprill, A., Weber, L. G., & Santoro, A. E. (2016). Distinguishing between Microbial Habitats Unravels Ecological Complexity in Coral Microbiomes. *MSystems*, *1*(5). https://doi.org/10.1128/mSystems.00143-16

Asamoto, C. K., Rempfert, K. R., Luu, V. H., Younkin, A. D., & Kopf, S. H. (2021). Enzyme-Specific Coupling of Oxygen and Nitrogen Isotope Fractionation of the Nap and Nar Nitrate Reductases. *Environmental Science & Technology*, *55*(8), 5537–5546. https://doi.org/10.1021/acs.est.0c07816

Asgari, S. (2014). *Epigenetic Modifications Underlying Symbiont–Host Interactions* (pp. 253–276). https://doi.org/10.1016/B978-0-12-800222-3.00010-3

Avila-Magaña, V., Kamel, B., DeSalvo, M., Gómez-Campo, K., Enríquez, S., Kitano, H., Rohlfs, R. V., Iglesias-Prieto, R., & Medina, M. (2021). Elucidating gene expression adaptation of phylogenetically divergent coral holobionts under heat stress. *Nature Communications*, *12*(1), 5731. https://doi.org/10.1038/s41467-021-25950-4

Babbin, A. R., Tamasi, T., Dumit, D., Weber, L., Rodríguez, M. V. I., Schwartz, S. L., Armenteros, M., Wankel, S. D., & Apprill, A. (2021). Discovery and quantification of anaerobic nitrogen metabolisms among oxygenated tropical Cuban stony corals. *The ISME Journal*, *15*(4), 1222–1235. https://doi.org/10.1038/s41396-020-00845-2

Bakshani, C. R., Morales-Garcia, A. L., Althaus, M., Wilcox, M. D., Pearson, J. P., Bythell, J. C., & Burgess, J. G. (2018). Evolutionary conservation of the antimicrobial function of mucus: a first defence against infection. *Npj Biofilms and Microbiomes*, *4*(1), 14. https://doi.org/10.1038/s41522-018-0057-2

Ballinger, M. J., & Perlman, S. J. (2019). The defensive Spiroplasma. *Current Opinion in Insect Science*, *32*, 36–41. https://doi.org/10.1016/j.cois.2018.10.004

Banahene, N., Kavunja, H. W., & Swarts, B. M. (2022). Chemical Reporters for Bacterial Glycans: Development and Applications. *Chemical Reviews*, *122*(3), 3336–3413. https://doi.org/10.1021/acs.chemrev.1c00729

Barshis, D. J., Ladner, J. T., Oliver, T. A., Seneca, F. O., Traylor-Knowles, N., & Palumbi, S. R. (2013). Genomic basis for coral resilience to climate change. *Proceedings of the National Academy of Sciences*, *110*(4), 1387–1392. https://doi.org/10.1073/pnas.1210224110

Baussant, T., Arnberg, M., Lyng, E., Ramanand, S., Bamber, S., Berry, M., Myrnes Hansen, I., Van Oevelen, D., & Van Breugel, P. (2022). Identification of tolerance levels on the cold-water coral Desmophyllum pertusum (Lophelia pertusa) from realistic exposure conditions to suspended bentonite, barite and drill cutting particles. *PLOS ONE*, *17*(2), e0263061. https://doi.org/10.1371/journal.pone.0263061

Bayer, T., Arif, C., Ferrier-Pagès, C., Zoccola, D., Aranda, M., & Voolstra, C. (2013). Bacteria of the genus Endozoicomonas dominate the microbiome of the Mediterranean gorgonian coral Eunicella cavolini. *Marine Ecology Progress Series*, *479*, 75–84. https://doi.org/10.3354/meps10197

Bayer, T., Neave, M. J., Alsheikh-Hussain, A., Aranda, M., Yum, L. K., Mincer, T., Hughen, K., Apprill, A., & Voolstra, C. R. (2013). The Microbiome of the Red Sea Coral Stylophora pistillata Is Dominated by Tissue-Associated Endozoicomonas Bacteria. *Applied and Environmental Microbiology*, *79*(15), 4759–4762. https://doi.org/10.1128/AEM.00695-13

Belser, C., Poulain, J., Labadie, K., Gavory, F., Alberti, A., Guy, J., Carradec, Q., Cruaud, C., Da Silva, C., Engelen, S., Mielle, P., Perdereau, A., Samson, G., Gas, S., Batisse, J., Beluche, O., Bertrand, L., Bohers, C., Bordelais, I., … Wincker, P. (2023). Integrative omics framework for characterization of coral reef ecosystems from the Tara Pacific expedition. *Scientific Data*, *10*(1), 326. https://doi.org/10.1038/s41597-023-02204-0

Benavides, M., Bednarz, V. N., & Ferrier-Pagès, C. (2017). Diazotrophs: Overlooked Key Players within the Coral Symbiosis and Tropical Reef Ecosystems? *Frontiers in Marine Science*, *4*. https://doi.org/10.3389/fmars.2017.00010

Béraud, E., Gevaert, F., Rottier, C., & Ferrier-Pagès, C. (2013). The response of the scleractinian coral *Turbinaria reniformis* to thermal stress depends on the nitrogen status of the coral holobiont. *Journal of Experimental Biology*. https://doi.org/10.1242/jeb.085183

Bernard, C. S., Brunet, Y. R., Gueguen, E., & Cascales, E. (2010). Nooks and Crannies in Type VI Secretion Regulation. *Journal of Bacteriology*, *192*(15), 3850–3860. https://doi.org/10.1128/JB.00370-10

Bhuvaneswari, G. (2013). Molecular Characterization of camphor utilizing bacterial isolates from refinery sludge and detection of target loci-Cytochrome P-450 cam mono oxygenase (cam C gene) by PCR and gene probe. *SpringerPlus*, *2*(1), 170. https://doi.org/10.1186/2193-1801-2-170

Boilard, A., Dubé, C. E., Gruet, C., Mercière, A., Hernandez-Agreda, A., & Derome, N. (2020). Defining Coral Bleaching as a Microbial Dysbiosis within the Coral Holobiont. *Microorganisms*, *8*(11), 1682. https://doi.org/10.3390/microorganisms8111682

Bonacolta, A. M., Miravall, J., Gómez-Gras, D., Ledoux, J.-B., Garrabou, J., Massana, R., & del Campo, J. (2022). *Apicomplexans predict thermal stress mortality in the Mediterranean coral Paramuricea clavata*. https://doi.org/10.1101/2022.11.23.517658

Bonacolta, A. M., Weiler, B. A., Porta-Fitó, T., Sweet, M., Keeling, P., & del Campo, J. (2023). Beyond the Symbiodiniaceae: diversity and role of microeukaryotic coral symbionts. *Coral Reefs*. https://doi.org/10.1007/s00338-023-02352-0

Bongaerts, P., Frade, P. R., Hay, K. B., Englebert, N., Latijnhouwers, K. R. W., Bak, R. P. M., Vermeij, M. J. A., & Hoegh-Guldberg, O. (2015). Deep down on a Caribbean reef: lower mesophotic depths harbor a specialized coral-endosymbiont community. *Scientific Reports*, *5*(1), 7652. https://doi.org/10.1038/srep07652

Bongaerts, P., Ridgway, T., Sampayo, E. M., & Hoegh-Guldberg, O. (2010). Assessing the 'deep reef refugia' hypothesis: focus on Caribbean reefs. *Coral Reefs*, *29*(2), 309–327. https://doi.org/10.1007/s00338-009-0581-x

Bontemps, Y., Vuillermoz, B., Antonicelli, F., Perreau, C., Danan, J.-L., Maquart, F.-X., & Wegrowski, Y. (2003). Specific Protein-1 Is a Universal Regulator of UDP-glucose Dehydrogenase Expression. *Journal of Biological Chemistry*, *278*(24), 21566–21575. https://doi.org/10.1074/jbc.M209366200

Bordenstein, S. R., & Theis, K. R. (2015). Host Biology in Light of the Microbiome: Ten Principles of Holobionts and Hologenomes. *PLOS Biology*, *13*(8), e1002226. https://doi.org/10.1371/journal.pbio.1002226

Böttjer, D., Dore, J. E., Karl, D. M., Letelier, R. M., Mahaffey, C., Wilson, S. T., Zehr, J., & Church, M. J. (2017). Temporal variability of nitrogen fixation and particulate nitrogen export at Station ALOHA. *Limnology and Oceanography*, *62*(1), 200–216. https://doi.org/10.1002/lno.10386

Bourne, D. G., Garren, M., Work, T. M., Rosenberg, E., Smith, G. W., & Harvell, C. D. (2009). Microbial disease and the coral holobiont. *Trends in Microbiology*, *17*(12), 554–562. https://doi.org/10.1016/j.tim.2009.09.004

Bourne, D. G., Morrow, K. M., & Webster, N. S. (2016). Insights into the Coral Microbiome: Underpinning the Health and Resilience of Reef Ecosystems. *Annual Review of Microbiology*, *70*(1), 317–340. https://doi.org/10.1146/annurev-micro-102215-095440

Bourne, D. G., & Munn, C. B. (2005). Diversity of bacteria associated with the coral Pocillopora damicornis from the Great Barrier Reef. *Environmental Microbiology*, *7*(8), 1162–1174. https://doi.org/10.1111/j.1462-2920.2005.00793.x

Brito-Morales, I., Schoeman, D. S., Molinos, J. G., Burrows, M. T., Klein, C. J., Arafeh-Dalmau, N., Kaschner, K., Garilao, C., Kesner-Reyes, K., & Richardson, A. J. (2020). Climate velocity reveals increasing exposure of deep-ocean biodiversity to future warming. *Nature Climate Change*, *10*(6), 576–581. https://doi.org/10.1038/s41558-020-0773-5

Brooke, S., Ross, S. W., Bane, J. M., Seim, H. E., & Young, C. M. (2013). Temperature tolerance of the deep-sea coral Lophelia pertusa from the southeastern United States. *Deep Sea Research Part II: Topical Studies in Oceanography*, *92*, 240–248. https://doi.org/10.1016/j.dsr2.2012.12.001

Buchfink, B., Xie, C., & Huson, D. H. (2015). Fast and sensitive protein alignment using DIAMOND. *Nature Methods*, *12*(1), 59–60. https://doi.org/10.1038/nmeth.3176

Buhl-Mortensen, P., Buhl-Mortensen, L., & Purser, A. (2016). Trophic Ecology and Habitat Provision in Cold-Water Coral Ecosystems. In *Marine Animal Forests* (pp. 1–26). Springer International Publishing. https://doi.org/10.1007/978-3-319-17001-5_20-1

Burke, L., Spalding, M. D., & Perry, A. (2011). *Reefs at Risk Revisited*. https://www.researchgate.net/publication/263705424

Cárdenas, A., Raina, J.-B., Pogoreutz, C., Rädecker, N., Bougoure, J., Guagliardo, P., Pernice, M., & Voolstra, C. R. (2022). Greater functional diversity and redundancy of coral endolithic microbiomes align with lower coral bleaching susceptibility. *The ISME Journal*, *16*(10), 2406–2420. https://doi.org/10.1038/s41396-022-01283-y

Cardini, U., van Hoytema, N., Bednarz, V. N., Rix, L., Foster, R. A., Al-Rshaidat, M. M. D., & Wild, C. (2016). Microbial dinitrogen fixation in coral holobionts exposed to thermal stress and bleaching. *Environmental Microbiology*, *18*(8), 2620–2633. https://doi.org/10.1111/1462-2920.13385

Carlos, C., Torres, T. T., & Ottoboni, L. M. M. (2013). Bacterial communities and species-specific associations with the mucus of Brazilian coral species. *Scientific Reports*, *3*(1), 1624. https://doi.org/10.1038/srep01624

Cassan, F. D., Coniglio, A., Amavizca, E., Maroniche, G., Cascales, E., Bashan, Y., & de-Bashan, L. E. (2021). The <scp> *Azospirillum brasilense* </scp> type <scp>VI</scp> secretion system promotes cell aggregation, biocontrol protection against phytopathogens and attachment to the microalgae <scp> *Chlorella sorokiniana* </scp>. *Environmental Microbiology*, *23*(10), 6257–6274. https://doi.org/10.1111/1462-2920.15749

Castellan, G., Abbiati, M., Angeletti, L., Foglini, F., Grande, V., Montagna, P., & Taviani, M. (2022). What are we protecting? An analysis of the current conservation framework addressing Mediterranean mesophotic habitats. *Frontiers in Environmental Science*, *10*. https://doi.org/10.3389/fenvs.2022.1009033

Cathalot, C., Van Oevelen, D., Cox, T. J. S., Kutti, T., Lavaleye, M., Duineveld, G., & Meysman, F. J. R. (2015). Cold-water coral reefs and adjacent sponge grounds: hotspots of benthic respiration and organic carbon cycling in the deep sea. *Frontiers in Marine Science*, *2*. https://doi.org/10.3389/fmars.2015.00037

Cerrano, C., Bavestrello, G., Bianchi, C. N., Cattaneo-vietti, R., Bava, S., Morganti, C., Morri, C., Picco, P., Sara, G., Schiaparelli, S., Siccardi, A., & Sponga, F. (2000). A catastrophic mass-mortality episode of gorgonians and other organisms in the Ligurian Sea (North-western Mediterranean), summer 1999. *Ecology Letters*, *3*(4), 284–293. https://doi.org/10.1046/j.1461-0248.2000.00152.x

Chapron, L., Galand, P. E., Pruski, A. M., Peru, E., Vétion, G., Robin, S., & Lartaud, F. (2021). Resilience of cold-water coral holobionts to thermal stress. *Proceedings of the Royal Society B: Biological Sciences*, *288*(1965). https://doi.org/10.1098/rspb.2021.2117

Chapron, L., Peru, E., Engler, A., Ghiglione, J. F., Meistertzheim, A. L., Pruski, A. M., Purser, A., Vétion, G., Galand, P. E., & Lartaud, F. (2018). Macro- and microplastics affect cold-water corals growth, feeding and behaviour. *Scientific Reports*, *8*(1), 15299. https://doi.org/10.1038/s41598-018-33683-6

Chaumeil, P.-A., Mussig, A. J., Hugenholtz, P., & Parks, D. H. (2020). GTDB-Tk: a toolkit to classify genomes with the Genome Taxonomy Database. *Bioinformatics*, *36*(6), 1925–1927. https://doi.org/10.1093/bioinformatics/btz848

"Chemel, M., "Erwan, P., "Mohammad, B., "Ramiro, L., "Franck, L., & "Pierre, G. (2024). Cold water coral Lophelia pertusa mortality under ocean warming is associated with pathogenic bacteria. *Preprint Authorea*.

Chen, C.-P., Tseng, C.-H., Chen, C. A., & Tang, S.-L. (2011). The dynamics of microbial partnerships in the coral Isopora palifera. *The ISME Journal*, *5*(4), 728–740. https://doi.org/10.1038/ismej.2010.151

Chen, N. H., Djoko, K. Y., Veyrier, F. J., & McEwan, A. G. (2016). Formaldehyde Stress Responses in Bacterial Pathogens. *Frontiers in Microbiology*, *7*. https://doi.org/10.3389/fmicb.2016.00257

Chimetto Tonon, L. A., Thompson, J. R., Moreira, A. P. B., Garcia, G. D., Penn, K., Lim, R., Berlinck, R. G. S., Thompson, C. C., & Thompson, F. L. (2017). Quantitative Detection of Active Vibrios Associated with White Plague Disease in Mussismilia braziliensis Corals. *Frontiers in Microbiology*, *8*. https://doi.org/10.3389/fmicb.2017.02272

Chiu, H.-H., Mette, A., Shiu, J.-H., Tang, S.-L., & Lin, S.-. (2012). *Bacterial Distribution in the Epidermis and Mucus of the Coral Euphyllia glabrescens by CARD-FISH*. http://zoolstud.sinica.edu.tw/Journals/51.8/1332.pdf

Chklovski, A., Parks, D. H., Woodcroft, B. J., & Tyson, G. W. (2024). Author Correction: CheckM2: a rapid, scalable and accurate tool for assessing microbial genome quality using machine learning. *Nature Methods*. https://doi.org/10.1038/s41592-024-02248-z

Chu, N. D., & Vollmer, S. V. (2016). Caribbean corals house shared and host-specific microbial symbionts over time and space. *Environmental Microbiology Reports*, *8*(4), 493–500. https://doi.org/10.1111/1758-2229.12412

Clark, M. R., Althaus, F., Schlacher, T. A., Williams, A., Bowden, D. A., & Rowden, A. A. (2016). The impacts of deep-sea fisheries on benthic communities: a review. *ICES Journal of Marine Science*, *73*(suppl_1), i51–i69. https://doi.org/10.1093/icesjms/fsv123

Cleves, P. A., Shumaker, A., Lee, J., Putnam, H. M., & Bhattacharya, D. (2020). Unknown to Known: Advancing Knowledge of Coral Gene Function. *Trends in Genetics*, *36*(2), 93–104. https://doi.org/10.1016/j.tig.2019.11.001

Cleves, P. A., Tinoco, A. I., Bradford, J., Perrin, D., Bay, L. K., & Pringle, J. R. (2020). Reduced thermal tolerance in a coral carrying CRISPR-induced mutations in the gene for a heat-shock transcription factor. *Proceedings of the National Academy of Sciences*, *117*(46), 28899–28905. https://doi.org/10.1073/pnas.1920779117

Croft, M. T., Lawrence, A. D., Raux-Deery, E., Warren, M. J., & Smith, A. G. (2005). Algae acquire vitamin B12 through a symbiotic relationship with bacteria. *Nature*, *438*(7064), 90–93. https://doi.org/10.1038/nature04056

Cumbo, V. R., Baird, A. H., Moore, R. B., Negri, A. P., Neilan, B. A., Salih, A., van Oppen, M. J. H., Wang, Y., & Marquis, C. P. (2013). Chromera velia is Endosymbiotic in Larvae of the Reef Corals Acropora digitifera and A. tenuis. *Protist*, *164*(2), 237–244. https://doi.org/10.1016/j.protis.2012.08.003

Cziesielski, M. J., Schmidt-Roach, S., & Aranda, M. (2019). The past, present, and future of coral heat stress studies. *Ecology and Evolution*, *9*(17), 10055–10066. https://doi.org/10.1002/ece3.5576

D Ainsworth, T., Krause, L., Bridge, T., Torda, G., Raina, J.-B., Zakrzewski, M., Gates, R. D., Padilla-Gamiño, J. L., Spalding, H. L., Smith, C., Woolsey, E. S., Bourne, D. G., Bongaerts, P., Hoegh-Guldberg, O., & Leggat, W. (2015). The coral core microbiome identifies rare bacterial taxa as ubiquitous endosymbionts. *The ISME Journal*, *9*(10), 2261–2274. https://doi.org/10.1038/ismej.2015.39

Dalsgaard, T., Stewart, F. J., Thamdrup, B., De Brabandere, L., Revsbech, N. P., Ulloa, O., Canfield, D. E., & DeLong, E. F. (2014). Oxygen at Nanomolar Levels Reversibly Suppresses Process Rates and Gene Expression in Anammox and Denitrification in the Oxygen Minimum Zone off Northern Chile. *MBio*, *5*(6). https://doi.org/10.1128/mBio.01966-14

DALY, M., FAUTIN, D. G., & CAPPOLA, V. A. (2003). Systematics of the Hexacorallia (Cnidaria: Anthozoa). *Zoological Journal of the Linnean Society*, *139*(3), 419–437. https://doi.org/10.1046/j.1096-3642.2003.00084.x

Damjanovic, K., van Oppen, M. J. H., Menéndez, P., & Blackall, L. L. (2019). Experimental Inoculation of Coral Recruits With Marine Bacteria Indicates Scope for Microbiome Manipulation in Acropora tenuis and Platygyra daedalea. *Frontiers in Microbiology*, *10*. https://doi.org/10.3389/fmicb.2019.01702

D'Angelo, T., Goordial, J., Lindsay, M. R., McGonigle, J., Booker, A., Moser, D., Stepanauskus, R., & Orcutt, B. N. (2023). Replicated life-history patterns and subsurface origins of the bacterial sister phyla Nitrospirota and Nitrospinota. *The ISME Journal*, *17*(6), 891–902. https://doi.org/10.1038/s41396-023-01397-x

Daniels, C. A., Baumgarten, S., Yum, L. K., Michell, C. T., Bayer, T., Arif, C., Roder, C., Weil, E., & Voolstra, C. R. (2015). Metatranscriptome analysis of the reef-building coral Orbicella faveolata indicates holobiont response to coral disease. *Frontiers in Marine Science*, *2*. https://doi.org/10.3389/fmars.2015.00062

Davies, A. J., & Guinotte, J. M. (2011). Global Habitat Suitability for Framework-Forming Cold-Water Corals. *PLoS ONE*, *6*(4), e18483. https://doi.org/10.1371/journal.pone.0018483

Davies, A. J., Wisshak, M., Orr, J. C., & Murray Roberts, J. (2008). Predicting suitable habitat for the cold-water coral Lophelia pertusa (Scleractinia). *Deep Sea Research Part I: Oceanographic Research Papers*, *55*(8), 1048–1062. https://doi.org/10.1016/j.dsr.2008.04.010

De Beul, E., Jongbloet, A., Franceus, J., & Desmet, T. (2021). Discovery of a Kojibiose Hydrolase by Analysis of Specificity-Determining Correlated Positions in Glycoside Hydrolase Family 65. *Molecules*, *26*(20), 6321. https://doi.org/10.3390/molecules26206321

Dean, J. F., Middelburg, J. J., Röckmann, T., Aerts, R., Blauw, L. G., Egger, M., Jetten, M. S. M., de Jong, A. E. E., Meisel, O. H., Rasigraf, O., Slomp, C. P., in't Zandt, M. H., & Dolman, A. J. (2018). Methane Feedbacks to the Global Climate System in a Warmer World. *Reviews of Geophysics*, *56*(1), 207–250. https://doi.org/10.1002/2017RG000559

Delgadillo-Ordoñez, N., Raimundo, I., Barno, A. R., Osman, E. O., Villela, H., Bennett-Smith, M., Voolstra, C. R., Benzoni, F., & Peixoto, R. S. (2022). Red Sea Atlas of Coral-Associated Bacteria Highlights Common Microbiome Members and Their Distribution across Environmental Gradients—A Systematic Review. In *Microorganisms* (Vol. 10, Issue 12). MDPI. https://doi.org/10.3390/microorganisms10122340

Deutsch, J. M., Jaiyesimi, O. A., Pitts, K. A., Houk, J., Ushijima, B., Walker, B. K., Paul, V. J., & Garg, N. (2021). Metabolomics of Healthy and Stony Coral Tissue Loss Disease Affected Montastraea cavernosa Corals. *Frontiers in Marine Science*, *8*. https://doi.org/10.3389/fmars.2021.714778

Ding, J.-Y., Shiu, J.-H., Chen, W.-M., Chiang, Y.-R., & Tang, S.-L. (2016). Genomic Insight into the Host–Endosymbiont Relationship of Endozoicomonas montiporae CL-33T with its Coral Host. *Frontiers in Microbiology*, *7*. https://doi.org/10.3389/fmicb.2016.00251

Dodds, L. A., Roberts, J. M., Taylor, A. C., & Marubini, F. (2007). Metabolic tolerance of the cold-water coral Lophelia pertusa (Scleractinia) to temperature and dissolved oxygen change. *Journal of Experimental Marine Biology and Ecology*, *349*(2), 205–214. https://doi.org/10.1016/j.jembe.2007.05.013

Dungan, A. M., Bulach, D., Lin, H., van Oppen, M. J. H., & Blackall, L. L. (2021). Development of a free radical scavenging bacterial consortium to mitigate oxidative stress in cnidarians. *Microbial Biotechnology*, *14*(5), 2025–2040. https://doi.org/10.1111/1751-7915.13877

Dunphy, C. M., Gouhier, T. C., Chu, N. D., & Vollmer, S. V. (2019). Structure and stability of the coral microbiome in space and time. *Scientific Reports*, *9*(1), 6785. https://doi.org/10.1038/s41598-019-43268-6

Eaton, K. R., Landsberg, J. H., Kiryu, Y., Peters, E. C., & Muller, E. M. (2021). Measuring Stony Coral Tissue Loss Disease Induction and Lesion Progression Within Two Intermediately Susceptible Species, Montastraea cavernosa and Orbicella faveolata. *Frontiers in Marine Science*, *8*. https://doi.org/10.3389/fmars.2021.717265

Edgar, R. C. (2010). Search and clustering orders of magnitude faster than BLAST. *Bioinformatics*, *26*(19), 2460–2461. https://doi.org/10.1093/bioinformatics/btq461

Emblem, Å., Karlsen, B. O., Evertsen, J., Miller, D. J., Moum, T., & Johansen, S. D. (2012). Mitogenome polymorphism in a single branch sample revealed by SOLiD deep sequencing of the Lophelia pertusa coral genome. *Gene*, *506*(2), 344–349. https://doi.org/10.1016/j.gene.2012.06.040

Epstein, H. E., Smith, H. A., Torda, G., & van Oppen, M. J. (2019). Microbiome engineering: enhancing climate resilience in corals. *Frontiers in Ecology and the Environment*, *17*(2), 100–108. https://doi.org/10.1002/fee.2001

Epstein, H. E., Torda, G., Munday, P. L., & van Oppen, M. J. H. (2019). Parental and early life stage environments drive establishment of bacterial and dinoflagellate communities in a common coral. *The ISME Journal*, *13*(6), 1635–1638. https://doi.org/10.1038/s41396-019-0358-3

Ezzat, L., Merle, P.-L., Furla, P., Buttler, A., & Ferrier-Pagès, C. (2013). The Response of the Mediterranean Gorgonian Eunicella singularis to Thermal Stress Is Independent of Its Nutritional Regime. *PLoS ONE*, *8*(5), e64370. https://doi.org/10.1371/journal.pone.0064370

Ezzat, L., Merolla, S., Clements, C. S., Munsterman, K. S., Landfield, K., Stensrud, C., Schmeltzer, E. R., Burkepile, D. E., & Vega Thurber, R. (2021). Thermal Stress Interacts With Surgeonfish Feces to Increase Coral Susceptibility to Dysbiosis and Reduce Tissue Regeneration. *Frontiers in Microbiology*, *12*. https://doi.org/10.3389/fmicb.2021.620458

Fennel, K., Brady, D., DiToro, D., Fulweiler, R. W., Gardner, W. S., Giblin, A., McCarthy, M. J., Rao, A., Seitzinger, S., Thouvenot-Korppoo, M., & Tobias, C. (2009). Modeling denitrification in aquatic sediments. *Biogeochemistry*, *93*(1–2), 159–178. https://doi.org/10.1007/s10533-008-9270-z

Fernandes de Barros Marangoni, L., Ferrier-Pagès, C., Rottier, C., Bianchini, A., & Grover, R. (2020). Unravelling the different causes of nitrate and ammonium effects on coral bleaching. *Scientific Reports*, *10*(1), 11975. https://doi.org/10.1038/s41598-020-68916-0

Ferrier-Pagès, C., Rottier, C., Beraud, E., & Levy, O. (2010). Experimental assessment of the feeding effort of three scleractinian coral species during a thermal stress: Effect on the rates of photosynthesis. *Journal of Experimental Marine Biology and Ecology*, *390*(2), 118–124. https://doi.org/10.1016/j.jembe.2010.05.007

Finn, D. R., Yu, J., Ilhan, Z. E., Fernandes, V. M. C., Penton, C. R., Krajmalnik-Brown, R., Garcia-Pichel, F., & Vogel, T. M. (2020). MicroNiche: an R package for assessing microbial niche breadth and overlap from amplicon sequencing data. *FEMS Microbiology Ecology*, *96*(8). https://doi.org/10.1093/femsec/fiaa131

Forcioli, D., Merle, P., Caligara, C., Ciosi, M., Muti, C., Francour, P., Cerrano, C., & Allemand, D. (2011). Symbiont diversity is not involved in depth acclimation in the Mediterranean sea whip Eunicella singularis. *Marine Ecology Progress Series*, *439*, 57–71. https://doi.org/10.3354/meps09314

Foster, Z. S. L., Sharpton, T. J., & Grünwald, N. J. (2017). Metacoder: An R package for visualization and manipulation of community taxonomic diversity data. *PLOS Computational Biology*, *13*(2), e1005404. https://doi.org/10.1371/journal.pcbi.1005404

Frias-Lopez, J., Zerkle, A. L., Bonheyo, G. T., & Fouke, B. W. (2002). Partitioning of Bacterial Communities between Seawater and Healthy, Black Band Diseased, and Dead Coral Surfaces. *Applied and Environmental Microbiology*, *68*(5), 2214–2228. https://doi.org/10.1128/AEM.68.5.2214-2228.2002

Galand, P. E., Ruscheweyh, H.-J., Salazar, G., Hochart, C., Henry, N., Hume, B. C. C., Oliveira, P. H., Perdereau, A., Labadie, K., Belser, C., Boissin, E., Romac, S., Poulain, J., Bourdin, G., Iwankow, G., Moulin, C., Armstrong, E. J., Paz-García, D. A., Ziegler, M., … Planes, S. (2023). Diversity of the Pacific Ocean coral reef microbiome. *Nature Communications*, *14*(1), 3039. https://doi.org/10.1038/s41467-023-38500-x

Galkiewicz, J. P., Pratte, Z. A., Gray, M. A., & Kellogg, C. A. (2011). Characterization of culturable bacteria isolated from the cold-water coral Lophelia pertusa. *FEMS Microbiology Ecology*, *77*(2), 333–346. https://doi.org/10.1111/j.1574-6941.2011.01115.x

Garren, M., & Azam, F. (2010). New Method for Counting Bacteria Associated with Coral Mucus. *Applied and Environmental Microbiology*, *76*(18), 6128–6133. https://doi.org/10.1128/AEM.01100-10

Ghanem, R., Soufi Kechaou, E., Ben Souissi, J., & Garrabou, J. (2018). Overview on the distribution of gorgonian species in Tunisian marine coastal waters (central Mediterranean). *Scientia Marina*, *82*(1), 55. https://doi.org/10.3989/scimar.04675.07A

Ghosal, D., Kim, K. W., Zheng, H., Kaplan, M., Truchan, H. K., Lopez, A. E., McIntire, I. E., Vogel, J. P., Cianciotto, N. P., & Jensen, G. J. (2019). In vivo structure of the Legionella type II secretion system by electron cryotomography. *Nature Microbiology*, *4*(12), 2101–2108. https://doi.org/10.1038/s41564-019-0603-6

Gissi, F., Reichelt-Brushett, A. J., Chariton, A. A., Stauber, J. L., Greenfield, P., Humphrey, C., Salmon, M., Stephenson, S. A., Cresswell, T., & Jolley, D. F. (2019). The effect of dissolved nickel and copper on the adult coral Acropora muricata and its microbiome. *Environmental Pollution*, *250*, 792–806. https://doi.org/10.1016/j.envpol.2019.04.030

Glasl, B., Bongaerts, P., Elisabeth, N. H., Hoegh-Guldberg, O., Herndl, G. J., & Frade, P. R. (2017). Microbiome variation in corals with distinct depth distribution ranges across a shallow–mesophotic gradient (15–85 m). *Coral Reefs*, *36*(2), 447–452. https://doi.org/10.1007/s00338-016-1517-x

Glasl, B., Herndl, G. J., & Frade, P. R. (2016). The microbiome of coral surface mucus has a key role in mediating holobiont health and survival upon disturbance. *The ISME Journal*, *10*(9), 2280–2292. https://doi.org/10.1038/ismej.2016.9

Glaze, T. D., Erler, D. V, & Siljanen, H. M. P. (2022). Microbially facilitated nitrogen cycling in tropical corals. *The ISME Journal*, *16*(1), 68–77. https://doi.org/10.1038/s41396-021-01038-1

Glynn, P. W., & Manzello, D. P. (2015). Bioerosion and Coral Reef Growth: A Dynamic Balance. In *Coral Reefs in the Anthropocene* (pp. 67–97). Springer Netherlands. https://doi.org/10.1007/978-94-017-7249-5_4

Godinot, C., Houlbrèque, F., Grover, R., & Ferrier-Pagès, C. (2011). Coral Uptake of Inorganic Phosphorus and Nitrogen Negatively Affected by Simultaneous Changes in Temperature and pH. *PLoS ONE*, *6*(9), e25024. https://doi.org/10.1371/journal.pone.0025024

Goldsmith, D. B., Kellogg, C. A., Morrison, C. L., Gray, M. A., Stone, R. P., Waller, R. G., Brooke, S. D., & Ross, S. W. (2018). Comparison of microbiomes of cold-water corals Primnoa pacifica and Primnoa resedaeformis, with possible link between microbiome composition and host genotype. *Scientific Reports*, *8*(1), 12383. https://doi.org/10.1038/s41598-018-30901-z

Golubic, S., Radtke, G., & Campion-Alsumard, T. Le. (2005). Endolithic fungi in marine ecosystems. *Trends in Microbiology*, *13*(5), 229–235. https://doi.org/10.1016/j.tim.2005.03.007

Gonzalez-Zapata, F. L., Gómez-Osorio, S., & Sánchez, J. A. (2018). Conspicuous endolithic algal associations in a mesophotic reef-building coral. *Coral Reefs*, *37*(3), 705–709. https://doi.org/10.1007/s00338-018-1695-9

Gori, A., Bramanti, L., López-González, P., Thoma, J. N., Gili, J.-M., Grinyó, J., Uceira, V., & Rossi, S. (2012). Characterization of the zooxanthellate and azooxanthellate morphotypes of the Mediterranean gorgonian Eunicella singularis. *Marine Biology*, *159*(7), 1485–1496. https://doi.org/10.1007/s00227-012-1928-3

Gori, A., Reynaud, S., Orejas, C., Gili, J.-M., & Ferrier-Pagès, C. (2014). Physiological performance of the cold-water coral Dendrophyllia cornigera reveals its preference for temperate environments. *Coral Reefs*, *33*(3), 665–674. https://doi.org/10.1007/s00338-014-1167-9

Gori, A., Rossi, S., Linares, C., Berganzo, E., Orejas, C., Dale, M. R., & Gili, J.-M. (2011). Size and spatial structure in deep versus shallow populations of the Mediterranean gorgonian Eunicella singularis (Cap de Creus, northwestern Mediterranean Sea). *Marine Biology*, *158*(8), 1721–1732. https://doi.org/10.1007/s00227-011-1686-7

Gori, A., Viladrich, N., Gili, J.-M., Kotta, M., Cucio, C., Magni, L., Bramanti, L., & Rossi, S. (2012). Reproductive cycle and trophic ecology in deep versus shallow populations of the Mediterranean gorgonian Eunicella singularis (Cap de Creus, northwestern Mediterranean Sea). *Coral Reefs*, *31*(3), 823–837. https://doi.org/10.1007/s00338-012-0904-1

Goslee, S. C., & Urban, D. L. (2007). The **ecodist** Package for Dissimilarity-based Analysis of Ecological Data. *Journal of Statistical Software*, *22*(7). https://doi.org/10.18637/jss.v022.i07

Grange, J. S., Rybarczyk, H., & Tribollet, A. (2015). The three steps of the carbonate biogenic dissolution process by microborers in coral reefs (New Caledonia). *Environmental Science and Pollution Research*, *22*(18), 13625–13637. https://doi.org/10.1007/s11356-014-4069-z

Gray, M. A., Stone, R. P., McLaughlin, M. R., & Kellogg, C. A. (2011). Microbial consortia of gorgonian corals from the Aleutian islands. *FEMS Microbiology Ecology*, *76*(1), 109–120. https://doi.org/10.1111/j.1574-6941.2010.01033.x

Grenié, M., Denelle, P., Tucker, C. M., Munoz, F., & Violle, C. (2017). funrar: An R package to characterize functional rarity. *Diversity and Distributions*, *23*(12), 1365–1371. https://doi.org/10.1111/ddi.12629

Grottoli, A. G., Rodrigues, L. J., & Palardy, J. E. (2006). Heterotrophic plasticity and resilience in bleached corals. *Nature*, *440*(7088), 1186–1189. https://doi.org/10.1038/nature04565

Gu, Z., Gu, L., Eils, R., Schlesner, M., & Brors, B. (2014). *circlize* implements and enhances circular visualization in R. *Bioinformatics*, *30*(19), 2811–2812. https://doi.org/10.1093/bioinformatics/btu393

Guillou, L., Bachar, D., Audic, S., Bass, D., Berney, C., Bittner, L., Boutte, C., Burgaud, G., de Vargas, C., Decelle, J., del Campo, J., Dolan, J. R., Dunthorn, M., Edvardsen, B., Holzmann, M., Kooistra, W. H. C. F., Lara, E., Le Bescot, N., Logares, R., … Christen, R. (2012). The Protist Ribosomal Reference database (PR2): a catalog of unicellular eukaryote Small Sub-Unit rRNA sequences with curated taxonomy. *Nucleic Acids Research*, *41*(D1), D597–D604. https://doi.org/10.1093/nar/gks1160

Hadaidi, G., Gegner, H. M., Ziegler, M., & Voolstra, C. R. (2019). Carbohydrate composition of mucus from scleractinian corals from the central Red Sea. *Coral Reefs*, *38*(1), 21–27. https://doi.org/10.1007/s00338-018-01758-5

Hagedorn, M., Carter, V., Zuchowicz, N., Phillips, M., Penfield, C., Shamenek, B., Vallen, E. A., Kleinhans, F. W., Peterson, K., White, M., & Yancey, P. H. (2015). Trehalose Is a Chemical Attractant in the Establishment of Coral Symbiosis. *PLOS ONE*, *10*(1), e0117087. https://doi.org/10.1371/journal.pone.0117087

Hanada, S. (2014). The Phylum Chloroflexi, the Family Chloroflexaceae, and the Related Phototrophic Families Oscillochloridaceae and Roseiflexaceae. In *The Prokaryotes* (pp. 515–532). Springer Berlin Heidelberg. https://doi.org/10.1007/978-3-642-38954-2_165

Hebbeln, D., Wienberg, C., Dullo, W.-C., Freiwald, A., Mienis, F., Orejas, C., & Titschack, J. (2020). Cold-water coral reefs thriving under hypoxia. *Coral Reefs*, *39*(4), 853–859. https://doi.org/10.1007/s00338-020-01934-6

Hernandez-Agreda, A., Leggat, W., Bongaerts, P., & Ainsworth, T. D. (2016). The Microbial Signature Provides Insight into the Mechanistic Basis of Coral Success across Reef Habitats. *MBio*, *7*(4). https://doi.org/10.1128/mBio.00560-16

Hernandez-Agreda, A., Leggat, W., Bongaerts, P., Herrera, C., & Ainsworth, T. D. (2018). Rethinking the Coral Microbiome: Simplicity Exists within a Diverse Microbial Biosphere. *MBio*, *9*(5). https://doi.org/10.1128/mBio.00812-18

Herndl, G. J., & Velimirov, B. (1985). Bacteria in the coelenteron of Anthozoa: Control of coelenteric bacterial density by the coelenteric fluid. *Journal of Experimental Marine Biology and Ecology*, *93*(1–2), 115–130. https://doi.org/10.1016/0022-0981(85)90153-4

Hochart, C., Paoli, L., Ruscheweyh, H.-J., Salazar, G., Boissin, E., Romac, S., Poulain, J., Bourdin, G., Iwankow, G., Moulin, C., Ziegler, M., Porro, B., Armstrong, E. J., Hume, B. C. C., Aury, J.-M., Pogoreutz, C., Paz-García, D. A., Nugues, M. M., Agostini, S., … Galand, P. E. (2023). Ecology of Endozoicomonadaceae in three coral genera across the Pacific Ocean. *Nature Communications*, *14*(1), 3037. https://doi.org/10.1038/s41467-023-38502-9

Hoegh-Guldberg, O. (1999). Climate change, coral bleaching and the future of the world's coral reefs. *Marine and Freshwater Research*. https://doi.org/10.1071/MF99078

Holm, J. B., & Heidelberg, K. B. (2016). Microbiomes of Muricea californica and M. fruticosa: Comparative Analyses of Two Co-occurring Eastern Pacific Octocorals. *Frontiers in Microbiology*, *7*. https://doi.org/10.3389/fmicb.2016.00917

Hoogenboom, M. O., Campbell, D. A., Beraud, E., DeZeeuw, K., & Ferrier-Pagès, C. (2012). Effects of Light, Food Availability and Temperature Stress on the Function of Photosystem II and Photosystem I of Coral Symbionts. *PLoS ONE*, *7*(1), e30167. https://doi.org/10.1371/journal.pone.0030167

Hou, Y., & Lin, S. (2009). Distinct Gene Number-Genome Size Relationships for Eukaryotes and Non-Eukaryotes: Gene Content Estimation for Dinoflagellate Genomes. *PLoS ONE*, *4*(9), e6978. https://doi.org/10.1371/journal.pone.0006978

Hrdlickova, R., Toloue, M., & Tian, B. (2017). <scp>RNA</scp> -Seq methods for transcriptome analysis. *WIREs RNA*, *8*(1). https://doi.org/10.1002/wrna.1364

Huggett, M. J., & Apprill, A. (2019). Coral microbiome database: Integration of sequences reveals high diversity and relatedness of coral-associated microbes. *Environmental Microbiology Reports*, *11*(3), 372–385. https://doi.org/10.1111/1758-2229.12686

Hyatt, D., Chen, G.-L., LoCascio, P. F., Land, M. L., Larimer, F. W., & Hauser, L. J. (2010). Prodigal: prokaryotic gene recognition and translation initiation site identification. *BMC Bioinformatics*, *11*(1), 119. https://doi.org/10.1186/1471-2105-11-119

Ikeuchi, M., Shukla, V. K., Pakrasi, H. B., & noue, Y. (1995). Directed inactivation of the psbl gene does not affect Photosystem II in the cyanobacterium Synechocystis sp. PCC 6803. *Molecular and General Genetics MGG*, *249*(6), 622–628. https://doi.org/10.1007/BF00418031

Janouškovec, J., Horák, A., Barott, K. L., Rohwer, F. L., & Keeling, P. J. (2012). Global analysis of plastid diversity reveals apicomplexan-related lineages in coral reefs. *Current Biology*, *22*(13), R518–R519. https://doi.org/10.1016/j.cub.2012.04.047

Jari Oksanen, G. L. S. F. G. B., Roeland Kindt, P. L. P. R. M., R.B. O'Hara, P. S. M. H. H. S., Eduard Szoecs, H. W. M. B., Michael Bedward, B. B. D. B., Gustavo Carvalho, M. C. M. D. C., Sebastien Durand, H. B. A. E. R. F. M. F. B. F. G. H. M. O. H. L. L. D. M. M.-H. O., Eduardo Ribeiro Cunha, T. S. A. S. C. J. F. T. B., & James Weedon. (2022). *Title Community Ecology Package*.

Järnegren, J., Brooke, S., & Jensen, H. (2017). Effects of drill cuttings on larvae of the cold-water coral Lophelia pertusa. *Deep Sea Research Part II: Topical Studies in Oceanography*, *137*, 454–462. https://doi.org/10.1016/j.dsr2.2016.06.014

Jensen, S., Hovland, M., Lynch, M. D. J., & Bourne, D. G. (2019). Diversity of deep-water coral-associated bacteria and comparison across depth gradients. *FEMS Microbiology Ecology*, *95*(7). https://doi.org/10.1093/femsec/fiz091

Jernigan, K. K., & Bordenstein, S. R. (2014). Ankyrin domains across the Tree of Life. *PeerJ*, *2*, e264. https://doi.org/10.7717/peerj.264

Jernigan, K. K., & Bordenstein, S. R. (2015). Tandem-repeat protein domains across the tree of life. *PeerJ*, *3*, e732. https://doi.org/10.7717/peerj.732

Joel A Boyd. (2019). Comparative genomics using EnrichM. Joel A Boyd Ben J Woodcroft Gene W Tyson. 2019. In preparation. *In Preparation*. https://github.com/geronimp/enrichM

Johnson, X., Wostrikoff, K., Finazzi, G., Kuras, R., Schwarz, C., Bujaldon, S., Nickelsen, J., Stern, D. B., Wollman, F.-A., & Vallon, O. (2010). MRL1, a Conserved Pentatricopeptide Repeat Protein, Is Required for Stabilization of *rbcL* mRNA in *Chlamydomonas* and *Arabidopsis* . *The Plant Cell*, *22*(1), 234–248. https://doi.org/10.1105/tpc.109.066266

Jorissen, H., Galand, P. E., Bonnard, I., Meiling, S., Raviglione, D., Meistertzheim, A.-L., Hédouin, L., Banaigs, B., Payri, C. E., & Nugues, M. M. (2021). Coral larval settlement preferences linked to crustose coralline algae with distinct chemical and microbial signatures. *Scientific Reports*, *11*(1), 14610. https://doi.org/10.1038/s41598-021-94096-6

Kahng, S. E., Garcia-Sais, J. R., Spalding, H. L., Brokovich, E., Wagner, D., Weil, E., Hinderstein, L., & Toonen, R. J. (2010). Community ecology of mesophotic coral reef ecosystems. *Coral Reefs*, *29*(2), 255–275. https://doi.org/10.1007/s00338-010-0593-6

Kanehisa, M. (2000). KEGG: Kyoto Encyclopedia of Genes and Genomes. *Nucleic Acids Research*, *28*(1), 27–30. https://doi.org/10.1093/nar/28.1.27

Kanehisa, M. (2019). Toward understanding the origin and evolution of cellular organisms. *Protein Science*, *28*(11), 1947–1951. https://doi.org/10.1002/pro.3715

Kang, D. D., Froula, J., Egan, R., & Wang, Z. (2015). MetaBAT, an efficient tool for accurately reconstructing single genomes from complex microbial communities. *PeerJ*, *3*, e1165. https://doi.org/10.7717/peerj.1165

Kanonenberg, K., Smits, S. H. J., & Schmitt, L. (2019). Functional Reconstitution of HlyB, a Type I Secretion ABC Transporter, in Saposin-A Nanoparticles. *Scientific Reports*, *9*(1), 8436. https://doi.org/10.1038/s41598-019-44812-0

Keller-Costa, T., Eriksson, D., Gonçalves, J. M. S., Gomes, N. C. M., Lago-Lestón, A., & Costa, R. (2017). The gorgonian coral Eunicella labiata hosts a distinct prokaryotic consortium amenable to cultivation. *FEMS Microbiology Ecology*, *93*(12). https://doi.org/10.1093/femsec/fix143

Keller-Costa, T., Kozma, L., Silva, S. G., Toscan, R., Gonçalves, J., Lago-Lestón, A., Kyrpides, N. C., Nunes da Rocha, U., & Costa, R. (2022). Metagenomics-resolved genomics provides novel insights into chitin turnover, metabolic specialization, and niche partitioning in the octocoral microbiome. *Microbiome*, *10*(1), 151. https://doi.org/10.1186/s40168-022-01343-7

Keller-Costa, T., Lago-Lestón, A., Saraiva, J. P., Toscan, R., Silva, S. G., Gonçalves, J., Cox, C. J., Kyrpides, N., Nunes da Rocha, U., & Costa, R. (2021). Metagenomic insights into the taxonomy, function, and dysbiosis of prokaryotic communities in octocorals. *Microbiome*, *9*(1), 72. https://doi.org/10.1186/s40168-021-01031-y

Keller-Costa, T., Silva, R., Lago-Lestón, A., & Costa, R. (2016). Genomic Insights into *Aquimarina* sp. Strain EL33, a Bacterial Symbiont of the Gorgonian Coral *Eunicella labiata*. *Genome Announcements*, *4*(4). https://doi.org/10.1128/genomeA.00855-16

Kellogg, C. A., Goldsmith, D. B., & Gray, M. A. (2017). Biogeographic Comparison of Lophelia-Associated Bacterial Communities in the Western Atlantic Reveals Conserved Core Microbiome. *Frontiers in Microbiology*, *8*. https://doi.org/10.3389/fmicb.2017.00796

Kellogg, C. A., Lisle, J. T., & Galkiewicz, J. P. (2009). Culture-Independent Characterization of Bacterial Communities Associated with the Cold-Water Coral

Lophelia pertusa in the Northeastern Gulf of Mexico. *Applied and Environmental Microbiology*, *75*(8), 2294–2303. https://doi.org/10.1128/AEM.02357-08

Kellogg, C. A., Ross, S. W., & Brooke, S. D. (2016). Bacterial community diversity of the deep-sea octocoral *Paramuricea placomus*. *PeerJ*, *4*, e2529. https://doi.org/10.7717/peerj.2529

Kim, K., & Rypien, K. (2015). Aspergillosis of Caribbean Sea Fan Corals, *Gorgonia* spp. In *Diseases of Coral* (pp. 236–241). John Wiley & Sons, Inc. https://doi.org/10.1002/9781118828502.ch16

Kim, S., & Kim, K.-J. (2018). Crystal Structure of Acyl-CoA Oxidase 3 from Yarrowia lipolytica with Specificity for Short-Chain Acyl-CoA. *Journal of Microbiology and Biotechnology*, *28*(4), 597–605. https://doi.org/10.4014/jmb.1711.11032

Kimes, N. E., Van Nostrand, J. D., Weil, E., Zhou, J., & Morris, P. J. (2010). Microbial functional structure of *Montastraea faveolata* , an important Caribbean reef-building coral, differs between healthy and yellow-band diseased colonies. *Environmental Microbiology*, *12*(2), 541–556. https://doi.org/10.1111/j.1462-2920.2009.02113.x

Klawonn, I., Bonaglia, S., Brüchert, V., & Ploug, H. (2015). Aerobic and anaerobic nitrogen transformation processes in N2-fixing cyanobacterial aggregates. *The ISME Journal*, *9*(6), 1456–1466. https://doi.org/10.1038/ismej.2014.232

Kooperman, N., Ben-Dov, E., Kramarsky-Winter, E., Barak, Z., & Kushmaro, A. (2007). Coral mucus-associated bacterial communities from natural and aquarium environments. *FEMS Microbiology Letters*, *276*(1), 106–113. https://doi.org/10.1111/j.1574-6968.2007.00921.x

Kořený, L., Sobotka, R., Janouškovec, J., Keeling, P. J., & Oborník, M. (2011). Tetrapyrrole Synthesis of Photosynthetic Chromerids Is Likely Homologous to the Unusual Pathway of Apicomplexan Parasites . *The Plant Cell*, *23*(9), 3454–3462. https://doi.org/10.1105/tpc.111.089102

Krediet, C. J., Ritchie, K. B., Alagely, A., & Teplitski, M. (2013). Members of native coral microbiota inhibit glycosidases and thwart colonization of coral mucus by an opportunistic pathogen. *The ISME Journal*, *7*(5), 980–990. https://doi.org/10.1038/ismej.2012.164

Kwong, W. K., del Campo, J., Mathur, V., Vermeij, M. J. A., & Keeling, P. J. (2019). A widespread coral-infecting apicomplexan with chlorophyll biosynthesis genes. *Nature*, *568*(7750), 103–107. https://doi.org/10.1038/s41586-019-1072-z

La Rivière, M., Garrabou, J., & Bally, M. (2015). Evidence for host specificity among dominant bacterial symbionts in temperate gorgonian corals. *Coral Reefs*, *34*(4), 1087–1098. https://doi.org/10.1007/s00338-015-1334-7

Laiolo, E., Alam, I., Uludag, M., Jamil, T., Agusti, S., Gojobori, T., Acinas, S. G., Gasol, J. M., & Duarte, C. M. (2024). Metagenomic probing toward an atlas of the taxonomic and metabolic foundations of the global ocean genome. *Frontiers in Science*, *1*. https://doi.org/10.3389/fsci.2023.1038696

Lamb, J. B., Willis, B. L., Fiorenza, E. A., Couch, C. S., Howard, R., Rader, D. N., True, J. D., Kelly, L. A., Ahmad, A., Jompa, J., & Harvell, C. D. (2018). Plastic waste associated with disease on coral reefs. *Science*, *359*(6374), 460–462. https://doi.org/10.1126/science.aar3320

Landsberg, J. H., Kiryu, Y., Peters, E. C., Wilson, P. W., Perry, N., Waters, Y., Maxwell, K. E., Huebner, L. K., & Work, T. M. (2020). Stony Coral Tissue Loss Disease in Florida Is Associated With Disruption of Host–Zooxanthellae Physiology. *Frontiers in Marine Science*, *7*. https://doi.org/10.3389/fmars.2020.576013

Lapointe, B. E., Brewton, R. A., Herren, L. W., Porter, J. W., & Hu, C. (2019). Nitrogen enrichment, altered stoichiometry, and coral reef decline at Looe Key, Florida Keys, USA: a 3-decade study. *Marine Biology*, *166*(8), 108. https://doi.org/10.1007/s00227-019-3538-9

Le Goff-Vitry, M. C., Pybus, O. G., & Rogers, A. D. (2004). Genetic structure of the deep-sea coral *Lophelia pertusa* in the northeast Atlantic revealed by microsatellites and internal transcribed spacer sequences. *Molecular Ecology*, *13*(3), 537–549. https://doi.org/10.1046/j.1365-294X.2004.2079.x

Lee, S., Inzerillo, S., Lee, G. Y., Bosire, E. M., Mahato, S. K., & Song, J. (2022). Glycan-mediated molecular interactions in bacterial pathogenesis. *Trends in Microbiology*, *30*(3), 254–267. https://doi.org/10.1016/j.tim.2021.06.011

Leggat, W., Ainsworth, T. D., Dove, S., & Hoegh-Guldberg, O. (2006). Aerial exposure influences bleaching patterns. *Coral Reefs*, *25*(3), 452–452. https://doi.org/10.1007/s00338-006-0128-3

Leite, D. C. A., Leão, P., Garrido, A. G., Lins, U., Santos, H. F., Pires, D. O., Castro, C. B., van Elsas, J. D., Zilberberg, C., Rosado, A. S., & Peixoto, R. S. (2017). Broadcast Spawning Coral Mussismilia hispida Can Vertically Transfer its Associated Bacterial Core. *Frontiers in Microbiology*, *8*. https://doi.org/10.3389/fmicb.2017.00176

Lema, K. A., Bourne, D. G., & Willis, B. L. (2014). Onset and establishment of diazotrophs and other bacterial associates in the early life history stages of the coral

Acropora millepora. *Molecular Ecology*, *23*(19), 4682–4695. https://doi.org/10.1111/mec.12899

Lesser, M., Mazel, C., Gorbunov, M., Science, P. F.-, & 2004, undefined. (2008). Discovery of symbiotic nitrogen-fixing cyanobacteria in corals. *Science.Org*, *305*(5686), 997–1000. https://doi.org/10.1126/science.1099128

Lesser, M. P. (2007). Coral reef bleaching and global climate change: Can corals survive the next century? *Proceedings of the National Academy of Sciences*, *104*(13), 5259–5260. https://doi.org/10.1073/pnas.0700910104

Levy Karin, E., Mirdita, M., & Söding, J. (2020). MetaEuk—sensitive, high-throughput gene discovery, and annotation for large-scale eukaryotic metagenomics. *Microbiome*, *8*(1), 48. https://doi.org/10.1186/s40168-020-00808-x

Li, D., Liu, C.-M., Luo, R., Sadakane, K., & Lam, T.-W. (2015a). MEGAHIT: an ultra-fast single-node solution for large and complex metagenomics assembly via succinct de Bruijn graph. *Bioinformatics*, *31*(10), 1674–1676. https://doi.org/10.1093/bioinformatics/btv033

Li, D., Liu, C.-M., Luo, R., Sadakane, K., & Lam, T.-W. (2015b). MEGAHIT: an ultra-fast single-node solution for large and complex metagenomics assembly via succinct de Bruijn graph. *Bioinformatics*, *31*(10), 1674–1676. https://doi.org/10.1093/bioinformatics/btv033

Li, H., & Durbin, R. (2009). Fast and accurate short read alignment with Burrows-Wheeler transform. *Bioinformatics (Oxford, England)*, *25*(14), 1754–1760. https://doi.org/10.1093/bioinformatics/btp324

Li, M., Sheng, H.-X., Dai, M., & Kao, S.-J. (2023). Understanding nitrogen dynamics in coral holobionts: comprehensive review of processes, advancements, gaps, and future directions. *Frontiers in Marine Science*, *10*. https://doi.org/10.3389/fmars.2023.1203399

Lima, L. F. O., Alker, A. T., Papudeshi, B., Morris, M. M., Edwards, R. A., de Putron, S. J., & Dinsdale, E. A. (2023). Coral and Seawater Metagenomes Reveal Key Microbial Functions to Coral Health and Ecosystem Functioning Shaped at Reef Scale. *Microbial Ecology*, *86*(1), 392–407. https://doi.org/10.1007/s00248-022-02094-6

Linares, D., Jean, N., Van Overtvelt, P., Ouidir, T., Hardouin, J., Blache, Y., & Molmeret, M. (2016). The marine bacteria *Shewanella frigidimarina* <scp>NCIMB400</scp> upregulates the type <scp>VI</scp> secretion system during early biofilm formation. *Environmental Microbiology Reports*, *8*(1), 110–121. https://doi.org/10.1111/1758-2229.12358

Littman, R. A., Willis, B. L., Pfeffer, C., & Bourne, D. G. (2009). Diversities of coral-associated bacteria differ with location, but not species, for three acroporid corals on the Great Barrier Reef. *FEMS Microbiology Ecology*, *68*(2), 152–163. https://doi.org/10.1111/j.1574-6941.2009.00666.x

Littman, R., Willis, B., & Bourne, D. (2009). Bacterial communities of juvenile corals infected with different Symbiodinium (dinoflagellate) clades. *Marine Ecology Progress Series*, *389*, 45–59. https://doi.org/10.3354/meps08180

LOBBAN, C. S., RAYMUNDO, L. M., & MONTAGNES, D. J. S. (2011). Porpostoma guamensis n. sp., a Philasterine Scuticociliate Associated With Brown-Band Disease of Corals. *Journal of Eukaryotic Microbiology*, *58*(2), 103–113. https://doi.org/10.1111/j.1550-7408.2010.00526.x

Lohr, K. E., Khattri, R. B., Guingab-Cagmat, J., Camp, E. F., Merritt, M. E., Garrett, T. J., & Patterson, J. T. (2019). Metabolomic profiles differ among unique genotypes of a threatened Caribbean coral. *Scientific Reports*, *9*(1), 6067. https://doi.org/10.1038/s41598-019-42434-0

Lombard, F., Bourdin, G., Pesant, S., Agostini, S., Baudena, A., Boissin, E., Cassar, N., Clampitt, M., Conan, P., Da Silva, O., Dimier, C., Douville, E., Elineau, A., Fin, J., Flores, J. M., Ghiglione, J.-F., Hume, B. C. C., Jalabert, L., John, S. G., … Gorsky, G. (2023). Open science resources from the Tara Pacific expedition across coral reef and surface ocean ecosystems. *Scientific Data*, *10*(1), 324. https://doi.org/10.1038/s41597-022-01757-w

Lu, Y., Jiang, J., Zhao, H., Han, X., Xiang, Y., & Zhou, W. (2020). Clade-Specific Sterol Metabolites in Dinoflagellate Endosymbionts Are Associated with Coral Bleaching in Response to Environmental Cues. *MSystems*, *5*(5). https://doi.org/10.1128/mSystems.00765-20

Lunak, Z. R., & Noel, K. D. (2015). A quinol oxidase, encoded by cyoABCD, is utilized to adapt to lower O2 concentrations in Rhizobium etli CFN42. *Microbiology*, *161*(1), 203–212. https://doi.org/10.1099/mic.0.083386-0

Lux, R., Jahreis, K., Bettenbrock, K., Parkinson, J. S., & Lengeler, J. W. (1995). Coupling the phosphotransferase system and the methyl-accepting chemotaxis protein-dependent chemotaxis signaling pathways of Escherichia coli. *Proceedings of the National Academy of Sciences*, *92*(25), 11583–11587. https://doi.org/10.1073/pnas.92.25.11583

Ma, W., Zhang, S., Li, Z., Jiang, M., Wang, S., Lu, W., Bi, X., Jiang, H., Zhang, H., & Wei, Z. (2022). Enhancing Protein Function Prediction Performance by Utilizing

AlphaFold-Predicted Protein Structures. *Journal of Chemical Information and Modeling*, *62*(17), 4008–4017. https://doi.org/10.1021/acs.jcim.2c00885

Magnusson, S., Fine, M., & Kühl, M. (2007). Light microclimate of endolithic phototrophs in the scleractinian corals Montipora monasteriata and Porites cylindrica. *Marine Ecology Progress Series*, *332*, 119–128. https://doi.org/10.3354/meps332119

Maher, R. L., Rice, M. M., McMinds, R., Burkepile, D. E., & Vega Thurber, R. (2019). Multiple stressors interact primarily through antagonism to drive changes in the coral microbiome. *Scientific Reports*, *9*(1), 6834. https://doi.org/10.1038/s41598-019-43274-8

Marcelino, V. R., & Verbruggen, H. (2016). Multi-marker metabarcoding of coral skeletons reveals a rich microbiome and diverse evolutionary origins of endolithic algae. *Scientific Reports*, *6*(1), 31508. https://doi.org/10.1038/srep31508

Mariño-Tapia, I., Enriquez, C., Silva, R., Mendoza-Baldwin, E., Escalante-Mancera, E., & Ruiz-Renteria, F. (2014). COMPARATIVE MORPHODYNAMICS BETWEEN EXPOSED AND REEF PROTECTED BEACHES UNDER HURRRICANE CONDITIONS. *Coastal Engineering Proceedings*, *1*(34), 55. https://doi.org/10.9753/icce.v34.sediment.55

Martin, M. (2011). Cutadapt removes adapter sequences from high-throughput sequencing reads. *EMBnet.Journal*, *17*(1), 10. https://doi.org/10.14806/ej.17.1.200

Mathur, V., del Campo, J., Kolisko, M., & Keeling, P. J. (2018). Global diversity and distribution of close relatives of apicomplexan parasites. *Environmental Microbiology*, *20*(8), 2824–2833. https://doi.org/10.1111/1462-2920.14134

Matos, F. L., Company, J. B., & Cunha, M. R. (2021). Mediterranean seascape suitability for Lophelia pertusa: Living on the edge. *Deep Sea Research Part I: Oceanographic Research Papers*, *170*, 103496. https://doi.org/10.1016/j.dsr.2021.103496

McFadden, C. S., Quattrini, A. M., Brugler, M. R., Cowman, P. F., Dueñas, L. F., Kitahara, M. V, Paz-García, D. A., Reimer, J. D., & Rodríguez, E. (2021). Phylogenomics, Origin, and Diversification of Anthozoans (Phylum Cnidaria). *Systematic Biology*, *70*(4), 635–647. https://doi.org/10.1093/sysbio/syaa103

Meistertzheim, Anne.-L., Lartaud, F., Arnaud-Haond, S., Kalenitchenko, D., Bessalam, M., Le Bris, N., & Galand, P. E. (2016). Patterns of bacteria-host associations suggest different ecological strategies between two reef building cold-water coral species. *Deep Sea Research Part I: Oceanographic Research Papers*, *114*, 12–22. https://doi.org/10.1016/j.dsr.2016.04.013

Menzel, L. P., Tondo, C., Stein, B., & Bigger, C. H. (2015). Histology and ultrastructure of the coenenchyme of the octocoral Swiftia exserta, a model organism for innate immunity/graft rejection. *Zoology*, *118*(2), 115–124. https://doi.org/10.1016/j.zool.2014.09.002

Mera, H., & Bourne, D. G. (2018). Disentangling causation: complex roles of coral-associated microorganisms in disease. *Environmental Microbiology*, *20*(2), 431–449. https://doi.org/10.1111/1462-2920.13958

Meron, D., Rodolfo-Metalpa, R., Cunning, R., Baker, A. C., Fine, M., & Banin, E. (2012). Changes in coral microbial communities in response to a natural pH gradient. *The ISME Journal*, *6*(9), 1775–1785. https://doi.org/10.1038/ismej.2012.19

Meyer, J. L., Castellanos-Gell, J., Aeby, G. S., Häse, C. C., Ushijima, B., & Paul, V. J. (2019a). Microbial Community Shifts Associated With the Ongoing Stony Coral Tissue Loss Disease Outbreak on the Florida Reef Tract. *Frontiers in Microbiology*, *10*. https://doi.org/10.3389/fmicb.2019.02244

Meyer, J. L., Castellanos-Gell, J., Aeby, G. S., Häse, C. C., Ushijima, B., & Paul, V. J. (2019b). Microbial Community Shifts Associated With the Ongoing Stony Coral Tissue Loss Disease Outbreak on the Florida Reef Tract. *Frontiers in Microbiology*, *10*. https://doi.org/10.3389/fmicb.2019.02244

Meyer, J. L., Paul, V. J., Raymundo, L. J., & Teplitski, M. (2017). Comparative Metagenomics of the Polymicrobial Black Band Disease of Corals. *Frontiers in Microbiology*, *8*. https://doi.org/10.3389/fmicb.2017.00618

Middelburg, J. J., Mueller, C. E., Veuger, B., Larsson, A. I., Form, A., & Oevelen, D. van. (2015a). Discovery of symbiotic nitrogen fixation and chemoautotrophy in cold-water corals. *Scientific Reports*, *5*(1), 17962. https://doi.org/10.1038/srep17962

Middelburg, J. J., Mueller, C. E., Veuger, B., Larsson, A. I., Form, A., & Oevelen, D. van. (2015b). Discovery of symbiotic nitrogen fixation and chemoautotrophy in cold-water corals. *Scientific Reports*, *5*(1), 17962. https://doi.org/10.1038/srep17962

Milne-Davies, B., Wimmi, S., & Diepold, A. (2021). Adaptivity and dynamics in type III secretion systems. *Molecular Microbiology*, *115*(3), 395–411. https://doi.org/10.1111/mmi.14658

Moberg, F., & Folke, C. (1999). Ecological goods and services of coral reef ecosystems. *Ecological Economics*, *29*(2), 215–233. https://doi.org/10.1016/S0921-8009(99)00009-9

Mohamed, A. R., Cumbo, V., Harii, S., Shinzato, C., Chan, C. X., Ragan, M. A., Bourne, D. G., Willis, B. L., Ball, E. E., Satoh, N., & Miller, D. J. (2016). The transcriptomic response of the coral *Acropora digitifera* to a competent *Symbiodinium* strain: the symbiosome as an arrested early phagosome. *Molecular Ecology*, *25*(13), 3127–3141. https://doi.org/10.1111/mec.13659

Mohamed, A. R., Cumbo, V. R., Harii, S., Shinzato, C., Chan, C. X., Ragan, M. A., Satoh, N., Ball, E. E., & Miller, D. J. (2018). Deciphering the nature of the coral–Chromera association. *The ISME Journal*, *12*(3), 776–790. https://doi.org/10.1038/s41396-017-0005-9

Mohamed, A. R., Ochsenkühn, M. A., Kazlak, A., Moustafa, A., & Amin, S. A. (2023). The coral microbiome: Towards an understanding of the molecular mechanisms of coral-microbiota interactions. *FEMS Microbiology Reviews*. https://doi.org/10.1093/femsre/fuad005

Moore, L. D., Le, T., & Fan, G. (2013). DNA Methylation and Its Basic Function. *Neuropsychopharmacology*, *38*(1), 23–38. https://doi.org/10.1038/npp.2012.112

Moriarity, J. L., Hurt, K. J., Resnick, A. C., Storm, P. B., Laroy, W., Schnaar, R. L., & Snyder, S. H. (2002). UDP-glucuronate Decarboxylase, a Key Enzyme in Proteoglycan Synthesis. *Journal of Biological Chemistry*, *277*(19), 16968–16975. https://doi.org/10.1074/jbc.M109316200

Morrison-Gardiner, S. (2002). *Dominant fungi from Australian coral reefs*.

Morrow, K. M., Muller, E., & Lesser, M. P. (2018). *How Does the Coral Microbiome Cause, Respond to, or Modulate the Bleaching Process?* (pp. 153–188). https://doi.org/10.1007/978-3-319-75393-5_7

Mueller, C. E., Larsson, A. I., Veuger, B., Middelburg, J. J., & van Oevelen, D. (2014). Opportunistic feeding on various organic food sources by the cold-water coral &lt;i&gt;Lophelia pertusa&lt;/i&gt; *Biogeosciences*, *11*(1), 123–133. https://doi.org/10.5194/bg-11-123-2014

Mulhall, M. (2009). *SAVING THE RAINFORESTS OF THE SEA: AN ANALYSIS OF INTERNATIONAL EFFORTS TO CONSERVE CORAL REEFS*. http://www.fao.org/newsroom/en/news/2005/102911/index.html.

Muscatine, L., & Porter, J. W. (1977). Reef Corals: Mutualistic Symbioses Adapted to Nutrient-Poor Environments. *BioScience*, *27*(7), 454–460. https://doi.org/10.2307/1297526

Naumann, M. S., Orejas, C., & Ferrier-Pagès, C. (2014). Species-specific physiological response by the cold-water corals Lophelia pertusa and Madrepora oculata to variations within their natural temperature range. *Deep Sea Research Part II:*

Topical Studies in Oceanography, *99*, 36–41. https://doi.org/10.1016/j.dsr2.2013.05.025

Neave, M. J., Apprill, A., Ferrier-Pagès, C., & Voolstra, C. R. (2016a). Diversity and function of prevalent symbiotic marine bacteria in the genus Endozoicomonas. *Applied Microbiology and Biotechnology*, *100*(19), 8315–8324. https://doi.org/10.1007/s00253-016-7777-0

Neave, M. J., Apprill, A., Ferrier-Pagès, C., & Voolstra, C. R. (2016b). Diversity and function of prevalent symbiotic marine bacteria in the genus Endozoicomonas. *Applied Microbiology and Biotechnology*, *100*(19), 8315–8324. https://doi.org/10.1007/s00253-016-7777-0

Neave, M. J., Apprill, A., Ferrier-Pagès, C., & Voolstra, C. R. (2016c). Diversity and function of prevalent symbiotic marine bacteria in the genus Endozoicomonas. *Applied Microbiology and Biotechnology*, *100*(19), 8315–8324. https://doi.org/10.1007/s00253-016-7777-0

Neave, M. J., Michell, C. T., Apprill, A., & Voolstra, C. R. (2017). Endozoicomonas genomes reveal functional adaptation and plasticity in bacterial strains symbiotically associated with diverse marine hosts. *Scientific Reports*, *7*(1), 40579. https://doi.org/10.1038/srep40579

Neave, M. J., Rachmawati, R., Xun, L., Michell, C. T., Bourne, D. G., Apprill, A., & Voolstra, C. R. (2017). Differential specificity between closely related corals and abundant *Endozoicomonas* endosymbionts across global scales. *The ISME Journal*, *11*(1), 186–200. https://doi.org/10.1038/ismej.2016.95

Neulinger, S. C., Gärtner, A., Järnegren, J., Ludvigsen, M., Lochte, K., & Dullo, W.-C. (2009). Tissue-Associated " *Candidatus* Mycoplasma corallicola" and Filamentous Bacteria on the Cold-Water Coral *Lophelia pertusa* (Scleractinia). *Applied and Environmental Microbiology*, *75*(5), 1437–1444. https://doi.org/10.1128/AEM.01781-08

Neulinger, S. C., Järnegren, J., Ludvigsen, M., Lochte, K., & Dullo, W.-C. (2008). Phenotype-Specific Bacterial Communities in the Cold-Water Coral *Lophelia pertusa* (Scleractinia) and Their Implications for the Coral's Nutrition, Health, and Distribution. *Applied and Environmental Microbiology*, *74*(23), 7272–7285. https://doi.org/10.1128/AEM.01777-08

Nguyen, M. T. H. D., Liu, M., & Thomas, T. (2014). Ankyrin-repeat proteins from sponge symbionts modulate amoebal phagocytosis. *Molecular Ecology*, *23*(6), 1635–1645. https://doi.org/10.1111/mec.12384

Obiol, A. (2020). *eukaryotesV4*. https://github.com/aleixop/eukaryotesV4

Obiol, A., Giner, C. R., Sánchez, P., Duarte, C. M., Acinas, S. G., & Massana, R. (2020). A metagenomic assessment of microbial eukaryotic diversity in the global ocean. *Molecular Ecology Resources*, *20*(3), 718–731. https://doi.org/10.1111/1755-0998.13147

Ochsenkühn, M. A., Schmitt-Kopplin, P., Harir, M., & Amin, S. A. (2018). Coral metabolite gradients affect microbial community structures and act as a disease cue. *Communications Biology*, *1*(1), 184. https://doi.org/10.1038/s42003-018-0189-1

Odum, H. T., & Odum, E. P. (1955). Trophic Structure and Productivity of a Windward Coral Reef Community on Eniwetok Atoll. *Ecological Monographs*, *25*(3), 291–320. https://doi.org/10.2307/1943285

Oevelen, D. van, Duineveld, G., Lavaleye, M., Mienis, F., Soetaert, K., & Heip, C. H. R. (2009). The cold-water coral community as hotspot of carbon cycling on continental margins: A food-web analysis from Rockall Bank (northeast Atlantic). *Limnology and Oceanography*, *54*(6), 1829–1844. https://doi.org/10.4319/lo.2009.54.6.1829

Olm, M. R., Brown, C. T., Brooks, B., & Banfield, J. F. (2017). dRep: a tool for fast and accurate genomic comparisons that enables improved genome recovery from metagenomes through de-replication. *The ISME Journal*, *11*(12), 2864–2868. https://doi.org/10.1038/ismej.2017.126

Orejas, C., Taviani, M., Ambroso, S., Andreou, V., Bilan, M., Bo, M., Brooke, S., Buhl-Mortensen, P., Cordes, E., Dominguez-Carrió, C., Ferrier-Pagès, C., Godinho, A., Gori, A., Grinyó, J., Gutiérrez-Zárate, C., Hennige, S., Jiménez, C., Larsson, A. I., Lartaud, F., … Carreiro-Silva, M. (2019). *38 Cold-Water Coral in Aquaria: Advances and Challenges. A Focus on the Mediterranean* (pp. 435–471). https://doi.org/10.1007/978-3-319-91608-8_38

Page, C. A., & Willis, B. L. (2008). Epidemiology of skeletal eroding band on the Great Barrier Reef and the role of injury in the initiation of this widespread coral disease. *Coral Reefs*, *27*(2), 257–272. https://doi.org/10.1007/s00338-007-0317-8

Pantos, O., Bongaerts, P., Dennis, P. G., Tyson, G. W., & Hoegh-Guldberg, O. (2015). Habitat-specific environmental conditions primarily control the microbiomes of the coral Seriatopora hystrix. *The ISME Journal*, *9*(9), 1916–1927. https://doi.org/10.1038/ismej.2015.3

Parks, D. H., Chuvochina, M., Chaumeil, P.-A., Rinke, C., Mussig, A. J., & Hugenholtz, P. (2020). A complete domain-to-species taxonomy for Bacteria and Archaea. *Nature Biotechnology*, *38*(9), 1079–1086. https://doi.org/10.1038/s41587-020-0501-8

Parks, D. H., Imelfort, M., Skennerton, C. T., Hugenholtz, P., & Tyson, G. W. (2015). CheckM: assessing the quality of microbial genomes recovered from isolates, single cells, and metagenomes. *Genome Research*, *25*(7), 1043–1055. https://doi.org/10.1101/gr.186072.114

Peano, C., Pietrelli, A., Consolandi, C., Rossi, E., Petiti, L., Tagliabue, L., De Bellis, G., & Landini, P. (2013). An efficient rRNA removal method for RNA sequencing in GC-rich bacteria. *Microbial Informatics and Experimentation*, *3*(1), 1. https://doi.org/10.1186/2042-5783-3-1

Pei, J.-Y., Yu, W.-F., Zhang, J.-J., Kuo, T.-H., Chung, H.-H., Hu, J.-J., Hsu, C.-C., & Yu, K.-F. (2022). Mass spectrometry–based metabolomic signatures of coral bleaching under thermal stress. *Analytical and Bioanalytical Chemistry*, *414*(26), 7635–7646. https://doi.org/10.1007/s00216-022-04294-y

Peixoto, R. S., Rosado, P. M., Leite, D. C. de A., Rosado, A. S., & Bourne, D. G. (2017). Beneficial Microorganisms for Corals (BMC): Proposed Mechanisms for Coral Health and Resilience. *Frontiers in Microbiology*, *8*. https://doi.org/10.3389/fmicb.2017.00341

Peng, L., Ni, B.-J., Ye, L., & Yuan, Z. (2015). The combined effect of dissolved oxygen and nitrite on N2O production by ammonia oxidizing bacteria in an enriched nitrifying sludge. *Water Research*, *73*, 29–36. https://doi.org/10.1016/j.watres.2015.01.021

Penn, K., Wu, D., Eisen, J. A., & Ward, N. (2006). Characterization of Bacterial Communities Associated with Deep-Sea Corals on Gulf of Alaska Seamounts. *Applied and Environmental Microbiology*, *72*(2), 1680–1683. https://doi.org/10.1128/AEM.72.2.1680-1683.2006

Pereira, C. S., Santos, A. J. M., Bejerano-Sagie, M., Correia, P. B., Marques, J. C., & Xavier, K. B. (2012). Phosphoenolpyruvate phosphotransferase system regulates detection and processing of the quorum sensing signal autoinducer-2. *Molecular Microbiology*, *84*(1), 93–104. https://doi.org/10.1111/j.1365-2958.2012.08010.x

Pereira, P. H. F., Fernandes, L., Jesus, H. E., Costa, P. G., Lacerda, C. H. F., Mies, M., Bianchini, A., & Santos, H. F. (2023). The Impact of Highly Weathered Oil from the Most Extensive Oil Spill in Tropical Oceans (Brazil) on the Microbiome of the Coral Mussismilia harttii. *Microorganisms*, *11*(8), 1935. https://doi.org/10.3390/microorganisms11081935

Pérez-Losada, M., Castro-Nallar, E., Bendall, M. L., Freishtat, R. J., & Crandall, K. A. (2015). Dual Transcriptomic Profiling of Host and Microbiota during Health and

Disease in Pediatric Asthma. *PLOS ONE*, *10*(6), e0131819. https://doi.org/10.1371/journal.pone.0131819

Pernice, M., & Levy, O. (2014). Novel tools integrating metabolic and gene function to study the impact of the environment on coral symbiosis. *Frontiers in Microbiology*, *5*. https://doi.org/10.3389/fmicb.2014.00448

Pernice, M., Raina, J.-B., Rädecker, N., Cárdenas, A., Pogoreutz, C., & Voolstra, C. R. (2020a). Down to the bone: the role of overlooked endolithic microbiomes in reef coral health. *The ISME Journal*, *14*(2), 325–334. https://doi.org/10.1038/s41396-019-0548-z

Pernice, M., Raina, J.-B., Rädecker, N., Cárdenas, A., Pogoreutz, C., & Voolstra, C. R. (2020b). Down to the bone: the role of overlooked endolithic microbiomes in reef coral health. *The ISME Journal*, *14*(2), 325–334. https://doi.org/10.1038/s41396-019-0548-z

Pinhassi, J., Pujalte, M. J., Pascual, J., Gonzalez, J. M., Lekunberri, I., Pedros-Alio, C., & Arahal, D. R. (2009). Bermanella marisrubri gen. nov., sp. nov., a genome-sequenced gammaproteobacterium from the Red Sea. *INTERNATIONAL JOURNAL OF SYSTEMATIC AND EVOLUTIONARY MICROBIOLOGY*, *59*(2), 373–377. https://doi.org/10.1099/ijs.0.002113-0

Planes, S., & Allemand, D. (2023). Insights and achievements from the Tara Pacific expedition. *Nature Communications*, *14*(1), 3131. https://doi.org/10.1038/s41467-023-38896-6

Planes, S., Allemand, D., Agostini, S., Banaigs, B., Boissin, E., Boss, E., Bourdin, G., Bowler, C., Douville, E., Flores, J. M., Forcioli, D., Furla, P., Galand, P. E., Ghiglione, J.-F., Gilson, E., Lombard, F., Moulin, C., Pesant, S., Poulain, J., … Zoccola, D. (2019a). The Tara Pacific expedition—A pan-ecosystemic approach of the "-omics" complexity of coral reef holobionts across the Pacific Ocean. *PLOS Biology*, *17*(9), e3000483. https://doi.org/10.1371/journal.pbio.3000483

Planes, S., Allemand, D., Agostini, S., Banaigs, B., Boissin, E., Boss, E., Bourdin, G., Bowler, C., Douville, E., Flores, J. M., Forcioli, D., Furla, P., Galand, P. E., Ghiglione, J.-F., Gilson, E., Lombard, F., Moulin, C., Pesant, S., Poulain, J., … Zoccola, D. (2019b). The Tara Pacific expedition—A pan-ecosystemic approach of the "-omics" complexity of coral reef holobionts across the Pacific Ocean. *PLOS Biology*, *17*(9), e3000483. https://doi.org/10.1371/journal.pbio.3000483

Plovie, A. (2009). *Comparison of bacterial communities associated with healthy and bleached Aiptasia pallida, a novel model organism for coral studies: implications and variation during bleaching*.

Pogoreutz, C., Oakley, C. A., Rädecker, N., Cárdenas, A., Perna, G., Xiang, N., Peng, L., Davy, S. K., Ngugi, D. K., & Voolstra, C. R. (2022). Coral holobiont cues prime Endozoicomonas for a symbiotic lifestyle. *The ISME Journal*, *16*(8), 1883–1895. https://doi.org/10.1038/s41396-022-01226-7

Pogoreutz, C., Rädecker, N., Cárdenas, A., Gärdes, A., Wild, C., & Voolstra, C. R. (2017). Nitrogen Fixation Aligns with nifH Abundance and Expression in Two Coral Trophic Functional Groups. *Frontiers in Microbiology*, *8*. https://doi.org/10.3389/fmicb.2017.01187

Pogoreutz, C., & Ziegler, M. (2024). Frenemies on the reef? Resolving the coral–Endozoicomonas association. *Trends in Microbiology*. https://doi.org/10.1016/j.tim.2023.11.006

Pollock, F. J., McMinds, R., Smith, S., Bourne, D. G., Willis, B. L., Medina, M., Thurber, R. V., & Zaneveld, J. R. (2018). Coral-associated bacteria demonstrate phylosymbiosis and cophylogeny. *Nature Communications*, *9*(1), 4921. https://doi.org/10.1038/s41467-018-07275-x

Pootakham, W., Mhuantong, W., Yoocha, T., Putchim, L., Jomchai, N., Sonthirod, C., Naktang, C., Kongkachana, W., & Tangphatsornruang, S. (2019). Heat-induced shift in coral microbiome reveals several members of the Rhodobacteraceae family as indicator species for thermal stress in *Porites lutea*. *MicrobiologyOpen*, *8*(12). https://doi.org/10.1002/mbo3.935

Prada, C., López-Londoño, T., Pollock, F. J., Roitman, S., Ritchie, K. B., Levitan, D. R., Knowlton, N., Woodley, C., Iglesias-Prieto, R., & Medina, M. (2022). Linking photoacclimation responses and microbiome shifts between depth-segregated sibling species of reef corals. *Royal Society Open Science*, *9*(3). https://doi.org/10.1098/rsos.211591

Price, D. R. G., Feng, H., Baker, J. D., Bavan, S., Luetje, C. W., & Wilson, A. C. C. (2014). Aphid amino acid transporter regulates glutamine supply to intracellular bacterial symbionts. *Proceedings of the National Academy of Sciences*, *111*(1), 320–325. https://doi.org/10.1073/pnas.1306068111

Priess, K., Le Campion-Alsumard, T., Golubic, S., Gadel, F., & Thomassin, B. A. (2000). Fungi in corals: black bands and density-banding of Porites lutea and P. lobata skeleton. *Marine Biology*, *136*(1), 19–27. https://doi.org/10.1007/s002270050003

Prog, S., Le Campion-~lsumard', T., Golubic2, S., & Priessl, K. (1995). *MARINE ECOLOGY PROGRESS SERIES*.

Puhar, A., & Sansonetti, P. J. (2014). Type III secretion system. *Current Biology*, *24*(17), R784–R791. https://doi.org/10.1016/j.cub.2014.07.016

Pushpakumara, B. L. D. U., Tandon, K., Willis, A., & Verbruggen, H. (2023). The Bacterial Microbiome of the Coral Skeleton Algal Symbiont Ostreobium Shows Preferential Associations and Signatures of Phylosymbiosis. *Microbial Ecology*, *86*(3), 2032–2046. https://doi.org/10.1007/s00248-023-02209-7

Quast, C., Pruesse, E., Yilmaz, P., Gerken, J., Schweer, T., Yarza, P., Peplies, J., & Glöckner, F. O. (2012). The SILVA ribosomal RNA gene database project: improved data processing and web-based tools. *Nucleic Acids Research*, *41*(D1), D590–D596. https://doi.org/10.1093/nar/gks1219

Quattrini, A. M., Rodríguez, E., Faircloth, B. C., Cowman, P. F., Brugler, M. R., Farfan, G. A., Hellberg, M. E., Kitahara, M. V., Morrison, C. L., Paz-García, D. A., Reimer, J. D., & McFadden, C. S. (2020). Palaeoclimate ocean conditions shaped the evolution of corals and their skeletons through deep time. *Nature Ecology & Evolution*, *4*(11), 1531–1538. https://doi.org/10.1038/s41559-020-01291-1

Quinn, R. A., Vermeij, M. J. A., Hartmann, A. C., Galtier d'Auriac, I., Benler, S., Haas, A., Quistad, S. D., Lim, Y. W., Little, M., Sandin, S., Smith, J. E., Dorrestein, P. C., & Rohwer, F. (2016). Metabolomics of reef benthic interactions reveals a bioactive lipid involved in coral defence. *Proceedings of the Royal Society B: Biological Sciences*, *283*(1829), 20160469. https://doi.org/10.1098/rspb.2016.0469

Quintanilla, E., Rodrigues, C. F., Henriques, I., & Hilário, A. (2022). Microbial Associations of Abyssal Gorgonians and Anemones (>4,000 m Depth) at the Clarion-Clipperton Fracture Zone. *Frontiers in Microbiology*, *13*. https://doi.org/10.3389/fmicb.2022.828469

Rädecker, N., Pogoreutz, C., Voolstra, C. R., Wiedenmann, J., & Wild, C. (2015). Nitrogen cycling in corals: the key to understanding holobiont functioning? *Trends in Microbiology*, *23*(8), 490–497. https://doi.org/10.1016/j.tim.2015.03.008

Raghukumar, C., & Ravindran, J. (2012). *Fungi and Their Role in Corals and Coral Reef Ecosystems* (pp. 89–113). https://doi.org/10.1007/978-3-642-23342-5_5

Rahman, M. A., Oomori, T., & Wörheide, G. (2011). Calcite Formation in Soft Coral Sclerites Is Determined by a Single Reactive Extracellular Protein. *Journal of Biological Chemistry*, *286*(36), 31638–31649. https://doi.org/10.1074/jbc.M109.070185

Rahmstorf, S. (2002). Ocean circulation and climate during the past 120,000 years. *Nature*, *419*(6903), 207–214. https://doi.org/10.1038/nature01090

Ralph, P. J., Larkum, A. W. D., & Kühl, M. (2007). Photobiology of endolithic microorganisms in living coral skeletons: 1. Pigmentation, spectral reflectance and variable chlorophyll fluorescence analysis of endoliths in the massive corals

Cyphastrea serailia, Porites lutea and Goniastrea australensis. *Marine Biology*, *152*(2), 395–404. https://doi.org/10.1007/s00227-007-0694-0

Ransome, E., Rowley, S. J., Thomas, S., Tait, K., & Munn, C. B. (2014). Disturbance to conserved bacterial communities in the cold-water gorgonian coral *Eunicella verrucosa*. *FEMS Microbiology Ecology*, n/a-n/a. https://doi.org/10.1111/1574-6941.12398

Ravindran, C., Bhagwat, P. V., Silveira, K. A., Shivaramu, M. S., & lele, U. P. (2020). Characterization of coral associated ciliates and their interactions with disease lesion progression of Indian Scleractinian corals. *Microbial Pathogenesis*, *149*, 104472. https://doi.org/10.1016/j.micpath.2020.104472

Reaka-Kudla, M. L. (1997). *Biodiversity II* (M. L. Reaka-Kudla, Ed.). Joseph Henry Press. https://doi.org/10.17226/4901

Reddy, M. M., Goossens, C., Zhou, Y., Chaib, S., Raviglione, D., Nicolè, F., Hume, B. C. C., Forcioli, D., Agostini, S., Boissin, E., Boss, E., Bowler, C., de Vargas, C., Douville, E., Flores, M., Furla, P., Galand, P. E., Gilson, E., Lombard, F., … Banaigs, B. (2023). Multi-omics determination of metabolome diversity in natural coral populations in the Pacific Ocean. *Communications Earth & Environment*, *4*(1), 281. https://doi.org/10.1038/s43247-023-00942-y

Reis, A. M. M., Araújo Jr, S. D., Moura, R. L., Francini-Filho, R. B., Pappas Jr, G., Coelho, A. M. A., Krüger, R. H., & Thompson, F. L. (2009). Bacterial diversity associated with the Brazilian endemic reef coral *Mussismilia braziliensis*. *Journal of Applied Microbiology*, *106*(4), 1378–1387. https://doi.org/10.1111/j.1365-2672.2008.04106.x

Reyes-Nivia, C., Diaz-Pulido, G., Kline, D., Guldberg, O.-H., & Dove, S. (2013). Ocean acidification and warming scenarios increase microbioerosion of coral skeletons. *Global Change Biology*, *19*(6), 1919–1929. https://doi.org/10.1111/gcb.12158

Ribicic, D., Netzer, R., Hazen, T. C., Techtmann, S. M., Drabløs, F., & Brakstad, O. G. (2018). Microbial community and metagenome dynamics during biodegradation of dispersed oil reveals potential key-players in cold Norwegian seawater. *Marine Pollution Bulletin*, *129*(1), 370–378. https://doi.org/10.1016/j.marpolbul.2018.02.034

Ricardo, G. F., Jones, R. J., Negri, A. P., & Stocker, R. (2016). That sinking feeling: Suspended sediments can prevent the ascent of coral egg bundles. *Scientific Reports*, *6*(1), 21567. https://doi.org/10.1038/srep21567

Ricci, F., Rossetto Marcelino, V., Blackall, L. L., Kühl, M., Medina, M., & Verbruggen, H. (2019). Beneath the surface: community assembly and functions of the coral skeleton microbiome. *Microbiome*, *7*(1), 159. https://doi.org/10.1186/s40168-019-0762-y

Richardson, L. L. (2004). Black Band Disease. In *Coral Health and Disease* (pp. 325–336). Springer Berlin Heidelberg. https://doi.org/10.1007/978-3-662-06414-6_18

Richter, D. J., Berney, C., Strassert, J. F. H., Poh, Y.-P., Herman, E. K., Muñoz-Gómez, S. A., Wideman, J. G., Burki, F., & de Vargas, C. (2022). EukProt: A database of genome-scale predicted proteins across the diversity of eukaryotes. *Peer Community Journal*, *2*, e56. https://doi.org/10.24072/pcjournal.173

Ritchie, M. E., Phipson, B., Wu, D., Hu, Y., Law, C. W., Shi, W., & Smyth, G. K. (2015). limma powers differential expression analyses for RNA-sequencing and microarray studies. *Nucleic Acids Research*, *43*(7), e47–e47. https://doi.org/10.1093/nar/gkv007

Roach, T. N. F., Little, M., Arts, M. G. I., Huckeba, J., Haas, A. F., George, E. E., Quinn, R. A., Cobián-Güemes, A. G., Naliboff, D. S., Silveira, C. B., Vermeij, M. J. A., Kelly, L. W., Dorrestein, P. C., & Rohwer, F. (2020). A multiomic analysis of in situ coral–turf algal interactions. *Proceedings of the National Academy of Sciences*, *117*(24), 13588–13595. https://doi.org/10.1073/pnas.1915455117

Robbins, S. J., Singleton, C. M., Chan, C. X., Messer, L. F., Geers, A. U., Ying, H., Baker, A., Bell, S. C., Morrow, K. M., Ragan, M. A., Miller, D. J., Forêt, S., Ball, E., Beeden, R., Berumen, M., Aranda, M., Ravasi, T., Bongaerts, P., Hoegh-Guldberg, O., … Bourne, D. G. (2019a). A genomic view of the reef-building coral Porites lutea and its microbial symbionts. *Nature Microbiology*, *4*(12), 2090–2100. https://doi.org/10.1038/s41564-019-0532-4

Robbins, S. J., Singleton, C. M., Chan, C. X., Messer, L. F., Geers, A. U., Ying, H., Baker, A., Bell, S. C., Morrow, K. M., Ragan, M. A., Miller, D. J., Forêt, S., Ball, E., Beeden, R., Berumen, M., Aranda, M., Ravasi, T., Bongaerts, P., Hoegh-Guldberg, O., … Bourne, D. G. (2019b). A genomic view of the reef-building coral Porites lutea and its microbial symbionts. *Nature Microbiology*, *4*(12), 2090–2100. https://doi.org/10.1038/s41564-019-0532-4

Roberts, J. M. (2019). Cold-Water Coral Reefs. In *Encyclopedia of Ocean Sciences* (pp. 675–687). Elsevier. https://doi.org/10.1016/B978-0-12-409548-9.04041-0

Roberts, J. M., Wheeler, A. J., & Freiwald, A. (2006). Reefs of the Deep: The Biology and Geology of Cold-Water Coral Ecosystems. *Science*, *312*(5773), 543–547. https://doi.org/10.1126/science.1119861

Rohwer, F., Seguritan, V., Azam, F., & Knowlton, N. (2002). Diversity and distribution of coral-associated bacteria. *Marine Ecology Progress Series*, *243*, 1–10. https://doi.org/10.3354/meps243001

Rosales, S. M., Clark, A. S., Huebner, L. K., Ruzicka, R. R., & Muller, E. M. (2020). Rhodobacterales and Rhizobiales Are Associated With Stony Coral Tissue Loss Disease and Its Suspected Sources of Transmission. *Frontiers in Microbiology*, *11*. https://doi.org/10.3389/fmicb.2020.00681

Rosales, S. M., Huebner, L. K., Clark, A. S., McMinds, R., Ruzicka, R. R., & Muller, E. M. (2022). Bacterial Metabolic Potential and Micro-Eukaryotes Enriched in Stony Coral Tissue Loss Disease Lesions. *Frontiers in Marine Science*, *8*. https://doi.org/10.3389/fmars.2021.776859

Rosales, S. M., Huebner, L. K., Evans, J. S., Apprill, A., Baker, A. C., Becker, C. C., Bellantuono, A. J., Brandt, M. E., Clark, A. S., del Campo, J., Dennison, C. E., Eaton, K. R., Huntley, N. E., Kellogg, C. A., Medina, M., Meyer, J. L., Muller, E. M., Rodriguez-Lanetty, M., Salerno, J. L., … Voss, J. D. (2023). A meta-analysis of the stony coral tissue loss disease microbiome finds key bacteria in unaffected and lesion tissue in diseased colonies. *ISME Communications*, *3*(1), 19. https://doi.org/10.1038/s43705-023-00220-0

Rosales, S. M., Miller, M. W., Williams, D. E., Traylor-Knowles, N., Young, B., & Serrano, X. M. (2019). Microbiome differences in disease-resistant vs. susceptible Acropora corals subjected to disease challenge assays. *Scientific Reports*, *9*(1), 18279. https://doi.org/10.1038/s41598-019-54855-y

Rose, N. H., Bay, R. A., Morikawa, M. K., & Palumbi, S. R. (2018). Polygenic evolution drives species divergence and climate adaptation in corals. *Evolution*, *72*(1), 82–94. https://doi.org/10.1111/evo.13385

Rosenberg, E., Koren, O., Reshef, L., Efrony, R., & Zilber-Rosenberg, I. (2007). The role of microorganisms in coral health, disease and evolution. *Nature Reviews Microbiology*, *5*(5), 355–362. https://doi.org/10.1038/nrmicro1635

Röthig, T., Yum, L. K., Kremb, S. G., Roik, A., & Voolstra, C. R. (2017). Microbial community composition of deep-sea corals from the Red Sea provides insight into functional adaption to a unique environment. *Scientific Reports*, *7*(1), 44714. https://doi.org/10.1038/srep44714

Rouzé, H., Galand, P. E., Medina, M., Bongaerts, P., Pichon, M., Pérez-Rosales, G., Torda, G., Moya, A., Raina, J.-B., & Hédouin, L. (2021). Symbiotic associations of the deepest recorded photosynthetic scleractinian coral (172 m depth). *The ISME Journal*, *15*(5), 1564–1568. https://doi.org/10.1038/s41396-020-00857-y

Rubio-Portillo, E., Kersting, D. K., Linares, C., Ramos-Esplá, A. A., & Antón, J. (2018). Biogeographic Differences in the Microbiome and Pathobiome of the Coral Cladocora caespitosa in the Western Mediterranean Sea. *Frontiers in Microbiology*, *9*. https://doi.org/10.3389/fmicb.2018.00022

Rubio-Portillo, E., Santos, F., Martínez-García, M., de los Ríos, A., Ascaso, C., Souza-Egipsy, V., Ramos-Esplá, A. A., & Anton, J. (2016). Structure and temporal dynamics of the bacterial communities associated to microhabitats of the coral <scp> *O* </scp> *culina patagonica*. *Environmental Microbiology*, *18*(12), 4564–4578. https://doi.org/10.1111/1462-2920.13548

Saghaï, A., Zivanovic, Y., Moreira, D., Tavera, R., & López-García, P. (2020). A Novel Microbialite-Associated Phototrophic Chloroflexi Lineage Exhibiting a Quasi-Clonal Pattern along Depth. *Genome Biology and Evolution*, *12*(7), 1207–1216. https://doi.org/10.1093/gbe/evaa122

Saini, M., Kashyap, A., Bindal, S., Saini, K., & Gupta, R. (2021). Bacterial Gamma-Glutamyl Transpeptidase, an Emerging Biocatalyst: Insights Into Structure–Function Relationship and Its Biotechnological Applications. *Frontiers in Microbiology*, *12*. https://doi.org/10.3389/fmicb.2021.641251

Salazar, G., Paoli, L., Alberti, A., Huerta-Cepas, J., Ruscheweyh, H.-J., Cuenca, M., Field, C. M., Coelho, L. P., Cruaud, C., Engelen, S., Gregory, A. C., Labadie, K., Marec, C., Pelletier, E., Royo-Llonch, M., Roux, S., Sánchez, P., Uehara, H., Zayed, A. A., … Wincker, P. (2019). Gene Expression Changes and Community Turnover Differentially Shape the Global Ocean Metatranscriptome. *Cell*, *179*(5), 1068-1083.e21. https://doi.org/10.1016/j.cell.2019.10.014

Salazar, G., Ruscheweyh, H.-J., Hildebrand, F., Acinas, S. G., & Sunagawa, S. (2021a). mTAGs: taxonomic profiling using degenerate consensus reference sequences of ribosomal RNA genes. *Bioinformatics*, *38*(1), 270–272. https://doi.org/10.1093/bioinformatics/btab465

Salazar, G., Ruscheweyh, H.-J., Hildebrand, F., Acinas, S. G., & Sunagawa, S. (2021b). mTAGs: taxonomic profiling using degenerate consensus reference sequences of ribosomal RNA genes. *Bioinformatics*, *38*(1), 270–272. https://doi.org/10.1093/bioinformatics/btab465

Salem, H., Bauer, E., Strauss, A. S., Vogel, H., Marz, M., & Kaltenpoth, M. (2014). Vitamin supplementation by gut symbionts ensures metabolic homeostasis in an insect host. *Proceedings of the Royal Society B: Biological Sciences*, *281*(1796), 20141838. https://doi.org/10.1098/rspb.2014.1838

Samuel A. Vohsen, Harald R. Gruber-Vodicka, Martina Meyer, Miriam Sadowski, Nicole Dubilier, Charles R. Fisher, & Iliana B. Baums. (2022). *The deep-sea coral, Callogorgia delta, associates with bacteria belonging to a novel marine branch of the Mollicutes*. https://doi.org/10.1101/2022.10.07.511369

Sangsawang, L., Casareto, B. E., Ohba, H., Vu, H. M., Meekaew, A., Suzuki, T., Yeemin, T., & Suzuki, Y. (2017). ^{13} C and ^{15} N assimilation and organic matter translocation by the endolithic community in the massive coral *Porites lutea*. *Royal Society Open Science*, *4*(12), 171201. https://doi.org/10.1098/rsos.171201

Santos, H. F., Carmo, F. L., Duarte, G., Dini-Andreote, F., Castro, C. B., Rosado, A. S., van Elsas, J. D., & Peixoto, R. S. (2014). Climate change affects key nitrogen-fixing bacterial populations on coral reefs. *The ISME Journal*, *8*(11), 2272–2279. https://doi.org/10.1038/ismej.2014.70

Sañudo-Wilhelmy, S. A., Gómez-Consarnau, L., Suffridge, C., & Webb, E. A. (2014). The Role of B Vitamins in Marine Biogeochemistry. *Annual Review of Marine Science*, *6*(1), 339–367. https://doi.org/10.1146/annurev-marine-120710-100912

Sargeant, S., Murrell, J., Nightingale, P., & Dixon, J. (2016). Seasonal variability in microbial methanol utilisation in coastal waters of the western English Channel. *Marine Ecology Progress Series*, *550*, 53–64. https://doi.org/10.3354/meps11705

Satomi, M., & Fujii, T. (2014). The Family Oceanospirillaceae. In *The Prokaryotes* (pp. 491–527). Springer Berlin Heidelberg. https://doi.org/10.1007/978-3-642-38922-1_286

Schleinkofer, N., Raddatz, J., Freiwald, A., Evans, D., Beuck, L., Rüggeberg, A., & Liebetrau, V. (2019). Environmental and biological controls on Na⁄Ca ratios in scleractinian cold-water corals. *Biogeosciences*, *16*(18), 3565–3582. https://doi.org/10.5194/bg-16-3565-2019

Schubert, N., Brown, D., & Rossi, S. (2016). Symbiotic Versus Non-symbiotic Octocorals: Physiological and Ecological Implications. In *Marine Animal Forests* (pp. 1–32). Springer International Publishing. https://doi.org/10.1007/978-3-319-17001-5_54-1

Seemann, T. (2014). Prokka: rapid prokaryotic genome annotation. *Bioinformatics*, *30*(14), 2068–2069. https://doi.org/10.1093/bioinformatics/btu153

Sharma, D., & Ravindran, C. (2020). Diseases and pathogens of marine invertebrate corals in Indian reefs. *Journal of Invertebrate Pathology*, *173*, 107373. https://doi.org/10.1016/j.jip.2020.107373

Sharp, K. H., Distel, D., & Paul, V. J. (2012). Diversity and dynamics of bacterial communities in early life stages of the Caribbean coral Porites astreoides. *The ISME Journal*, *6*(4), 790–801. https://doi.org/10.1038/ismej.2011.144

Shashar, N., Banaszak, A. T., Lesser, M. P., & Amrami, A. D. (1997). Coral Endolithic Algae: Life in a Protected Environment! In *Pacific Science* (Vol. 51, Issue 2).

Shi, T., Shi, T. ;, Zheng, X. ;, Zhang, H. ;, Wang, Q. ;, & Zhong, X. (. (2021). *Coral Reefs: Potential Blue Carbon Sinks for Climate Change Coral Reefs: Potential Blue Carbon Sinks for Climate Change Mitigation Mitigation Recommended Citation Recommended Citation*. *36*, 3–20. https://doi.org/10.16418/j.issn.1000-3045.20210217102

Shinzato, C., Inoue, M., & Kusakabe, M. (2014). A Snapshot of a Coral "Holobiont": A Transcriptome Assembly of the Scleractinian Coral, Porites, Captures a Wide Variety of Genes from Both the Host and Symbiotic Zooxanthellae. *PLoS ONE*, *9*(1), e85182. https://doi.org/10.1371/journal.pone.0085182

Shinzato, C., Shoguchi, E., Kawashima, T., Hamada, M., Hisata, K., Tanaka, M., Fujie, M., Fujiwara, M., Koyanagi, R., Ikuta, T., Fujiyama, A., Miller, D. J., & Satoh, N. (2011). Using the Acropora digitifera genome to understand coral responses to environmental change. *Nature*, *476*(7360), 320–323. https://doi.org/10.1038/nature10249

Shoguchi, E., Beedessee, G., Tada, I., Hisata, K., Kawashima, T., Takeuchi, T., Arakaki, N., Fujie, M., Koyanagi, R., Roy, M. C., Kawachi, M., Hidaka, M., Satoh, N., & Shinzato, C. (2018). Two divergent Symbiodinium genomes reveal conservation of a gene cluster for sunscreen biosynthesis and recently lost genes. *BMC Genomics*, *19*(1), 458. https://doi.org/10.1186/s12864-018-4857-9

Shoguchi, E., Shinzato, C., Kawashima, T., Gyoja, F., Mungpakdee, S., Koyanagi, R., Takeuchi, T., Hisata, K., Tanaka, M., Fujiwara, M., Hamada, M., Seidi, A., Fujie, M., Usami, T., Goto, H., Yamasaki, S., Arakaki, N., Suzuki, Y., Sugano, S., … Satoh, N. (2013a). Draft Assembly of the Symbiodinium minutum Nuclear Genome Reveals Dinoflagellate Gene Structure. *Current Biology*, *23*(15), 1399–1408. https://doi.org/10.1016/j.cub.2013.05.062

Shoguchi, E., Shinzato, C., Kawashima, T., Gyoja, F., Mungpakdee, S., Koyanagi, R., Takeuchi, T., Hisata, K., Tanaka, M., Fujiwara, M., Hamada, M., Seidi, A., Fujie, M., Usami, T., Goto, H., Yamasaki, S., Arakaki, N., Suzuki, Y., Sugano, S., … Satoh, N. (2013b). Draft Assembly of the Symbiodinium minutum Nuclear Genome Reveals Dinoflagellate Gene Structure. *Current Biology*, *23*(15), 1399–1408. https://doi.org/10.1016/j.cub.2013.05.062

Siboni, N., Ben-Dov, E., Sivan, A., & Kushmaro, A. (2008). Global distribution and diversity of coral-associated *Archaea* and their possible role in the coral holobiont nitrogen cycle. *Environmental Microbiology*, *10*(11), 2979–2990. https://doi.org/10.1111/j.1462-2920.2008.01718.x

Siguier, P., Gourbeyre, E., & Chandler, M. (2014). Bacterial insertion sequences: their genomic impact and diversity. *FEMS Microbiology Reviews*, *38*(5), 865–891. https://doi.org/10.1111/1574-6976.12067

Smits, S. H. J., Schmitt, L., & Beis, K. (2020). Self-immunity to antibacterial peptides by ABC transporters. *FEBS Letters*, *594*(23), 3920–3942. https://doi.org/10.1002/1873-3468.13953

Soler-Hurtado, M. M., Sandoval-Sierra, J. V., Machordom, A., & Diéguez-Uribeondo, J. (2016). Aspergillus sydowii and Other Potential Fungal Pathogens in Gorgonian Octocorals of the Ecuadorian Pacific. *PLOS ONE*, *11*(11), e0165992. https://doi.org/10.1371/journal.pone.0165992

Sostare, J., Di Guida, R., Kirwan, J., Chalal, K., Palmer, E., Dunn, W. B., & Viant, M. R. (2018). Comparison of modified Matyash method to conventional solvent systems for polar metabolite and lipid extractions. *Analytica Chimica Acta*, *1037*, 301–315. https://doi.org/10.1016/j.aca.2018.03.019

Steinegger, M., & Söding, J. (2017a). *Linclust: clustering billions of protein sequences per day on a single server*. https://doi.org/10.1101/104034

Steinegger, M., & Söding, J. (2017b). MMseqs2 enables sensitive protein sequence searching for the analysis of massive data sets. *Nature Biotechnology*, *35*(11), 1026–1028. https://doi.org/10.1038/nbt.3988

Stephens, T. G., Ragan, M. A., Bhattacharya, D., & Chan, C. X. (2018). Core genes in diverse dinoflagellate lineages include a wealth of conserved dark genes with unknown functions. *Scientific Reports*, *8*(1), 17175. https://doi.org/10.1038/s41598-018-35620-z

Stien, D., Suzuki, M., Rodrigues, A. M. S., Yvin, M., Clergeaud, F., Thorel, E., & Lebaron, P. (2020). A unique approach to monitor stress in coral exposed to emerging pollutants. *Scientific Reports*, *10*(1), 9601. https://doi.org/10.1038/s41598-020-66117-3

Stoskopf, M. K., Westmoreland, L. S., & Lewbart, G. A. (2022). OCTOCORALLIA, HEXACORALLIA, SCLERACTINIA, AND OTHER CORALS. In *Invertebrate Medicine* (pp. 65–105). Wiley. https://doi.org/10.1002/9781119569831.ch5

Suantika, G. (2013). The Use of Indigenous Probiotic Halomonas aquamarina and Shewanella algae for White Shrimp (Litopenaeus vannamei Boone) Hatchery Productivity in Zero Water Discharge System. *Journal of Aquaculture Research & Development*, *04*(05). https://doi.org/10.4172/2155-9546.1000194

Sun, C., Xu, L., Yu, X.-Y., Zhao, Z., Wu, Y.-H., Oren, A., Wang, C.-S., & Xu, X.-W. (2018). Minwuia thermotolerans gen. nov., sp. nov., a marine bacterium forming a deep branch in the Alphaproteobacteria, and proposal of Minwuiaceae fam. nov. and Minwuiales ord. nov. *International Journal of Systematic and Evolutionary Microbiology*, *68*(12), 3856–3862. https://doi.org/10.1099/ijsem.0.003073

Sunda, W., Kieber, D. J., Kiene, R. P., & Huntsman, S. (2002). An antioxidant function for DMSP and DMS in marine algae. *Nature*, *418*(6895), 317–320. https://doi.org/10.1038/nature00851

Sundahl, H., Buhl-Mortensen, P., & Buhl-Mortensen, L. (2020). Distribution and Suitable Habitat of the Cold-Water Corals Lophelia pertusa, Paragorgia arborea, and Primnoa resedaeformis on the Norwegian Continental Shelf. *Frontiers in Marine Science*, *7*. https://doi.org/10.3389/fmars.2020.00213

Sweet, M., & Bythell, J. (2012). Ciliate and bacterial communities associated with White Syndrome and Brown Band Disease in reef-building corals. *Environmental Microbiology*, *14*(8), 2184–2199. https://doi.org/10.1111/j.1462-2920.2012.02746.x

Sweet, M. J., Croquer, A., & Bythell, J. C. (2011). Bacterial assemblages differ between compartments within the coral holobiont. *Coral Reefs*, *30*(1), 39–52. https://doi.org/10.1007/s00338-010-0695-1

Sweetman, A. K., Thurber, A. R., Smith, C. R., Levin, L. A., Mora, C., Wei, C.-L., Gooday, A. J., Jones, D. O. B., Rex, M., Yasuhara, M., Ingels, J., Ruhl, H. A., Frieder, C. A., Danovaro, R., Würzberg, L., Baco, A., Grupe, B. M., Pasulka, A., Meyer, K. S., … Roberts, J. M. (2017). Major impacts of climate change on deep-sea benthic ecosystems. *Elementa: Science of the Anthropocene*, *5*. https://doi.org/10.1525/elementa.203

Tandon, K., Chiou, Y.-J., Yu, S.-P., Hsieh, H. J., Lu, C.-Y., Hsu, M.-T., Chiang, P.-W., Chen, H.-J., Wada, N., & Tang, S.-L. (2022a). Microbiome Restructuring: Dominant Coral Bacterium *Endozoicomonas* Species Respond Differentially to Environmental Changes. *MSystems*, *7*(4). https://doi.org/10.1128/msystems.00359-22

Tandon, K., Chiou, Y.-J., Yu, S.-P., Hsieh, H. J., Lu, C.-Y., Hsu, M.-T., Chiang, P.-W., Chen, H.-J., Wada, N., & Tang, S.-L. (2022b). Microbiome Restructuring: Dominant Coral Bacterium *Endozoicomonas* Species Respond Differentially to

Environmental Changes. *MSystems*, *7*(4). https://doi.org/10.1128/msystems.00359-22

Tandon, K., Lu, C.-Y., Chiang, P.-W., Wada, N., Yang, S.-H., Chan, Y.-F., Chen, P.-Y., Chang, H.-Y., Chiou, Y.-J., Chou, M.-S., Chen, W.-M., & Tang, S.-L. (2020a). Comparative genomics: Dominant coral-bacterium Endozoicomonas acroporae metabolizes dimethylsulfoniopropionate (DMSP). *The ISME Journal*, *14*(5), 1290–1303. https://doi.org/10.1038/s41396-020-0610-x

Tandon, K., Lu, C.-Y., Chiang, P.-W., Wada, N., Yang, S.-H., Chan, Y.-F., Chen, P.-Y., Chang, H.-Y., Chiou, Y.-J., Chou, M.-S., Chen, W.-M., & Tang, S.-L. (2020b). Comparative genomics: Dominant coral-bacterium *Endozoicomonas acroporae* metabolizes dimethylsulfoniopropionate (DMSP). *The ISME Journal*, *14*(5), 1290–1303. https://doi.org/10.1038/s41396-020-0610-x

Tandon, K., Ricci, F., Costa, J., Medina, M., Kühl, M., Blackall, L. L., & Verbruggen, H. (2022). Genomic view of the diversity and functional role of archaea and bacteria in the skeleton of the reef-building corals *Porites lutea* and *Isopora palifera*. *GigaScience*, *12*. https://doi.org/10.1093/gigascience/giac127

Tang, K., Wang, Y., & Wang, X. (2019). Recent progress on signalling molecules of coral-associated microorganisms. *Science China Earth Sciences*, *62*(4), 609–618. https://doi.org/10.1007/s11430-018-9332-1

Technau, U., Genikhovich, G., & Kraus, J. E. M. (2015). Cnidaria. In *Evolutionary Developmental Biology of Invertebrates 1* (pp. 115–163). Springer Vienna. https://doi.org/10.1007/978-3-7091-1862-7_6

Teplitski, M., & Ritchie, K. (2009). How feasible is the biological control of coral diseases? *Trends in Ecology & Evolution*, *24*(7), 378–385. https://doi.org/10.1016/j.tree.2009.02.008

Thurber, R. V., Willner-Hall, D., Rodriguez-Mueller, B., Desnues, C., Edwards, R. A., Angly, F., Dinsdale, E., Kelly, L., & Rohwer, F. (2009). Metagenomic analysis of stressed coral holobionts. *Environmental Microbiology*, *11*(8), 2148–2163. https://doi.org/10.1111/j.1462-2920.2009.01935.x

Tignat-Perrier, R., van de Water, J. A. J. M., Guillemain, D., Aurelle, D., Allemand, D., & Ferrier-Pagès, C. (2022). The Effect of Thermal Stress on the Physiology and Bacterial Communities of Two Key Mediterranean Gorgonians. *Applied and Environmental Microbiology*, *88*(6). https://doi.org/10.1128/aem.02340-21

Tilstra, A., El-Khaled, Y. C., Roth, F., Rädecker, N., Pogoreutz, C., Voolstra, C. R., & Wild, C. (2019). Denitrification Aligns with N2 Fixation in Red Sea Corals. *Scientific Reports*, *9*(1), 19460. https://doi.org/10.1038/s41598-019-55408-z

Tilstra, A., Roth, F., El-Khaled, Y. C., Pogoreutz, C., Rädecker, N., Voolstra, C. R., & Wild, C. (2021). Relative abundance of nitrogen cycling microbes in coral holobionts reflects environmental nitrate availability. *Royal Society Open Science*, *8*(6), 201835. https://doi.org/10.1098/rsos.201835

Tong, R., Davies, A. J., Purser, A., Liu, X., & Liu, F. (2022). Global distribution of the cold-water coral Lophelia pertusa. *IOP Conference Series: Earth and Environmental Science*, *1004*(1), 012010. https://doi.org/10.1088/1755-1315/1004/1/012010

Tresguerres, M., Barott, K. L., Barron, M. E., Deheyn, D. D., Kline, D. I., & Linsmayer, L. B. (2017). Cell Biology of Reef-Building Corals: Ion Transport, Acid/Base Regulation, and Energy Metabolism. In *Acid-Base Balance and Nitrogen Excretion in Invertebrates* (pp. 193–218). Springer International Publishing. https://doi.org/10.1007/978-3-319-39617-0_7

Tribollet, A. (2008). The boring microflora in modern coral reef ecosystems: a review of its roles. In *Current Developments in Bioerosion* (pp. 67–94). Springer Berlin Heidelberg. https://doi.org/10.1007/978-3-540-77598-0_4

Tribollet, A., & Golubic, S. (2011). Reef Bioerosion: Agents and Processes. In *Coral Reefs: An Ecosystem in Transition* (pp. 435–449). Springer Netherlands. https://doi.org/10.1007/978-94-007-0114-4_25

Uritskiy, G. V., DiRuggiero, J., & Taylor, J. (2018). MetaWRAP—a flexible pipeline for genome-resolved metagenomic data analysis. *Microbiome*, *6*(1), 158. https://doi.org/10.1186/s40168-018-0541-1

Vad, J., Orejas, C., Moreno-Navas, J., Findlay, H. S., & Roberts, J. M. (2017). Assessing the living and dead proportions of cold-water coral colonies: implications for deep-water Marine Protected Area monitoring in a changing ocean. *PeerJ*, *5*, e3705. https://doi.org/10.7717/peerj.3705

van Bleijswijk, J. D. L., Whalen, C., Duineveld, G. C. A., Lavaleye, M. S. S., Witte, H. J., & Mienis, F. (2015). Microbial assemblages on a cold-water coral mound at the SE Rockall Bank (NE Atlantic): interactions with hydrography and topography. *Biogeosciences*, *12*(14), 4483–4496. https://doi.org/10.5194/bg-12-4483-2015

van de Water, J. A. J. M., Ainsworth, T. D., Leggat, W., Bourne, D. G., Willis, B. L., & van Oppen, M. J. H. (2015). The coral immune response facilitates protection against microbes during tissue regeneration. *Molecular Ecology*, *24*(13), 3390–3404. https://doi.org/10.1111/mec.13257

van de Water, J. A. J. M., Allemand, D., & Ferrier-Pagès, C. (2018). Host-microbe interactions in octocoral holobionts - recent advances and perspectives. *Microbiome*, *6*(1), 64. https://doi.org/10.1186/s40168-018-0431-6 van de Water, J. A. J. M., Coppari, M., Enrichetti, F., Ferrier-Pagès, C., & Bo, M. (2020). Local Conditions Influence the Prokaryotic Communities Associated With the Mesophotic Black Coral Antipathella subpinnata. *Frontiers in Microbiology*, *11*. https://doi.org/10.3389/fmicb.2020.537813

van de Water, J. A. J. M., Melkonian, R., Voolstra, C. R., Junca, H., Beraud, E., Allemand, D., & Ferrier-Pagès, C. (2017). Comparative Assessment of Mediterranean Gorgonian-Associated Microbial Communities Reveals Conserved Core and Locally Variant Bacteria. *Microbial Ecology*, *73*(2), 466–478. https://doi.org/10.1007/s00248-016-0858-x

van de Water, J. A. J. M., Voolstra, C. R., Rottier, C., Cocito, S., Peirano, A., Allemand, D., & Ferrier-Pagès, C. (2018). Seasonal Stability in the Microbiomes of Temperate Gorgonians and the Red Coral Corallium rubrum Across the Mediterranean Sea. *Microbial Ecology*, *75*(1), 274–288. https://doi.org/10.1007/s00248-017-1006-y

van Oppen, M. J. H., & Blackall, L. L. (2019). Coral microbiome dynamics, functions and design in a changing world. *Nature Reviews Microbiology*, *17*(9), 557–567. https://doi.org/10.1038/s41579-019-0223-4

Vaulot, D., Sim, C. W. H., Ong, D., Teo, B., Biwer, C., Jamy, M., & Lopes dos Santos, A. (2022). <scp> metaPR ^{2} </scp> : A database of eukaryotic <scp>18S rRNA</scp> metabarcodes with an emphasis on protists. *Molecular Ecology Resources*, *22*(8), 3188–3201. https://doi.org/10.1111/1755-0998.13674

Vega Thurber, R. L., Burkepile, D. E., Fuchs, C., Shantz, A. A., McMinds, R., & Zaneveld, J. R. (2014). Chronic nutrient enrichment increases prevalence and severity of coral disease and bleaching. *Global Change Biology*, *20*(2), 544–554. https://doi.org/10.1111/gcb.12450

Vilela, C. L. S., Villela, H. D. M., Duarte, G. A. S., Santoro, E. P., Rachid, C. T. C. C., & Peixoto, R. S. (2021). Estrogen induces shift in abundances of specific groups of the coral microbiome. *Scientific Reports*, *11*(1), 2767. https://doi.org/10.1038/s41598-021-82387-x

Villela, H. (2020). Microbiome Flexibility Provides New Perspectives in Coral Research. *BioEssays*, *42*(7), 2000088. https://doi.org/10.1002/bies.202000088

Villela, H., Modolon, F., Schultz, J., Delgadillo-Ordoñez, N., Carvalho, S., Soriano, A. U., & Peixoto, R. S. (2023). Genome analysis of a coral-associated bacterial consortium highlights complementary hydrocarbon degradation ability and other beneficial mechanisms for the host. *Scientific Reports*, *13*(1), 12273. https://doi.org/10.1038/s41598-023-38512-z

Vohsen, S. A., Fisher, C. R., & Baums, I. B. (2019). Metabolomic richness and fingerprints of deep-sea coral species and populations. *Metabolomics*, *15*(3), 34. https://doi.org/10.1007/s11306-019-1500-y

Wada, N., Hsu, M.-T., Tandon, K., Hsiao, S. S.-Y., Chen, H.-J., Chen, Y.-H., Chiang, P.-W., Yu, S.-P., Lu, C.-Y., Chiou, Y.-J., Tu, Y.-C., Tian, X., Chen, B.-C., Lee, D.-C., Yamashiro, H., Bourne, D. G., & Tang, S.-L. (2022). High-resolution spatial and genomic characterization of coral-associated microbial aggregates in the coral *Stylophora pistillata*. *Science Advances*, *8*(27). https://doi.org/10.1126/sciadv.abo2431

Wang, Z., You, R., Han, H., Liu, W., Sun, F., & Zhu, S. (2024). Effective binning of metagenomic contigs using contrastive multi-view representation learning. *Nature Communications*, *15*(1), 585. https://doi.org/10.1038/s41467-023-44290-z

Ward, L. M., Hemp, J., Shih, P. M., McGlynn, S. E., & Fischer, W. W. (2018). Evolution of Phototrophy in the Chloroflexi Phylum Driven by Horizontal Gene Transfer. *Frontiers in Microbiology*, *9*. https://doi.org/10.3389/fmicb.2018.00260

Water, J. A. J. M., Chaib De Mares, M., Dixon, G. B., Raina, J., Willis, B. L., Bourne, D. G., & Oppen, M. J. H. (2018). Antimicrobial and stress responses to increased temperature and bacterial pathogen challenge in the holobiont of a reef-building coral. *Molecular Ecology*, *27*(4), 1065–1080. https://doi.org/10.1111/mec.14489

Wegley, L., Edwards, R., Rodriguez-Brito, B., Liu, H., & Rohwer, F. (2007). Metagenomic analysis of the microbial community associated with the coral Porites astreoides. *Environmental Microbiology*, *9*(11), 2707–2719. https://doi.org/10.1111/j.1462-2920.2007.01383.x

Wegley, L., Yu, Y., Breitbart, M., Casas, V., Kline, D., & Rohwer, F. (2004). Coral-associated Archaea. *Marine Ecology Progress Series*, *273*, 89–96. https://doi.org/10.3354/meps273089

Weil, E., Rogers, C. S., & Croquer, A. (2016). Octocoral Diseases in a Changing Ocean. In *Marine Animal Forests* (pp. 1–55). Springer International Publishing. https://doi.org/10.1007/978-3-319-17001-5_43-1

Weinbauer, M. G., Oregioni, D., Großkurth, A., Kerros, M.-E., Harder, T., DuBow, M., Gattuso, J.-P., & Maier, C. (2019). *33 Diversity of Bacteria Associated with the Cold Water Corals Lophelia pertusa and Madrepora oculata* (pp. 377–386). https://doi.org/10.1007/978-3-319-91608-8_33

Weinnig, A. M., Gómez, C. E., Hallaj, A., & Cordes, E. E. (2020). Cold-water coral (Lophelia pertusa) response to multiple stressors: High temperature affects recovery from short-term pollution exposure. *Scientific Reports*, *10*(1), 1768. https://doi.org/10.1038/s41598-020-58556-9

Weis, V. M., Davy, S. K., Hoegh-Guldberg, O., Rodriguez-Lanetty, M., & Pringle, J. R. (2008). Cell biology in model systems as the key to understanding corals. *Trends in Ecology & Evolution*, *23*(7), 369–376. https://doi.org/10.1016/j.tree.2008.03.004

Welsh, R. M., Rosales, S. M., Zaneveld, J. R., Payet, J. P., McMinds, R., Hubbs, S. L., & Vega Thurber, R. L. (2017). Alien vs. predator: bacterial challenge alters coral microbiomes unless controlled by *Halobacteriovorax* predators. *PeerJ*, *5*, e3315. https://doi.org/10.7717/peerj.3315

West, P. T., Probst, A. J., Grigoriev, I. V., Thomas, B. C., & Banfield, J. F. (2018). Genome-reconstruction for eukaryotes from complex natural microbial communities. *Genome Research*, *28*(4), 569–580. https://doi.org/10.1101/gr.228429.117

Wickham, H. (2016). *ggplot2*. Springer International Publishing. https://doi.org/10.1007/978-3-319-24277-4

Wickham, H., Averick, M., Bryan, J., Chang, W., McGowan, L., François, R., Grolemund, G., Hayes, A., Henry, L., Hester, J., Kuhn, M., Pedersen, T., Miller, E., Bache, S., Müller, K., Ooms, J., Robinson, D., Seidel, D., Spinu, V., … Yutani, H. (2019). Welcome to the Tidyverse. *Journal of Open Source Software*, *4*(43), 1686. https://doi.org/10.21105/joss.01686

Wienhausen, G., Bruns, S., Sultana, S., Dlugosch, L., Groon, L.-A., Wilkes, H., & Simon, M. (2022). The overlooked role of a biotin precursor for marine bacteria - desthiobiotin as an escape route for biotin auxotrophy. *The ISME Journal*, *16*(11), 2599–2609. https://doi.org/10.1038/s41396-022-01304-w

Wild, C., Huettel, M., Klueter, A., Kremb, S. G., Rasheed, M. Y. M., & Jørgensen, B. B. (2004). Coral mucus functions as an energy carrier and particle trap in the reef ecosystem. *Nature*, *428*(6978), 66–70. https://doi.org/10.1038/nature02344

Wild, C., Naumann, M., Niggl, W., & Haas, A. (2010). Carbohydrate composition of mucus released by scleractinian warm- and cold-water reef corals. *Aquatic Biology*, *10*(1), 41–45. https://doi.org/10.3354/ab00269

Williams, A., Chiles, E. N., Conetta, D., Pathmanathan, J. S., Cleves, P. A., Putnam, H. M., Su, X., & Bhattacharya, D. (2021a). Metabolomic shifts associated with heat stress in coral holobionts. *Science Advances*, *7*(1). https://doi.org/10.1126/sciadv.abd4210

Williams, A., Chiles, E. N., Conetta, D., Pathmanathan, J. S., Cleves, P. A., Putnam, H. M., Su, X., & Bhattacharya, D. (2021b). Metabolomic shifts associated with heat stress in coral holobionts. *Science Advances*, *7*(1). https://doi.org/10.1126/sciadv.abd4210

Woo, S., Yang, S.-H., Chen, H.-J., Tseng, Y.-F., Hwang, S.-J., De Palmas, S., Denis, V., Imahara, Y., Iwase, F., Yum, S., & Tang, S.-L. (2017). Geographical variations in bacterial communities associated with soft coral Scleronephthya gracillimum. *PLOS ONE*, *12*(8), e0183663. https://doi.org/10.1371/journal.pone.0183663

Woodcroft et al. (n.d.). *CoverM*. Retrieved April 4, 2024, from https://github.com/wwood/CoverM

Wooldridge, S. A. (2013). Breakdown of the coral-algae symbiosis: towards formalising a linkage between warm-water bleaching thresholds and the growth rate of the intracellular zooxanthellae. *Biogeosciences*, *10*(3), 1647–1658. https://doi.org/10.5194/bg-10-1647-2013

Work, T. M., Aeby, G. S., Stanton, F. G., & Fenner, D. (2008). Overgrowth of fungi (endolithic hypermycosis) associated with multifocal to diffuse distinct amorphous dark discoloration of corals in the Indo-Pacific. *Coral Reefs*, *27*(3), 663–663. https://doi.org/10.1007/s00338-008-0374-7

Work, T. M., Weatherby, T. M., Landsberg, J. H., Kiryu, Y., Cook, S. M., & Peters, E. C. (2021). Viral-Like Particles Are Associated With Endosymbiont Pathology in Florida Corals Affected by Stony Coral Tissue Loss Disease. *Frontiers in Marine Science*, *8*. https://doi.org/10.3389/fmars.2021.750658

Wright, R. M., Strader, M. E., Genuise, H. M., & Matz, M. (2019). Effects of thermal stress on amount, composition, and antibacterial properties of coral mucus. *PeerJ*, *7*, e6849. https://doi.org/10.7717/peerj.6849

Wu, T., Gómez-Coronado, P. A., Kubis, A., Lindner, S. N., Marlière, P., Erb, T. J., Bar-Even, A., & He, H. (2023). Engineering a synthetic energy-efficient formaldehyde assimilation cycle in Escherichia coli. *Nature Communications*, *14*(1), 8490. https://doi.org/10.1038/s41467-023-44247-2

Wu, Y.-W., Tang, Y.-H., Tringe, S. G., Simmons, B. A., & Singer, S. W. (2014). MaxBin: an automated binning method to recover individual genomes from metagenomes using an expectation-maximization algorithm. *Microbiome*, *2*(1), 26. https://doi.org/10.1186/2049-2618-2-26

Xiang, N., Hassenrück, C., Pogoreutz, C., Rädecker, N., Simancas-Giraldo, S. M., Voolstra, C. R., Wild, C., & Gärdes, A. (2022). Contrasting Microbiome Dynamics of Putative Denitrifying Bacteria in Two Octocoral Species Exposed to Dissolved

Organic Carbon (DOC) and Warming. *Applied and Environmental Microbiology*, *88*(2). https://doi.org/10.1128/AEM.01886-21

Xue, C.-X., Lin, H., Zhu, X.-Y., Liu, J., Zhang, Y., Rowley, G., Todd, J. D., Li, M., & Zhang, X.-H. (2021). DiTing: A Pipeline to Infer and Compare Biogeochemical Pathways From Metagenomic and Metatranscriptomic Data. *Frontiers in Microbiology*, *12*. https://doi.org/10.3389/fmicb.2021.698286

Yang, S.-H., Tandon, K., Lu, C.-Y., Wada, N., Shih, C.-J., Hsiao, S. S.-Y., Jane, W.-N., Lee, T.-C., Yang, C.-M., Liu, C.-T., Denis, V., Wu, Y.-T., Wang, L.-T., Huang, L., Lee, D.-C., Wu, Y.-W., Yamashiro, H., & Tang, S.-L. (2019). Metagenomic, phylogenetic, and functional characterization of predominant endolithic green sulfur bacteria in the coral Isopora palifera. *Microbiome*, *7*(1), 3. https://doi.org/10.1186/s40168-018-0616-z

Yoshii, K., Hosomi, K., Sawane, K., & Kunisawa, J. (2019). Metabolism of Dietary and Microbial Vitamin B Family in the Regulation of Host Immunity. *Frontiers in Nutrition*, *6*. https://doi.org/10.3389/fnut.2019.00048

Yu, G., Wang, L.-G., Han, Y., & He, Q.-Y. (2012). clusterProfiler: an R Package for Comparing Biological Themes Among Gene Clusters. *OMICS: A Journal of Integrative Biology*, *16*(5), 284–287. https://doi.org/10.1089/omi.2011.0118

Yu, X., Yu, K., Liao, Z., Chen, B., Deng, C., Yu, J., Yao, Q., Qin, Z., & Liang, J. (2021). Seasonal fluctuations in symbiotic bacteria and their role in environmental adaptation of the scleractinian coral Acropora pruinosa in high-latitude coral reef area of the South China Sea. *Science of The Total Environment*, *792*, 148438. https://doi.org/10.1016/j.scitotenv.2021.148438

Yuh, J., Marani, G., & Blidberg, D. R. (2011). Applications of marine robotic vehicles. *Intelligent Service Robotics*, *4*(4), 221–231. https://doi.org/10.1007/s11370-011-0096-5

Zhang, X.-Y., & Qi, S.-H. (2019). Microbes in Gorgonian and Soft Corals. In *Symbiotic Microbiomes of Coral Reefs Sponges and Corals* (pp. 69–79). Springer Netherlands. https://doi.org/10.1007/978-94-024-1612-1_6

Zhang, Y., Chen, Q., Xie, J. Y., Yeung, Y. H., Xiao, B., Liao, B., Xu, J., & Qiu, J.-W. (2019). Development of a transcriptomic database for 14 species of scleractinian corals. *BMC Genomics*, *20*(1), 387. https://doi.org/10.1186/s12864-019-5744-8

Zhang, Y., Ling, J., Yang, Q., Wen, C., Yan, Q., Sun, H., Van Nostrand, J. D., Shi, Z., Zhou, J., & Dong, J. (2015). The functional gene composition and metabolic potential of coral-associated microbial communities. *Scientific Reports*, *5*(1), 16191. https://doi.org/10.1038/srep16191

Zhu, W., Lomsadze, A., & Borodovsky, M. (2010). Ab initio gene identification in metagenomic sequences. *Nucleic Acids Research*, *38*(12), e132–e132. https://doi.org/10.1093/nar/gkq275

Ziv-El, M. C., & Rittmann, B. E. (2009). Systematic evaluation of nitrate and perchlorate bioreduction kinetics in groundwater using a hydrogen-based membrane biofilm reactor. *Water Research*, *43*(1), 173–181. https://doi.org/10.1016/j.watres.2008.09.035